Characterisation of G protein-coupled receptor 56-signalling and its potential role in tumour progression

by

Lea Maria Bauer, Dipl. Biol.

2014

Extracellular Matrix in Repair & Remodelling
Cardiff University
School of Dentistry
Cardiff, United Kingdom

A thesis submitted to the Cardiff University for the degree of
Doctor of Philosophy

Acknowledgements

I would like to thank my supervisors Dr Vera Knäuper and Prof Daniel Aeschlimann for their support and inspiration throughout my PhD.

I would like to acknowledge Tenovus for funding this project.

I would like to thank my colleagues Katarzyna Gaweł-Bęben, Magdalena Adamczyk, Ana Mafalda dos Reis Jegundo, Andreas Heil and Tim Wanger for their help and motivation.

Finally, I would like to thank Andreas, my parents Irmgard and Peter and my sister Lisa for their love and support.

Abstract

The adhesion G protein-coupled receptor 56 (GPR56) plays a major role in early brain development. Mutations in *Gpr56* cause the developmental brain disease bilateral frontoparietal polymicrogyria (BFPP), which is recapitulated in *Gpr56*$^{-/-}$ mice. GPR56 interacts with collagen III in the brain pial basement membrane and with tissue transglutaminase (TG2) in melanoma, where it potentially acts as a tumour suppressor by antagonising TG2-related functions. In glioblastoma, however, GPR56 is highly overexpressed and might play an important role for the invasive behaviour of these cells, which could be regulated by TG2 in the tumour stroma.

The main aim of this thesis was to analyse GPR56 signalling in response to TG2, thus exploring a potential link to cancer development and progression. Identifying downstream signalling pathways activated by GPR56 in response to TG2 could provide valuable information regarding potential targets for future therapeutic intervention in the context of anti-cancer therapies.

In order to investigate GPR56 signalling, a cell-based assay was established that measures GPR56 activation as metalloproteinase-dependent ectodomain shedding of alkaline phosphatase-tagged amphiregulin (AP-AR) in HEK293 cells. The assay was used to demonstrate for the first time activation of GPR56 by TG2. RhoA/Rho-associated protein kinase (ROCK) are activated by GPR56, which likely requires G$\alpha_{12/13}$ coupling to GPR56. RhoA/ROCK activity is required for the activation of a disintegrin and metalloproteinase 17 (ADAM17), the main metalloproteinase responsible for GPR56-dependent AP-AR shedding. Shedding of EGF-like ligands such as amphiregulin leads to the activation of epidermal growth factor receptors, inducing cellular responses such as cell proliferation and migration.

Further investigations using different GPR56 mutants revealed that the N-terminal domain of GPR56 is required for activation by TG2. The crosslinking activity of TG2 is dispensable for GPR56 activation and the C-terminal β-barrel domains of TG2 are sufficient to stimulate GPR56 signalling. Moreover, two novel potential GPR56 ligands, TG6 and TG7, were shown to stimulate GPR56-dependent AP-AR shedding.

Using confocal microscopy, GPR56-dependent internalisation of TG2 via clathrin-coated pits was demonstrated, a mechanism that is well known for agonist-activated GPCRs. Finally, the potential role of GPR56 in glioblastoma was investigated by generating stable GPR56 knockdown glioma cells. Analysis of GPR56 knockdown cells indicated that GPR56 may play a role for glioblastoma migration and invasion.

These results present a novel signalling pathway activated by GPR56 in response to TG2 that is involved in cell proliferation, growth and migration, potentially providing an explanation for the supposed tumour promoting functions of GPR56 in glioblastoma.

1 Introduction 1

1.1 Why study GPR56? 1
1.2 G protein-coupled receptors 3
  1.2.1 Phylogenetic classification of GPCRs 3
  1.2.2 Structure of GPCRs 4
  1.2.3 Activation of GPCRs 6
  1.2.4 G protein-dependent signalling 9
  1.2.5 Desensitisation of G protein-dependent signalling 12
  1.2.6 Internalisation of GPCRs 13
    1.2.6.1 Clathrin-dependent endocytosis 14
    1.2.6.2 Clathrin-independent endocytosis 15
    1.2.6.3 Endosomal sorting 17
  1.2.7 G protein-independent signalling 19
  1.2.8 EGFR transactivation 21
    1.2.8.1 A disintegrin and metalloproteinases (ADAMs) 25
      1.2.8.1.1 Structure of ADAMs 26
      1.2.8.1.2 Biological functions of ADAMs 27
      1.2.8.1.3 ADAM17 28
      1.2.8.1.4 ADAM inhibitors 29
1.3 Adhesion GPCRs 30
  1.3.1 Structure of adhesion GPCRs 30
  1.3.2 GPS cleavage and the GAIN domain 32
  1.3.3 Physiological functions of adhesion GPCRs 33
    1.3.3.1 De-orphanised adhesion GPCRs 33
    1.3.3.2 Adhesion GPCRs in immunology 34
    1.3.3.3 Adhesion GPCRs in embryonic developmental 34
    1.3.3.4 Adhesion GPCRs in the CNS 35
  1.3.4 Signalling by adhesion GPCRs 36
  1.3.5 Adhesion GPCRs in tumorigenesis 37
1.4 GPR56 39

1.4.1 Expression of GPR56 ... 39
1.4.2 Structure of GPR56 ... 39
1.4.3 GPR56 interaction partners and potential ligands ... 41
1.4.4 GPR56 in brain development ... 41
1.4.4.1 GPR56 knockout mice ... 44
1.4.5 GPR56 and cancer ... 45
1.4.5.1 GPR56 as a tumour suppressor ... 45
1.4.5.2 GPR56 as a tumour promoter ... 46
1.4.6 GPR56 in immune cells ... 48
1.4.7 The role of N-GPR56 in GPR56 activation ... 48
1.4.8 Natural splice variants ... 49
1.5 Transglutaminases ... 51
1.6 Tissue transglutaminase (TG2) ... 53
1.6.1 Expression of TG2 in the human body ... 53
1.6.2 Enzymatic activities of TG2 ... 53
1.6.3 Biological functions of TG2-mediated transamidation ... 57
1.6.4 Regulation of the transamidation activity ... 57
1.6.5 TG2 as a GTPase and G protein ... 59
1.6.6 Non-enzymatic functions of extracellular TG2 and their physiological roles ... 60
1.6.7 TG2 and cancer ... 61
1.6.8 TG2 knockout mice ... 62
1.7 Glioblastoma multiforme ... 64
1.8 Aims of the thesis ... 67
2 Material and methods ... 68
2.1 DNA manipulation ... 68
2.1.1 Agarose gel electrophoresis ... 68
2.1.2 Restriction digest ... 68
2.1.3 Ligation ... 69
2.1.4 Transformation ... 69
2.1.5 Identifying positive clones ... 69

2.1.6 Plasmid DNA midiprep 70

2.2 DNA mutagenesis 70

2.2.1 PCR reactions 70
2.2.2 Generating an intermediate GPR56 expression vector 72
2.2.3 Restriction digest of PCR reactions 72
2.2.4 Purification of cleaved PCR products 73
2.2.5 Cloning of C-terminal GPR56 phosphorylation mutants 73

2.3 Cell culture 74

2.3.1 Cell lines 74

2.3.1.1 HEK293 model system 75
2.3.1.2 HCA2 fibroblasts 75
2.3.1.3 Glioblastoma cell line 76

2.3.1.3.1 Generating GPR56 knockdown cells 76
2.3.1.3.2 Linearization of shRNA plasmid DNA 76
2.3.1.3.3 Phenol-chloroform extraction of shRNA plasmid DNA.. 77
2.3.1.3.4 Stable transfection of cells 77
2.3.1.3.5 Hygromycin kill curve of U373 cells 78
2.3.1.3.6 Selection of stably transfected cells 78
2.3.1.3.7 Isolating single cell colonies 78

2.4 Alkaline phosphatase-Amphiregulin (AP-AR) shedding assay 79

2.4.1 Transient transfection of HEK293 cells 79
2.4.2 Inhibition of ADAM10 and ADAM17 79
2.4.3 Treatment with potential ligands for GPR56 80
2.4.4 Measurement of AP-activity in the medium 80
2.4.5 Statistical analysis 81

2.5 Protein analysis by Western Blotting 82

2.5.1 Production of cell lysates 82
2.5.2 Protein concentration assay (DC assay) 82
2.5.3 SDS polyacrylamide gel electrophoresis (SDS-PAGE) 83
2.5.4 Western blotting 83

2.6 Immunofluorescence 85
2.6.1 Immunodetection of GPR56 in eukaryotic cells 86
2.6.1.1 Endogenous GPR56 expression in U373 cells as detected with N-GPR56 antibody 86
2.6.1.2 GPR56 expression in transiently transfected HEK293 cells 86
2.6.2 Immuno-colocalisation of GPR56 and TG2 in stable HEK293 cells 87
2.6.3 SNAP-tag staining of GPR56 in HEK293 cells 87
2.6.3.1 Immunolocalisation of TG2 88
2.6.3.2 Immuno-colocalisation of TG2 and lysosomes or caveolae 88
2.6.3.3 Co-staining of transferrin receptors 89
2.6.3.4 Inhibition of endocytosis with sucrose 89
3 Investigations of GPR56 downstream signalling using an AP-AR shedding assay 90
3.1 Introduction 90
3.1.1 Aims of the chapter 93
3.2 Results 94
3.2.1 Principle of the AP-AR shedding assay 94
3.2.2 Validation of the GPR56 signalling response 97
3.2.2.1 C_{230}-A TG2 activates GPR56 97
3.2.2.2 Comparison of wild type TG2, C_{230}-A TG2 and an anti-N-GPR56 antibody 102
3.2.2.3 The putative ligand collagen III 103
3.2.3 Identification of the metalloproteinase involved in GPR56-dependent AP-AR shedding 105
3.2.4 Identifying mediator proteins downstream of GPR56 108
3.2.4.1 Interfering with the Protein kinase C (PKC) / Phospholipase C (PLC) pathway 108
3.2.4.2 Inhibition of the RhoA signalling mechanism 113
3.2.4.3 Inhibition of the epidermal growth factor receptor (EGFR)115

3.3 Discussion ... 117

4 Characterisation of GPR56-TG interactions ... 125

4.1 Introduction ... 125

4.1.1 Aims of the chapter ... 126

4.2 Results ... 127

4.2.1 GPR56 activation by TG2 is independent of transglutaminase activity ... 127

4.2.2 Other TG isoenzymes ... 129

4.2.2.1 Neuronal transglutaminase (TG6, TG$_Y$) induces GPR56-dependent AP-AR shedding ... 129

4.2.2.2 Transglutaminase 7 (TG7, TG$_z$) activates GPR56 ... 131

4.2.2.3 A transglutaminase lacking the β-barrel domains fails to activate GPR56 ... 132

4.2.2.4 The β-barrel domains of TG2 are sufficient to activate GPR56 ... 134

4.3 Discussion ... 135

5 Identifying GPR56 structural domains involved in downstream signalling ... 141

5.1 Introduction ... 141

5.1.1 Aims of the chapter ... 143

5.2 Results ... 144

5.2.1 Cloning of the C-terminal tail phosphorylation site mutants ... 144

ΔS-A-GPR56, T$_{688}$A-GPR56, ΔS/T-A GPR56 ... 144

5.2.2 Analysis of wild type and mutant GPR56 expression levels in transiently transfected HEK293 cells ... 148

5.2.3 GPR56 mutants in the AP-AR shedding assay ... 153

5.2.3.1 Basal- and C$_{230}$-A TG2-induced AP-AR shedding is impaired in the BFPP-mutant R$_{565}$W-GPR56 and the natural splice variant Δ$_{430\text{-}35}$-GPR56 ... 153

5.2.3.2 TG2-stimulated GPR56-dependent AP-AR shedding requires the N-terminal domain of the receptor 157

5.2.3.2.1 The ligand interaction site deletion mutant ΔSTP-GPR56 157

5.2.3.2.2 The N-terminal domain deletion mutant ΔN-GPR56 ... 160

5.2.3.3 Multiple mutations of six serine residues alone or in conjunction with threonine-688 in the C-terminal tail of GPR56 do not affect receptor-induced signalling.. 162

5.2.3.4 The GPR56 C-terminal tail regulates basal, but not TG2-induced AP-AR shedding 168

5.3 Discussion 170

6 Exploring the mechanism of GPR56-dependent internalisation of TG2 using confocal microscopy.. 175

6.1 Introduction.. 175

6.1.1 Aims of the chapter 177

6.2 Results... 178

6.2.1 Interaction of GPR56 and TG2 in stably transfected HEK293 cells 178

6.2.2 Internalisation of GPR56 and TG2 in HEK293 cells transiently expressing SNAP-tagged GPR56... 184

6.2.2.1 Optimisation of SNAP-GPR56 staining and comparison to the SNAP-β_2-adrenergic receptor.. 184

6.2.2.2 Co-internalisation of SNAP-GPR56 and TG2 189

6.2.2.3 Internalisation of GPR56 and TG2 is clathrin-dependent. 193

6.2.2.3.1 The clathrin-inhibitor sucrose prevents internalisation 193

6.2.2.3.2 SNAP-GPR56 internalises with transferrin receptors . 198

6.2.2.3.3 Endocytosis of SNAP-GPR56 is caveolae-independent... 201

6.2.2.4 Internalised GPR56 and TG2 do not co-localise in lysosomes 204

6.3 Discussion 211

7 Generation and preliminary characterisation of stable GPR56 knockdown glioblastoma cells 218

7.1 Introduction.. 218

7.1.1 Aims of the chapter 219

7.2 Results... 220

7.2.1 Hygromycin dose-response.. 220

7.2.1.1 GPR56 expression levels and pattern 222

7.3 Discussion 225

8 General discussion and future experiments 228

8.1 Summary of the results.. 228

8.2 Conclusions 230

8.2.1 TG2 stimulates GPR56-dependent activation of ADAM17..... 230

8.2.2 TG2-dependent GPR56 signalling is independent of TG2 crosslinking activity 231

8.2.3 GPR56 downstream signalling 233

8.2.3.1 GPR56 activates RhoA signalling................................... 233

8.2.3.2 GPR56-mediated ADAM17-activation is independent of G_q-signalling.. 236

8.2.3.3 A role for β-arrestins in GPR56-dependent signalling?.... 237

8.2.4 Novel GPR56 ligands... 238

8.2.5 Internalisation of GPR56 240

8.2.6 Controversial roles of GPR56 in cancer 241

8.3 Future outlook.. 246

References.. 249

Appendix I: Solutions and buffer 283

Appendix II: Chemicals 284

Appendix III: Consumables and laboratory equipment.............................. 285

Appendix IV: DNA sequences endcoding shRNAs used to stably transfect U373 glioblastoma cells 287

Appendix V: Sequence of wild type GPR56, 693 aa 288
Appendix VI: Stably transfected HEK293 control cells stained for GPR56 and TG2. 289

List of abbreviations

7TM	Seven transmembrane
aa	Amino acid
AC	Adenylyl cyclase
ADAM	A disintegrin and metalloproteinase
ADPKD	Autosomal-dominant polycystic kidney disease
aGPCR	Adhesion G protein-coupled receptor
AP	Alkaline phosphatase
AP-2	Adaptor protein-2
AR	Amphiregulin
ATR	Angiotensin II receptor
ATP	Adenosine triphosphate
BAI	Brain angiogenesis inhibitor
β_2AR	β_2-adrenergic receptor
BSA	Bovine serum albumine
BFPP	Bilateral frontoparietal polymicrogyria
BM	Basement membrane
cAMP	Cyclic adenosine monophosphate
CaMKII	Calcium-calmodulin-dependent kinase II
Cav-1	Caveolin-1
Cdc42	Cell division control protein 42 homolog
CD	Cluster of differentiation
CHO	Chinese hamster ovary
CIRL	Calcium-independent receptor of latrotoxin
CNS	Central nervous system
CXCR	Chemokine receptor
DAF	Decay accelerating factor
DAG	Diacylglycerol
DAPI	2-(4-amidinophenyl)-1H-indole-6-carboxamidine
DMEM	Dulbecco’s modified eagle’s medium
DMSO	Dimethyl sulfoxide
DOCK	Dedicator of cytokines protein

ECD	Ectodomain
ECL	Extracellular loop
ECM	Extracellular matrix
EDTA	Ethylenediaminetetraacetic acid
EGTA	Ethylene glycol tetraacetic acid
EGF	Epidermal growth factor
EGFR	Epidermal growth factor receptor
ELMO	Engulfment and cell motility
EMEM	Eagle’s minimum essential medium
EMR	EGF-like module containing mucin-like receptor protein
ER	Endoplasmic reticulum
ETR	Endothelian receptor
ERK	Extracellular signal-related kinase
ESCC	Esophageal squamous cell carcinoma
FXIII	Factor 13
FLRT	Fibronectin leucine-rich repeat transmembrane protein
FBS	Fetal bovine serum
FN	Fibronectin
GAIN	GPCR-autoproteolysis inducing
GAG	Glycosaminoglycan
GAPDH	Glyceraldehyde 3-phosphate dehydrogenase
GBM	Glioblastoma multiforme
GDP	Guanine nucleotide diphosphate
GEF	Guanine nucleotide exchange factor
GPCR	G protein-coupled receptor
GPR56	G protein-coupled receptor 56
G protein	Guanine nucleotide binding protein
GPS	G protein-coupled receptor proteolytic site
GRAFS	Glutamate, rhodopsin, adhesion, frizzled/taste2, secretin
GRK	G protein-coupled receptor kinase
GTP	Guanine nucleotide triphosphate
GTPγS	Guanosine-(γ-thio)triphosphate
HBF	heparin-binding epidermal growth factor

HEK293	human embryonic kidney 293
HRP	Horseradish peroxidase
ICL	intracellular loop
IgG	Immunoglobulin G
IP_3	Inositol triphosphate
KD	Knockdown
LAMP	Lysosome-associated membrane protein
LPA	Lysophosphatidic acid
LRP	Lipoprotein-receptor related protein
MAPK	Mitogen-activated protein kinase
MEK	Mitogen-activated protein kinase kinase
MMP	Matrix metalloproteinase
NF-κB	Nuclear factor κB
NK	Natural killer
NPC	Neural progenitor cell
PAGE	Polyacrylamide gel electrophoresis
PAR	Protease-activated receptor
PBS	Phosphate buffered saline
PCP	Planar cell polarity
PDGF	Platelet derived growth factor
PDZ	PSD95, Dlg, ZO-1/2
PFA	Paraformaldehyde
PI3K	Phosphatidylinositol 3-kinase
PKD	Polycystic kidney disease
PMA	Phorbol 12-myristate 13-acetate
p-NPP	*para*-nitrophenol phosphate
PNGase F	peptide-N-glycosidase F
PKA	Protein kinase A
PKC	Protein kinase C
PLC	Phospholipase C
PTEN	Phosphatase and tensin homolog
PVDF	Polyvinyliden-difluorid
Rab	Ras-related in brain

Rho	Ras homolog gene family
ROCK	Rho-associated protein kinase
RTK	Receptor tyrosine kinase
SDS	Sodium dodecyl sulfate
Sh	Short hairpin
Src	Proto-oncogene tyrosine-protein kinase
SRE	Serum-response element
STP	Serine, threonine, proline
TBST	Tris-buffered saline and Tween-20
Tf	Transferrin
TG	Transglutaminase
TG2	Transglutaminase 2
TGF	Transforming growth factor
TM	Transmembrane
TMPS	Triple-membrane-passing-signalling
TR	Transferrin receptor
V_2R	Vasopressin receptor 2
VEGF	Vascular endothelial growth factor
VLGR	Very large G protein-coupled receptor

CHAPTER 1:

Introduction

1 Introduction

1.1 Why study GPR56?

The adhesion G protein-coupled receptor 56 (GPR56) plays an important role during early brain development, where it regulates neural progenitor migration by interacting with its ligand collagen III in the pial basement membrane (Piao et al. 2004; Luo, Jeong, et al. 2011). Another potential function of GPR56 is related to the development and progression of cancer and GPR56 expression levels are deregulated in certain types of cancer (Xu et al. 2006; Ke et al. 2007; Sud et al. 2006; Huang et al. 2008; Shashidhar et al. 2005). GPR56 is down-regulated in highly metastatic melanoma and overexpression of GPR56 in melanoma cells leads to stop of tumour growth and metastasis *in vivo* (Xu et al. 2006; Yang et al. 2011). It was supposed that GPR56 interacts with its second known ligand tissue transglutaminase (TG2) in the tumour stroma, thus antagonising the tumour promoting effects of TG2 (Yang et al. 2014). In contrast to the situation in metastatic melanoma, GPR56 is highly overexpressed in glioblastoma and associated with cell adhesion, potentially contributing to the invasive properties of aggressive glioblastoma cells (Shashidhar et al. 2005). Glioblastoma multiforme (GBM) is a deadly disease and despite extensive treatments, most patients die shortly after diagnosis (Holland 2000). There is a strong need to identify and characterise novel cellular players involved in the development and progression of GBM, which could be targeted by drugs to treat the disease more efficiently. GPCRs and their signalling networks are involved in most physiological processes and they have important functions for many diseases including cancer, making them a major target for drug development (Dorsam and Gutkind 2007; Lappano and Maggiolini 2011). Being a member of this large protein family, GPR56 represents a potential candidate for novel therapeutic interventions in the context of glioblastoma and other tumours.

In addition to its controversial roles in different types and stages of cancer outlined above, a study by Edwards (2010) suggested that GPR56 might be involved in keratinocyte migration in response to TG2, as shown in the context of re-epithelialisation. The study showed that matrix TG2 induces a disintegrin and metalloproteinase 17 (ADAM17)-dependent shedding of epidermal growth factors, leading to the activation of epidermal growth factor receptor (EGFR) in keratinocytes, inducing migration and proliferation (Edwards 2010). The underlying signalling mechanism is also referred to as EGFR transactivation and it plays a major role in cellular migration, survival and proliferation, also in the context of cancer (Lappano and Maggiolini 2011; Gschwind et al. 2001; Fischer et al. 2003). It was hypothesised that the missing link between TG2 and ADAM17 activation might be GPR56 (Edwards 2010). This working hypothesis and the published data about GPR56's potential roles in cancer (Xu et al. 2006; Yang et al. 2011; Yang et al. 2014; Shashidhar et al. 2005) led to the current project, which set out to investigate GPR56-mediated signalling in response to TG2, potentially resulting in EGFR transactivation. Understanding this GPR56 downstream signalling pathway, which likely contributes to oncogenic transformation in tumours, as well as further characterising the nature and function of the GPR56-TG2 interaction could help to understand the potential role of GPR56 in cancer. In order to connect these basic investigations with the situation in GBM, this projects set out to investigate the specific role of GPR56 in GBM by characterising the effects of depleting GPR56 in glioblastoma cells. This study could help to advance the existing knowledge of GPR56's role in cancer and might help to identify points for therapeutic intervention in order to block invasion and proliferation of glioblastoma more efficiently in the future.

1.2 G protein-coupled receptors

G protein-coupled receptors (GPCRs) are the largest family of membrane proteins involved in signal transduction, represented by more than 800 members (~4 % of the coding sequence) in the human genome (Hill 2006). GPCRs are ubiquitously expressed in the human body and mediate most of cellular responses to neurotransmitters, hormones, amines, peptides, proteins, ions, nucleotides, growth factors, lipids or sensory stimuli like photons, odorants and taste ligands by transducing extracellular signals to intracellular effectors. GPCRs play very important roles in fundamental biological processes such as cellular growth, migration, differentiation, or apoptosis (Dorsam and Gutkind 2007). They are involved in physiological processes such as the visual sense, the sense of smell, immune responses, regulation of blood pressure, contraction of cardiac- and smooth-muscle, synaptic transmission and far more. They also play key functions in many diseases and are currently targeted by ~50 % of all therapeutic agents (Dorsam and Gutkind 2007; Hill 2006; Lagerström and Schiöth 2008; Rosenbaum et al. 2009). For ~120 receptors neither their physiological role, nor their endogenous ligands are known. These receptors are called "orphan GPCRs" (Lappano and Maggiolini 2011).

1.2.1 Phylogenetic classification of GPCRs

Due to physiological and structural similarities, the GPCR superfamily was originally subdivided into six classes (A-F classification system): class A - rhodopsin-like, class B - secretin receptor family, class C - metabotropic glutamate/pheromone, class D - fungal mating pheromone receptors, class E - cAMP receptors and class F - frizzled/smoothened (Kolakowski 1994). More recently, an alternative, phylogenetic classification system was established by Fredriksson et al. (2003), announcing five different GPCR families, called "GRAFS": the glutamate, rhodopsin, adhesion, frizzled/taste2 and secretin GPCRs. In 2008, the glutamate family consisted of 22, the rhodopsin family of 672, the adhesion family of 33, the frizzled/taste2 family of 11/25 and the secretin family of 15 members (Lagerström and Schiöth 2008). The main difference between the classification by Kolakowski (1994) and Fredriksson et al. (2003) is the subdivision of class B receptors into the adhesion and secretin families. The new system also provides a subdivision of the largest group of GPCRs, the rhodopsin family, into four main groups with 13 sub-branches (Fredriksson et al. 2003; Lagerström and Schiöth 2008).

1.2.2 Structure of GPCRs

The first identified GPCR was bovine rhodopsin, found in the rod photoreceptor cells of the retina. Its primary structure was resolved in 1983 (Hargrave et al. 1983; Nathans and Hogness 1983) and its crystal structure in 2000, the first one of a GPCR (Palczewski et al. 2000). These analyses revealed that rhodopsin consists of the 40 kDa opsin that is linked to the chromophore 11-*cis*-retinal, a derivate of vitamin A (Hargrave et al. 1983). The binding of a photon induces a conformational change of rhodopsin through isomerisation of 11-*cis*-retinal to all-*trans*-retinal, which transiently activates opsin, before the all-*trans*-retinal is hydrolysed and dissociates. It was shown that the absorption of one photon activates hundreds of rhodopsin receptors, converting energy into intracellular signalling via the G protein transducin, thus enabling vision (Yoshizawa and Wald 1963; Fung et al. 1981; Palczewski et al. 2000). The amino acid sequence analysis predicted the existence of hydrophobic α-helical seven transmembrane (7TM) domains, waving in and out the membrane, as well as hydrophilic extracellular (ECLs) and intracellular loops (ICLs) connecting these transmembrane domains, as well as an extracellular N-terminus and a C-terminal cytoplasmic tail (Hargrave et al. 1983). This model was later confirmed by x-ray structural analysis of the three-dimensional structure (Palczewski et al. 2000).

Cloning of another GPCR, the β_2-adrenergic receptor (β_2AR), revealed significant homology with bovine rhodopsin (Dixon et al. 1986). However, the idea of a common protein family emerged later with the cloning and structural analysis of other GPCRs. The existence of a 7TM domain as well as the ability to couple guanine nucleotide-binding proteins (G proteins) represent the two main requirements for a receptor to be called GPCR, although the latter requirement has not been demonstrated for all GPCRs, thus they are sometimes also referred to as 7TM-receptors (Fredriksson et al. 2003).

In order to compare residues between the different receptors of the largest class of GPCRs, the rhodopsin-like GPCRs, different official GPCR nomenclatures were introduced. The Schwartz numbering scheme marks the most conserved residue within a TM-domain with a generic number according to its position within the helix (Schwartz 1994). For example, AspII:10 is the most conserved residue in TM2 and it is located at position 10 within this helix. In the Ballesteros-Weinstein nomenclature, each residue is marked by two numbers (Ballesteros and Weinstein 1995). The first number refers to the helix the residue is located in and the second number provides information about the position of this residue relative to the most conserved residue, which has been given number 50, within the same TM-domain. For example, the most conserved residue within TM1 is Pro$^{1.50}$, the next residue C-terminally to it is Asn$^{1.51}$ and the residue N-terminally to it is Cys$^{1.49}$. Comparison of rhodopsin-like GPCR structures using these numbering schemes has helped to identify certain highly conserved residues that are important for receptor activation, as discussed in section 1.2.3.

Functionally, the N-terminal domain, ECLs and the 7TM domain comprise the ligand recognition parts, while the ICLs and cytoplasmic domain are involved in G protein-dependent/-independent signal transduction (Dorsam and Gutkind 2007). The greatest structural variance among the different GPCRs is observed in the N-terminus, which can be very short or very long, depending on the GPCR family (Fig. 1.1).

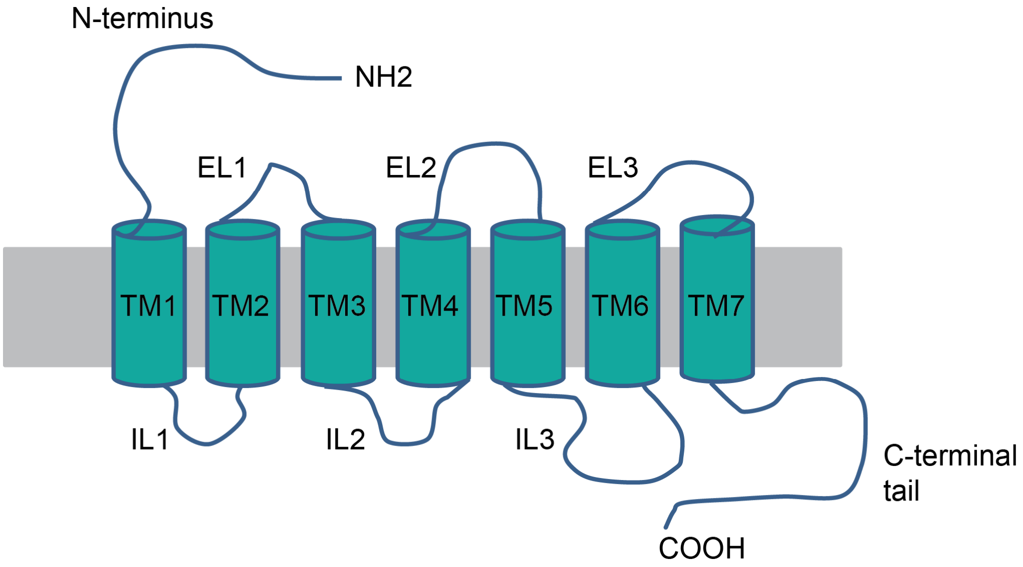

Figure 1.1 Secondary structure of a typical GPCR.
All GPCRs consist of a seven transmembrane domain (TM1-7). The N-terminus and the extracellular loops (ECLs) comprise the extracellular domains, whereas the intracellular loops (ICLs) and the cytoplasmic C-terminus are located intracellularly.

1.2.3 Activation of GPCRs

Although there is huge ligand diversity, there seems to be a common mechanism of receptor activation. Analysis of rhodopsin demonstrated conformational changes occurring within the 7TM domain upon light activation. A rotation of TM6 relative to TM3, as well as conformational changes in the cytoplasmic ends of TM1, TM2 and TM7 were shown (Farrens et al. 1996; Altenbach et al. 2001). Analysis of the β_2AR showed similar changes in TM3 and TM6 upon adrenalin binding (Ghanouni et al. 2001). An ionic interaction between the cytoplasmic end of TM6 and the highly conserved D(/E)RY motif, localised in ICL2, was identified (Yao et al. 2006). This so-called “ionic lock” is one of several non-covalent interactions that keep GPCRs in their inactive state (Kobilka and Deupi 2007) and its disruption upon agonist stimulation leads to the active receptor conformation.

GPCRs that are activated by completely different ligands can couple to the same G protein. Thus, the induced changes in their cytoplasmic regions upon agonist activation must be quite similar, as observed for rhodopsin and β_2AR (Kobilka 2007) and others (Warne et al. 2011; Xu et al. 2011; Deupi and Standfuss 2011; Lebon et al. 2012).

Many GPCRs have some basal (constitutive) activity, which means they activate G protein signalling in the absence of agonist. The simplest kinetic model to explain activation of GPCRs is a two-state model, in which the GPCR exists primarily in an inactive (R) or active state (R*) (Leff 1995) (Fig. 1.2 A). The constitutive activity of a GPCR is defined as the equilibrium between these two states in the absence of a ligand. A full agonist shifts the equilibrium to the active state R*, while an inverse agonist binds and stabilises the inactive state R, inhibiting basal activity. Partial agonists have some affinity for both states, thus shift the equilibrium less efficiently towards R* and activate only submaximal. Antagonists do not affect constitutive activity, thus the equilibrium between R and R*, but block access for other ligands (Fig. 1.2 B) (Kobilka 2007).

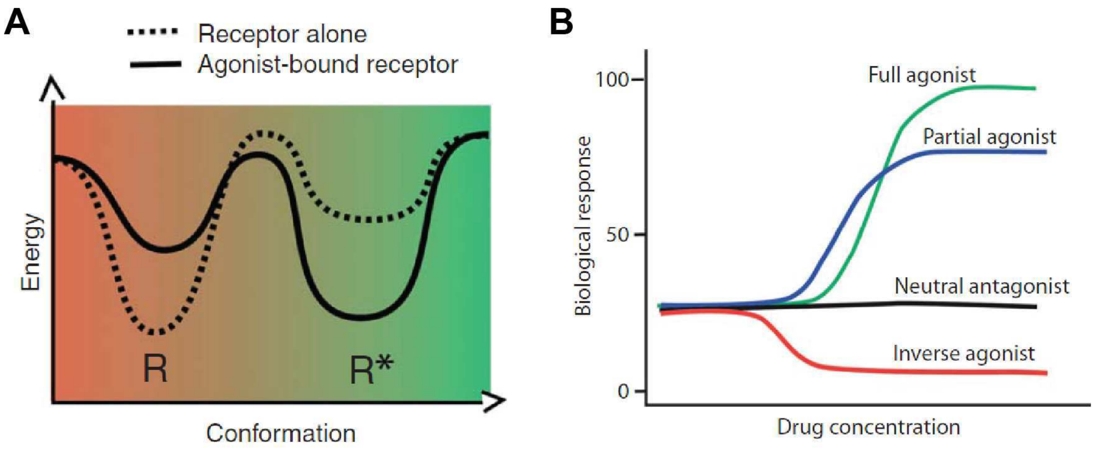

Figure 1.2 Activation of GPCRs.

(A) Energy landscape diagram for a possible mechanism of GPCR activation. In this simple model, the GPCR can switch only between two conformations, an inactive (R) and an agonist-activated (R*) state. The energy difference between the two states determines the probability that the GPCR will undergo a conformational change. The height of the energy barrier defines the kinetics of the transition between the states. A binding ligand can provide energy that reduces the height of the energy barrier.

(B) Different types of ligands have varying effects on a GPCR that shows some basal activity.

Taken from (Deupi and Kobilka 2007).

It must be noted that this is a very simple model and that most GPCRs are very dynamic proteins that may exist in multiple conformational states (Kobilka and Deupi 2007). In addition, each ligand could stabilize a unique receptor conformation, as indicated for the β_2AR (Ghanouni et al. 2001).

Rhodopsin is a special GPCR regarding receptor activation, since it shows no basal (constitutive) activity. Rhodopsin behaves as a simple on-off switch, in which a single photon fully activates the receptor. This is accompanied by the transition of the inverse agonist *cis*-retinal, bound in the 7TM domain of opsin, to the full agonist *all*-trans-retinal, followed by a series of conformational changes leading to the formation of the active conformation metarhodopsin II (Kobilka 2007).

1.2.4 G protein-dependent signalling

One major feature of GPCRs is their ability to bind G proteins. Upon agonist activation, GPCRs undergo structural changes within their 7TM domain, which mainly affects the conformation of the ICLs, thus uncovering G protein binding sites within ICL2, 3 and 4 (Hamm 2001). It is thought that receptor activation leads to the formation of a ternary complex consisting of agonist, GPCR and G protein. However, many receptors activate G protein signalling in the absence of an agonist, thus are constitutively active (Gether 1998).

Conventional G proteins are heterotrimeric proteins, consisting of a Gβ/γ-heterodimer and a Gα-subunit that binds guanosine diphosphate (GDP) and guanosine triphosphate (GTP) and acts as a GTPase. GDP-bound Gα tightly binds to Gβ/γ, leading to cell membrane association of the G protein where it can couple a GPCR. The GPCR acts as a guanosine nucleotide exchange factor (GEF), inducing the release of GDP from Gα, followed by binding of GTP. This, however, induces conformational changes within Gα, leading to the dissociation of the Gβ/γ-dimer. Both subunits, GTP-Gα and Gβ/γ, may activate different downstream effectors. Once GTP is hydrolysed by Gα, downstream signalling is terminated, since inactive Gα-GDP binds again to Gβ/γ. The hydrolysis of GTP is regulated by RGS (regulator of G protein signalling) proteins (McCudden et al. 2005; Pierce et al. 2002).

A variety of different Gα and Gβ/γ subunits have been identified, with 16 human Gα-genes, 5 human Gβ-genes ($G\beta_{1\text{-}5}$) and 12 Gγ-genes ($G\gamma_{1\text{-}12}$) resulting in a huge number of possible combinations for the Gβγ-dimer (McCudden et al. 2005). Some of the Gβγ-combinations preferably target specific GPCRs and specifically activate certain effector proteins. The 39-45 kDa Gα-proteins consist of a nucleotide-binding domain with homology to Ras-like GTPases and an α-helical domain. They can be subdivided into four major classes: G_s, G_q, G_{12}, G_i. Each of the classes is composed of specific isotypes showing a high degree of amino acid similarities, as shown in table 1.1 (Simon et al. 1991; McCudden et al. 2005).

Table 1.1 Classification of human Gα proteins. ***After Simon et al. (1991)*.**

G protein class	Isotypes within the class
G_s	$G\alpha_s$, $G\alpha_{olf}$
G_i	$G\alpha_{i1}$, $G\alpha_{i2}$, $G\alpha_{i3}$, $G\alpha_o$, $G\alpha_{t1}$, $G\alpha_{t2}$, $G\alpha_{gust,}$ $G\alpha_z$
G_q	$G\alpha_q$, $G\alpha_{11}$, $G\alpha_{14}$, $G\alpha_{16}$
G_{12}	$G\alpha_{12}$, $G\alpha_{13}$

The different Gα subfamilies also activate different downstream effectors such as second-messenger producing enzymes or ion channels. Adenylyl cyclase (AC) was the first recognized effector, activated by $G\alpha_s$, whereas $G\alpha_i$ was later found to inhibit AC (Ross and Gilman 1977; Hildebrandt et al. 1983). AC hydrolyses ATP to cAMP, which activates effectors such as protein kinase A (PKA) or Ca^{2+}-channels. cAMP and Ca^{2+} are ubiquitous second messengers, involved in many physiological functions. $G\alpha_i$ proteins also activate mitogen-activated protein kinase (MAPK) and phosphatidylinositol 3-kinase (PI3K), signalling pathways that are involved in cell growth, proliferation and survival (Fig. 1.3) (Leurs et al. 2005).

$G\alpha_{12/13}$ proteins regulate Rho-family guanine nucleotide exchange factors (Rho-GEFs) that activate small GTPases such as RhoA, Rac1, Ras or Cdc42 by inducing the exchange of GDP to GTP. The small GTPases in turn activate a wide range of effector proteins which are mainly involved in the organisation of the actin cytoskeleton, including the formation of stress fibers or focal adhesion complexes. These processes play important roles for biological functions such as cell adhesion and migration. Moreover, signalling through the small GTPases is also involved in cell cycle progression, cell proliferation, apoptosis or oncogenic transformation (Fig. 1.3) (Sah et al. 2000; Chiariello et al. 2010; Schwartz 2004).

G_q proteins activate the β-isoforms of PLC (PLCβ) that hydrolyses phosphatidylinositol bisphosphate to the second messengers diacylglycerol (DAG) and inositol triphosphate (IP_3). DAG activates protein kinase C (PKC) and IP_3 mobilises Ca^{2+}-release from intracellular stores (Mizuno and Itoh 2009). Similar to $G\alpha_{12/13}$, G_q proteins initiate RhoA signalling, which is independent of PLCβ. However, G_q activates different Rho-GEFs than $G\alpha_{12/13}$ proteins (Fig. 1.3) (Mizuno and Itoh 2009).

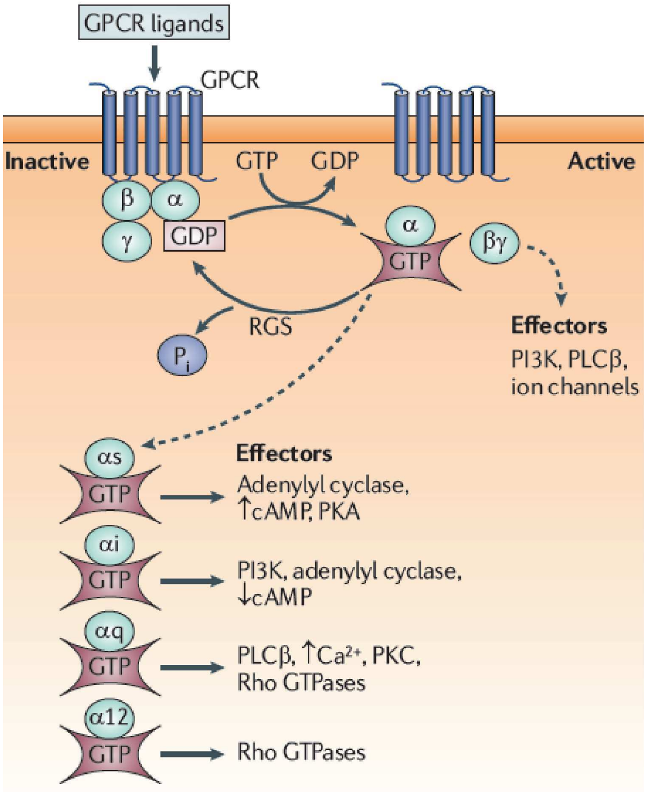
GPCR ligands
GPCR
Inactive
GTP
GDP
Active
β
α
γ
GDP
α
GTP
βγ
RGS
Pi
Effectors
PI3K, PLCβ,
ion channels
αs
GTP
Effectors
Adenylyl cyclase,
↑cAMP, PKA
αi
GTP
PI3K, adenylyl cyclase,
↓cAMP
αq
GTP
PLCβ, ↑Ca2+, PKC,
Rho GTPases
α12
GTP
Rho GTPases

Figure 1.3 Examples for G protein-dependent signalling.

Following agonist activation, GPCRs can couple to different heterotrimeric G proteins, inducing the dissociation of the Gβγ-subunit and the activation of the Gα-subunit. There are four different classes of Gα proteins ($G\alpha_s$, $G\alpha_i$, $G\alpha_q$ and $G\alpha_{12}$) with varying signalling abilities. Typical $G\alpha_s$-signalling involves activation of adenylyl cyclase (AC), which converts ATP to cyclic AMP (cAMP), a second messenger that activates protein kinase A (PKA); $G\alpha_i$-signalling inhibits AC, leading to a decrease in intracellular cAMP levels. Gαi can also induce phosphoinositide 3-kinase (PI3K), leading to activation of the PI3K/Akt/mTOR pathway; $G\alpha_q$ activates PLCβ, which hydrolyses phosphatidylinositol bisphosphate (PIP2) to the second messengers inositol triphosphate (IP_3) and diacylglycerol (DAG). IP_3 binds Ca^{2+}-permeable channels located at the endoplasmic reticulum, increasing intracellular Ca^{2+}-levels. DAG activates protein kinase C (PKC), which phosphorylates several intracellular targets. $G\alpha_q$-signalling can also lead to Rho activation; $G\alpha_{12}$ activates Rho GTPases, leading to structural rearrangements of the cytoskeleton.

Taken from Lappano & Maggiolini (2011).

1.2.5 Desensitisation of G protein-dependent signalling

G protein-dependent signalling through GPCRs can quickly be dampened by a process called receptor desensitization (Ferguson 2001; Lefkowitz 1998). Desensitization means the loss of responsiveness of the GPCR to an ongoing stimulus and serves as a regulatory mechanism to protect the cell against acute and chronic receptor overstimulation. The process is controlled through the phosphorylation of GPCRs by protein kinases such as the second-messenger kinases PKA and PKC or G protein-coupled receptor kinases (GRKs). These kinases phosphorylate serines and threonines within ICL3 and the cytoplasmic tail of GPCRs.

Phosphorylation by second-messenger kinases represents a negative feedback-loop, which leads to the disruption of the GPCR-G protein interaction. Protein kinase-activation by one GPCR can lead to the phosphorylation and subsequent desensitisation of another GPCR (Pierce et al. 2002). Thus, second-messenger kinases can phosphorylate GPCRs independently of agonist activation (Ferguson 2001). However, specific phosphorylation can also lead to the generation of novel G protein binding sites allowing coupling to a different G protein. This was shown for the G_s-coupled β_2AR, where PKA-mediated receptor phosphorylation promotes G_i coupling, thus promoting the activation of a different signalling pathway (Pierce et al. 2002; Daaka et al. 1997).

There are seven different GPCR kinases (GRKs) expressed in human, which are subdivided into three groups: the retinal enzymes GRK1 (rhodopsin kinase) and GRK7 (cone opsin kinase), GRK2 (βAR kinase-1, βARK1) and GRK3 (βARK2), GRK4 (expressed in testis) and the ubiquitously expressed GRK5 and GRK6 (Pitcher et al. 1998; Ferguson 2001). The phosphorylation of GPCRs by GRKs leads to the recruitment of arrestins. There are two groups of arrestins each consisting of two members: visual and cone arrestin (also called arrestin 1 and 4), as well as β-arrestin 1 and 2 (also called arrestin 2 and 3). Expression of visual and cone arrestin is restricted to the retina, whereas the β-arrestins are expressed ubiquitously with high expression levels in neuronal tissue and spleen (Craft et al. 1994; Attramadal et al. 1992; Ferguson 2001). The interaction of arrestins with GPCRs desensitises the receptor as it sterically inhibits further G protein binding, thus terminating G protein-dependent signalling (Pierce et al. 2002). Depending on the GPCR, arrestin binding sites are located in one of the ICLs, as well as the cytoplasmic tail (Cen et al. 2001; Cheng 2000; Wu et al. 1997; Krupnick et al. 1994; DeGraff et al. 2002). In rhodopsin-like receptors, the D(/E)RY motif located in ICL2 was shown to be involved in both G protein and arrestin binding (Marion et al. 2006; Barak et al. 1994).

For a long time, the dogma existed that GRKs only phosphorylate agonist-occupied GPCRs, leading to arrestin-recruitment (Oakley et al. 2001). However, GRKs can phosphorylate GPCRs in the absence of ligand stimulation, which is likely due to the constitutive activity of certain GPCRs that acquire an activated conformation in the absence of agonist (Ferguson 2001). In general, arrestins preferentially bind to agonist-activated and GRK-phosphorylated GPCRs and visual arrestin only binds GRK-phosphorylated rhodopsin (Gurevich et al. 1995). However, there are exceptions, where arrestins bind to agonist-activated, non-phosphorylated receptors, as well as unliganded, but phosphorylated GPCRs. Thus, GRK-phosphorylation increases the affinity of arrestins for the GPCRs, but more important than receptor phosphorylation is a conformational change of the receptor, promoting the interaction with arrestins (Marion et al. 2006; Oakley et al. 2001).

1.2.6 Internalisation of GPCRs

Endocytosis or internalisation of GPCRs is a very important mechanism to regulate GPCR activity. GPCRs can internalise via multiple endocytic mechanisms and receptor internalisation rates, as well as their intracellular trafficking routes can vary enormously (Ferguson 2001).

1.2.6.1 Clathrin-dependent endocytosis

The processes of GPCR desensitisation, including GRK phosphorylation and arrestin binding, are usually followed by GPCR endocytosis. Binding of β-arrestins to GPCRs specifically targets them to endocytosis via clathrin-coated vesicles, as shown for the β_2AR and angiotensin II type 1A receptor ($AT_{1A}R$) (Zhang et al. 1996). β-arrestins directly interact via their cytoplasmic tails with proteins required for the formation of clathrin-coated pits such as the major adaptor protein AP-2 and other components of this machinery (Goodman et al. 1997; Laporte et al. 1999; Laporte et al. 2000). Monomeric clathrin triskelia polymerise and form a coat around the vesicles (“vesicles in a basket”) by binding to the adaptor proteins, but never directly to the membrane or the receptor (Patel et al. 2008). Vesicle budding, the next stage of internalisation, is mediated by the GTPase-activity of dynamin, which is recruited to clathrin-coated pits (Fig. 1.4). However, dynamin action is not restricted to clathrin-coated vesicles (McMahon and Boucrot 2011; Henley et al. 1998). Finally, clathrin detaches from the vesicles and is recycled, whereas the vesicles fuse with early endosomes.

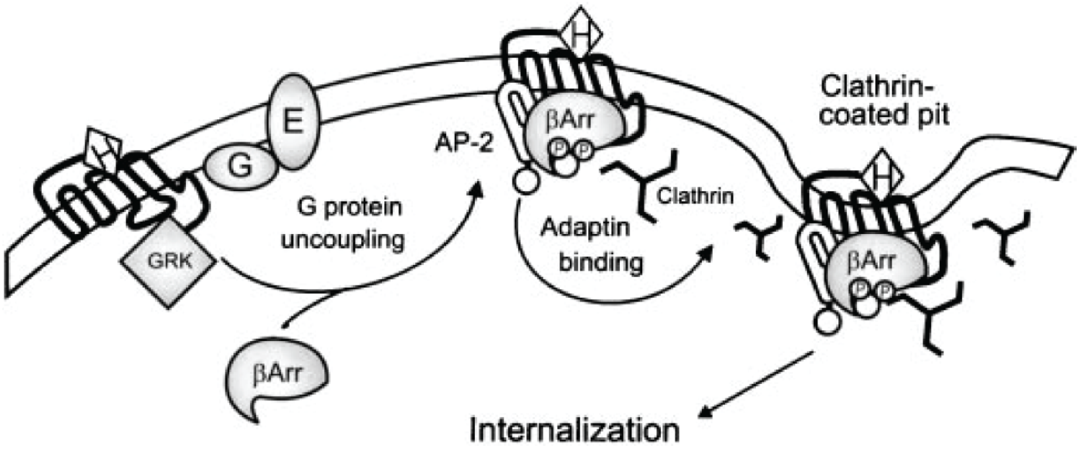

Figure 1.4 Clathrin-dependent endocytosis of GPCRs.

The cytoplasmic tail and ICL3 of agonist-activated GPCRs are phosphorylated by GRKs, leading to binding of β-arrestin to the phosphorylated GPCR. β-arrestin recruits proteins of the clathrin endocytotic machinery, such as the adapter protein AP-2 and clathrin itself that bind to the GPCR and form an intracellular coat. Vesicle budding is followed by pinching off the vesicle, which is mediated by the large GTPase dynamin (not shown).

AP-2, AP-2 heterotetrameric adaptor complex; βArr, β-arrestin; H, hormone; G, G protein; E, enzyme; GRK, GPCR kinase; P, phosphate group; ICL3, intracellular loop 3. Taken from Ferguson (2001).

1.2.6.2 Clathrin-independent endocytosis

Increasing evidence for β-arrestin- and clathrin-independent endocytosis of GPCRs was demonstrated more recently. These mechanisms may even apply for receptors that are usually internalised via clathrin, at least in the presence of a clathrin-inhibitor like a dominant-negative β-arrestin (Zhang et al. 1996). This indicates that some GPCRs can switch the mode of internalisation depending on the cellular environment. The best described alternative route for clathrin-independent endocytosis is internalisation via caveolae. Caveolae are flask- or omega-shaped membrane invaginations (“little caves”) with a diameter of 50-80 nm that can be detected using electron microscopy (Fig. 1.5).

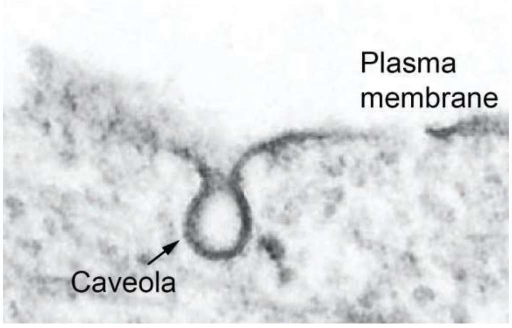

Figure 1.5 Electron microscopy image of a caveola in pulmonary artery smooth muscle cells (8900x).

Taken from Patel et al. 2008, modified.

Caveolae are present in many but not all eukaryotic cells and are marked by the presence of integral membrane proteins belonging to the family of caveolins (cav-1, -2, -3) that serve as scaffolds. Caveolae are rich in hydrophobic cholesterols and glycosphingolipids and are detergent-resistant, thus called non-planar membrane (lipid) rafts (Patel et al. 2008; Kiss and Botos 2009). Caveolae form in golgi and traffick to the cell membrane, where they are anchored to the cytoskeleton by proteins like filamin (Tagawa et al. 2005; Mundy et al. 2002), thus forming quite immobile structures. However, the interaction of cav-1/caveolae with a variety of proteins like receptor tyrosine kinases (RTKs), ion channels or GPCRs triggers their endocytosis.

Caveolae budding and the release from the membrane is regulated by Src-dependent caveolin tyrosine phosphorylation (Kiss and Botos 2009). Caveolins assemble in oligomers and form a cytoplasmic coat located on the invaginations. Similar to internalisation of clathrin-coated pits, dynamin is required for the fission of caveolae by constricting their necks (De Camilli et al. 1995). Once pinched off, caveolae are transported along microtubules into the cytoplasm. The actin cytoskeleton needs to be re-organised, as filamin physically prevents detachment of caveolae from the membrane (Parton et al. 1994). This is achieved by temporary actin depolymerisation (Pelkmans and Helenius 2002).

Caveolae do not exclusively play a role in GPCR endocytosis, but also for GPCR signalling. As part of membrane rafts, caveolae enrich components for GPCR signalling, including GPCRs and G proteins by directly interacting with them. Thus, caveolae bring GPCRs and their downstream effectors into close proximity, facilitating signalling (Patel et al. 2008; Ostrom and Insel 2004).

1.2.6.3 Endosomal sorting

Once internalised, the vesicles fuse with early endosomes and their GPCR cargo is sorted to different endocytic pathways. It was shown that members of the Rab family of small GTPases play important roles in vesicle budding at the cell surface, their transport and fusion with endosomes (Somsel Rodman and Wandinger-Ness 2000). Sorting has partially occurred already at the plasma membrane, as the fate of the GPCR may be influenced by post-translational modifications including phosphorylation or ubiquitination, interactions with proteins such as β-arrestins and the “choice” of the endocytic machinery (e.g. clathrin-dependent/-independent) that can deliver the receptor to different endocytic vesicles (Hanyaloglu and von Zastrow 2008). Nonetheless, the main sorting seems to occur in early endosomes, where interactions with adaptor proteins determine whether GPCRs are recycled or degraded (Hanyaloglu and von Zastrow 2008; von Zastrow 2003; Sorkin and Von Zastrow 2002). The two traffic routes lead to opposite receptor fates, as GPCRs targeted to lysosomes are typically degraded, whereas their recycling to the cell membrane leads to rapid receptor recovery (resensitisation) (Pierce et al. 2002; von Zastrow 2003). Additionally, evidence is accumulating for the initiation of new signalling pathways from GPCRs that remain intact in endocytic vesicles (Fig. 1.6) (Sorkin and von Zastrow 2009; Irannejad et al. 2013).

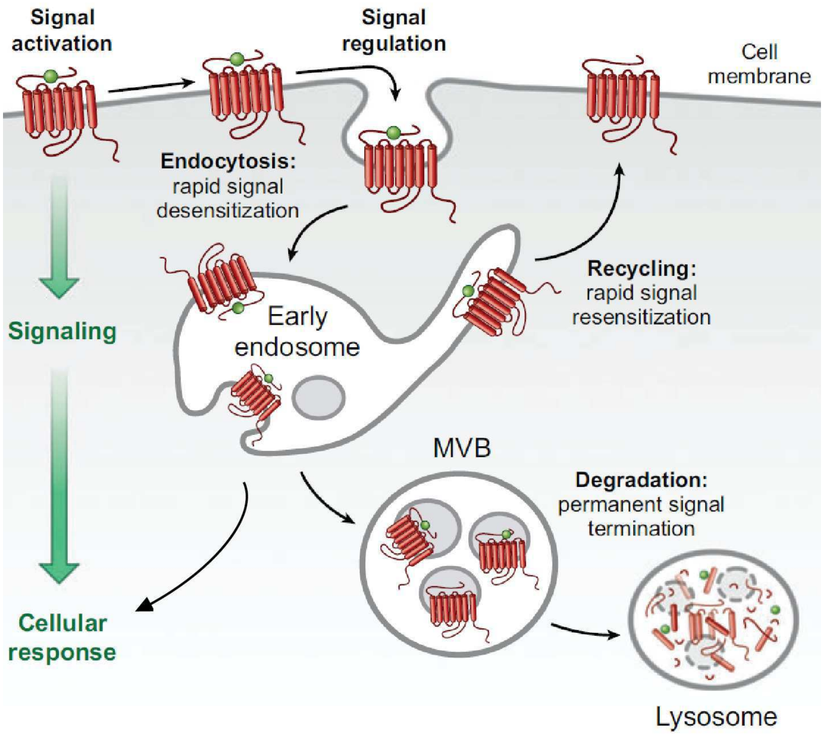
Signal activation
Signal regulation
Cell membrane
Endocytosis:
rapid signal desensitization
Signaling
Early endosome
Recycling:
rapid signal resensitization
MVB
Degradation:
permanent signal termination
Cellular response
Lysosome

Figure 1.6 Sorting of endocytosed GPCRs.

Internalised vesicles containing GPCRs fuse with early endosomes, in which GPCRs are sorted to different intracellular compartments. Sorting to multivesicular bodies (MVBs) and lysosomes leads to proteolytic degradation of the GPCR, whereas the receptor is recycled back to the cell surface, if sorted to recycling endosomes. In addition, intact GPCRs can induce signalling responses from the endosomes. *Taken from Hanyaloglu & von Zastrow 2008, modified.*

For β-arrestin-dependent internalisation, it was shown that variations in the persistence of the GPCR-β-arrestin association affect their intracellular fate. Thus, some GPCRs such as the β_2AR or β_{1B}AR quickly dissociate from β-arrestin near the cell membrane during endocytosis, are dephosphorylated in endosomes and recycle back to the cell surface. These GPCRs are called “class A” receptors. This nomenclature must not to be confused with the original A-F classification scheme regarding the different GPCR families, in which rhodopsin-like GPCRs were called “class A GPCRs” (Kolakowski 1994). The class A and class B receptor nomenclature in the context of internalisation is independent of the GPCR family and does only refer to the strength of the GPCR-β-arrestin interaction, which influences the fate of the endocytosed receptor.

In contrast to β_2AR or β_{1B}AR, vasopressin receptor 2 (V_2R) and the AT_{1A}R internalise complexed with β-arrestin in endocytic vesicles, which prevents GPCR recycling. Instead, the GPCRs are retained in endosomes or targeted to lysosomes. These so called “class B” GPCRs usually contain a cluster of phosphorylated serines or threonines within their C-terminal tail, which reduces β-arrestin dissociation, preventing recycling (Oakley et al. 1999; Ferguson 2001; Hanyaloglu and von Zastrow 2008; Oakley et al. 2001).

Moreover, the intracellular fate of a GPCR changes upon prolonged agonist-stimulation, leading to down-regulation of recycled receptors (e.g. β_2AR), contributing to loss of drug effectiveness (von Zastrow 2001).

The receptor-bound ligand may dissociate from the receptor within endosomes, probably due to the acidic milieu with pH~5, followed by lysosomal degradation. This is also the case if receptor and ligand are transported to lysosomes as a complex. However, other ligands remain associated with the receptor and recycle back to the cell surface in a receptor-ligand complex, such as transferrin and its receptor (Goldstein et al. 1985).

1.2.7 G protein-independent signalling

In addition to their role in desensitisation and internalisation of GPCRs, it is now appreciated that β-arrestins initiate GPCR signalling in their own right. β-arrestins serve as scaffolds and adaptors, connecting the activated and endocytosed GPCR with different signalling pathways (Ferguson 2001; Lefkowitz and Shenoy 2005). This mainly accounts for class B GPCRs, since they show prolonged association with β-arrestins.

The best-studied β-arrestin-dependent signalling mechanism following GPCR endocytosis is activation of mitogen-activated protein kinases (MAPKs). Receptor-bound β-arrestins can recruit and bind non-receptor tyrosine kinases such as c-Src, leading to the activation of a signalling cascade involving MAP kinase kinase kinases (MAP3K such as Raf) that phosphorylate MAP kinase kinases (MAPKKs such as MEK) which in turn phosphorylate MAPKs such as extracellular signal-regulated kinases (ERK1 and ERK2). In case of class B receptors that stably associate and endocytose with β-arrestins, ERK signalling persists for a longer period than in case of class A receptors, which only transiently interact with β-arrestins. In endocytic vesicles, β-arrestins serve as scaffolds for the components involved in ERK1/2 activation, which leads to the formation of a multiprotein complex consisting of the endocytosed GPCR, β-arrestin, Ras, MEK and ERK. This prevents the translocation of ERK1/2 to the nucleus, which inhibits cell proliferation, but enables ERK to phosphorylate cytosolic substrates, inducing protein-translation and anti-apoptotic signals (Ferguson 2001; Lefkowitz and Shenoy 2005) (Fig. 1.7).

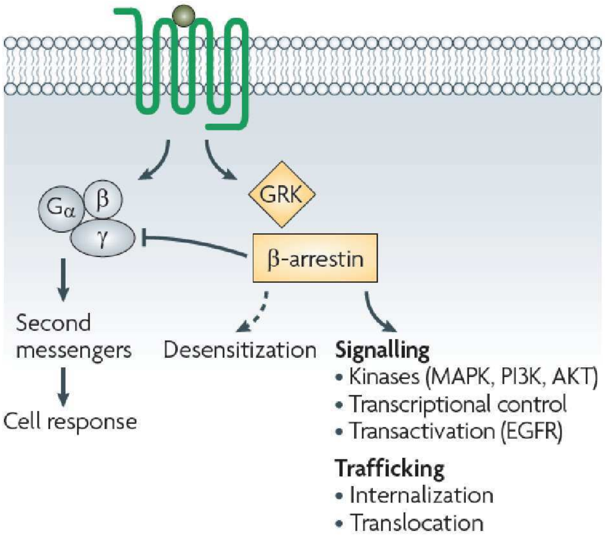
Gα
β
γ
GRK
β-arrestin
Second messengers
Cell response
Desensitization
Signalling
• Kinases (MAPK, PI3K, AKT)
• Transcriptional control
• Transactivation (EGFR)
Trafficking
• Internalization
• Translocation

Figure 1.7 G protein- and β-arrestin-dependent signalling.

Activation of GPCRs can lead to classical G protein-dependent signalling resulting in the production of second messengers, which induce cellular responses. Additionally, activated GPCRs are phosphorylated by GRKs and bind β-arrestins, which leads to receptor desensitisation, thus physically interrupting G protein-dependent signalling. Moreover, β-arrestins induce a couple of downstream signalling pathways in their own right and are also involved in receptor internalisation.

GRK, GPCR kinase; MAPK, mitogen-activated protein kinase, PI3K, phosphoinositide 3-kinase, EGFR, epidermal growth factor receptor.

Taken from Rajagopal et al. (2010).

Following the activation of the $AT_{1A}R$, concurrent recruitment of β-arrestin 1 and activation of $G\alpha_{q/11}$ activates RhoA, which induces stress fiber formation (Barnes et al. 2005). β-arrestins can also directly interact with the inhibitor of NF-κB, IκBα, as well as upstream kinases that regulate the activity of IκB, leading to the inhibition of NF-κB activity (Witherow et al. 2004). Stimulation of the β_2AR enhances the interaction between β-arrestin 2 and IκB and in that way β_2AR modulates NF-κB-dependent transcription (Gao et al. 2004). Additionally, activation of the $G_{i/o}$-coupled receptor GPR109A by nicotinic acid recruits β-arrestin 1, which binds and activates cytosolic phospholipase A2 (Walters et al. 2009; Reiter et al. 2012).

In addition, there are biased ligands for GPCRs that either activate G protein-dependent or β-arrestin-dependent signalling cascades such as ERK-activation (Lefkowitz and Shenoy 2005; Rajagopal et al. 2010).

1.2.8 EGFR transactivation

Agonist-activation of GPCRs can lead to the activation of the ERK/MAPK signalling cascade by transactivating the epidermal growth factor receptor (EGFR), inducing cell proliferation (Daub et al. 1996). The crosstalk between GPCRs and EGFR occurs in non-transformed and transformed cells. It is implicated in processes such as fertilisation, neurogenesis, wound healing, heart development, but also in diseases such as cardiac hypertrophy and cancer, since it promotes cellular functions such as growth, survival, migration and metastasis (Lappano and Maggiolini 2011; Wetzker and Böhmer 2003). Activation of GPCRs leads to intracellular activation of metalloproteinases (MPs) which cleave membrane-tethered growth factors such as the epidermal growth factor (EGF), heparin-binding EGF (HB-EGF), transforming growth factor α (TGFα) or amphiregulin (AR), which activate the EGFR (Fischer et al. 2003; Prenzel et al. 1999). This mechanism is also called “triple-membrane-passing-signalling” (TMPS), since it involves three signalling steps passing the cell membrane (Wetzker and Böhmer 2003). Activation of the EGFR induces EGFR dimerization and intracellular tyrosine auto-phosphorylation by the receptor’s intrinsic kinase activity. The protease-activated receptor 1 (PAR1), the CXC chemokine receptor type 4 (CXCR4), AT_1R, LPA receptors or the endothelian A subtype receptor (ET_AR) all participate in this signalling pathway (Lappano and Maggiolini 2011). MPs cleaving the EGF-like ligands belong to the ADAM (a disintegrin and metalloproteinase) family of zinc-dependent proteases, with ADAM9, 10, 12, 15 and 17 playing a role (Werb and Yan 1998; Ohtsu et al. 2006; Werry et al. 2005). Knockout of ADAM17 in mice is embryonic lethal and resembles mice lacking EGFR or TGFα, as they share the same defects in maturation and morphogenesis of epithelial structures (Peschon et al. 1998). GPCR-dependent EGFR transactivation can be mediated by both G protein- and β-arrestin-dependent signalling. However, especially the signalling mediators downstream of the activated GPCR controlling MP activity are not well characterised (Fig. 1.8).

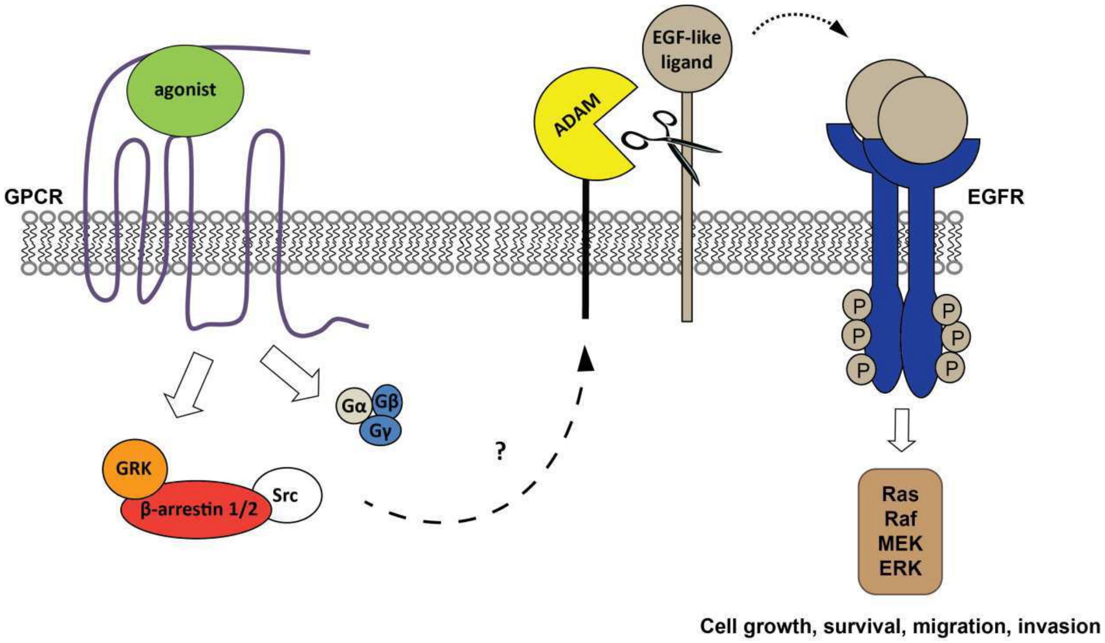

Figure 1.8 GPCR-dependent EGFR transactivation ("triple-membrane-passing-mechanism", TMPS).

The agonist-activated GPCR binds G proteins and is phosphorylated by GRKs, leading to binding of β-arrestins. Second messengers and other signalling mediators activated by G proteins or β-arrestins induce ADAM-activation. The ADAM cleaves the membrane-tethered pro-EGF-like ligand leading to its release and interaction with the EGFR, which is activated by ligand binding. The downstream signalling mechanisms activated by the EGFR induce mitogenic and anti-apoptotic cellular signalling responses.

Early investigations revealed that G_q-and G_i-coupled GPCRs transactivate EGFR in Cos-7 (Faure et al. 1994), HEK293, U373 glioblastoma cells and others (Gschwind et al. 2001). Later, G_{13}-coupled receptors were identified (Gohla et al. 1998; Gohla et al. 1999), while G_s-coupled receptors cannot transactivate EGFRs (Gschwind et al. 2001; Fischer et al. 2003). In response to activation of the G_i-coupled α_{2A}ARs, the dissociated Gβγ-subunit activates c-Src, leading to shedding of HB-EGF by an unidentified ADAM (Pierce et al. 2001). Induction of PLC-signalling through the G_q-coupled AT_1R is required for ADAM17-dependent shedding (Mifune et al. 2005). PKC is well known to activate ADAM17 (Horiuchi et al. 2007; Kveiborg et al. 2011) and AT_1R-

dependent activation of HB-EGF shedding involves PKC and Src in particular cell lines (Shah et al. 2004). In addition, Ca^{2+} and reactive oxygen species (ROS) are good candidates for GPCR-dependent ADAM activation (Ohtsu et al. 2006). Activated LPA-receptors activate ADAM-dependent shedding through Ras/ERK-signalling (Umata et al. 2001).

In contrast, the β_1AR transactivates the EGFR in a β-arrestin dependent manner. In this model, β-arrestin binds the agonist-activated β_1AR, recruits Src which in turn activates an ADAM, inducing cleavage of HB-EGF and activation of the EGFR (Noma and Lemaire 2007). More recently, it was demonstrated that GPCR-dependent EGFR transactivation can also occur in the absence of agonist, due to constitutive GPCR activity. A subtype of the α_{1A}-AR constitutively transactivates EGFR through β-arrestin-coupling and ADAM12/matrix metalloproteinase 7 (MMP7) activation, leading to cell proliferation (Oganesian et al. 2011).

Besides the triple-membrane-passing-mechanism of EGFR transactivation outlined above, there are also some examples for a mode of transactivation that is independent of ADAM-mediated EGFR-ligand shedding. In these cases, several GPCR signalling mediators such as Src, PKC, Ca^{2+}, Ca^{2+}-regulated tyrosine-kinase Pyk2, Ca^{2+}-calmodulin-dependent kinase II (CaMKII) or PI3K were identified (Fischer et al. 2003; Buchanan et al. 2003; Ohtsu et al. 2006). The exact mechanism of transactivation varies, but often involves phosphorylation and activation of the EGFR by Src tyrosine kinase (Werry et al. 2005). Moreover, a direct association between agonist-bound GPCRs and EGFRs leading to second-messenger independent transactivation was demonstrated for AT_1R and β_2AR (Maudsley et al. 2000; Seta and Sadoshima 2003).

1.2.8.1 A disintegrin and metalloproteinases (ADAMs)

A disintegrin and metalloproteinases (ADAMs) are membrane-anchored zinc-dependent proteases that belong to the group of adamalysin proteases, a family of the metzincin superfamily. The family of adamalysins also includes the secreted ADAM-TS (ADAMs with thrombospondin repeats) and class III snake venom metalloproteinases (SVMPs). Matrix metalloproteinases (MMPs) and membrane-type MMPs (MT-MMPs) represent further families within the metzincin clan (Fig. 1.9) (Murphy 2008; Hooper 1994).

22 different ADAMs are expressed in human, some of them are predominantly found in the testis and others broadly in somatic tissues, such as ADAM17 (Wolfsberg et al. 1995; Seals and Courtneidge 2003; Edwards et al. 2008).

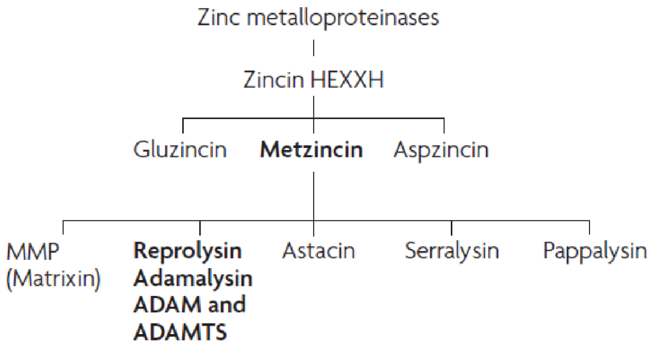
Zinc metalloproteinases
Zincin HEXXH
Gluzincin
Metzincin
Aspzincin
MMP (Matrixin)
Reprolysin Adamalysin ADAM and ADAMTS
Astacin
Serralysin
Pappalysin

Figure 1.9 Classification of zinc metalloproteinases. *Taken from Murphy (2008).* The zinc metalloproteinases comprise 3 superfamilies: the gluzincins, metzincins and aspzincins. The major families within the metzincin superfamily are the matrix metalloproteinases (MMPs), reprolysins (also known as adamalysins, including a disintegrin and metalloproteinases (ADAMs) and ADAMs with thrombospondin repeats (ADAMTS) proteins) and the astacins.

1.2.8.1.1 Structure of ADAMs

ADAMs are multidomain proteins consisting of an extracellular prodomain, a metalloproteinase domain, a disintegrin domain, a cysteine-rich domain and an EGF-like domain, a transmembrane domain and a cytoplasmic domain (Fig. 1.10) (Edwards et al. 2008).

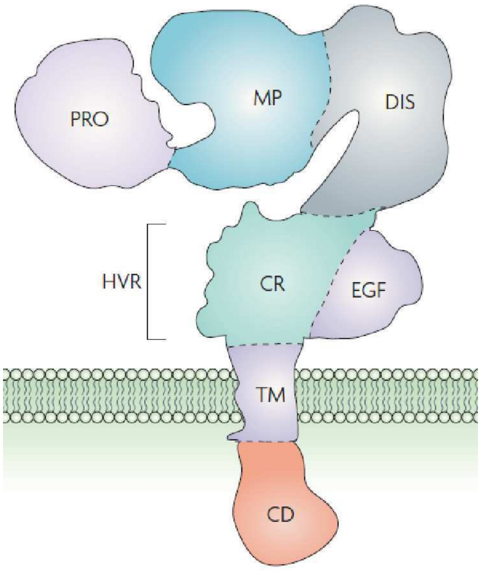

Figure 1.10 Domain structure of the ADAM family. *Taken from Murphy (2008). Pro, prodomain; MP, metalloproteinase domain; DIS, disintegrin domain; CR, cysteine-rich domain; EGF, EGF-like domain; TM, transmembrane domain; CD, cytoplasmic domain; HVR, highly variable region (within cysteine-rich domain).*

The prodomain keeps the metalloproteinase domain in an inactive state by interacting with the active site zinc ion within the catalytic cavity. During maturation in the golgi, the prodomain is cleaved and released from the rest of the protein, which activates the ADAM. The prodomain is required for proper folding of ADAMs and in its absence, catalytically inactive proteases are formed (Seals and Courtneidge 2003).

The metalloproteinase domain is required for the main function of ADAMs, which is the proteolytic shedding of substrates. It comprises the active site, containing the zinc-binding consensus sequence HEXGHXXGXXHD, which is characteristic for the superfamily of metzincins. 13 of 22 human ADAMs contain this catalytic site and are predicted to be proteolytically active, including ADAM10 and 17 (Edwards et al. 2008; Seals and Courtneidge 2003).

The disintegrin domain of ADAMs shows close homology to a domain found in snake venom metalloproteinases (SVMPs), which inhibits integrin-mediated adhesion of platelets to fibrinogen via an Arg-Gly-Asp (RGD) sequence present in a disintegrin loop of SVMPs. However, most ADAMs, except ADAM15, lack the RGD sequence within their disintegrin domain, but contain the consensus motif CRXXXXXCDXXEXC, which is thought to enable binding to integrins (Edwards et al. 2008).

Information on the function of the cysteine-rich and the EGF-like domains of ADAMs is scarce. It was proposed that those domains mediate adhesive interactions (Edwards et al. 2008; Gaultier et al. 2002; Iba et al. 2000). For ADAM10 and 17, the cysteine-rich domain is required for shedding activity (Gaultier et al. 2002), whereas the EGF-like domain is absent in ADAM10 and 17 (Edwards et al. 2008).

The cytoplasmic tails of ADAMs have variable length and sequences. They contain binding sites for Src-homology region 3 (SH3) domain-containing proteins and phosphorylation sites for serine/threonine or tyrosine kinases. Therefore, the cytoplasmic domain represents an important structure for the intracellular signalling function of ADAMs, as it defines interactions with adapter molecules and/or kinases (Poghosyan et al. 2002; Seals and Courtneidge 2003).

1.2.8.1.2 Biological functions of ADAMs

Ectodomain (ECD) shedding of membrane-tethered growth factors, cytokines, receptors and adhesion molecules was demonstrated for several ADAMs (Edwards et al. 2008). Shedding is an important mechanism for cellular signalling by either releasing soluble ECDs of cytokines and growth factors, which then stimulate cells in an autocrine or paracrine manner, or by reducing the amount of membrane-tethered proteins, thus decreasing cellular responsiveness to selected stimuli (Hundhausen et al. 2003). Shedding activity is constitutive, but can also be induced by GPCRs, PKC or Ca^{2+} ionophores (Edwards et al. 2008).

Due to the integrin binding function of the disintegrin domain, an adhesive function was described for many ADAMs (Schlöndorff and Blobel 1999). While family members such as ADAM17 and 10 act as sheddases, others remain “orphan proteases”, because of their unknown functions (Seals and Courtneidge 2003).

Members of the ADAM family are involved in the regulation of many processes such as signal transduction, cell migration, fertilisation, cell-cell communication or cell adhesion (Black and White 1998). Dysregulation of their functions can lead to pathology, including Alzheimer disease, rheumatoid arthritis, asthma or cancer (Kodama et al. 2004; Seals and Courtneidge 2003; Edwards et al. 2008).

1.2.8.1.3 ADAM17

ADAM17 or tumour necrosis factor (TNF)-α-converting enzyme (TACE) was the first member of the ADAM family demonstrating shedding activity towards the EGFR ligand TNF-α and other substrates (Blobel et al. 1992; Black et al. 1997). It was demonstrated that ADAM17 plays a role not only for the activation of TNF-α, but also for signalling through the EGFR during development. ADAM17 knockout mice die shortly after birth and have open eye lids, skin and hair abnormalities, as well as defects in epithelial maturation and in many other organs (Peschon et al. 1998). This phenotype closely resembles the phenotype of mice lacking EGFR or its ligands heparin-binding-EGF (HB-EGF), amphiregulin or transforming growth factor-α (TGF-α), which are also substrates of ADAM17 (Peschon et al. 1998; Blobel 2005; Sternlicht et al. 2005; Jackson et al. 2003). Further ADAM17 substrates are L-selectin adhesion molecule, TNF receptor and the amyloid precursor protein (APP) (Peschon et al. 1998; Buxbaum et al. 1998). The identification of these substrates demonstrated that there is a high variability of sequences cleaved by ADAM17.

1.2.8.1.4 ADAM inhibitors

The four natural tissue inhibitors of metalloproteinases (TIMP1-4) regulate ADAM activity by interacting with their catalytic domain. TIMPs also inhibit MMPs, but have greater selectivity towards ADAMs (Edwards et al. 2008).

The hydroxamate-based compounds GI254023X, which preferentially blocks ADAM10 but not ADAM17, and GW280264X, which inhibits both ADAM10 and 17, were used to demonstrate that ADAM10 is involved in the constitutive shedding of interleukin-6 receptor and the transmembrane chemokine CX3CL1 from the cell surface, whereas ADAM17 mediates phorbol-12-myristate-13-acetate (PMA)-stimulated shedding (Hundhausen et al. 2003; Ludwig et al. 2005). Synthetic ADAM inhibitors represent promising therapeutic agents for the treatment of different diseases. ADAM10 is involved in shedding of the human epidermal growth factor receptor 2 (HER2) and is an interesting target for anti-cancer therapies. Several selective ADAM17 inhibitors are in clinical trials for the treatment of rheumatoid arthritis, since ADAM17 plays a central role in TNF-α shedding (Moss et al. 2008; Edwards et al. 2008). Another ADAM10/17 inhibitor was shown to reduce tumour growth by inhibiting the shedding of the EGFR ligands HB-EGF, amphiregulin and TGF-α (Fridman et al. 2007).

1.3 Adhesion GPCRs

1.3.1 Structure of adhesion GPCRs

The family of adhesion GPCRs (aGPCRs) is, with 33 members, the second largest family of GPCRs in the human genome and can be further subdivided into nine groups (I-IX), based on the phylogenetic relationship between the 7TM-domains (Fig. 1.11) (Langenhan et al. 2013). Group I contains the lectomedin receptors (LEC1-3) that are often called latrophilins, group II contains the EGF-like module containing mucin-like receptors (EMR1-3), GPR127 and the cell differentiation antigen receptor (CD97), group III contains GPR123-125, group IV contains the cadherin, EGF LAG seven-pass G-type receptors (CELSR1-3), group V contains GPR133 and GPR144, group VI contains GPR110-116, group VII contains brain angiogenesis inhibitor receptors (BAI1-3), group VIII contains GPR56, GPR97, GPR112, GPR114, GPR126, GPR128 and human epididymal gene product 6 (HE6) and group IX consists of the very large GPCR (VLGR1) (Bjarnadóttir et al. 2004; Lagerström and Schiöth 2008; Langenhan et al. 2013).

Structurally, aGPCRs contain an unusually long extracellular N-terminus that is linked to the 7TM-domain via a GPCR proteolytic site (GPS)-containing stalk region. The long N-termini are often highly glycosylated and may contain structural motifs such as EGF-like, immunoglobulin-like, cadherin-like, leucine-rich or thrombospondin-like repeats that are known to be involved in cell-cell contacts or cell-matrix adhesion. Therefore, aGPCRs likely play dual roles in adhesion and signalling (Fig. 1.11) (Yona et al. 2008; Araç, Boucard, et al. 2012).

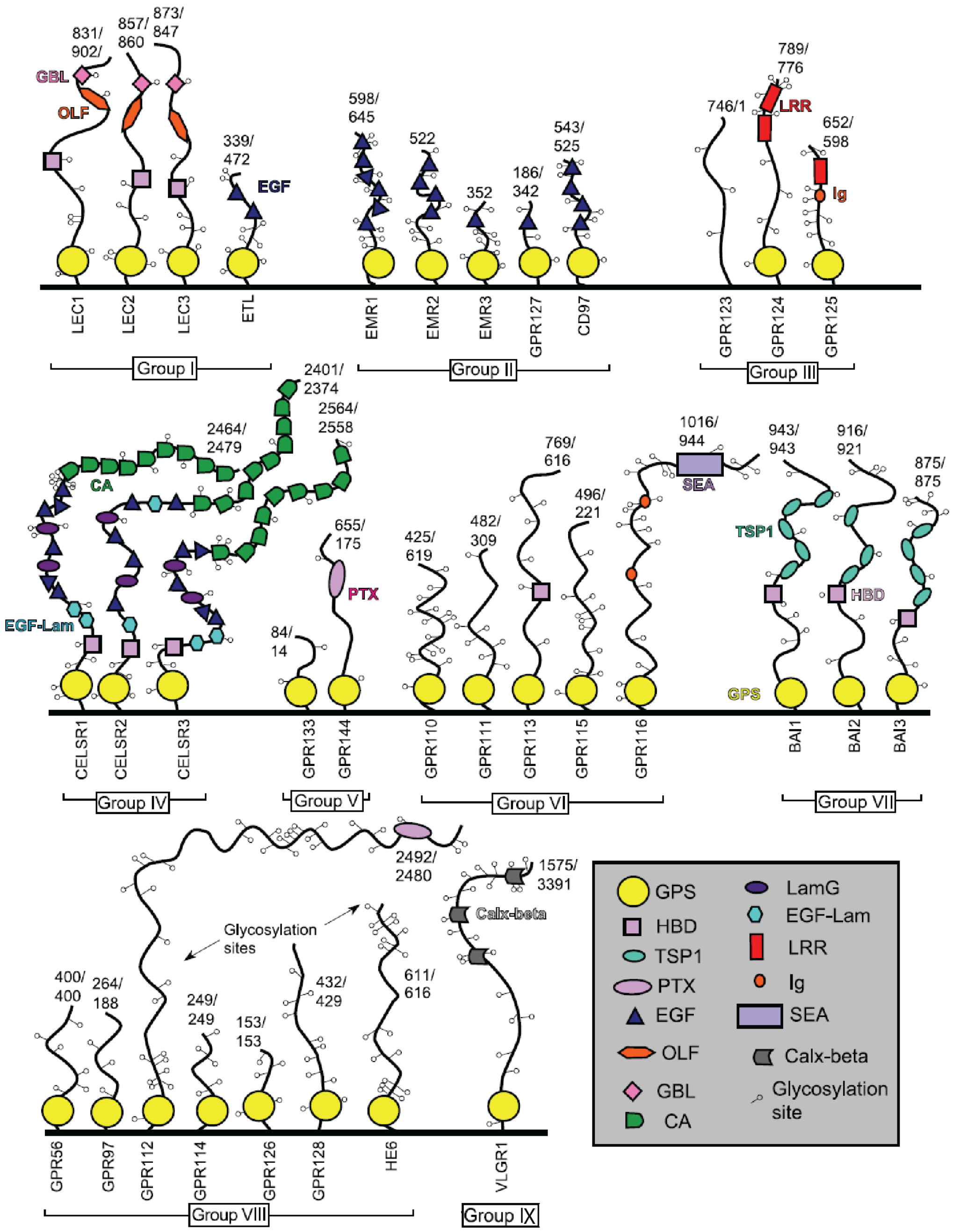
831/ 902/
857/ 860
873/ 847
GBL
OLF
339/ 472
EGF
598/ 645
522
352
186/ 342
543/ 525
746/1
789/ 776
LRR
652/ 598
Ig
LEC1
LEC2
LEC3
ETL
EMR1
EMR2
EMR3
GPR127
CD97
GPR123
GPR124
GPR125
Group I
Group II
Group III
2401/ 2374
2564/ 2558
2464/ 2479
CA
EGF-Lam
655/ 175
PTX
84/ 14
425/ 619
482/ 309
769/ 616
496/ 221
1016/ 944
SEA
943/ 943
916/ 921
875/ 875
TSP1
HBD
GPS
CELSR1
CELSR2
CELSR3
GPR133
GPR144
GPR110
GPR111
GPR113
GPR115
GPR116
BAI1
BAI2
BAI3
Group IV
Group V
Group VI
Group VII
2492/ 2480
1575/ 3391
Calx-beta
Glycosylation sites
400/ 400
264/ 188
249/ 249
153/ 153
432/ 429
611/ 616
GPR56
GPR97
GPR112
GPR114
GPR126
GPR128
HE6
VLGR1
Group VIII
Group IX
GPS
HBD
TSP1
PTX
EGF
OLF
GBL
CA
LamG
EGF-Lam
LRR
Ig
SEA
Calx-beta
Glycosylation site

Figure 1.11 Schematic representation of the extracellular N-terminal domains of the 33 human adhesion GPCRs as predicted by RPS-BLAST at NCBI.

GPS, GPCR proteolytic site; domains: EGF, epidermal growth factor; HBD, hormone-binding domain; Ig, immunoglobulin; OLF, olfactomedin; GBL, galactose-binding lectin; CA, cadherin; LamG, laminin G; LRR, leucine-rich repeats, SEA, sea urchin sperm protein, enterokinase and arginine; TSP, thrombospondin; PTX, pentraxin; Numbers at the end of N-termini indicate the number of amino acids found in the N-termini from the predicted start at TM1.

Taken from Bjarnadóttir et al. (2004).

1.3.2 GPS cleavage and the GAIN domain

The GPS domain was originally identified in the calcium-independent receptor of latrotoxin-1, called CIRL-1, latrophilin-1, CL-1 or LEC-2 (Krasnoperov et al. 1999; Araç, Aust, et al. 2012). The GPS domain is located proximal to the first TM-helix, at the end of the N-terminal extracellular region and is ~40 aa long. It contains conserved cysteine and tryptophan residues and cleavage occurs between a leucine and a threonine, serine or cysteine residue (H-L|T/S/C) (Araç, Boucard, et al. 2012). Self-catalytic (*cis*-autoproteolytic) GPS cleavage occurs early during GPCR biosynthesis in the endoplasmic reticulum (ER) and produces two independent proteins, an N-terminal and a C-terminal domain. Recent investigation of the aGPCRs latrophilin-1 and brain angiogenesis inhibitor 3 (BAI3) revealed that the GPS motif is part of a larger domain, the GPCR-Autoproteolysis INducing (GAIN) domain, previously called stalk region (Araç, Boucard, et al. 2012). It is now known that the GAIN domain is ~320 aa long, conserved in all 33 human aGPCRs and five human polycystic kidney disease (PKD) proteins, 11-pass membrane proteins that are not GPCRs.

Experiments with latrophilin-1 mutants showed that deletion of the GAIN domain except for the GPS motif abolishes autoproteolysis. Therefore, the GPS motif is not functional by itself and is probably unfolded when expressed in the absence of the GAIN domain. The presence of the entire GAIN domain is both required and sufficient for GPCR autoproteolysis (Araç, Boucard, et al. 2012). Despite the cleavage event, several aGPCRs, such as latrophilin-1 and -3 or GPR56 were shown to remain associated as heterodimers at the cell surface, thus the N-terminal domain does not dissociate (Araç, Boucard, et al. 2012; Xu et al. 2006). The GAIN domain seems to play an important role in this process, since it forms non-covalent interactions with the secondary structure comprising the GPS cleavage site, generating a tightly associated heterodimer. In addition to its autoproteolytic functions, the GAIN domain can also serve as a ligand binding domain, as shown for the GAIN domain of latrophilin-1 and its binding partner α-latrotoxin (Araç, Boucard, et al. 2012).

Mutations within the GAIN domain of the transmembrane protein PKD1 abolish autoproteolysis and cause autosomal-dominant polycystic kidney disease (ADPKD) (Qian et al. 2002). Mutations within the GAIN domains of aGPCRs are associated with a variety of diseases, including bilateral frontoparietal polymicrogyria (BFPP) for GPR56 (Piao et al. 2004), attention-deficit/hyperactivity disorder for latrophilin-3 (Arcos-Burgos et al. 2010), Usher syndrome 2 for very large GPCR-1 (VLGR1) (Ebermann et al. 2009) or cancer for latrophilin-1/-3 and BAI3 (Kan et al. 2010). Cancer-inducing mutations in the GAIN domains of latrophilin-1 and -3 do not affect autoproteolysis or cell surface localisation. Thus, the cancer-mutations may interfere with other functions of the GAIN domain, such as the regulation of GPCR signalling through interaction of the GAIN domain with the 7TM-domain or ligand binding (Araç, Boucard, et al. 2012; Araç, Aust, et al. 2012)

1.3.3 Physiological functions of adhesion GPCRs

1.3.3.1 De-orphanised adhesion GPCRs

Most aGPCRs are still considered to be orphan GPCRs, which means that their ligand and physiological functions are unknown. The first de-orphanised aGPCR was CD97, which binds the complement regulatory protein decay accelerating factor (CD55 or DAF) (Hamann et al., 1996; Lin et al., 2001). In addition, CD97 and the closely related receptor EGF-like module containing mucin-like receptor protein 2 (EMR2) were found to bind the extracellular matrix (ECM) component chondroitin sulphate, a glycosaminoglycan (Stacey et al., 2003; Kwakkenbos et al., 2005). Latrophilin-1 binds the neurotoxin α-latrotoxin (Krasnoperov et al. 1997) and a splice variant of the transmembrane protein teneurin-2, Lasso, its endogenous ligand in rat brain (Silva et al., 2011). Fibronectin leucine-rich repeat transmembrane protein 3 (FLRT3) is an endogenous ligand for latrophilin-3 (Sullivan et al. 2012). BAI1 expressed on macrophages binds phosphatidylserine on apoptotic cells (Park et al. 2007). Finally, GPR56 binds tissue transglutaminase 2 (Xu et al. 2006) and collagen III, components of the ECM (Luo et al. 2011).

1.3.3.2 Adhesion GPCRs in immunology

Several aGPCRs play active roles in the immune system. The EGF-7TM receptors CD97 and EMR1-4 are predominantly expressed in leucocytes and involved in several aspects of leucocyte development and activation, which play a role in the activation phase of an inflammatory response (Yona et al. 2008). Whereas expression of EMR1 in human is restricted to eosinophils, EMR2-4 are more ubiquitously expressed in myeloid leucocytes such as monocytes, neutrophils, dendritic cells and macrophages. Additionally, CD97, the leucocyte activation antigen, is also expressed in smooth muscle cells, as well as activated T and B cells. Interactions of the closely related EMR2 and CD97 with chondroitin sulfate play a role in myeloid cell migration during inflammation, whereas binding of CD97 to CD55 co-stimulates T cells during the adaptive immune response (Yona et al. 2008; Yona and Stacey 2010). BAI1 is expressed on macrophages and binds phosphatidylserine on the plasma membrane of apoptotic cells. This interaction induces the clearance of apoptotic cells by phagocytosis, which occurs during the subsequent resolution phase of the inflammatory response (Park et al. 2007). Other aGPCRs are also expressed in leucocytes such as GPR56, which is found in CD56$^+$ natural killer cells (NK cells) present in peripheral blood and inflamed tissues, as well as GPR97 in whole blood. Thus, it is likely that more aGPCRs play a role in immunology then previously appreciated (Della Chiesa et al. 2010; Yona et al. 2008).

1.3.3.3 Adhesion GPCRs in embryonic developmental

The most extensively studied aGPCRs in embryonic development are the members of the 7TM-cadherin subfamily (Celsr/Flamingo/Starry night).

CELSR1-3 are found in mammals, whereas Flamingo or Starry night is the CELSR1 homologue in *Drosophila melanogaster*. The extracellular domain of 7TM-cadherins contains nine cadherin-repeats and a combination of EGF-like and laminin G-like domains (Hulpiau and van Roy 2009). Studies of *Drosophila* embryogenesis showed that Flamingo is involved in the formation of the nervous system and in the regulation of tissue polarity, which is important during wing and eye development. Planar cell polarity (PCP) describes the coordinated polarity of cells or tissue, either with neighbouring cells or along an embryonic axis. Flamingo functions in the PCP-signalling cascade and a “Flamingo bridge” model was proposed, in which Flamingo senses activity of the GPCR Frizzled between neighbouring cells and acts with Frizzled to propagate polarising information (Yona and Stacey 2010; Lawrence et al. 2007). Latrophilins are structurally related to the 7TM-cadherin family and studies in *C.elegans* revealed a role of latrophilin-1 in the generation of anterior to posterior cell polarity during embryogenesis (Langenhan et al. 2009). Analysis of Wnt/Frizzled-signalling in *C.elegans* embryos showed that multiple parallel Wnt signals are required for the transmission of the polarising information and latrophilin-1 might be involved in the propagation of these signals (Rocheleau et al. 1997; Schlesinger et al. 1999).

1.3.3.4 Adhesion GPCRs in the CNS

In rodents, 17 out of 30 aGPCRs are expressed in the central nervous system (CNS) and investigations showed that BAI1-3, CELSR1-3, latrophilin-1-3, VLGR1 and GPR56 play important roles in the CNS of mice and human (Yona and Stacey 2010).

Whereas latrophilin-2 is expressed more ubiquitously, latrophilin-1 and -3 are predominantly expressed in the brain and are associated with synaptic cell adhesion and cell signalling in the CNS (Matsushita et al. 1999). BAI1-3 are almost exclusively expressed in embryonic and adult brain, where they are likely involved in angiogenesis and neuronal differentiation (Kee et al. 2004;

Koh et al. 2001). CELSR1-3 are expressed broadly within the developing CNS. CELSR1 is mostly found in the ventricular zone, whereas CELSR3 is expressed in the cortical plate. CELSR2 is found in the entire developing cerebral cortex (Shima et al. 2002). CELSR2 and 3 are activated through homophilic interactions and it was shown that they have opposite effects during neurogenesis. Whereas CELSR2 enhances neurite growth, CELSR3 suppresses it (Shima et al. 2007). During embryonal neurogenesis, VLGR1 is strongly expressed in the CNS (Weston et al. 2004). VLGR1 is involved in the normal development of auditory hair bundles and mutations in VLGR1 are associated with Usher syndrome 2, causing blindness and deafness (McMillan et al. 2002). In brain, GPR56 is expressed in the cerebral cortex, ventricular and subventricular zones and rostral cerebellum during CNS development and mutations in GPR56 are associated with the brain malformation BFPP, which will be discussed in detail in a later chapter (Li et al. 2008; Koirala et al. 2009; Piao et al. 2004; Bai et al. 2009; Jeong et al. 2013; Iguchi et al. 2008).

1.3.4 Signalling by adhesion GPCRs

The large amount of orphan receptors in the aGPCR family is one reason for the lack of evidence of G protein-dependent signalling. Another explanation is the complicated structure of aGPCRs, with their variable N-termini and the existence of two independent proteins upon GPS cleavage, which may interact independently of each other and may even cross-interact with other aGPCRs. The 7TM of latrophilin-1 interacts not only with its own N-terminus, but also with that of EMR2 or GPR56 (Silva et al. 2009). Thus, binding of α-latrotoxin to the N-terminus of latrophilin-1 could activate GPR56-dependent signalling, indicating the complexity of aGPCR signal transduction (Yona and Stacey 2010). Finally, alternative splicing of aGPCRs, such as CD97, EMRs and GPR56 result in naturally occurring splice variants that may activate different downstream signalling pathways (Kwakkenbos et al. 2004; Kim et al. 2010).

For some aGPCRs, G protein-dependent signalling was demonstrated. α-latrotoxin binds to latrophilin-1, inducing Ca^{2+}-signalling and transmitter release from synaptosomes. Latrophilin-1 associates with $G\alpha_o$ and $G\alpha_q$ and it is likely that it induces $G\alpha_q$/Gβγ-dependent PLCβ activation, leading to Ca^{2+}-mobilisation and neurotransmitter release (Lelianova et al. 1997; Davletov et al. 1998; Rahman et al. 1999). Moreover, GPR56 forms a complex with the tetraspanins CD81/9 and $G\alpha_q$ and inhibits neural progenitor signalling via coupling to $G\alpha_{12/13}$ leading to RhoA activation (Little et al. 2004; Iguchi et al. 2008). On the other hand, BAI1, GPR124 and GPR125 interact with the PDZ (**P**SD-95, **D**lg, **Z**O-1/2)-domains of intracellular proteins via an xTxV motif in their cytoplasmic tails, indicating G protein-independent signalling by aGPCRs (Lagerström et al. 2007; Shiratsuchi et al. 1998; Yona et al. 2008). Moreover, binding of phosphatidylserine to BAI1 induces the interaction of BAI1 with the ELMO1-DOCK180 (**e**ngu**l**fment and cell **mo**tility 1 & **d**edicator **o**f **c**yto**k**ines) complex and the small GTPase Rac, promoting phagocytosis of apoptotic cells (Park et al. 2007).

1.3.5 Adhesion GPCRs in tumorigenesis

Several aGPCRs are aberrantly expressed on cancer cells and involved in processes such as angiogenesis, migration and invasion. GPR124, a tumour endothelial marker, interacts with glycosaminoglycans (GAGs) and integrin $\alpha_v\beta_3$, mediating endothelial survival and tumour angiogenesis (Carson-Walter et al. 2001; Vallon and Essler 2006). EMR2 is overexpressed in invasive breast cancer cells (Davies et al. 2011) and mediates adhesion and migration in glioblastoma cells. High expression levels of EMR2 are correlated with poor overall survival in glioblastoma patients (Rutkowski et al. 2011). CD97 expression at the front of many different cancer cells is associated with tumour invasion. Overexpression of CD97 promotes tumour growth in immunodeficient mice, stimulates cell motility, increases the metalloproteinase activity of MMPs and the secretion of chemokines. These effects can increase the invasion capacity of tumours (Galle et al. 2006).

Additionally, CD97 acts as a pro-angiogenic factor by interacting with $\alpha_5\beta_1/\alpha_v\beta_3$ integrins on endothelial cells, which promotes endothelial cell migration and invasion (Wang et al. 2005). BAIs are involved in the regulation of brain tumour progression and BAI1 inhibits angiogenesis by binding $\alpha_v\beta_5$ integrin on endothelial cells, inhibiting their proliferation (Nishimori et al. 1997; Koh et al. 2004; Yona et al. 2008). BAI1 expression levels are decreased in glioblastoma and overexpression of BAI1 impairs glioma angiogenesis. Therefore, BAI1 represents a biomarker for high grade gliomas (Kee et al. 2004; Kaur et al. 2003). GPR56 is down-regulated in highly metastatic melanoma cells and its expression inhibits tumour growth and metastases, likely through interaction with TG2 (Xu et al. 2006; Yang et al. 2014). However, GPR56 is overexpressed in glioblastoma and might promote cell adhesion and signalling (Shashidhar et al. 2005). The role of GPR56 in cancer will be discussed in detail in one of the following sections.

1.4 GPR56

1.4.1 Expression of GPR56

The *Gpr56* gene (also called TM7XN1) consists of 14 exons, is located on chromosome 16q13 and was initially cloned by two groups that isolated the gene from a human heart cDNA library (Liu et al. 1999) and a human melanoma metastasis model (Zendman et al. 1999), respectively. The two identified genes are 98% identical, but differ by an insertion of six amino acids in ICL1 (Terskikh et al. 2001). Thus, Zendman et al. (1999) likely identified the natural occurring splice variant $\Delta_{430\text{-}35}$-GPR56, whereas Liu et al. (1999) isolated the gene encoding wild type GPR56.

GPR56 is ubiquitously expressed in human tissues, with moderate mRNA expression levels in kidney, prostate, testis and weak expression in bladder, lung, thyroid gland, uterus and brain (Zendman et al. 1999). Liu et al. (1999) presented slightly different results with the highest expression of GPR56 mRNA in thyroid gland and lower expression levels in brain, heart, kidney, pancreas, testis and skeletal muscle. Analysis of GPR56 protein expression revealed very low expression levels in human lung, liver and adult brain (Shashidhar et al. 2005). In mouse, high levels of GPR56 protein were detected in kidney and pancreas, medium levels in liver, spleen, ovary, uterus and brain and low levels in heart and lung (Huang et al. 2008).

1.4.2 Structure of GPR56

GPR56 full-length protein consists of 693 amino acids, with a molecular weight of ~75 kDa and has a predicted three-dimensional structure typical for aGPCRs (Fig. 1.12). During protein maturation, GPR56 is cleaved in the ER, resulting in an N- and C-terminal domain. Cleavage occurs at the GPS site between aa382/383 that is located within the GPS domain (aa343-394). The long, extracellular N-terminus (aa26-382) is highly N-glycosylated at seven Asn-residues and contains a serine, threonine, proline (STP)-rich domain (aa108-177), forming a mucin-like stalk that is ~ 65 kDa in size. The C-terminus consists of the 7TM-domains (aa383-657) and the short, cytoplasmic C-terminal tail (aa658-693), resulting in a ~25 kDa protein (Xu et al. 2006; Jin et al. 2007; Huang et al. 2008; Chiang et al. 2011).

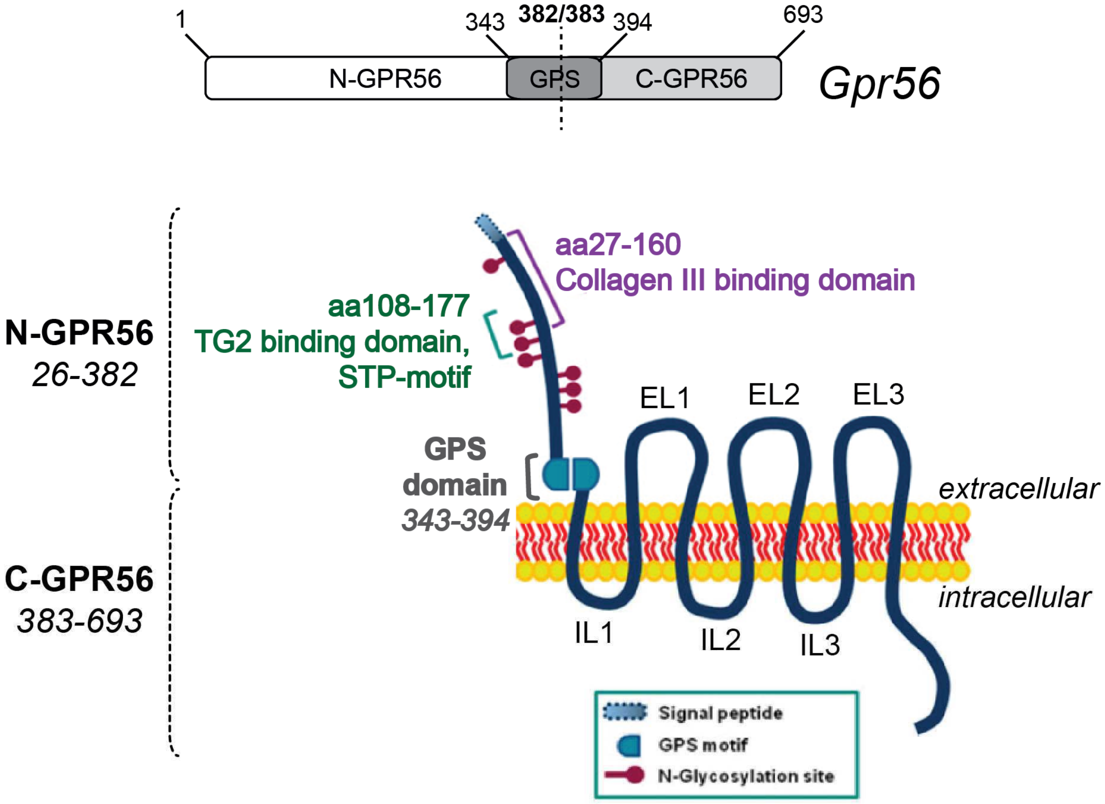
1
343
382/383
394
693
N-GPR56
GPS
C-GPR56
Gpr56
N-GPR56
26-382
C-GPR56
383-693
aa27-160
Collagen III binding domain
aa108-177
TG2 binding domain,
STP-motif
GPS
domain
343-394
EL1
EL2
EL3
extracellular
intracellular
IL1
IL2
IL3
Signal peptide
GPS motif
N-Glycosylation site

Figure 1.12 GPR56 gene and schematic protein structure.

GPR56 consists of an N-terminal domain containing two partially overlapping ligand binding sites for collagen III and TG2, 7 N-glycosylation sites and the GPS motif that separates N-GPR56 from C-GPR56 upon cleavage. C-GPR56 consists of the 7TM-domain and the short intracellular tail.

Taken from Singer et al. (2012), modified.

1.4.3 GPR56 interaction partners and potential ligands

Firstly, Little et al. (2004) reported the identification of the tetraspanins CD81 and CD9, forming a membrane-spanning complex with GPR56 that intracellularly couples Gα_q, without performing any signalling studies. Later, Xu et al. (2006) demonstrated the interaction of N-GPR56 with mouse tissue transglutaminase (mTG2), a component of the extracellular matrix. The TG2 binding site was identified between aa107-177 of N-GPR56 (Yang et al. 2011). However, a potential mechanism of signal transduction due to the GPR56-TG2 interaction was not presented. Yang et al. (2014) showed that GPR56 antagonises the tumorigenic effect of exogenous TG2 in melanoma MC-1 cells by GPR56-dependent internalisation of TG2, likely leading to lysosomal degradation of both GPR56 and TG2. Additionally, an unknown ligand was identified in the pial basement membrane (BM) of the developing mouse cerebral cortex and deletion of aa93-143 in an N-GPR56-Fc probe completely abolished ligand binding (Li et al. 2008). This ligand was identified as collagen III, another component of the ECM, present in the pial BM of the developing brain (Luo et al. 2011). Collagen III induces GPR56-dependent RhoA activation and inhibits migration of neural progenitor cells (NPCs) (Luo et al. 2011). Further analysis of the ligand binding site revealed that collagen III binds to aa27-160 within N-GPR56. In addition, an N-GPR56-Fc probe failed to bind to *Col3a1*$^{-/-}$ mouse brains, suggesting that the ligand of GPR56 in brain is indeed collagen III (Luo et al. 2012).

1.4.4 GPR56 in brain development

Although many of the known aGPCRs are expressed in the central nervous system (CNS), GPR56 is the only one that was associated with a developmental brain malformation in humans, which is called bilateral frontoparietal polymicrogyria (BFPP). BFPP is caused by mutations in GPR56 and *Gpr56* knockout mice display a similar cobblestone-like cortical malformation (Piao et al. 2004; Li et al. 2008; Bahi-Buisson et al. 2010).

BFPP is an autosomal-recessive hereditary disorder and the brains of patients are characterised by numerous, abnormally small gyri (folds) in the frontal and parietal lobes, as well as hypoplasia of cerebellum and pons (Piao et al. 2004; Li et al. 2008; Piao et al. 2005). BFPP patients show mental retardation, language impairment, motor development delay, seizures, ataxia and severe epilepsy (Chiang et al. 2011; Jin et al. 2007; Piao et al. 2004; Li et al. 2008).

25 mutations within *Gpr56* associated with BFPP were identified, including missense, splicing and frameshift mutations (Piao et al. 2004; Quattrocchi et al. 2013; Singer et al. 2012; Fujii et al. 2013). 18 mutations are located in extracellular domains, including the N-terminus, the GPS-domain and ECLs of the receptor and only 7 of them are found in the 7TM-region. Similar to the frameshift and splicing mutations, the missense mutations located in the extracellular domains of GPR56 cause BFPP, indicating loss-of-function of the mutant receptors (Ke et al. 2008; Bahi-Buisson et al. 2010; Singer et al. 2012; Quattrocchi et al. 2013). The two missense mutations within the GPS-domain, $W_{349}S$ and $C_{346}S$, impair GPS-cleavage and cause a trafficking defect of GPR56, as the receptors largely remain in the ER (Jin et al. 2007; Ke et al. 2008). This indicates the importance of GPS-cleavage for GPR56 trafficking, as shown for other aGPCRs (Krasnoperov et al. 2002), but it is not the general rule as evolutionary loss of the GPS cleavage site does not affect the function of aGPCRs belonging to the subfamilies of EMR, CELSR or BAI receptors (Prömel et al. 2012). Moreover, in contrast to BAI3 endogenously expressed in neurons, in HEK293 cells ectopically expressed BAI3 in not cleaved, but still efficiently transported to the cell membrane (Araç, Boucard, et al. 2012). However, the N-terminal GPR56 missense mutations ($R_{38}Q$, $R_{38}W$, $Y_{88}C$, $C_{91}S$) result in reduced cell surface expression caused by protein misfolding and impaired intracellular trafficking (Jin et al. 2007; Chiang et al. 2011).

A crucial event for the development of a cobblestone cortex, as observed in BFPP patients, is a defective pial basement membrane (BM), a specialised extracellular matrix (ECM) overlying the surface of the developing brain. This is accompanied by abnormal neural migration. Although GPR56 expression is almost undetectable in adult brain (Shashidhar et al. 2005), GPR56 is highly expressed in neural stem and progenitor cells, localised in the ventricular and subventricular zones of the developing mouse and human fetal brain (Piao et al. 2004; Iguchi et al. 2008; Bai et al. 2009). During development and differentiation, the neural stem and progenitor cells lose GPR56 expression (Bai et al. 2009). In mice, GPR56 is expressed at the cell surface of neural progenitor cells (NPCs) from embryonic day 13 till postnatal day 7 (Iguchi et al. 2008; Piao et al. 2004). GPR56 overexpression inhibits NPC migration from neurospheres. In NIH/3T3 cells, GPR56 overexpression induces Rho-dependent F-actin reorganisation and stress fiber formation. Additionally, GPR56 overexpression in HEK293 cells activates transcription through SRE- and NF-κB-responsive elements in a $G\alpha_{12/13}$ and Rho-dependent manner, which is elevated by treatment with anti-N-GPR56 antibody (Iguchi et al. 2008). In summary, GPR56 negatively regulates migration of NPCs by activating Rho signalling via $G\alpha_{12/13}$.

During cortical development, NPCs migrate along radial glial fibers from the ventricular zone to the cortical plate, a process called radial migration. Thus, inhibition of NPC migration mediated by GPR56 might be involved in brain development, since terminating signals in radial migration are important for proper lamination of the cortex (Iguchi et al. 2008).

The ECM component collagen III was identified as the major ligand for GPR56 in the developing mouse brain that is present in meningeal fibroblasts, the meninges and pial BM (Luo et al. 2011). *Col3a1*$^{-/-}$ mice develop cobblestone lissencephaly as observed in *Gpr56*$^{-/-}$ mice (Jeong et al. 2012). Additionally, collagen III treatment inhibits migration of NPCs. Collagen III activates RhoA in a GPR56- and $G\alpha_{12/13}$-dependent manner in NIH/3T3 cells and NPCs (Luo et al. 2011), similar to what was shown for the anti-N-GPR56 antibody (Iguchi et al. 2008).

Taken together, GPR56 likely plays an important physiological role in the regulation of the pial BM integrity by binding collagen III in the ECM during cortical development, thus regulating the migration of NPCs and neurons.

1.4.4.1 GPR56 knockout mice

Analysis of *Gpr56*$^{-/-}$ mice showed that loss of GPR56 expression results in a disruption of the pial BM accompanied by neuronal progenitors migrating through the breaches in the defective BM during early brain development, causing the cobblestone-like brain malformation observed in BFPP patients (Li et al. 2008). GPR56 is expressed in NPCs in murine fetal forebrain. Radial glial cells, a special type of neural progenitors, attach via their end feet to the pial BM. GPR56 is expressed at the cell surface of these end feet and binds to collagen III in the pial BM (Li et al. 2008; Luo et al. 2011). The defects in the pial BM observed in *Gpr56*$^{-/-}$ mice lead to an abnormal anchorage of the radial glial end feet that extend beyond the pial surface, which is accompanied by overmigrating neurons (Li et al. 2008).

Analysis of the brain defects in adult *Gpr56*$^{-/-}$ mice revealed a malformation of the rostral cerebellum that becomes evident at perinatal age and only in regions where GPR56 is normally expressed (Koirala et al. 2009). At this stage of development, GPR56 expression is restricted to developing rostral granule cells, including precursors and young postmitotic neurons. Due to *Gpr56* knockout, these cells lose the ability to adhere to ECM molecules such as laminin-1 and fibronectin, present in the pial BM. However, despite loss of GPR56 expression, granule cells show normal proliferation *in vivo* or migration and neurite outgrowth *in vitro*. As observed by Li et al. (2008), loss of GPR56 expression causes breaches in the pial BM, through which the granule cells migrate outward (Koirala et al. 2009).

Defects in integrins and their ligand laminin are associated with pial BM breakdown and neuronal overmigration. Since rostral granule cells from *Gpr56*$^{-/-}$ mice lose the ability to adhere to laminin-1 (Koirala et al. 2009), Jeong et al. (2013) investigated a potential interaction between $\alpha_3\beta_1$-integrin and GPR56. Loss of $\alpha_3\beta_1$-integrin in NPCs attenuates the inhibitory effect of collagen III treatment on migration from neurospheres, similar to what was observed before in *Gpr56*$^{-/-}$ mice. Moreover, $\alpha_3\beta_1^{-/-}$ *Gpr56*$^{-/-}$ double knockout mice display a more severe cortical phenotype than *Gpr56*$^{-/-}$ single knockouts with defects in the pial BM that appear earlier in development, suggesting a potential interaction between the two cell surface receptors. GPR56 and $\alpha_3\beta_1$-integrin colocalise in rostral granule cells and neurons, however, $\alpha_3\beta_1$-integrin does not bind directly to collagen III. Thus, GPR56 and $\alpha_3\beta_1$-integrin function together in cortical development, likely via an unknown mediator (Jeong et al. 2013).

The only phenotype in *Gpr56*$^{-/-}$ mice outside the CNS was reported by Chen et al. (2010), showing that GPR56 is involved in the regulation of mouse testis development and fertility. Interestingly, the authors reported that TG2 co-localises with laminin-1 in mouse testes and that the distribution pattern of TG2 is altered in *Gpr56*$^{-/-}$ mice. However, *Tg2*$^{-/-}$ mice do not show any defects in testis development, indicating that TG2 might not be the ligand for GPR56 during testes development or that there is compensation by another ligand (Chen et al. 2010).

1.4.5 GPR56 and cancer

1.4.5.1 GPR56 as a tumour suppressor

Zendman and colleagues (1999) originally isolated GPR56 from human melanoma cells where they demonstrated that GPR56 mRNA expression levels decrease with increasing potential of the melanoma cells to form metastases in the lung. This was later confirmed by Xu et al. (2006), showing down-regulation of GPR56 mRNA and protein in highly metastatic melanoma cells. Experiments using a xenograft tumour model indicated that overexpression of GPR56 in MC-1 melanoma cells results in reduced cell growth and fewer lung metastases. However, high GPR56 expression levels do not affect proliferation *in vitro*, suggesting that GPR56 interacts with a factor in the microenvironment *in vivo*, which was identified as TG2.

However, Xu et al. (2010) themselves later demonstrated that GPR56 actually does not influence endogenous melanoma progression by crossing *Gpr56*$^{-/-}$ mice with mice from a melanoma model expressing GPR56. In their study, all of the offspring (*Gpr56*$^{+/+}$, *Gpr56*$^{+/-}$ and *Gpr56*$^{-/-}$ mice) develop melanoma, but tumour progression does not differ among the animals. These results indicated that GPR56 has no effect on endogenous melanoma progression, which is in contrast to the results obtained with the xenograft tumour model (Xu et al. 2006).

Nonetheless, analysis of tumour sections from MC-1 melanoma cells overexpressing GPR56 by Yang et al. (2011) showed reduced amounts of blood vessels and much lower vascular endothelial growth factor (VEGF) concentrations in cell supernatants when compared to vector control MC-1 cells, thus expression of GPR56 inhibits melanoma angiogenesis. On the other hand, knockdown of TG2 by shRNA does not result in increased levels of VEGF in GPR56-positive MC-1 cells, indicating that TG2 does not mediate inhibition of VEGF secretion by GPR56 (Yang et al. 2011).

A recent report by (Yang et al. 2014) confirmed previous observations made by Xu et al. (2006) regarding a reduction in tumour growth following the interaction of GPR56 with TG2. Injection of GPR56-overexpressing MC-1 cells into $Tg2^{+/+}Rag2^{-/-}$ mice results in reduced tumour weight when compared to control MC-1 cells (low endogenous GPR56 expression). Moreover, injection of TG2-ablated MC-1 cells into $Tg2^{-/-}Rag2^{-/-}$ mice causes a reduction in tumour weight, indicating that TG2 itself promotes melanoma growth. The tumour weight is not further reduced, when TG2-ablated MC-1 cells overexpressing GPR56 are injected into $Tg2^{-/-}Rag2^{-/-}$ mice, indicating that TG2 mediates the inhibitory effect of GPR56.

In addition to highly metastatic melanoma cells, GPR56 protein expression is down-regulated in human pancreatic cancer cell lines, despite high GPR56 mRNA levels. The down-regulation, however, is not due to proteasomal degradation of GPR56, thus GPR56 expression is likely suppressed at the translational level (Huang et al. 2008).

1.4.5.2 GPR56 as a tumour promoter

GPR56 mRNA is up-regulated in human esophageal squamous cell carcinoma (ESCC) tissue and cell lines, whereas it is undetectable in normal esophageal tissues (Sud et al. 2006). GPR56 protein expression is up-regulated in human glioma tumours and cell lines (Shashidhar et al. 2005). In these cells, GPR56 is believed to play a role for cell adhesion, since it is expressed at the front of migrating cells. Moreover, GPR56 overexpression in HEK293 cells activates TCF (T-cell factor), PAI-1 (plasminogen activator inhibitor-1) and NF-κB (nuclear factor kappa-light-chain-enhancer of activated B cells) responsive elements (Shashidhar et al. 2005), which is in line with the report from Iguchi et al. (2008). Kim et al (2010) demonstrated increased promoter activities of COX2 (cyclooxigenase 2), iNOS (inducible nitric oxide synthase) and VEGF genes following GPR56 overexpression. Moreover, GPR56 mRNA is up-regulated in many other cancer types outside the CNS such as ovarian, pancreatic, colon, breast, brain and non-small cell lung cancers, suggesting a general role of GPR56 in tumorigenicity (Ke et al. 2007). GPR56 expression is also associated with the transformation phenotype in HeLa cells. ShRNA-mediated silencing of GPR56 in several cancer cell lines induces apoptosis, suggesting that GPR56 normally prevents intrinsic apoptosis of cancer cells. Moreover, GPR56-silenced A2058 melanoma cells display impaired adhesion to fibronectin *in vitro* and partially dephosphorylated ERK, indicating a role for GPR56 in adhesion signalling (Ke et al. 2007). The same authors presented opposing results to Xu et al. (2006) regarding the effect of GPR56 expression on tumour progression, using a similar melanoma xenograft model. In their model, shRNA-mediated down-regulation of GPR56 in A2058 melanoma cells results in inhibition of tumour growth, demonstrating the oncogenic properties of GPR56 (Ke et al. 2007). This was also observed by others, when GPR56- and TG2-ablated MC-1 melanoma cells were injected into $Tg2^{-/-}Rag2^{-/-}$ mice, leading to a complete inhibition of melanoma tumour growth. The result indicated that GPR56 itself has tumour promoting functions in the absence of TG2, as tumour growth is not entirely ablated when MC-1 control cells with low endogenous GPR56 expression and ablated TG2 expression are injected into the same mice (Yang et al. 2014).

The discrepancies between the different reports highlight that GPR56 is either a tumour suppressor or promoter and it is likely that additional ligands and therefore functions may be discovered in the future.

1.4.6 GPR56 in immune cells

GPR56 is a marker of cytotoxic natural killer cells (NK cells) and cytotoxic T lymphocytes (Della Chiesa et al. 2010; Peng et al. 2011). GPR56 expression is down-regulated upon activation of NK cells by cytokines such as interleukins. GPR56 down-regulation is regulated at the transcriptional level and does not include retention of the protein in the cytoplasm (Della Chiesa et al. 2010). The role of GPR56 in these cells remains completely unknown, however overexpression of GPR56 in a cytotoxic NK cell line reduces migration dramatically *in vitro* (Peng et al. 2011). Thus, GPR56 might regulate migration of cytotoxic lymphocytes, which would concur with reports on the regulation of migration in NPCs.

1.4.7 The role of N-GPR56 in GPR56 activation

Like other aGPCRs, GPR56 is cleaved into two independent proteins, N-GPR56 and C-GPR56, which remain non-covalently associated at the cell surface (Xu et al. 2006; Jin et al. 2007; Huang et al. 2008). In addition to its ligand binding ability (Xu et al. 2006; Luo et al. 2011), several results indicated that N-GPR56 serves as an endogenous antagonist for C-GPR56. In contrast to wild type GPR56, overexpression of an N-terminal deletion mutant (“C-GPR56”) in MC-1 melanoma cells results in a significant induction of melanoma growth and angiogenesis *in vivo*, whereas addition of N-GPR56-Fc reduces GPR56-dependent VEGF-production (Yang et al. 2011). These data indicated an antagonistic relationship between C- and N-GPR56, in which N-GPR56 inhibits GPR56 activity. Deletion of the TG2-binding site (aa108-177), a motif rich in serines, threonines and prolines (STP), results in induction of tumour growth and angiogenesis, indicating that the STP-region is required for the inhibitory effect of N-GPR56. It was speculated that the deletion of the STP-domain results in a conformational change of N-GPR56, thus it is unable to inhibit GPR56 activity (Yang et al. 2011).

Overexpression of another N-terminally truncated GPR56 mutant ("ΔNT") in HEK293 cells actives RhoA (Paavola et al. 2011). The high degree of GPR56 ubiquitination, increased co-localisation with β-arrestin-2 and cytotoxicity is caused by prolonged expression of ΔNT. This was associated with high auto-activity of truncated ΔNT, confirming the inhibitory function of N-GPR56.

In a co-culture system, *trans-trans* N-terminal interactions (interactions of the same receptor type on adjacent cells) between full-length GPR56 expressed on the surface of HEK293 base cells and N-GPR56 or full-length GPR56 expressed in the co-cultured HEK293 cells, induce GPR56-dependent Rho activation in the base cells. This result indicated that GPR56 *trans-trans* or potential ligand-GPR56 interactions could lead to the removal of N-GPR56 or induce a conformational change within N-GPR56, resulting in the activation of the receptor as seen with truncated ΔNT (Paavola et al. 2011).

1.4.8 Natural splice variants

Four natural splice variants of GPR56 were reported by Kim et al (2010). Variant 1, $\Delta_{430\text{-}35}$-GPR56, results from alternative splicing in exon 10 and lacks six amino acids in ICL1. Variant 2 is similar to $\Delta_{430\text{-}35}$-GPR56, but additionally contains five amino acids surrounding the region of the signal peptide cleavage site. Compared to wild type GPR56, overexpression of variant 1 and 2 in HEK293 cells increases SRE-mediated transcription, indicating that the 6 amino acid deletion in the first intracellular loop might facilitate activation of the Rho signalling pathway (Kim et al. 2010). Variant 3 lacks 170 amino acids (Δ38-208) within N-GPR56, but has an intact signal peptide and variant 4 lacks the first 175 amino acids (Δ1-175) including the signal peptide. Overexpression of variants 3 and 4 result in reduced promoter activities, including the VEGF promoter (Kim et al. 2010). These findings contradict the hypothesis that N-terminal deletion mutants are constitutively more active than wild type GPR56 (Yang et al. 2011; Paavola et al. 2011). However, folding and trafficking defects resulting in impaired cell surface expression levels might explain the result, as observed for BFPP-mutants (Jin et al. 2007) and another N-terminally truncated GPR56 variant before (Iguchi et al. 2008).

1.5 Transglutaminases

Transglutaminases (TGs) are a family of structurally and functionally related proteins. The human genome encodes nine TGs that belong to the structurally related papain-like superfamily of cysteine proteases (Lorand and Graham 2003). Eight of the TGs found in man, TG1-7 and FXIIIa, are catalytically active (Lorand and Graham 2003; Thomas et al. 2013). One member of the TG family, erythrocyte band 4.2, is catalytically inactive and has scaffolding functions. Enzymatically active TGs catalyse a variety of post-translational protein modifications that are involved in biological processes such as blood coagulation or ECM assembly (Lorand and Graham 2003). However, TGs also contribute to auto-immune reactions, where TG2-modified gliadin peptides are immunogenic and cause coeliac disease (Sollid 2002).

The human TGs are expressed in different tissues and recognize various substrates for their enzymatic reactions. However, all catalytically active TGs require Ca^{2+} to perform post-translational protein modifications. Interestingly, even extracellular TGs such as FXIIIa and TG2 lack a signal sequence and it remains elusive how they are secreted (Aeschlimann and Paulsson 1994).

The human TGs share a high degree of sequence conservation and they all have a similar tertiary structure consisting of 4 domains: the N-terminal β-sandwich, the α/β-catalytic core and the C-terminal β-barrels 1&2 (Fig. 1.13). All of the catalytically active TGs share a common catalytic site containing a catalytic triad (Cys-His-Asp). In addition, TG1 and FXIIIa exist as pro-enzymes with an N-terminal sequence that is cleaved to generate active enzymes (Fig. 1.13 A) (Iismaa et al. 2009).

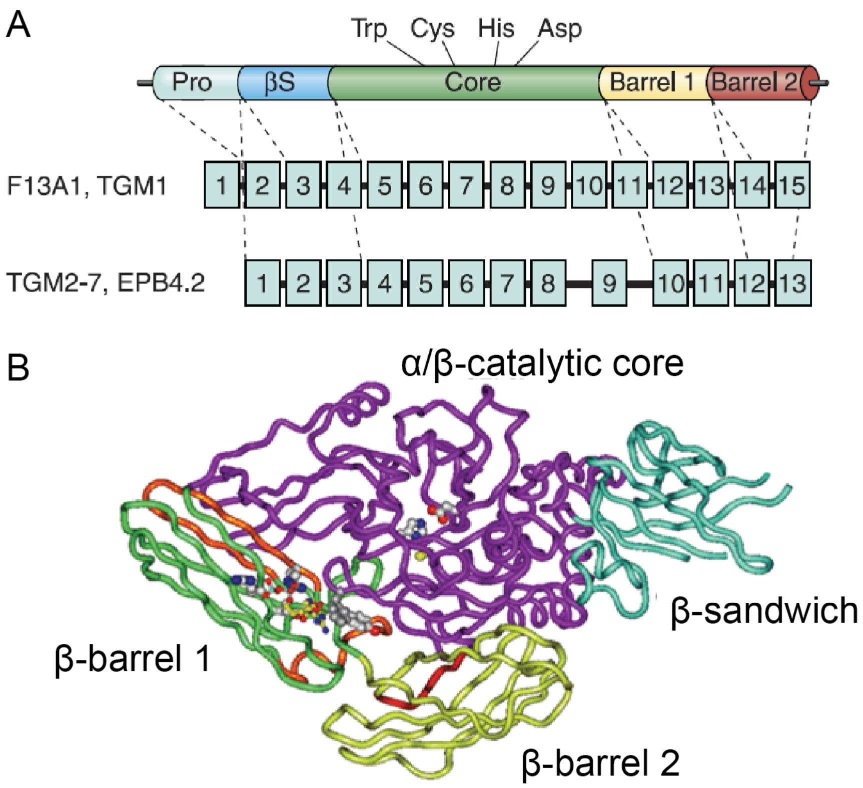
A
Trp
Cys
His
Asp
Pro
βS
Core
Barrel 1
Barrel 2
F13A1, TGM1
1 2 3 4 5 6 7 8 9 10 11 12 13 14 15
TGM2-7, EPB4.2
1 2 3 4 5 6 7 8 9 10 11 12 13
B
α/β-catalytic core
β-sandwich
β-barrel 1
β-barrel 2

Figure 1.13 Genomic organisation, protein domains and tertiary structure of human TGs.

(A) FXIIIa and TG1 consist of 15 exons (numbered) and 14 introns, whereas exon 1 is non-coding and exon 2 encodes an N-terminal pro-peptide. TG2-7 and erythrocyte band 4.2 consist of 13 exons and 12 introns. All TGs are composed of 4 structural domains: N-terminal β-sandwich, α/β-catalytic core and β-barrels 1&2.

(B) Crystal structure of GDP-bound TG2.

Orange, α$_{1B}$*-adrenergic receptor binding site; red, phospholipase Cδ1-recognition domain; balls and sticks, catalytic residues (Cys*$_{277}$*, His*$_{335}$*, Asp*$_{358}$*) and key GTP-binding residues (Phe*$_{174}$*, Arg*$_{478}$*, Val*$_{479}$*, Arg*$_{580}$*, Tyr*$_{583}$*).*

Taken from Lorand & Graham (2003) and Iismaa et al. (2009), modified.

1.6 Tissue transglutaminase (TG2)

1.6.1 Expression of TG2 in the human body

The TGM2 gene is localised on chromosome 20q11-12 and encodes an ~80 kDa protein. In contrast to the other TGs that show a restricted expression pattern in specific organs and tissues, TG2 is ubiquitously expressed is the human body. However, its physiological role remains elusive (Lorand and Graham 2003). TG2 is expressed in cells of different lineages including mesenchymal, epithelial and hematopoietic and is constitutively expressed in endothelial cells, smooth muscle cells and fibroblasts (Iismaa et al. 2009). TG2 localises intracellularly in the cytoplasm, nucleus and mitochondria, as well as extracellularly in the ECM or at the cell surface in association with the ECM (Nurminskaya and Belkin 2012).

Amino acid sequence alignments of all human TGs revealed a close relationship between TG2, TG3, TG5, TG6, TG7 and band 4.2, which belong to one phylogenetic lineage (Grenard et al. 2001). TG2 was the first recognized member of the TG family (Sarkar et al. 1957).

1.6.2 Enzymatic activities of TG2

Like other members of the TG family, TG2 catalyses several post-translational modifications of proteins, which are Ca^{2+}- and thiol-dependent. Essential for the reactions is the presence of the catalytic triad located within the catalytic core domain, consisting of Cys_{277}, His_{335} and Asp_{358}, as well as two stabilizing tryptophans (Iismaa et al. 2009; Lorand and Graham 2003).

The three main reactions catalysed by TG2 will be briefly explained in the following section: transamidation, hydrolysis and esterification. All of these reactions involve an initial acylation step, where a Gln-containing peptide or protein, the first substrate, reacts with the active site Cys of TG2. As a result, the substrate is covalently bound to the active site Cys, forming a γ-glutamylthioester, known as the acyl-enzyme intermediate (Fig. 1.14). This initial step is followed by the nucleophilic attack of the thioester bond by a second substrate, leading to the cleavage of the thioester bond of the intermediate. Depending on the nature of the second substrate, the following step may be a transamidation (amine attacks) or esterification (alcohol attacks) reaction. In the absence of a second substrate, water can drive a hydrolysis reaction (Fig. 1.15).

If the amino-group of a Lys within another protein (second substrate) serves as the attacking nucleophile, a transamidation reaction occurs. The most important and best studied transamidation reaction is protein cross-linking (Fig. 1.14 & 1.15). During the reaction, the Gln of the first substrate is cross-linked to the Lys of the second substrate, forming an N^{ε}(γ-glutamyl)lysyl isopeptide bond (Iismaa et al. 2009). The crosslinking reaction is unique for the family of TGs (Lorand & Graham, 2003; Pinkas et al. 2007). Another transamidation reaction is amine incorporation into the Gln of the first substrate (Fig. 1.15).

Esterification of the Gln in the first substrate occurs if a suitable alcohol serves as the second substrate. Hydrolysis reactions occur in the absence of a second substrate and result in the replacement of the $-NH_2$ group of Gln in the first substrate by an –OH group. This hydrolysis reaction is called deamidation and converts the Gln into a Glu. Peptides present in glutenins and gliadins, two major components of wheat gluten proteins, which are deamidated by TG2, are the dominant epitopes for activating T cells and cause coeliac disease (Lorand and Graham 2003; Sollid 2002). Hydrolysis can also follow the crosslinking of two peptides and reverse the crosslinking reaction by cleavage of the isopeptide bond. (Fig. 1.15) (Iismaa et al. 2009; Lorand and Graham 2003).

.

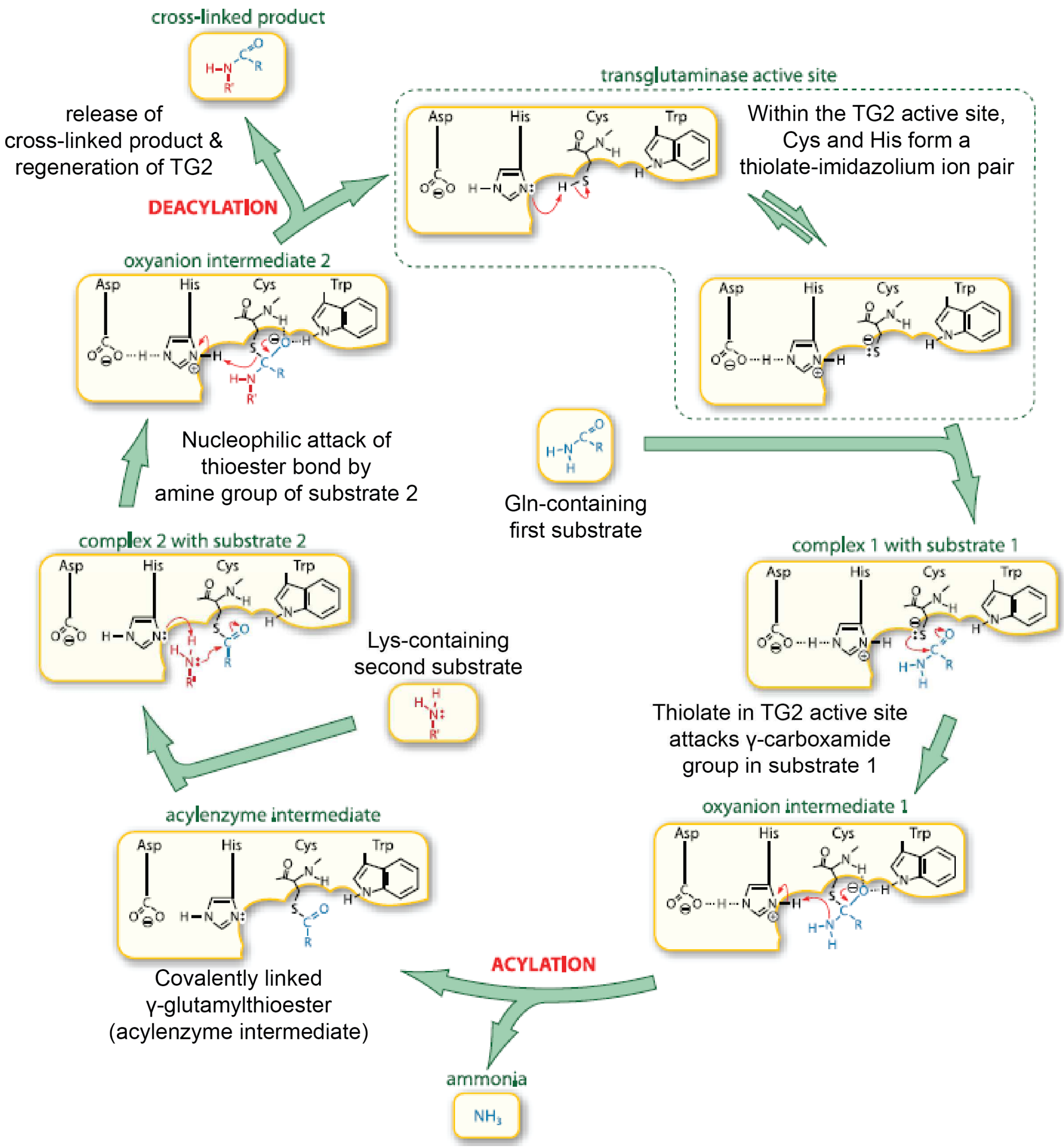
cross-linked product
release of cross-linked product & regeneration of TG2
DEACYLATION
transglutaminase active site
Within the TG2 active site, Cys and His form a thiolate-imidazolium ion pair
Asp
His
Cys
Trp
oxyanion intermediate 2
Nucleophilic attack of thioester bond by amine group of substrate 2
Gln-containing first substrate
complex 2 with substrate 2
complex 1 with substrate 1
Lys-containing second substrate
Thiolate in TG2 active site attacks γ-carboxamide group in substrate 1
oxyanion intermediate 1
acylenzyme intermediate
Covalently linked γ-glutamylthioester (acylenzyme intermediate)
ACYLATION
ammonia
NH₃

Figure 1.14 Mechanism of post-translational protein modifications catalysed by TG2.

The initial acylation step is similar for all post-translational modifications catalysed by TG2 and involves the reaction of a Gln-containing first substrate with TG2. The reaction results in the formation of a covalent bond between the substrate and the TG2 active site Cys, forming a γ-glutamylthioester, the acyl-enzyme intermediate. The following reactions depend on the nature of nucleophile donor that is present, in this case a Lys-containing second substrate. Nucleophilic attack of the thioester bond of the acyl-enzyme intermediate by the amine group of the Lys results in cleavage of the thioester group. This causes the release of the crosslinked product, followed by regeneration of TG2. *Taken from Iismaa et al. (2009), modified.*

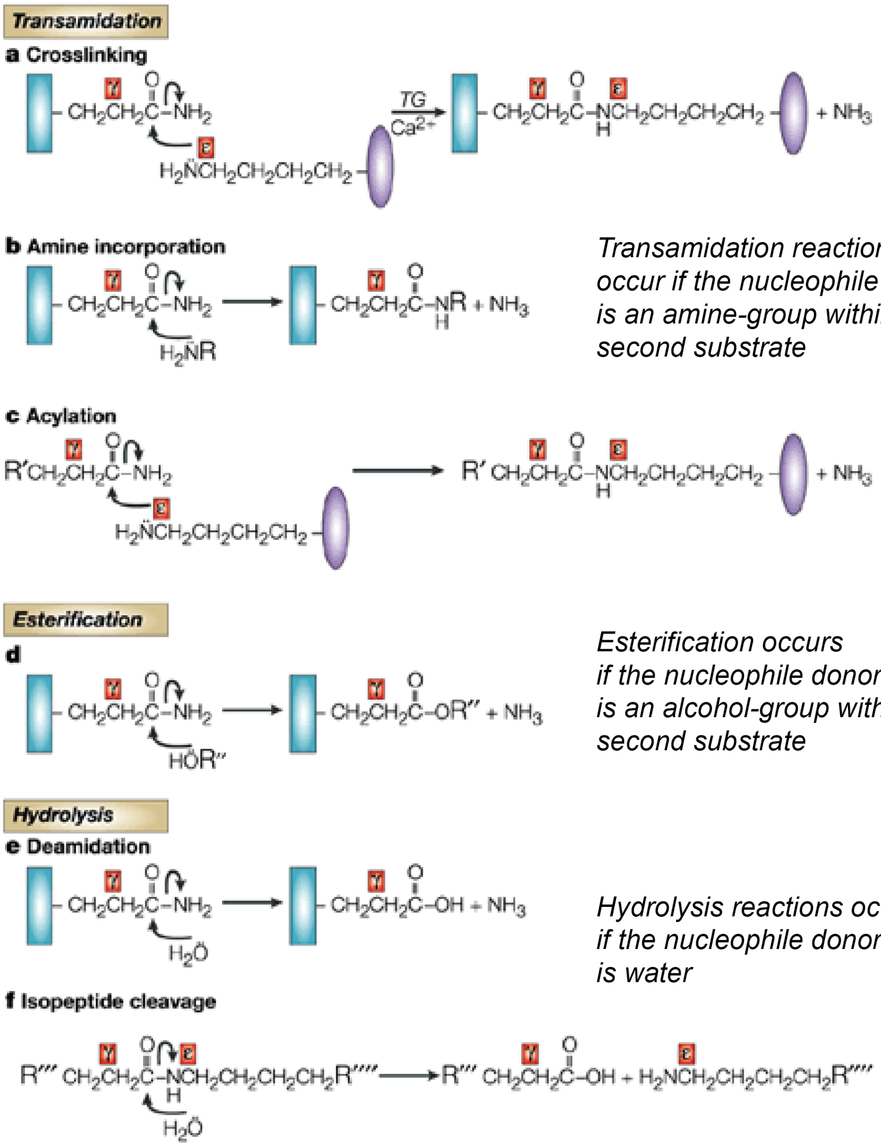
Transamidation
a Crosslinking
TG
Ca2+
+ NH3
b Amine incorporation
c Acylation
Esterification
d
Hydrolysis
e Deamidation
f Isopeptide cleavage

Transamidation reactions occur if the nucleophile donor is an amine-group within a second substrate

Esterification occurs if the nucleophile donor is an alcohol-group within a second substrate

Hydrolysis reactions occur if the nucleophile donor is water

Figure 1.15 Reactions catalysed by TG2.

The three main categories of Ca^{2+}-dependent post-translational modifications catalysed by TG2 are transamidation reactions including protein crosslinking (a), amine incorporation (b) and acylation (c); esterification reactions (d); hydrolysis reactions including deamidation (e) and isopeptidase cleavage (f). The type of reaction that is catalysed by TG2 depends on the nature of the nucleophile donor.

Blue rectangle, first substrate containing acceptor-Gln; purple ellipse, second substrate with Lys donor residue; R, side chain of a primary amine; R’, Gln-containing peptide; R’’, a ceramide (sphingolipid); R’’’ & R’’’’, side chains in branched isopeptides.

Taken from Lorand & Graham (2003), modified.

1.6.3 Biological functions of TG2-mediated transamidation

TG2 catalyses the formation of intra- and intermolecular crosslinks. Extracellular TG2 generates intramolecular crosslinks that mainly affect protein conformations and interactions (Nemes et al. 2009). Intermolecular crosslinking of ECM proteins such as fibronectin, collagen or fibrinogen leads to the formation of covalently linked, highly stable polymers (Barsigian et al. 1988; Collighan and Griffin 2009). TG2 also crosslinks itself to these ECM proteins (Barsigian et al. 1991). Crosslinking of ECM proteins contributes to the stabilisation and the resistance of the ECM to proteolytic degradation. In addition, it unmasks binding sites for cell surface receptors such as integrins, promoting cell-ECM adhesion (Belkin et al. 2005).

ECM crosslinking plays an important role in the process of wound healing and angiogenesis (Aeschlimann and Thomazy 2000; Iismaa et al. 2009; Nurminskaya and Belkin 2012). However, inappropriate crosslinking of the ECM by TG2 leads to fibrosis (Jones et al. 2006).

Intracellularly, protein crosslinking is involved in apoptosis. Moreover, cytosolic TG2 stimulates inflammation by crosslinking IκBα, resulting in the activation of NFκB signalling (Iismaa et al. 2009).

Amine incorporation to small GTPases such as RhoA, Rab4A, Rab3A, Rab27a or Rac1 by intracellular TG2 was shown to alter their activities. In case of RhoA, this modification leads to its constitutive activation and enhanced degradation, which activates AKT1 and inhibits contractility in vascular smooth muscle cells (Guilluy et al. 2007).

1.6.4 Regulation of the transamidation activity

The transamidation activity of TG2 is Ca^{2+}-dependent. Activation of TG2 by Ca^{2+}-binding, however, is inhibited by binding of GTP to TG2 and vice versa. Intracellularly, GTP concentrations are high and Ca^{2+}-concentrations are low, thus TG2 is bound to GTP and exists in a compact, “closed” conformation, with the active site buried (Fig. 1.16 A).

In the closed conformation, TG2 acts as a G protein, but lacks transglutaminase activity (Nakaoka et al. 1994). Activation of TG2 requires the binding of at least two Ca^{2+}-ions, inducing a large conformational change of the enzyme by moving the two β-barrels away from the catalytic core (Fig. 1.16 B) (Pinkas et al. 2007).

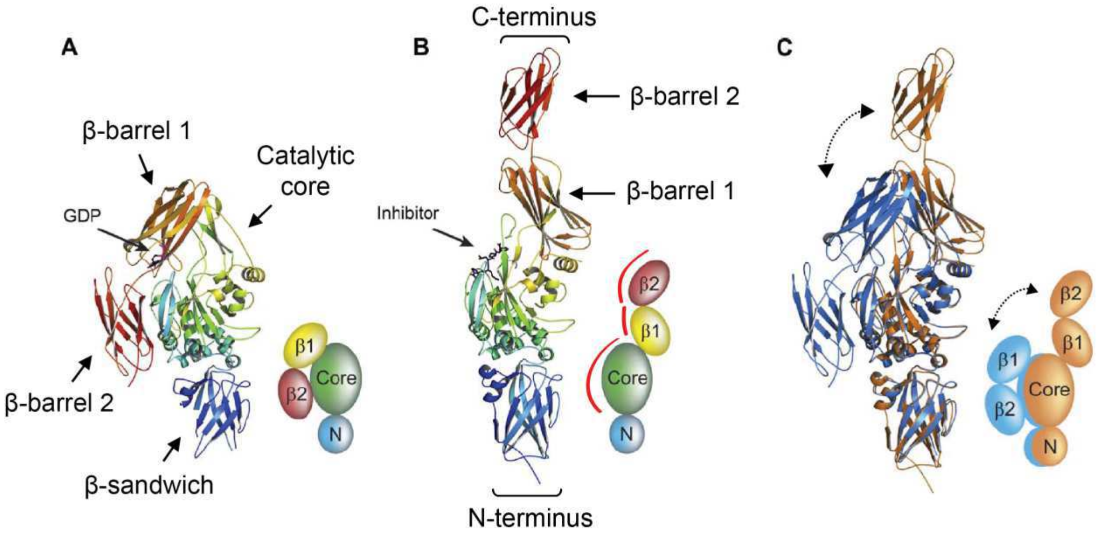
A
β-barrel 1
Catalytic core
GDP
β-barrel 2
β-sandwich
β1
β2
Core
N
B
C-terminus
β-barrel 2
β-barrel 1
Inhibitor
β2
β1
Core
N
N-terminus
C
β2
β1
β1
β2
Core
N

Figure 1.16 Crystal structures and schematics of TG2 closed and open conformations.

(A) GDP-bound, “closed”, catalytically inactive conformation of TG2.

(B) Inhibitor-bound, catalytically arrested, “open” conformation of TG2. Accessible motifs that were buried in the closed conformation are marked red in the schematic.

(C) Conformational change during enzymatic activation of TG2.

Blue, N-terminal β-sandwich; green, catalytic core domain; yellow, C-terminal β-barrel 1; red, β-barrel 2.

Taken from Pinkas et al. (2007), modified.

It is thought that TG2 can be activated intra- and extracellularly upon increased Ca^{2+}-levels (Pinkas et al. 2007). Although extracellular Ca^{2+}-concentrations are relatively high under normal physiological conditions, extracellular TG2 is mostly inactive. Therefore, it was investigated how TG2 activity is regulated. Pinkas et al. (2007) speculated that externalised TG2 remains in a closed, inactive conformation, which results from guanine nucleotide- and/or integrin-binding. Chemical injury however, might activate TG2 rapidly. Others showed that the oxidative state of the extracellular milieu regulates TG2 activity, as oxidation leads to disulphide bond formation and TG2 inactivation (Stamnaes et al. 2010). Moreover, it was speculated that Ca^{2+} is not the only trigger for TG2 activation and there might be additional factors such as conformational changes due to interacting proteins on the cell surface and in the ECM that stabilize TG2 in an active conformation (Nurminskaya and Belkin 2012).

In addition, it remains elusive as to which conformation Ca^{2+}-activated TG2 acquires, due to the lack of a crystal structure of the Ca^{2+}-bound form (Király et al. 2011). The inhibitor-bound, open conformation was presented as the prototypical structure of catalytically active TG2 (Pinkas et al. 2007), but others speculated that it might represent one of the transition states occurring during the enzymatic reaction (Király et al. 2011).

1.6.5 TG2 as a GTPase and G protein

Besides the enzymatic functions described above, TG2 can act as a GTPase by hydrolysing GTP, which is independent of its transamidating activity (Achyuthans and Greenberg 1987). Intracellular TG2 functions as a Gα protein and mediates GPCR signalling by coupling to several GPCRs such as α_{1B}- and α_{1D}-ARs, thromboxane A2, oxytocin and follicle stimulating hormone receptors, where it induces PLC signalling (Nakaoka et al. 1994; Chen et al. 1996; Nurminskaya and Belkin 2012). However, TG2 shows no structural homology to the Gα subunits of other heterotrimeric G proteins or small GTPases. Whereas $G\alpha_q$ proteins induce PLCβ-signalling, TG2 specifically interacts with PLCδ1 (Nakaoka et al. 1994; Kang et al. 2002). The Ca^{2+}-binding protein calreticulin acts as the Gβ-subunit for intracellular TG2 and inhibits the GTPase- and transamidating-activities of TG2 by keeping the protein in its inactive, GDP-bound conformation, ready for the initiation of GPCR signalling. Intracellular TG2 is activated and deactivated similar to Gα subunits of heterotrimeric G proteins (Mhaouty-Kodja 2004). The agonist-activated GPCR induces the exchange of GDP to GTP and TG2 dissociates from calreticulin (Gβ). TG2 is deactivated by GTP-hydrolysis and reassociates with calreticulin (Nurminskaya and Belkin 2012).

In its function as a GTPase, TG2 is involved in several other signalling pathways. α_1-AR dependent activation of intracellular TG2 induces hypertrophy in cardiomyocytes by inducing ERK signalling (Lee et al. 2003) and proliferation in hepatocytes (Wu et al. 2000). Intracellular TG2 can promote or inhibit cell migration. GTPase activity of TG2 promotes cell migration of fibroblasts by activating PKCα signalling and phosphorylation of focal adhesion kinase (FAK), which is required for the turnover of focal adhesions (Stephens et al. 2004). On the other hand, the α_{1B}-AR-induced interaction of intracellular TG2 with the cytoplasmic tails of integrins inhibits migration of smooth muscle cells (Kang et al. 2004).

Although the GTPase activity of TG2 was shown to activate several signalling pathways, their pathophysiological implication remains elusive. However, signalling mediated by intracellular TG2 seems to have rather pro-survival effects, since the GTPase activity of intracellular TG2 protects NIH/3T3 and HeLa cells against apoptosis (Datta et al. 2007).

1.6.6 Non-enzymatic functions of extracellular TG2 and their physiological roles

Besides ample enzymatic functions, several non-covalent interactions with numerous binding partners in the nucleus, cytoplasm, cell surface and ECM have been identified that promote signalling and/or adaptor/scaffolding functions of TG2. Often, these interaction partners also serve as transamidating substrates for TG2.

Extracellular TG2 interacts with matrix metalloproteinase 2 (MMP2) and cell surface receptors such as integrins, syndecan-4, platelet-derived growth factor receptor, GPR56 and others (Belkin et al. 2004; Akimov et al. 2000; Zemskov et al. 2009; Xu et al. 2006).

In addition to stabilising the ECM by crosslinking, extracellular TG2 also interacts with the ECM independently of its enzymatic functions. Thus, TG2 interacts with fibronectin (FN) (Turner and Lorand 1989), mediating the assembly of FN fibrils, which does not require TG2's transamidating activity, but promotes the deposition of soluble FN into the ECM (Akimov and Belkin 2001). Moreover, TG2 acts as a bridge between integrins and FN, promoting cell-ECM adhesion and cell migration (Akimov et al. 2000; Zemskov et al. 2006). Independently of FN, TG2-integrin complexes enhance the formation of focal adhesion complexes and stress fibers by activating FAK, as well as RhoA. Taken together, the TG2-integrin interactions affect cellular processes including adhesion, migration and spreading (Stephens et al. 2004; Nurminskaya and Belkin 2012).

1.6.7 TG2 and cancer

The role of TG2 in cancer progression is controversial and there are several reports demonstrating either down- or up-regulation of TG2 in this process (Kotsakis and Griffin 2007; Mehta et al. 2010). It was shown that TG2 is down-regulated in primary tumours from breast (Ai et al. 2008), liver (Barnes et al. 1985) and prostate (Birckbichler et al. 2000) and that its expression level and activity decrease with tumour progression. In breast cancer, the expression of TG2 might be reduced by epigenetic gene silencing in primary tumours (Ai et al. 2008). Down-regulation of TG2 promotes matrix destabilisation and degradation, which is accompanied with tumour cell invasion. In secondary metastatic tumours, however, TG2 is highly overexpressed and promotes cell survival (Kotsakis and Griffin 2007).

In contrast, analysis of drug-resistant cancer cells obtained from glioblastoma, melanoma, as well as breast, lung, pancreatic and ovarian carcinoma show increased TG2 expression levels (Han and Park 1999; Mehta 1994; van Groningen et al. 1995; Mehta et al. 2010). Cells derived from metastases show even higher TG2 expression levels when compared to their primary tumours. It is believed that TG2 expression levels positively correlate with the potential of tumours to metastasise (Mehta et al. 2010; Chen et al. 2002).

The resistance of cancer cells to apoptosis is a property that allows them to metastasise and to develop drug-resistance (Kerbel et al. 1994). Increased expression of TG2 can prevent apoptosis and prolong cell survival. TG2 down-regulates the tumour suppressor protein phosphatase and tensin homolog (PTEN) and constitutively activates the pro-survival factors NF-κB and Akt, which is associated with cancer progression, including chemoresistance and metastasis (Wang et al. 2012; Mann et al. 2006; Verma and Mehta 2007; Cao et al. 2008). Down-regulation of TG2 by siRNA or inhibition of TG2 by small molecule inhibitors in various cancer cell types increases their sensitivity to chemotherapeutics and inhibits invasion *in vitro* and *in vivo* (Verma and Mehta 2007).

Integrins influence the ability of cells to proliferate, migrate and undergo apoptosis and mediate processes such as invasion and metastasis (Giancotti and Ruoslahti 1999). TG2 associates with β_1, β_3 and β_5 integrins, which enhances the adhesion of ovarian cancer cells to FN and induces directional migration of these cells, promoting cell invasion (Satpathy et al. 2007). Moreover, TG2 up-regulates anti-apoptotic and pro-survival signalling pathways, rendering cancer cells drug-resistant (Mehta et al. 2010). Thus, association of TG2 with integrins increases binding of breast cancer cells to FN, leading to FAK-activation, which initiates downstream signalling by PI3K/Akt, Ras/Erk or Crk/Dock180/Rac. These downstream pathways are pro-survival and increase the invasive properties of cancer cells (Mehta and Eckert 2005; Levental et al. 2009).

1.6.8 TG2 knockout mice

Despite numerous cellular functions of TG2, *Tg2*$^{-/-}$ mice are viable and develop and reproduce normally. The ECM structure and composition, as well as the onset of apoptosis are unaltered (De Laurenzi and Melino 2001). The lack of a lethal phenotype can be partially explained by compensation of

TG2 functions by other TGs. However, clearance by phagocytosis seems to be altered in the thymus and the liver in these mice and they develop inflammatory and autoimmune reactions (Szondy et al. 2003). In the late phase of apoptosis, crosslinking by TG2 normally stabilizes the structure of a dying cell prior to phagocytosis, preventing the release of intracellular components and inflammatory responses (Chhabra et al. 2009). Moreover, *Tg2*$^{-/-}$ mice display defects in wound healing, which is associated with impaired adherence of fibroblasts to the ECM (Nanda et al. 2001). *Tg2*$^{-/-}$ mouse embryonic fibroblasts show impaired cell migration, which can be partially rescued by addition of exogenous TG2, confirming the critical role for extracellular TG2 in wound repair (Mehta and Eckert 2005; Telci and Griffin 2006).

Studies with *Tg2*$^{-/-}$ mice have also shown that TG2 activity contributes to the autosomal-dominant neurodegenerative disorder Huntington’s disease (HD). HD is associated with extensive apoptosis of neuronal cells in the cerebral cortex, resulting in progressive motor dysfunction and dementia. The disease is caused by the expansion of CAG repeats, encoding glutamine, within the gene encoding the cytosolic protein huntingtin (htt) (MacDonald et al. 1993). Originally, insoluble aggregates of htt proteins, which result from non-covalent hydrogen bond interactions, were thought to cause HD (MacDonald et al. 1993). However, more recently it was shown that the soluble complexes of mutant htt are neurotoxic (Ruan and Johnson 2007). Crossing of *Tg2*$^{-/-}$ mice and HD R6/1 transgenic mice resulted in reduced cell death and improved motor function, but increased formation of htt aggregates, indicating that TG2 might inhibit aggregate formation (Mastroberardino et al. 2002). Therefore, it was suggested that TG2 increases the formation of soluble high-molecular weight htt complexes, which cause HD, by crosslinking insoluble, poly-glutamine htt-aggregates, thus increasing their solubility (Lai et al. 2004).

1.7 Glioblastoma multiforme

Glioblastoma multiforme (GBM) is the most aggressive and most common type of primary brain tumour in humans. The origin of the cells that give rise to glioblastomas is still under investigation. However, it was proposed that neural stem and progenitor cells can transform into glioblastoma cells, as well as mature glia (astrocytes and oligodendrocytes) that de-differentiate due to multiple genetic mutations (Hadjipanayis and Van Meir 2009a; Hadjipanayis and Van Meir 2009b; Bachoo et al. 2002). According to the classification of the World Health Organisation, which clinically distinguishes four classes of gliomas, GBM is a grade IV astrocytoma, thus the highest grade glioma tumour and most malignant astrocytoma (Holland 2000; Zhang et al. 2003). Histologically, the presence of necrotic cells in the tumour centre and the increase of blood vessels around the tumour distinguishes GBM from lower grade gliomas (Salcman 2012). In general, glioblastomas are considered to be one of the most vascularised tumours, which enables them to grow extremely fast and which makes them highly invasive (Shashidhar et al. 2005). With respect of the genetics of GBM, there are diverse modifications such as gene deletions, amplifications or point mutations. Mutations of the phosphatase and tensin homolog (*PTEN*), normally regulating the PI3K-pathway involved in cell proliferation, loss of the tumour suppressors p16 and p19 (also called Ink4a-ARF) and amplification of the *EGFR* gene are associated with primary (de novo) GBM. In addition, rearrangements of the *EGFR* gene such as an in-frame deletion result in the expression of a truncated EGFR, showing constitutive tyrosine kinase activity (Sehgal 1998; Nagane et al. 2001). Moreover, platelet-derived growth factor receptor (*PDGFR*) amplification and p53 mutations often occur in secondary glioblastomas that develop from lower grade astrocytomas (Sehgal 1998; James and Olson 1996; Geevimaan and Babu 2013).

The Cancer Genome Atlas (TCGA) is a project that analyses expression profiles and genetic data of cancer. The analysis of primary GBM tumours led to a subdivision of grade IV glioblastomas into four groups (classical, mesenchymal, neural and proneural) (Fig. 1.17). Comparison of the gene profiles of the 4 glioblastoma subtypes with neurons and glia *in vitro* suggests different cell origin for the GBM subtypes (Van Meir et al. 2010).

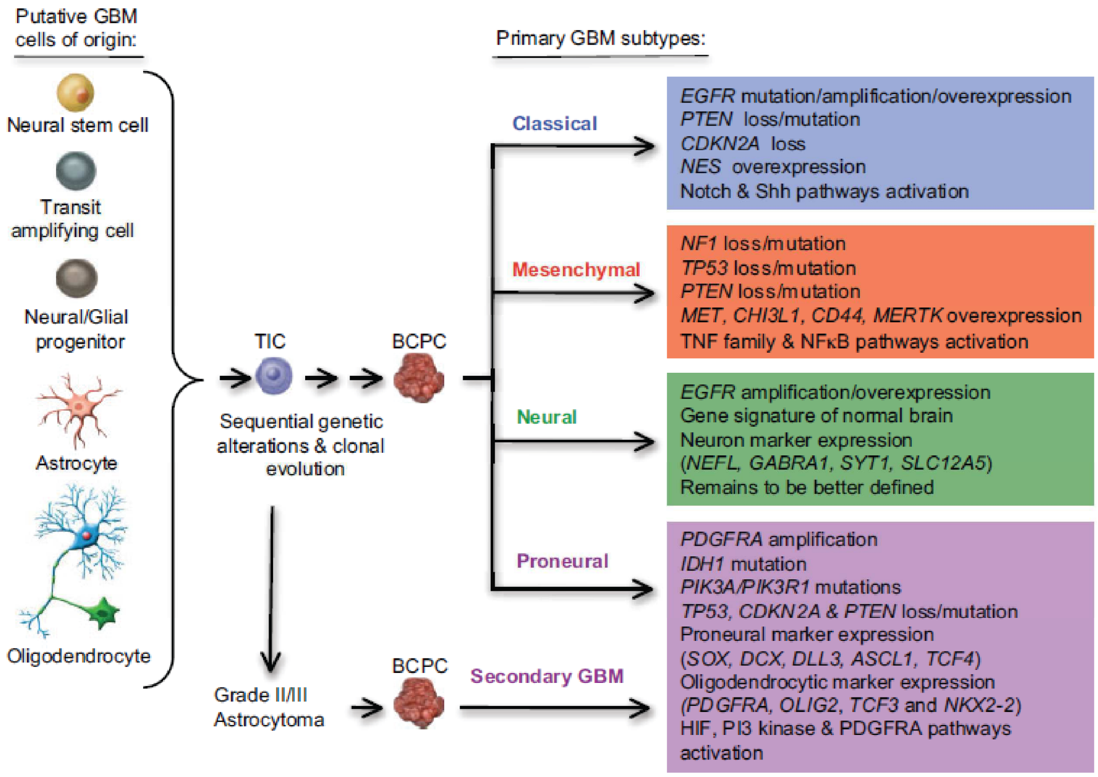
Putative GBM cells of origin:
Neural stem cell
Transit amplifying cell
Neural/Glial progenitor
Astrocyte
Oligodendrocyte
TIC
BCPC
Sequential genetic alterations & clonal evolution
Grade II/III Astrocytoma
BCPC
Secondary GBM
Primary GBM subtypes:
Classical
Mesenchymal
Neural
Proneural
EGFR mutation/amplification/overexpression
PTEN loss/mutation
CDKN2A loss
NES overexpression
Notch & Shh pathways activation
NF1 loss/mutation
TP53 loss/mutation
PTEN loss/mutation
MET, CHI3L1, CD44, MERTK overexpression
TNF family & NFκB pathways activation
EGFR amplification/overexpression
Gene signature of normal brain
Neuron marker expression
(*NEFL, GABRA1, SYT1, SLC12A5*)
Remains to be better defined
PDGFRA amplification
IDH1 mutation
PIK3A/PIK3R1 mutations
TP53, CDKN2A & PTEN loss/mutation
Proneural marker expression
(*SOX, DCX, DLL3, ASCL1, TCF4*)
Oligodendrocytic marker expression
(*PDGFRA, OLIG2, TCF3* and *NKX2-2*)
HIF, PI3 kinase & PDGFRA pathways activation

Figure 1.17 Subdivision of GBM into 4 subgroups, based on genetic alterations and gene expression profiles. *Taken from Meir et al. (2010)*

Normal brain cells of different origin undergo genetic alterations, leading to a cell population of tumour-initiating cells (TIC). This cell population can accumulate further genetic and epigenetic changes and become a brain cancer-propagating cell (BCPC) population, leading to the formation of GBM. Based on different genetic alterations, 4 different subgroups of GBM can be distinguished: the classical, mesenchymal, neural and proneural types of GBM.

GBM, glioblastoma multiforme; EGFR, epidermal growth factor receptor; PDGFR, platelet-dervied growth factor receptor, PTEN, phosphatase and tensin homolog; TNF, tumour necrosis factor; IDH, isocitrate dehydrogenase; PI3K, phosphoinositide 3-kinase; HIF, hypoxia-inducible factor.

The “classical” subtype has a typical genetic profile of highly proliferative cells and shows gene amplification of *EGFR* and loss of *PTEN*. Neural precursors and stem cell markers, as well as Notch- and Sonic hedgehog-signalling mediators are up-regulated. The “mesenchymal” subtype is characterised by an expression profile associated with angiogenesis and mesenchyme and expresses astrocytic markers. *NF1*, *TP53* and *PTEN* tumour suppressor genes are often mutated or lost. The “proneural” subtype expresses oligodendrocytic and proneural developmental marker genes. Overexpression or amplification of *PDGFR* and *TP53* mutations are typical. Mutations in the *IDH1* (isocitrate dehydrogenase 1) gene that are usually found in lower grade gliomas suggest that secondary glioblastomas belong to this subtype. The “neural” subtype is poorly defined, but shows gene expression profiles similar to differentiated cells in normal brain tissue with expression of neuronal markers.

It must be noted that despite a classification into 4 subgroups may help to treat the different tumours more efficiently, all subgroups of GBMs demonstrate inactivation of the tumour suppressors p53 and Rb and activation of receptor tyrosine kinase pathways (Van Meir et al. 2010).

About 50% of all gliomas are GBMs, which can occur in any age group, but they are most commonly observed in 50-70 years old adults. The standard therapy of GBM includes surgical resection of the tumour, followed by radiation therapy, often in combination with chemotherapy. In many cases, however, tumour recurrences occur even outside of the region of prior resection and it is impossible to remove all tumour cells. Glioblastoma cells often migrate away from the primary tumour and form metastases within the brain, however they rarely spread outside the brain to distinct regions in the body (Salcman 2012). Due to the complex character of GBM and the non-efficient therapies, most of the patients have a poor prognosis and die of the disease within 14 months of diagnosis (Holland 2000; Zhang et al. 2003; Van Meir et al. 2010).

1.8 Aims of the thesis

GPR56 is a member of the novel family of adhesion G protein-coupled receptors. GPR56 plays a role during early brain development and mutations or loss of *Gpr56* expression result in a severe malformation of the brain.

The role of GPR56 in cancer is controversial, as the receptor can act as a tumour suppressor or promoter, depending on the cancer type and stage (Xu et al. 2006; Ke et al. 2007; Huang et al. 2008; Sud et al. 2006; Shashidhar et al. 2005). In highly invasive glioblastoma, GPR56 may act as a tumour promoter, as it is overexpressed and involved in adhesion signalling (Shashidhar et al. 2005). However, downstream signalling pathways induced by GPR56 are poorly understood and an activation of GPR56 by its potential ligand TG2 was not demonstrated to date. Understanding the signalling pathways induced by GPR56 and the potential role of the GPR56-TG2 interaction in cancer may provide valuable information for novel anti-cancer therapies, since GPCRs represent very interesting drug targets.

The main aim of this project was to characterise the interaction between TG2 and GPR56 and to investigate GPR56 downstream signalling. In order to achieve this aim, the following questions were addressed:

- Does TG2 activate GPR56-dependent signalling?
- Does GPR56 activation require specific domains or the catalytic activity of TG2?
- Are there other putative ligands for GPR56 among the family of transglutaminases?
- How do GPR56 mutations or domain deletions affect GPR56 activity and the interaction with TG2?
- What downstream signalling proteins are activated by GPR56?
- Is GPR56 internalised?
- Is TG2 internalised in a GPR56-dependent manner?
- What is the mechanism of GPR56 internalisation?
- What happens to endocytosed GPR56 and TG2?
- What is the role of GPR56 in glioblastoma?

CHAPTER 2:

Materials and methods

2 Material and methods

The formulations of the used solutions and buffers are summarised in Appendix I, the used chemicals are listed in Appendix II, as well as the consumables and laboratory equipment in Appendix III.

2.1 DNA manipulation

2.1.1 Agarose gel electrophoresis

Plasmid DNA was mixed with 6x DNA loading buffer (Promega) and loaded onto a 1 % (w/v) agarose gel containing 0.1 mg/ml ethidium bromide (Sigma-Aldrich) in 1x TAE buffer (40 mM Tris acetate, 1 mM EDTA). The DNA fragments were separated at a voltage of 100 V for 20-30 mins and visualized under UV light. 1 kb plus DNA marker (Invitrogen) was used to estimate the size and amount of DNA analysed. To purify DNA from agarose gels, the QIAquick gel extraction kit (QIAGEN) was used according to manufacturer’s instructions.

2.1.2 Restriction digest

2-5 µg plasmid DNA was mixed with 1 µl (20 U) of each restriction enzyme (New England Biolabs (NEB) or Promega) using the recommended NEB buffer and double distilled water to reach a final volume of 50 µl. The restriction mixtures were incubated at 37 °C for 1 h, separated by agarose gel electrophoresis and extracted from the gel as outlined in 2.1.1.

2.1.3 Ligation

5 µl of purified vector DNA, 4 µl of purified insert DNA fragment, 1x rapid ligation buffer (Promega) and 3 U of T4 DNA ligase (Promega) was mixed and incubated for 1 h at room temperature to perform ligation (20 µl reaction volume).

2.1.4 Transformation

5 µl of the ligation mixture was added to 100 µl frozen NovaBlue GigaSingles competent *E.coli* (Novagen, MerckKGaA) and incubated for 10 mins on ice. Heat shock transformation was performed at 37 °C for 1 min and cells were put back on ice immediately for 2 mins. Bacteria were streaked at varying dilutions on LB plates containing 50 µg/ml carbenicillin (Melford) using several plates and incubated overnight at 37 °C.

2.1.5 Identifying positive clones

Single colonies were picked using a sterile pipette tip and transferred into 3 ml LB medium containing 50 µg/ml carbenicillin. Bacteria were incubated at 37 °C and 220 rpm overnight. 1.5 ml of overnight bacterial culture was centrifuged at 4,000 rpm for 10 mins. The supernatants were discarded and the plasmid DNA was purified from the bacterial pellets using the QIAprep Spin MiniPrep Kit (QIAGEN) according to manufacturer’s instructions.

5 µl of purified plasmid DNA was cleaved with the same restriction enzymes that were used to generate complementary restriction sites within the vector and the insert DNA fragment (2.1.2), followed by agarose gel electrophoresis (2.1.1). A positive clone was identified as it contained a DNA insert fragment of the right size and was sent for dideoxy sequencing (MWG Operon).

2.1.6 Plasmid DNA midiprep

To amplify large amounts of DNA, a positive *E.coli* clone was grown overnight in 100 ml LB medium containing 50 µg/ml carbencillin at 37 °C and 220 rpm agitation. The bacterial suspension was centrifuged at 4,500 rpm for 20 mins to pellet *E.coli*. DNA was extracted from the pellet using the GenElute HP Plasmid Midiprep Kit (Sigma-Aldrich) according to manufacturer's instructions.

2.2 DNA mutagenesis

2.2.1 PCR reactions

In order to replace potential serine (S684, S685, S687, S689, S690, S691) and threonine (T688) phosphorylation sites in the C-terminal tail of GPR56 by alanine, three reverse primers were designed (Table 2.1). The wild type GPR56-pOTP7-CA plasmid was used as a template for the production of the T_{688}-A GPR56 mutant. To generate the $\Delta_{684\text{-}91}$S-A-GPR56 mutant, the $\Delta_{687/689}$S-A-GPR56 plasmid served as a template (generated by Dr. Vera Knäuper). The generated $\Delta_{684\text{-}91}$S-A-GPR56 mutant was used as a template for the production of the $\Delta_{684\text{-}91}$S/T-A-GPR56 mutant. For all PCR reactions the forward primer $GPR56_{for}$ was used.

The results of cloning the T_{688}-A GPR56, $\Delta_{684\text{-}91}$S-A-GPR56 and $\Delta_{687/689}$S-A-GPR56 mutants are discussed in Chapter 5.2.1.

Table 2.1 Oligonucleotides used for PCR mutagenesis

Reverse primer	**Primer sequence**
Primer #1 (T_{688}-A)	5’AAATCTAAGATGCGGCTGGACGAGGCGCTGCCCGAGCTGATGGGGAG3’
Primer #2 ($\Delta_{687/689}$S-A)	5’AAATCTAGAGATGCGGGCGGCAGCGGTGGCGCCAGCACCGATGGGGAGCCTGGC3’
Primer #3 ($\Delta_{687/689}$S/T-A)	5’AAATCTAGAGATGCGGGCGGCAGCGGCGGCGCCAGCACCGATGGGGAG3’
Forward primer	**Primer sequence**
GPR56for	5’AAAAGATCTAAAATGACTCCCCAGTCGCTGCTGCAGA3’

Primers were synthesised by MWG Operon and the PCR reactions were carried out using a 96-well thermal cycler (VWR). Table 2.2 outlines the composition of the PCR master mixes and table 2.3 the programmes used to amplify the DNA.

Table 2.2 Composition of PCR master mixes (50 µl reaction volume)

Component
1x Herculase II reaction buffer (Agilent Technologies)
300-700 ng Template DNA (GPR56-pOTP7-CA, $\Delta_{687/689}$S-A-GPR56 or Δ_{684-91}S-A GPR56)
1 mM dNTP mix (Agilent Technologies)
0.5 µM Reverse primer (#1, #2 or #3)
0.5 µM Forward primer (GPR56for)
1 U Herculase II Fusion DNA Polymerase (Agilent Technologies)
2% DMSO (Agilent Technologies)
Double distilled water up to a total volume of 50 µl

Table 2.3 PCR cycling parameters

Segment	Number of cycles	Stage	Temperature	Duration
1	1	Initialization step	95 °C	2 mins
2	20	Denaturation	95 °C	30 sec
		Annealing	63 °C	30 sec
		Elongation	72 °C	2 mins
3	1	Final elongation	72 °C	3 mins
4	---	Storage	4 °C	---

To remove primers, nucleotides, polymerases and salts from the PCR sample, the QIAquick PCR Purification kit (QIAGEN) was used according to manufacturer's instructions.

2.2.2 Generating an intermediate GPR56 expression vector

A GPR56 fragment (GPR56^f) lacking the C-terminal residues 564 to 693 was created by cleaving the wild type GPR56 expression vector pcDNA4-GPR56/V5-His with *Bam*H I and *Hind* III (2.1.2). The cleaved DNA fragment GPR56^f was purified using a 1 % agarose gel (2.1.1) and ligated into *Bam*H I and *Hind* III cleaved pcDNA4/V5-His (Invitrogen). The resulting intermediate expression vector pcDNA4-GPR56^f/V5-His was amplified as described above (2.1.4-2.1.6).

2.2.3 Restriction digest of PCR reactions

In order to reconstitute the C-terminal tail of GPR56^f, the 800 bp long, purified PCR products (2.2.1) were cleaved with *Xba* I/*Bam*H I/*Xho* I restriction enzymes (NEB) at 37 °C overnight, as PCR products need prolonged incubation times to ensure a complete digest. *Xho* I was added to the mixture to distinguish between wanted and unwanted fragments, as a digest with *Xba* I/*Bam*H I alone would result in the generation of two fragments of the same size (400 bp).

2.2.4 Purification of cleaved PCR products

The cleaved PCR products were separated using a 1% agarose gel (2.1.1). Due to the addition of *Xho* I to the digestion mixture, three fragments, one of 400 bp and two of 200 bp were produced. The 400 bp fragment was extracted from the gel and purified as described before (2.1.1).

2.2.5 Cloning of C-terminal GPR56 phosphorylation mutants

In order to extend the C-terminal end of truncated GPR56^{f} with mutant PCR products (2.2.4), the intermediate pcDNA4-GPR56^{f}-V5/His construct was cleaved with *Bam*H I and *Xba* I restriction enzymes (NEB) to generate complementary restriction sites. The cleaved DNA vector was purified from a 1% agarose gel (2.1.1). Cleaved vector and PCR fragments were ligated (2.1.2). The final products, pcDNA4-T$_{688}$A-GPR56/V5-His, pcDNA4-$\Delta_{684\text{-}91}$S-A-GPR56/V5-His and pcDNA4-$\Delta_{684\text{-}91}$S/T-A-GPR56/V5-His were amplified in *E.coli* (2.1.4-2.1.6) and sent for dideoxy sequencing to MWG operon.

2.3 Cell culture

All plastic ware used in tissue culture was obtained from Sarstedt Ltd., unless otherwise stated. Foetal bovine serum (FBS), Opti-MEM and advanced DMEM culture media, MEM non-essential amino acids, Penicillin/Streptomycin and trypsin/EDTA were purchased from Gibco, EMEM and DMEM culture media from Lonza, Hygromycin B and Blasticidin from Invitrogen and poly-L-lysine solution from Sigma-Aldrich.

2.3.1 Cell lines

Culture conditions for the cell lines used are outlined in table 2.4.

In general, cell lines were maintained at 37 °C in humidified air containing 5 % CO_2, and passaged every 4-5 days or upon confluency. Cells were washed once with PBS (without Ca^{2+} and Mg^{2+}), followed by incubation with 1 ml trypsin/EDTA per 75 cm^2 tissue culture flask for 5 mins at 37 °C. Trypsin activity was stopped by adding 7 ml of DMEM/10% FBS. Cells were collected by centrifugation for 5 mins at 1,500 rpm, medium removed and cells resuspended in growth medium and diluted in a ratio of 1:5 to 1:10, respectively.

Table 2.4 Culture conditions for cell lines.

Cell line	Origin	Medium
HEK293 Flip-In	Human embryonic kidney	90% DMEM, 10% FBS
HEK293 N-Strep/HA-GPR56/V5	Human embryonic kidney	90% DMEM, 10% FBS, 15 µg/ml blasticidin, 100 µg/ml hygromycin
U373	Human brain tumour (glioblastoma)	89% DMEM, 10% FBS, 1 % MEM non-essential amino acids
U373 shGPR56 (stably transfected)	Human brain tumour (glioblastoma)	89% DMEM, 10% FBS, 1 % MEM non-essential amino acids, 200 µg/ml hygromycin B
HCA2 TG2 sense (S)	Human fibroblasts	89% DMEM, 10% FBS, 1% Pen/Strep, 400 µg/ml geneticin
HCA2 TG2 antisense (As)	Human fibroblasts	89% DMEM, 10% FBS, 1% Pen/Strep, 400 µg/ml geneticin

2.3.1.1 HEK293 model system

The HEK293 Flip-In cell line was purchased from Invitrogen. The stable HEK293 N-Strep/HA-GPR56/V5 cell line inducibly expressing GPR56 was established by Dr Vera Knäuper. Briefly, full-length GPR56 cDNA was cloned into pcDNA5-FRT-TO (Invitrogen), followed by transfection and selection of the TET-on HEK293 Flp-In cell line according to the manufacturers' instructions (Invitrogen).

2.3.1.2 HCA2 fibroblasts

Stably transfected HCA2 cell lines were obtained from Prof. Daniel Aeschlimann. Briefly, the HCA2 strain of normal diploid fibroblasts was immortalised by stable transfection with amphotrophic retrovirus pBABE-hTERT (human telomerase). Immortalised HCA2 cells were then transfected with different expression constructs for stable expression of TG2 mRNA: one construct with the coding sequence for TG2 inserted in sense (TG2 overexpression) and the other construct with the coding sequence in antisense orientation (TG2 null). Stably transfected cells were isolated and maintained in selection medium containing 400 µg/ml geneticin (Stephens et al. 2004).

2.3.1.3 Glioblastoma cell line

The glioblastoma cell line U373 was purchased from the American Type Culture Collection (ATCC). U373 glioblastoma cells are human brain tumour cells derived from a grade IV glioblastoma. GPR56 is highly expressed in glioblastoma cells compared to non-tumourigenic brain tissue (Shashidhar et al. 2005) and therefore U373 cells were chosen as a model cell line to generate GPR56 knockdown cell lines.

2.3.1.3.1 Generating GPR56 knockdown cells

Two SureSilencing shRNA plasmids targeting GPR56 mRNA and a non-coding shRNA plasmid (negative control) were purchased from SABiosciences (QIAGEN) in order to stably transfect the glioblastoma cell line U373. The DNA sequences encoding the shRNAs are outlined in Appendix IV.

2.3.1.3.2 Linearization of shRNA plasmid DNA

2 µg of each shRNA plasmid DNA was cleaved with *Nae* I restriction enzyme (NEB) for 3 h at 37 °C as described in 2.1.2. *Nae* I was inactivated by incubation for 20 mins at 65 °C.

2.3.1.3.3 Phenol-chloroform extraction of shRNA plasmid DNA

The linearized shRNA plasmid DNA was diluted in double distilled water to a final volume of 500 µl. An equal amount of phenol:chloroform:isoamyl alcohol (25:24:1 v/v, Promega) was added and vortexed to mix the organic and water phases. The mixture was centrifuged for 3 mins at 13,000 rpm and the top aqueous phase containing the DNA was removed and transferred into a new microcentrifuge tube. 1/10 volume of 3 M sodium acetate (pH 5.5) and 2 volumes 100 % ethanol was added to the DNA and incubated at - 20 °C for 1 h. Precipitated DNA was collected by centrifugation for 30 mins at 13,000 rpm and 4 °C. The ethanol supernatant was carefully removed and the pellet dried for 30 mins at 37 °C. The linearized, purified DNA was resuspended in 40 µl double distilled water and stored at - 20 °C.

2.3.1.3.4 Stable transfection of cells

Cells were stably transfected using the reverse transfection protocol supplied by SABiosciences. 100 µl of serum-free Opti-MEM was pipetted into each well of a 24-well plate. 0.4 µg of linearized shRNA plasmid DNA was added and mixed by gently rocking the plate. FuGENE 6 Transfection Reagent (Promega) was pre-diluted 1:2 in fresh Opti-MEM, and 2.4 µl of the mixture was added to each well (1:3 ratio DNA:FuGENE 6), mixed by rocking the plate and incubated for 30 mins at room temperature to allow DNA-FuGENE-complex formation.

U373 glioblastoma cells were resuspended in culture medium to a density of $1.6x10^6$ cells/ml and 500 µl the cell suspension was added to the wells containing the FuGENE-DNA-complexes ($8x10^5$ cells/well). Cells were incubated for 24 h as they already reached confluency.

2.3.1.3.5 Hygromycin kill curve of U373 cells

In order to select for stably transfected cells, the hygromycin concentration killing all non-transfected cells was determined. $5x10^4$ non-transfected U373 cells were plated at a low density (~ 10 % confluence) in a 6-well plate containing growth medium supplemented with hygromycin B (Invitrogen) at final concentrations ranging from 0-800 µg/ml. Medium was changed every two days and cells were allowed to grow until the hygromycin-free cells reached confluency. The effective hygromycin concentration was determined at 200 µg/ml.

2.3.1.3.6 Selection of stably transfected cells

ShRNA transfected cells were re-plated onto 24-well plates at 10% confluency in growth medium containing 200 µg/ml hygromycin B. The medium was changed every 5-7 days, until small single cell colonies appeared.

2.3.1.3.7 Isolating single cell colonies

To lift single cell clones, the selection medium was taken off and cells were washed twice with PBS. Sterile cloning cylinders (internal diameter: 4.7 mm, height: 8 mm; Sigma-Aldrich) were placed over single colonies and sealed by dropwise adding 1 % (w/v) low-melting point agarose (Gibco-BRL) around the cylinders. 50 µl of accutase (Millipore) was dispensed into the cloning cylinders and incubated for 5 mins at 37 °C. According to the size of the colony, the cells were then transferred to individual wells of either 24- or 6-well plates containing selection medium that was changed every two days. Upon confluency, cells were transferred into bigger plates or tissue culture flasks.

2.4 Alkaline phosphatase-Amphiregulin (AP-AR) shedding assay

2.4.1 Transient transfection of HEK293 cells

Cells were seeded onto poly-L-lysine coated wells of a 24-well plate at a density of $1x10^5$ cells/well in 0.5 ml DMEM/10 % FBS and grown for 24 h. To co-transfect one well, 0.5 µg of a GPR56 expression construct and 0.25 µg of Alkaline Phosphatase-tagged Amphiregulin (AP-AR) were mixed with 2.25 µl FuGENE 6 transfection reagent (Promega) in 200 µl serum-free Opti-MEM. The mixture was incubated for 20 mins at room temperature to allow formation of DNA-FuGENE 6 complexes and added dropwise to the cells. After rocking the plate gently, the cells were incubated at 37 °C, 5% CO_2 for 48 h.

2.4.2 Inhibition of ADAM10 and ADAM17

ADAM inhibitors targeting ADAM10 (GI254023x) and ADAM10/17 (GW280264x) were obtained from Dr. Amour, GlaxoSmithKline (GSK).

Cells were transfected with wild type GPR56 and AP-AR as outline in 2.4.1. and 48 h later the experiments were started.

When ADAM inhibitors were used at a final concentration of 10 µM, cells were serum starved for 1 h in DMEM containing 10 µM ADAM inhibitor or DMSO solvent control. Medium was removed and cells were washed 1x with 250 µl serum-free Opti-MEM prior to incubation in serum-free, gassed Opti-MEM for 30 mins at 37 °C.

When ADAM inhibitors were used at a final concentration of 1 µM, cells were washed 1x with warm, serum-free advanced DMEM, followed by serum-starvation in advanced DMEM containing 1 µM ADAM inhibitor or DMSO solvent control for 1 h. The medium was removed and cells were stimulated with 20 µg/ml C_{230}-A TG2 or buffer control in the presence of ADAM inhibitors or DMSO solvent control in advanced DMEM for 1 h at 37 °C.

For experiments using an inhibitory ADAM17 antibody (Prof. G. Murphy, Cambridge, UK), cells were washed 1x with advanced DMEM and serum starved in the presence of 100 nM D1A12 ADAM17 inhibitory antibody or human IgG control for 1 h. Medium was removed and cells were treated with 20 µg/ml C_{230}-A TG2 or buffer control in advanced DMEM in the presence of 100 nM D1A12 ADAM17 inhibitory antibody or human IgG control for 1 h at 37 °C.

2.4.3 Treatment with potential ligands for GPR56

Cells were washed 1x with warm, serum-free advanced DMEM, followed by a serum-starvation step for 1 h in advanced DMEM. Medium was removed and cells were treated with different transglutaminases (Table 2.5) or collagen III in advanced DMEM for 1 h at 37 °C at the indicated final concentrations.

Table 2.5 Transglutaminases and their storage buffers.

Transglutaminase	Buffer
C_{230}-A TG2	20 mM Tris-HCl (pH 7.5), 300 mM NaCl, 1mM EDTA
TG2	10 mM Tris-HCl (pH 7.5), 300 mM NaCl, 1mM EDTA
OC-TG2	10 mM Tris-HCl (pH 7.4), 100 mM NaCl, 1 mM EDTA
C_{277}-S TG2	20 mM Tris-HCl (pH 7.5), 300 mM NaCl, 1mM EDTA
TG6	10 mM Tris-HCl (pH 7.8), 500 mM NaCl, 10 mg/ml sucrose
TG7	50 mM Tris-HCl (pH 8.0), 10 mM reduced glutathione
∆FXIII	50 mM Tris-HCl (pH 8.0), 300 mM NaCl, 15 % glycerol

2.4.4 Measurement of AP-activity in the medium

At the end of the stimulation period, medium was collected and transferred into 1.5 ml tubes, followed by centrifugation for 3 mins at 13,000 rpm to remove cells. 50 µl of AP-AR containing supernatant was placed in duplicates in a 96-well plate. Alkaline phosphatase substrate solution

(2 mg/ml *p*-NPP; Sigma-Aldrich) was prepared by mixing 600 µl of 50 mg/ml *p*-NPP with 15 ml AP buffer (100 mM Tris-HCl (pH 9.5), 100 mM NaCl, 20 mM $MgCl_2$). 150 µl of substrate solution was added to the supernatants in the plate (final concentration of *p*-NPP on 96-well plate was 1.5 mg/ml) and AP-activity was determined. The hydrolysis of *p*-NPP to *p*-nitrophenol was measured at 405 nm every 10 to 30 mins over a period of several hours using a microplate reader (OMEGA plate reader, BMG Labtech).

2.4.5 Statistical analysis

The GraphPad Prism software was used to analyse data by One-way Anova with Tukey post-test. P values below 0.05 (95 % confidence interval) were considered significant. For the final analysis of every experiment, at least 3 independent shedding assays were performed, with usually 4 repeats per condition and construct in each assay (n=12). Data are shown as mean +/- SEM.

2.5 Protein analysis by Western Blotting

2.5.1 Production of cell lysates

A “GPCR lysis buffer” containing 50 mM HEPES (pH 7.5), 10 mM NEM, 100 µM benzamidine, 0.5 % Nonident P-40, 250 mM NaCl, 2 mM EDTA, 10% (v/v) glycerol was produced. For the production of cell lysates, 10 µl of a protease inhibitor cocktail (#P8340 from Sigma-Aldrich; final concentrations: 1.04 mM AEBSF, 0.8 µM aprotinin, 40 µM bestatin, 14 µM E-64, 20 µM leupeptin, 15 µM pepstatin A) and 5 µl Na_3VO_4 (final concentration = 1.5 mM; Sigma-Aldrich) were added to 1ml of the buffer.

After removing the medium, the cell monolayer was lysed with 35 µl lysis buffer per well of a 24-well plate and incubated for 30 mins on ice. Cell lysates were transferred into 1.5 ml microcentrifuge tubes and centrifuged at 13,000 rpm for 5 mins to remove cell debris. The supernatants were stored at - 80 ˚C to avoid protein degradation.

2.5.2 Protein concentration assay (DC assay)

Protein concentrations were determined using the colorimetric DC protein assay (Bio-Rad). A protein standard curve was created by analysing different BSA concentrations ranging from 0.2 - 1.5 mg/ml for each assay. 5 µl of each protein standard and sample were pipetted in duplicates into a 96-well plate, then 25 µl of Reagent A’ (20 µl Reagent S in 1 ml Reagent A) and 200 µl of Reagent B was added per well. The plate was gently mixed by rocking and incubated for 15 mins at room temperature. The absorbance was measured at 570 nm and protein concentrations determined from the standard curve.

2.5.3 SDS polyacrylamide gel electrophoresis (SDS-PAGE)

50 µg of cell lysate or 25 µl of cell supernatant was diluted 1:2 using 2x SDS reducing sample buffer. To denature proteins, the mixtures were incubated at 95 °C for 5 mins. To analyse C-GPR56 by western blotting, the samples were incubated for 10 mins at room temperature in order to avoid induction of aggregation by boiling. Samples were then centrifuged for 1 min at 13,000 rpm, followed by separation using 4 % stacking and 10 %, 11 % or 12.5 % resolving SDS polyacrylamide gels at 50-100 mA (max 250 V) until the dye front reached the bottom of the gel.

2.5.4 Western blotting

Polyvinyliden-difluorid (PVDF) membranes (Thermo Fisher Scientific) were activated for 20 sec in methanol, followed by equilibration in transfer buffer in conjunction with the SDS polyacrylamide gels. Proteins were then transferred to the PVDF membrane at 75 V for 1 h or at 15-20 V overnight (at least 16 h) in a transfer cell (Bio-Rad) containing transfer buffer and a cooling block. Non-specific protein binding sites of the membrane were blocked by incubating the membrane for 1 h with 5 % skimmed milk dissolved in TBST using a shaker. The membrane was incubated for 4 h or overnight with the primary antibody diluted in 5 % skimmed milk/TBST on a rotator plate. Membranes were washed 3x 5 mins in 1x TBST and incubated for 1 h at room temperature with the secondary antibody diluted in 5 % skimmed milk/TBST on a rotator plate. All primary and secondary antibodies used for Western Blotting are outlined in Table 2.6. Membranes were washed 4x 10 mins with 1x TBST on a shaker. Membranes were removed and 1 ml EZ-ECL reagent (Solution A:Solution B 1:2; Geneflow) was added and incubated for 1 min. Membranes were exposed to ECL hyperfilms (Amersham Bioscience) and developed in a CURIX 60 automated developer (Agfa HealthCare GmbH).

Table 2.6 Antibodies used for Western Blotting

	Primary antibodies		
Antibody	**Working dilution**	**Working concentration**	**Manufacturer**
Sheep anti-GPR56	1:1,000	200 ng/ml	R&D Systems
Mouse anti-V5	1:5,000	20 ng/ml	Invitrogen
Mouse anti-TG2 (CUB)	1:1,000	200 ng/ml	Thermo Scientific
Mouse anti-GAPDH	1:5,000	12.5 ng/ml	Sigma-Aldrich
	Secondary antibodies		
Antibody	**Working dilution**	**Working concentration**	**Manufacturer**
Donkey anti-sheep-HRP	1:5,000	20 ng/ml	Jackson ImmunoResearch
Donkey anti-mouse-HRP	1:5,000	16 ng/ml	Jackson ImmunoResearch

2.6 Immunofluorescence

All primary and secondary antibodies used for immunofluorescence are outlined in table 2.7. Cells were analysed using a Leica SP5 confocal microscope (Leica Microsystems). Images were acquired with a 63x oil immersion objective, using the 488, 543 and 633 laser lines, respectively.

Table 2.7 Antibodies used for immunofluorescence

Primary antibodies			
Antibody	**Working dilution**	**Working concentration**	**Manufacturer**
Sheep anti-N-GPR56	1:200	1 µg/ml	R&D Systems
Mouse anti-V5	1:500	1 µg/ml	Invitrogen
Mouse anti-Flag M2	1:200	1 µg/ml	Sigma-Aldrich
Rabbit anti-LAMP1	1:200	5 µg/ml	Sigma-Aldrich
Mouse anti-LAMP2	1:200	5 µg/ml	DSHB
Mouse anti-TG2 (CUB7402)	1:200	1 µg/ml	Thermo Scientific
Rabbit anti-Caveolin-1	1:200	5 µg/ml	Abcam
Secondary antibodies			
Antibody	**Working dilution**	**Working concentration**	**Manufacturer**
Donkey anti-sheep AF 568	1:500	4 µg/ml	Invitrogen
Donkey anti-mouse AF 594	1:500	4 µg/ml	Invitrogen
Donkey anti-mouse AF 488	1:500	4 µg/ml	Invitrogen
Donkey anti-rabbit AF 488	1:500	4 µg/ml	Invitrogen

2.6.1 Immunodetection of GPR56 in eukaryotic cells

2.6.1.1 Endogenous GPR56 expression in U373 cells as detected with N-GPR56 antibody

U373 parental or stable GPR56 knockdown cells were plated onto poly-L-lysine coated glass coverslips in 24-well plates at a density of $0.1x10^5$ cells/well in 0.5 ml DMEM/10% FBS. Detection of endogenously expressed GPR56 was performed 72 h after seeding. Cells were washed using PBS and fixed with 4% paraformaldehyde (PFA)/PBS for 5 mins. Cells were washed 3x with PBS for 5 mins, blocked for 30 mins in 1% BSA/PBS prior to incubation with primary sheep anti-N-GPR56 antibody (1 µg/ml) for 2 h in a humidified chamber. Cells were washed 3x with PBS, incubated for 1 h with secondary donkey anti-sheep Alexa Fluor 568 antibody (4 µg/ml) in blocking buffer and washed 3x with PBS for 5 mins. Nuclei were counter stained with DAPI-containing vectashield mounting medium (Vector Laboratories).

2.6.1.2 GPR56 expression in transiently transfected HEK293 cells

Cells were plated onto poly-L-lysine coated glass coverslips in a 24-well plate at a density of $0.3x10^5$ cells/well in 0.5 ml DMEM/10% FBS. The next day, cells were transfected. To transfect one well, 0.5 µg of a GPR56 expression construct was mixed with 1.5 µl FuGENE 6 transfection reagent (Promega) in 200 µl serum-free Opti-MEM. The mixture was incubated for 20 mins at room temperature to allow the formation of DNA-FuGENE complexes. 200 µl was then added dropwise to the cells. Two days post-transfection, the extracellular N-terminus of GPR56 was detected on fixed cells as described in 2.6.1.1.

The C-terminal domain of GPR56 was detected via the V5 epitope-tag. Therefore, fixed cells were permeabilised for 10 mins using 0.5% saponin/PBS. Cells were washed 3x with PBS and blocked with 1%

BSA/PBS for 30 mins. Primary mouse anti-V5 antibody (1 µg/ml) was incubated for 2 h in a humidified chamber prior to the appropriate wash steps. Donkey anti-mouse Alexa 594 (4 µg/ml) was used as secondary antibody and incubated for 1 h. Cells were washed 3x with PBS and nuclei stained with DAPI.

2.6.2 Immuno-colocalisation of GPR56 and TG2 in stable HEK293 cells

HEK293 cells inducibly expressing GPR56 were seeded at 0.3×10^5 cells per well onto poly-L-lysine coated glass coverslips in a 24-well plate in 0.5 ml DMEM/10% FBS without antibiotics. The next day, GPR56 expression was induced in half the wells by adding DMEM/10% FBS medium supplemented with 10 µg/ml doxycycline. The second half of the plate was cultured in DMEM/10% FBS alone and was used as a GPR56 negative control. After 48 h, cells were washed with serum-free advanced DMEM and serum starved for 1 h at 37 °C prior to C_{230}-A TG2 treatment (20 µg/ml) for 5 sec, 15 mins and 30 mins at 37 °C. Cells were fixed as described in 2.6.1.1. In order to follow internalisation of N-GPR56, cells were also permeabilised as outlined in 2.6.1.2. Following a blocking step for 30 mins in 1% BSA/PBS, TG2 and GPR56 were stained using the primary mouse anti-TG2 CUB7402 antibody at 1 µg/ml and the primary sheep anti-N-GPR56 at 1 µg/ml for 2 h in a humidified chamber. Donkey anti-mouse Alexa 488 and donkey anti-sheep Alexa 568 secondary antibodies were used at 4 µg/ml dilution and incubated for 1 h. Coverslips were washed 3x with PBS and mounted onto slides using vecta shield containing DAPI.

2.6.3 SNAP-tag staining of GPR56 in HEK293 cells

Cells were plated onto poly-L-lysine coated glass coverslips in a 24-well plate at a density of 0.3×10^5 cells/well in 0.5 ml DMEM/10% FBS. The next day, four wells were transfected with 2 µg SNAP-GPR56/V5 (or SNAP-β2-adrenergic receptor as control) as described in 2.4. 48 h post-transfection, cells were washed with serum-free advanced DMEM and serum starved for 1 h at 37 °C in advanced DMEM. In the meantime, 1 µl of 1 mM SNAP-surface substrate (in DMSO; NEB) was diluted in 1 ml advanced DMEM. Medium was removed from the cells, 250 µl of 1 µM SNAP-substrate solution was added and incubated for 15 mins at 37 °C or 4 °C, as indicated. SNAP-tag surface substrates 488, 549 or 647 were used. Cells were washed 3x with 0.5% BSA/advanced DMEM to remove excessive SNAP-tag surface substrate, followed by 1x wash in serum-free advanced DMEM. Cells were then ready for further treatments as outlined below.

2.6.3.1 Immunolocalisation of TG2

SNAP-surface label 647 (NEB) was used to stain SNAP-GPR56 for 15 mins at 4 °C (2.6.3), followed by pulse-treatment with 20 µg/ml C_{230}-A TG2 for 5 sec. Medium was removed and cells fixed immediately to investigate cell surface co-localisation of GPR56 and TG2. In order to follow receptor internalisation, cells were incubated in serum-free medium for up to 1 h at 37 °C following TG2 treatment. Cells were fixed, permeabilised and blocked as described above. TG2 was detected using the mouse anti-TG2 CUB7402 antibody at 1 µg/ml as described in 2.6.2. Either donkey anti-mouse Alexa 488 or donkey anti-mouse Alexa 594 secondary antibodies were used at 4 µg/ml dilution.

2.6.3.2 Immuno-colocalisation of TG2 and lysosomes or caveolae

Cells were stained with SNAP-surface substrate 647 (NEB) and treated with C_{230}A-TG2 as described in 2.6.3.1 and cells were incubated in serum-free medium for up to 6 h prior to fixation (2.6.1). For visualization of late endosomes/early lysosomes, fixed and permeabilised cells were stained with rabbit anti-LAMP1 (5 µg/ml) or mouse anti-LAMP2 (5 µg/ml) antibodies for 2 h in a humidified chamber. For caveolae staining, a rabbit anti-Cav1 antibody (5 µg/ml) was used and incubated for 2 h. In both cases, donkey anti-rabbit Alexa 488 served as secondary antibody conjugate and was incubated for 1 h. Cells were co-stained for TG2 as described in 2.6.2. All wash steps were carried out as explained in 2.6.1.1.

2.6.3.3 Co-staining of transferrin receptors

SNAP-GPR56 transfected cells were serum starved for 1 h. Transferrin receptor/Transferrin-488 complexes were formed by incubating cells with 10 µg/ml Transferrin-488 (Molecular probes, Invitrogen) for 30 mins at 4 °C in cold advanced DMEM. Cells were washed 3x in ice-cold PBS, prior to staining with SNAP-surface substrate 647 for 15 mins at 4 °C, as described in 2.6.3. Cells were pulse treated with 20 µg/ml C_{230}-A TG2 for 5 sec, fixed directly with 4% PFA/PBS or incubated in serum free medium for 15 mins prior to fixation. Cells were washed 3x with PBS and nuclei stained with DAPI.

2.6.3.4 Inhibition of endocytosis with sucrose

Following serum starvation for 30 mins in 0.45 M sucrose in advanced DMEM, cells were stained with SNAP-surface substrate 647 (NEB) for 15 mins at 4 °C (2.6.3) and pulse treated with 20 µg/ml C_{230}-A TG2 for 5 sec. Cells were either fixed with 4% PFA/PBS immediately, or incubated in advanced DMEM in the presence or absence of 0.45 M sucrose for 30 mins prior to fixation, followed by permeabilisation in 0.5 % saponin/PBS. Cells were blocked as described above in 1% BSA/PBS and TG2 was detected using mouse anti-TG2 CUB7402 antibody at 1 µg/ml and incubated for 2 h. Donkey anti-mouse Alexa 594 secondary antibody was used at 4 µg/ml dilution and incubated for 1 h. Coverslips were washed 3x with PBS and mounted onto slides using vecta shield containing DAPI.

CHAPTER 3:

Investigations of GPR56 downstream signalling using an AP-AR shedding assay

3 Investigations of GPR56 downstream signalling using an AP-AR shedding assay

3.1 Introduction

Adhesion GPCRs (aGPCRs) are the second biggest family of GPCRs, but they are by far the most poorly understood. Most of aGPCRs are still considered orphan receptors with no known ligands. Therefore, aGPCRs are difficult to study.

In recent years, the major approach to de-orphanise aGPCRs was to use soluble, recombinant protein probes, consisting of the ligand binding N-terminal ectodomain (ECD) of the aGPCR fused to a truncated Fc-fragment with an optional C-terminal biotinylation signal sequence (Lin et al., 2009; Lin, et al., 2005). These Fc-fusion proteins are used to isolate binding partners of the aGPCR.

In order to de-orphanise GPR56, this “ligand fishing” approach was applied by several groups using different N-GPR56-Fc probes. Xu and colleagues (2006) used mGPR56^{N}-hFc to identify an ~80 kDa ligand from extracted mouse lungs, which was identified as TG2.

Li et al. (2008) used an mGPR56^{N}-mFc probe to find potential ligands for GPR56 in mouse brain. The probe bound to the pial basement membrane (BM) in the cerebral cortex and this interaction was entirely lost or discontinuous on brain sections from *Gpr56*$^{-/-}$ mice. The results indicated a GPR56-dependent expression of the putative ligand and partial breakdown of the pial BM due to GPR56 depletion. The nature of the potential ligand was not characterised in this study (Li et al. 2008), but was later identified in meningeal fibroblasts (MFs) as the ECM component collagen III (Luo et al. 2011).

Chiang et al. (2011) identified a third potential ligand for GPR56, which was not TG2. Using an hGPR56-mFc fusion protein, the unknown binding partner was detected in several cell lines. It was described as a trypsin-sensitive cell surface protein and the interaction with GPR56 was EDTA- and EGTA-sensitive, but was restored by the addition of Ca^{2+} or Mg^{2+}. However, its identity remained elusive to date. The identified binding partner might be an integrin, as their receptor function is dependent on the presence of Ca^{2+} and Mg^{2+} (Leitinger et al., 2000). Moreover, Jeong et al. (2013) revealed a link between GPR56 and $\alpha_3\beta_1$-integrin, as double knockout mice showed an even more severe cortical malformation than *Gpr56*$^{-/-}$ single knockout mice. However, $\alpha_3\beta_1$-integrin does not bind to the GPR56 ligand collagen III and it was not shown whether $\alpha_3\beta_1$-integrin may directly interact with GPR56. Thus it is not clear, how the two transmembrane receptors function together. Moreover, TG2 was shown to interact with β_1-, β_3-, and β_5-integrins and acts as a co-receptor for ECM proteins (Iismaa et al. 2006; Akimov et al. 2000). Thus, the binding partner identified by Chiang et al. (2011) might be a TG2-bound integrin.

Using Co-IP experiments, Little et al. (2004) identified the tetraspanin CD81 in a complex with CD9 as interacting partners of GPR56. A complex formation between CD81/9, GPR56 and $G\alpha_{q/11}$-proteins was described, but a signalling outcome as a result of the protein association was not shown.

The first real evidence for a GPR56-dependent signalling response was presented by Shashidhar et al. (2005), who showed that overexpression of GPR56 increased the activity of NF-κB, PAI-I and TCF response elements, all of which have been implicated in tumorigenesis and adhesion. Iguchi et al. (2008) then showed that the GPR56-dependent transcription through activation of NF-κB and SRE responsive elements was mediated by $G\alpha_{12/13}$ and Rho signalling. However, co-expression of TG2 did not increase SRE-mediated transcriptional activity.

Kim et al. (2010) also showed an increased transcriptional activity of SRE, E2F, NFAT response elements and COX2, iNOS, VEGF promoters following GPR56 overexpression. These signalling pathways are involved in cell proliferation, invasion, angiogenesis and tumour growth, respectively.

Regarding ligand-induced responses mediated through GPR56, Iguchi et al. (2008) demonstrated for the first time that treatment of GPR56-expressing cells with a self-made, polyclonal anti-N-GPR56 antibody elevated Rho activation and GPR56-mediated transcriptional activity of NF-κB and SRE responsive elements. Additionally, anti-N-GPR56 treatment inhibited migration of neural progenitor cells (NPCs). Luo and colleagues (2011) then showed that treatment of NIH/3T3 cells as well as NPCs derived from *Gpr56*$^{+/-}$, but not *Gpr56*$^{-/-}$ mice, with recombinant human collagen III also activated Rho signalling. GPR56-KD by shRNA, as well as the expression of a dominant negative mutant of $G\alpha_{13}$ ablated GPR56-dependent activation of RhoA by collagen III. Supporting evidence for the inhibition of migratory signals following the interaction between collagen III and GPR56 was presented from neurosphere migration assays. Collagen III treatment of neurospheres derived from *Gpr56*$^{+/-}$ mice, but not *Gpr56*$^{-/-}$ mice, inhibited migration, again indicating that GPR56 expression was required (Luo et al. 2011).

This chapter introduces a shedding assay that enables the investigation of GPR56 signalling. A very similar approach was described by Inoue et al. (2012) who tested 116 different GPCRs with known ligands using a TGF-α shedding assay, by measuring GPCR activation as ectodomain (ECD) shedding of a membrane-tethered proform of Alkaline Phosphatase-tagged TGF-α (AP-TGF-α). Likewise, the principle of the assay used in this project is based on GPR56-induced shedding of pro-AP-Amphiregulin (AP-AR) and quantification of the released AP-AR ECD in the conditioned medium.

Among the 116 GPCRs tested by Inoue et al. (2012), 75 were active in their assay. Interestingly, GPCRs known to couple $G\alpha_{12/13}$ and $G\alpha_q$ induced potent AP-TGFα shedding, whereas $G\alpha_i$- and $G\alpha_s$-coupled receptors induced only weak shedding. The results indicated that the TGF-α shedding assay, which relies on the same principle as the AP-AR shedding assay used here, represented a very useful and sensitive tool to measure signalling of $G\alpha_{12/13}$- and $G\alpha_q$-coupled receptors such as GPR56.

In this project, the AP-AR shedding assay was thus used to investigate the signalling capacity of GPR56 in non-stimulated and stimulated conditions. The assay was also used to identify potential downstream pathways involved in AP-AR shedding. HEK293 cells were chosen as a model cell line, as they are easy to culture and transfect. Moreover, as shown by Inoue and colleagues (2012) who compared 6 different cell lines, HEK293 cells showed low endogenous AP-activity, the highest expression of the ADAM substrate chosen (AP-TGF-α) and showed the most potent shedding response of AP-TGF-α to TPA-stimulation.

3.1.1 Aims of the chapter

- To establish a sensitive and reliable, cell-based assay in order to investigate GPR56 signalling in response to treatment with potential ligands.
- To identify the metalloproteinase involved in GPR56-dependent shedding of amphiregulin.
- To identify signalling pathways downstream of GPR56.

3.2 Results

3.2.1 Principle of the AP-AR shedding assay

Investigating migration of keratinocytes from spheroids placed on TG2-containing fibroblast matrices, Edwards (2010) showed that extracellular TG2 activates ADAM17-mediated cleavage of EGF-like ligands in keratinocytes. This led to activation of the EGFR and subsequent keratinocyte migration and proliferation. It was speculated that GPR56, expressed on the keratinocyte cell surface, might represent the missing link as a binding partner for matrix TG2, activating the intracellular signalling cascades that lead to EGFR transactivation (Edwards 2010).

In order to investigate signalling through GPR56, a shedding assay was established based on the idea that GPR56 would activate a metalloproteinase leading to cleavage of an EGFR ligand (Inoue et al. 2012; Edwards 2010) (Fig. 3.1 A). Shedding was measured by monitoring the activity of released alkaline phosphatase-tagged amphiregulin (AP-AR), as an example of an ADAM substrate (Sahin et al. 2004).

The first step in order to optimise the assay was to investigate whether GPR56 was constitutively active in non-stimulated conditions. Therefore, HEK293 cells were co-transfected with AP-AR and GPR56 or the negative control N-GPR56, consisting of the ECD up to the GPS cleavage site of GPR56 (aa1-382). Two days post-transfection, GPR56-dependent activation of ADAM(s), leading to the release of AP-AR ECD, was determined by measuring changes in OD_{405nm} due to hydrolysis of the AP substrate *p*-NPP.

The example in figure 3.1 B&C shows a single representative shedding assay, in which cells were serum starved for 1 h, followed by incubation in serum-free medium for 1 h. This combination of serum starvation and subsequent incubation (or ligand treatment) was found to be optimal, ensuring that the release of AP-AR from the cell membrane was assayed in the linear range prior to substrate depletion (data not shown). It is also in good agreement with the experimental regimen used by Inoue et al. (2012).

As shown in figure 3.1 C, *p*-NPP hydrolysis was 2.8-fold higher in non-stimulated, GPR56 co-transfected cells compared to N-GPR56 expressing cells. This result indicated that overexpression of GPR56 in HEK293 cells leads to AP-AR shedding, reflecting a high auto-activity of the receptor in this assay. This is in good agreement with previous literature reports for GPR56 (Iguchi et al. 2008; Shashidhar et al. 2005) and other adhesion GPCRs being auto-active (Simundza and Cowin 2013).

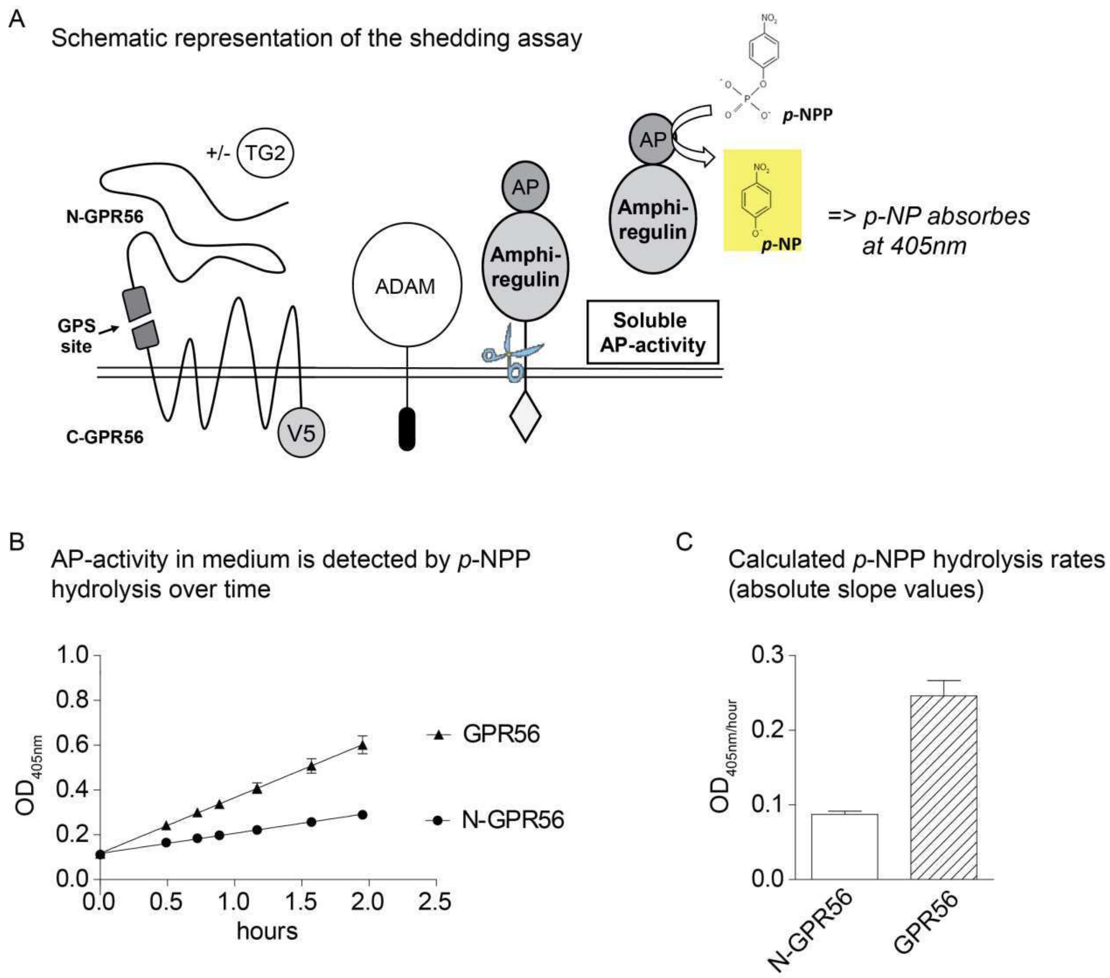

A Schematic representation of the shedding assay

B AP-activity in medium is detected by *p*-NPP hydrolysis over time

C Calculated *p*-NPP hydrolysis rates (absolute slope values)

Figure.3.1 Principle of AP-AR shedding assay and data analysis.

(A) Schematic of the assay. GPR56 induces ADAM-dependent shedding of membrane-bound AP-AR. Release of AP-AR ECD was quantified by collecting conditioned medium and measuring AP-activity based on *p*-NPP hydrolysis (production of yellow *p*-NP).

(B) Exemplary analysis of *p*-NPP hydrolysis in conditioned medium. HEK293 cells expressing GPR56 and AP-AR were serum starved for 1 h, followed by incubation in serum-free medium for 1 h. Conditioned medium was transferred into a 96-well pate, *p*-NPP substrate added and AP-activity measured by monitoring the colorimetric reaction of AP (OD_{405nm}) using an optical plate reader. Linear regression of the change in absorbance over time was performed using GraphPad Prism.

(C) The calculated slopes of the hydrolysis reaction shown in (B) represent the *p*-NPP hydrolysis rates ($OD_{405nm/hour}$) due to AP-AR ECD activity released into medium. A single representative experiment with 4 repeats for each construct is shown (n=4) and data are presented as mean +/- SEM.

3.2.2 Validation of the GPR56 signalling response

3.2.2.1 C_{230}-A TG2 activates GPR56

The section above outlined the principle of the shedding assay used to investigate signalling through GPR56 in transiently transfected cells. The first experiments using this assay already indicated that GPR56 was auto-active (Fig. 3.1 C). The next step was to investigate whether GPR56 activity could be further stimulated by treatment with its potential ligand TG2.

As the cell-based shedding assay was performed in an extracellular, oxidative environment, an oxidation-resistant cysteine-to-alanine mutant TG2 (C_{230}-A TG2) was used in most of the assays. At this stage it was unclear, whether catalytic activity of TG2 and therefore a certain conformation would be relevant for binding and activation of GPR56. The C_{230}-A TG2 mutant was used, as it is less prone to oxidation and disulfide bond formation, hence catalytic inactivation (Stamnaes et al., 2010). The catalytic activity of C_{230}-A TG2 under the experimental conditions of the shedding assay was demonstrated using a real-time fluorescence assay, which measures TG-dependent isopeptidase activity. These experiments showed that the activity of C_{230}-A TG2 was comparable to WT-TG2 (Adamczyk 2013; data not shown).

Figure 3.2 shows the final analyses of experiments in which HEK293 cells co-transfected with N-GPR56 and AP-AR or GPR56 and AP-AR were compared.

Two days post-transfection, cells were serum starved and treated with 20 µg/ml C_{230}-A TG2 for 1 h. In order to overcome variance resulting from differences in transfection efficiencies between the single experiments, the *p*-NPP hydrolysis rate of each experimental repeat was normalised to 1 for the non-stimulated GPR56 transfection control. The relative ratios between experimental conditions and controls were thus determined, allowing for inter-assay comparisons and subsequent statistical evaluation of results.

When compared to N-GPR56, the *p*-NPP hydrolysis rate in medium of cells expressing GPR56 was ~70 % higher when treated with control buffer, indicating activation of shedding by GPR56 (Fig. 3.2). Thus, the data confirmed that GPR56 had a high basal activity. Shedding was further increased by about 45 % in GPR56 transfected cells upon C_{230}-A TG2 stimulation, whereas N-GPR56 transfected cells showed no response to C_{230}-A TG2 treatment. The endogenous AP-activity measured in non-transfected cells was negligible.

These experiments indicated that GPR56 overexpression activates shedding of amphiregulin in transiently transfected HEK293 cells due to the high basal activity of the receptor and the data showed that C_{230}-A TG2 acts as an agonist for GPR56.

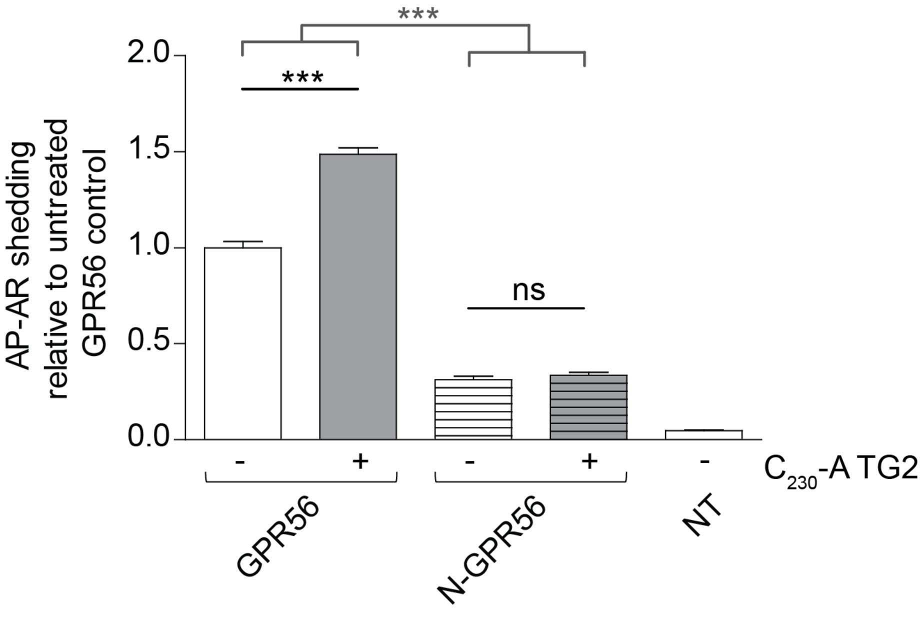

Figure 3.2 Overexpression of GPR56 activates shedding of AP-AR which is further increased by C_{230}-A TG2 treatment.

Cells were co-transfected with GPR56 and AP-AR or N-GPR56 and AP-AR, or left non-transfected (NT). 48 h later, cells were serum starved for 1 h, followed by treatment with 20 µg/ml C_{230}-A TG2 or control buffer for 1 h.

Data presented show mean of 3 to 6 independent experiments with 4 repeats each +/- SEM (n=12 to 24). Statistical significance denoted as follows: ***, $p<0.001$; ns, non-significant.

In order to verify that GPR56 and N-GPR56 were expressed in co-transfected cells, total lysates of the cells used for the AP-AR shedding assay were analysed by western blotting. The expression of N-GPR56 and GPR56 in cell lysates was compared using anti-N-GPR56 (Fig. 3.3 A), anti-V5 (Fig. 3.3 B) and anti-TG2 (Fig. 3.3 C) antibodies.

Analysis using anti-N-GPR56 antibody showed a banding pattern for wild type GPR56 consisting of 4 main bands running at approximately 60, 65, 70 and 75 kDa. The latter band likely represents uncleaved full-length GPR56. The lower running bands probably reflect variation in posttranslational modifications of cleaved N-GPR56, as there are 7 N-glycosylation sites present in the ECD and in addition those N-linked sugars can carry several sialic acid moieties (Jin et al. 2007). This banding pattern is in good agreement with previous reports from the literature (Chiang et al., 2011; Jin et al., 2007; Paavola et al., 2011).

Cells expressing N-GPR56 showed one major band running between 60-65 kDa and a high molecular weight band at ~180 kDa, probably representing polyubiquitinated or multimeric protein. It must be noted that this band was only detected, when lysates were analysed using non-boiling conditions. Treatment with C_{230}-A TG2 did not influence the banding pattern detected with anti-N-GPR56 antibody, indicating no crosslinking of proteins by TG2, although I cannot preclude that a small amount of crosslinking occurs.

Staining with anti-V5 antibody (Fig. 3.3 B) showed 3 major bands for GPR56 running at ~ 27, 50 and 75 kDa. The latter band most likely represents full length GPR56, as it was the same band detected with the anti-N-GPR56 antibody (Fig. 3.3 A). The bands running at 27 and 50 kDa probably represent monomeric and dimeric C-GPR56. Again, this banding pattern is in good agreement with reports from the literature (Chiang et al. 2011). Note that detection of C-GPR56, especially the monomeric isoform, required that protein samples were incubated in SDS sample buffer without heat treatment in order to avoid protein aggregation, as shown by others (Chiang et al. 2011). Interestingly, expression levels of dimeric C-GPR56 were reduced in GPR56 expressing cells following treatment with C_{230}-A TG2, potentially indicating elevated receptor internalisation and degradation. Lysates of N-GPR56 expressing cells were negative for anti-V5 staining, as N-GPR56 carries a C-terminal Flag-tag (Fig. 3.3 B).

Analyses of cell lysates using the anti-TG2 antibody showed that N-GPR56 and GPR56 expressing cells were negative for endogenous TG2 expression, as shown for HEK293 cells by others (Cho et al. 2010; D’Eletto et al. 2012). In lysates treated with C_{230}-A TG2, a major band running at ~80 kDa for monomeric TG2, as well as higher molecular weight bands running between ~180-260 kDa were present, probably representing crosslinked dimeric and multimeric TG2, respectively. It must be noted that prior to preparation of the cell lysates, the supernatants were just removed and cells were not washed extensively, thus TG2 was found in lysates of GPR56 as well as N-GPR56 expressing cells treated with C_{230}-A TG2. In addition, TG2 could potentially be matrix bound and soluble ECM proteins may be present in the cell lysates. However, confocal analysis of GPR56-expressing HEK293 cells treated with C_{230}-A TG2 showed that TG2 was only cell surface-associated (see Chapter 6).

The supernatants used in the AP-AR shedding assay were also analysed by western blotting for GPR56 secretion and TG2 using anti-N-GPR56 (Fig. 3.3 D) and anti-TG2 (Fig. 3.3 E) antibodies, respectively. Staining of conditioned medium with anti-N-GPR56 showed a specific band running at 78 kDa in N-GPR56 transfected cells, whereas GPR56 expressing cells were negative, irrespective of TG2 treatment (Fig. 3.3 D). Using anti-TG2 antibody, a major band at 80 kDa for monomeric TG2, a band at 180 kDa representing dimeric TG2 and a faint band at 55 kDa likely representing TG2 lacking the β-barrel domains was found in supernatants of cells treated with C_{230}-A TG2.

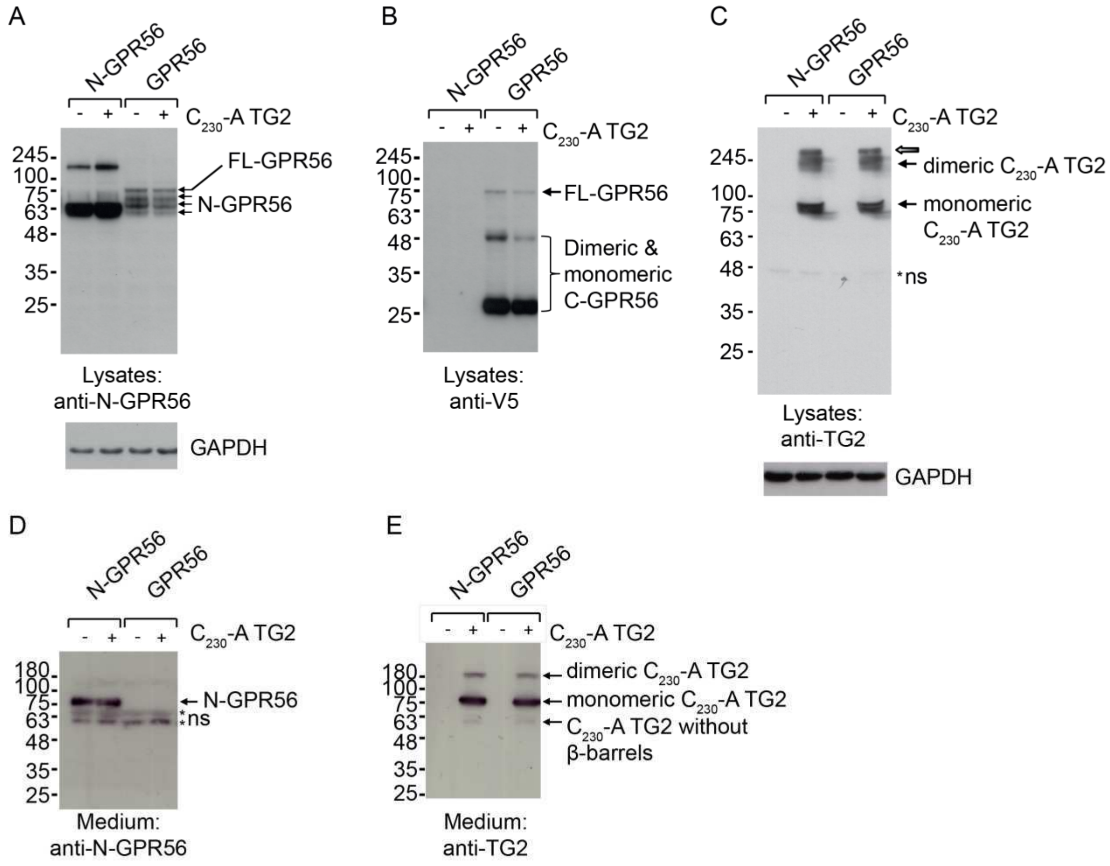
A
N-GPR56
GPR56
- + - + C230-A TG2
245-
100-
75-
63-
48-
35-
25-
FL-GPR56
N-GPR56
Lysates:
anti-N-GPR56
GAPDH
B
N-GPR56
GPR56
- + - + C230-A TG2
245-
100-
75-
63-
48-
35-
25-
FL-GPR56
Dimeric &
monomeric
C-GPR56
Lysates:
anti-V5
C
N-GPR56
GPR56
- + - + C230-A TG2
245-
100-
75-
63-
48-
35-
25-
dimeric C230-A TG2
monomeric
C230-A TG2
*ns
Lysates:
anti-TG2
GAPDH
D
N-GPR56
GPR56
- + - + C230-A TG2
180-
100-
75-
63-
48-
35-
25-
N-GPR56
*ns
Medium:
anti-N-GPR56
E
N-GPR56
GPR56
- + - + C230-A TG2
180-
100-
75-
63-
48-
35-
25-
dimeric C230-A TG2
monomeric C230-A TG2
C230-A TG2 without
β-barrels
Medium:
anti-TG2

Figure 3.3 Expression of N-GPR56 and GPR56 in transiently transfected HEK293 cells.

Cells were co-transfected with GPR56 and AP-AR or N-GPR56 and AP-AR. Two days post-transfection, cells were serum starved for 1 h, followed by treatment with 20 µg/ml C_{230}-A TG2 or control buffer for 1 h. Total cell lysates were prepared and separated in 10% resolving gels, blotted onto PVDF membranes and stained with (A) anti-N-GPR56, (B) anti-V5 or (C) anti-TG2 antibodies. Anti-GAPDH staining served as loading control. Conditioned medium of the same cells was analysed using (D) anti-N-GPR56 and (E) anti-TG2 antibodies.

Data are representative for 6 independent experiments.

3.2.2.2 Comparison of wild type TG2, C_{230}-A TG2 and an anti-N-GPR56 antibody

In order to verify that stimulation of GPR56 by TG2 was specific, an anti-N-GPR56 antibody (R&D Systems) was compared in the shedding assay with the TG2 response. Iguchi et al. (2008) had previously shown that a different anti-N-GPR56 antibody activated GPR56, inducing Rho responses using a neurosphere migration model as the readout. Therefore it was likely that the polyclonal anti-N-GPR56 antibody used in this project potentially acts as a ligand for GPR56. This hypothesis was examined using the AP-AR shedding assay.

Figure 3.4 shows the analysis of GPR56 and AP-AR co-expressing cells treated with 5 µg/ml anti-N-GPR56 antibody or sheep IgG control for 1 h. Treatment with the antibody led to a comparable stimulation of GPR56-dependent AP-AR shedding when compared to 20 µg/ml C_{230}A-TG2. Additionally, wild type TG2 was tested in parallel. As shown in Figure 3.4, C_{230}-A TG2 or 20 µg/ml wild type TG2 stimulated the release of AP-AR into the medium by ~40 % when compared to control buffer treatment.

These data showed for the first time that TG2, C_{230}-A TG2 and anti-N-GPR56 activated GPR56-dependent AP-AR release, confirming Inoue et al.'s (2012) observation that GPCR activity can be assayed using this methodology. Thus, aGPCR signalling can be assessed using this experimental approach.

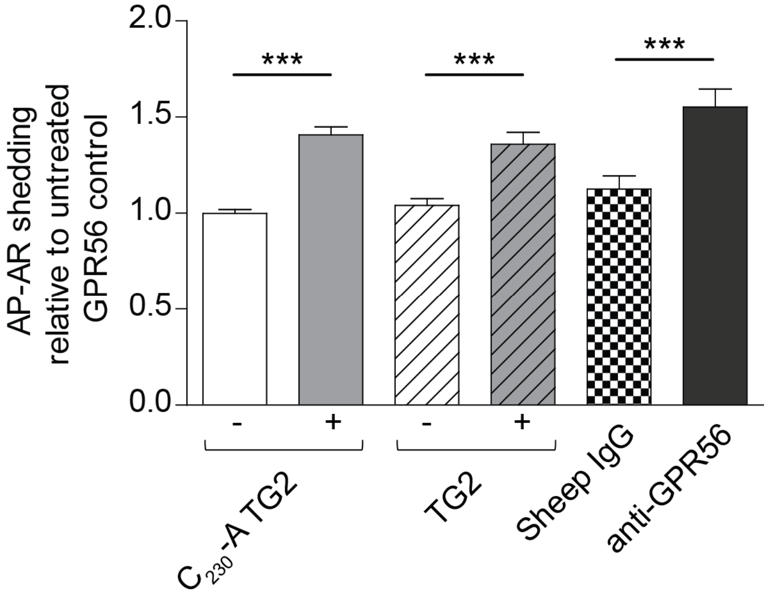

Figure 3.4 Wild type TG2 and an anti-N-GPR56 antibody stimulate GPR56 in a comparable manner to C230-A TG2.

GPR56 and AP-AR co-transfected cells were serum starved for 1 h and treated with either 5 µg/ml sheep anti-N-GPR56 antibody (R&D Systems) or 20 µg/ml of TG2 or C_{230}-A TG2 for 1 h.

Data presented show mean of 3 to 7 independent experiments with 4 repeats each +/- SEM (n=12 to 28). Statistical significance denoted as follows: ***, $p<0.001$.

3.2.2.3 The putative ligand collagen III

The results described above revealed that TG2, the first discovered extracellular binding partner of GPR56 (Xu et al. 2006), was able to stimulate GPR56-dependent AP-AR shedding. The next step was to investigate whether the second potential ligand, collagen III, also activated the receptor using the same assay. Cells co-expressing N-GPR56 and AP-AR or GPR56 and AP-AR were treated with collagen III for 1 h. To keep the experiments comparable to those using TG2 for stimulation, collagen III was used at the same molarity as TG2, 250 nM (≡ 75 µg/ml). Collagen III (Abcam, ab73160) was stored in 10 mM HCl, which was used as the buffer control. Figure 3.5

shows that treatment with collagen III did not stimulate basal GPR56-dependent shedding, which was in contrast to the treatments with TG2, C_{230}-A TG2 and anti-N-GPR56 antibody.

These data suggested that collagen III does not act as an agonist for GPR56-dependent AP-AR shedding.

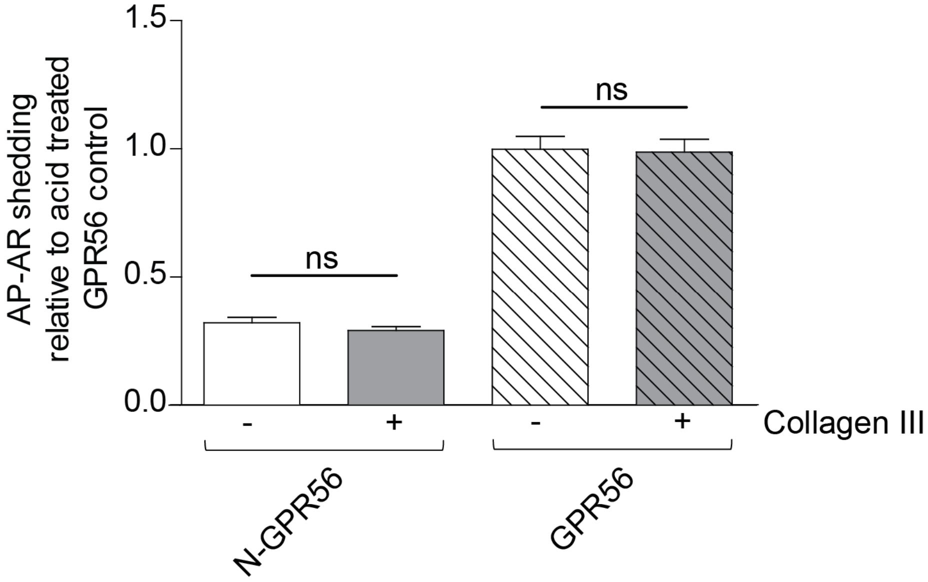

Figure 3.5 Collagen III does not activate GPR56.

Cells were co-transfected with N-GPR56 and AP-AR or GPR56 and AP-AR. Two days post-transfection, cells were serum starved for 1 h, followed by treatment with 250 nM collagen III (≡ 75 µg/ml) or buffer control for 1 h.

Data presented show mean of 3 independent experiments with 4 repeats each +/- SEM (n=12). Statistical significance denoted as follows: ns, non-significant.

3.2.3 Identification of the metalloproteinase involved in GPR56-dependent AP-AR shedding

Initial experiments demonstrated that activation of GPR56 leads to AP-AR shedding, which is further stimulated by TG2 or an agonistic anti-N-GPR56 antibody. The next set of experiments aimed to identify the metalloproteinase responsible for GPR56-dependent cleavage of AP-AR. Therefore, two ADAM inhibitors from GlaxoSmithKline were selected. One inhibits both ADAM10 and ADAM17 equally well (GW280264x, ADAM10/17 inhibitor) and the other specifically inhibits ADAM10 with a ~100-fold increased potency when compared to ADAM17 (GI254034x, ADAM10 inhibitor) (Hundhausen et al. 2003).

N-GPR56 or GPR56 and AP-AR expressing cells were serum starved in the presence or absence of the inhibitors, followed by incubation in medium in their presence or absence, which was optionally combined with C_{230}-A TG2 treatment.

Initially, both ADAM inhibitors were used at a 10 µM dose in the absence of ligand. At this dose, both inhibitors blocked ADAM10 and ADAM17 activity leading to significantly reduced *p*-NPP hydrolysis rates in GPR56 transfected cells in comparison to the DMSO solvent control (Fig. 3.6). Both the ADAM10 and ADAM10/17 inhibitor had no effect on the background shedding of AP-AR seen in N-GPR56 transfected cells, suggesting that this does not require these enzymes.

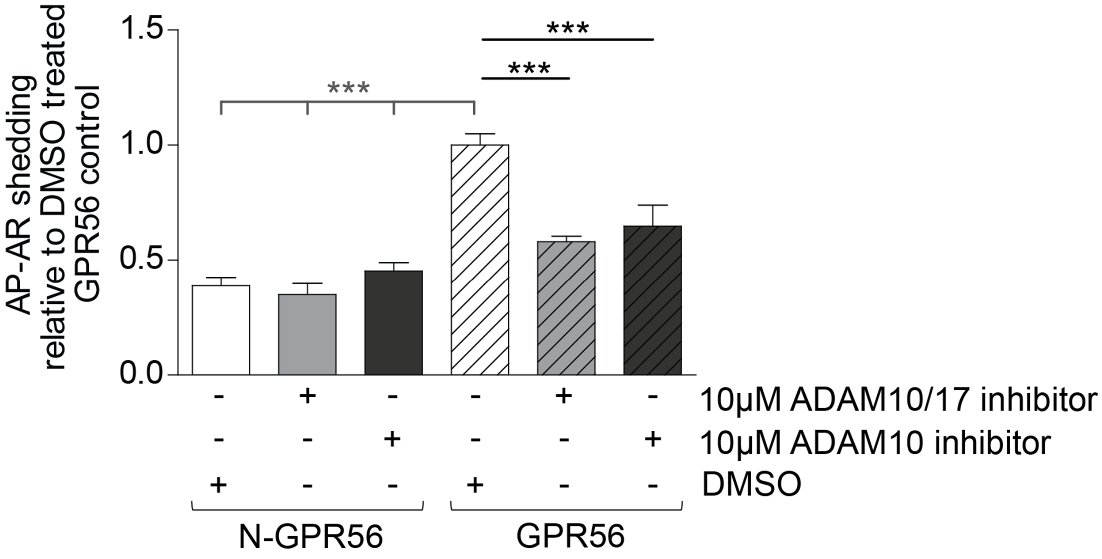

Figure 3.6 GPR56-dependent AP-AR shedding requires metalloproteinase activity.

Cells were co-transfected with GPR56 and AP-AR or N-GPR56 and AP-AR. Two days later, cells were serum-starved for 1 h in 10 µM ADAM10 or ADAM10/17 inhibitor or DMSO solvent control containing medium. Cells were incubated in Opti-MEM for 30 mins.

Data presented show mean of 3 independent experiments with 4 repeats each +/- SEM (n=12). Statistical significance denoted as follows: ***, $p<0.001$.

Inhibitors were then used at a 1 µM dose and only the ADAM10/17 inhibitor blocked GPR56-dependent AP-AR shedding (Fig. 3.7 A). Moreover, in the presence of 1 µM ADAM10/17 inhibitor, C_{230}-A TG2 lost its stimulating effect on GPR56, whereas shedding in the presence of the ADAM10 inhibitor was comparable to DMSO control. This result indicated that ADAM17 and not ADAM10 is involved in the reaction.

In order to confirm the specific involvement of ADAM17, an inhibitory ADAM17 antibody (Prof. G. Murphy) was used at a concentration of 100 nM during the serum starvation and ligand treatment period, to see whether this also ablated signalling. The results obtained show a highly significant reduction in shedding in the presence of the inhibitory antibody (Fig. 3.7 B), similar to what was seen using the ADAM10/17 inhibitor (Fig. 3.7 A).

The results shown in this section revealed that ADAM17 is required for GPR56-dependent shedding of amphiregulin.

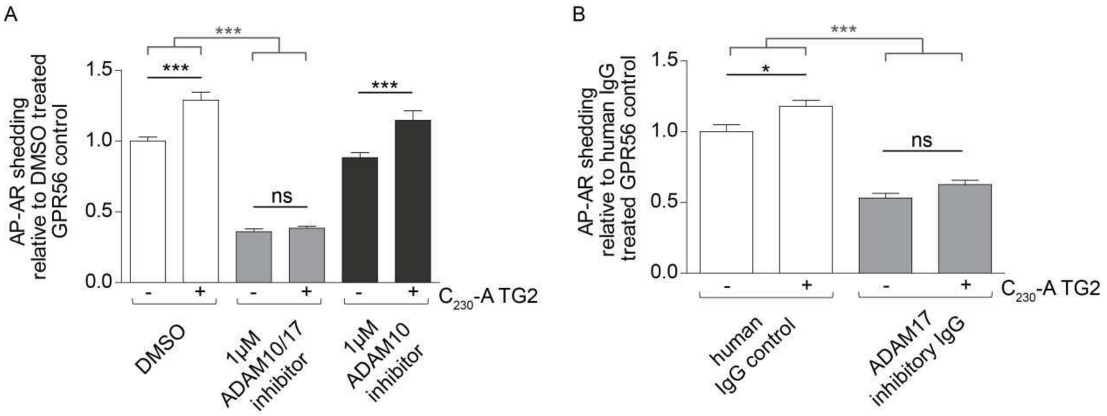

Figure 3.7 ADAM17 is required for GPR56-dependent AP-AR shedding.

Cells were co-transfected with GPR56 and AP-AR and experiments were started 48 h post-transfection with 1 h serum starvation.

(A) Cells were serum-starved in medium containing 1 µM ADAM10 or ADAM10/17 inhibitor or DMSO solvent control, followed by 1 h treatment with control buffer or 20 µg/ml C_{230}-A TG2 in the presence or absence of the same inhibitor.

(B) Cells were serum-starved and stimulated for 1 h with 20 µg/ml C_{230}-A TG2 in the presence of 100 nM ADAM17 inhibitory antibody or human IgG control.

Data presented show mean of 3 independent experiments with 4 repeats each +/- SEM (n=12). Statistical significance denoted as follows: *, $p<0.05$; ***, $p<0.001$; ns, non-significant.

3.2.4 Identifying mediator proteins downstream of GPR56

Experiments illustrated in the previous sections identified TG2 as an agonist for GPR56 activating ADAM17. In order to further characterise GPR56 signalling, the next step was to identify signalling mediators acting downstream of GPR56. Work here focussed on downstream mediators of G_q- and $G_{12/13}$-pathways, as they have been implicated in GPR56 signalling (Iguchi et al. 2008; Little et al. 2004; Luo et al. 2011; Yang et al. 2011).

3.2.4.1 Interfering with the Protein kinase C (PKC) / Phospholipase C (PLC) pathway

To address the question whether GPR56-dependent AP-AR shedding was mediated via $G\alpha_{q/11}$-proteins leading to activation of the PKC/PLC signalling pathway, the shedding assay was used as outlined before. Cells were serum starved in the presence or absence of different inhibitors blocking either PLC, PKC or IP_3-receptors prior to C_{230}-A TG2 stimulation in their presence or absence.

In order to investigate whether Phospholipase C was activated downstream of GPR56, the aminosteroid and PLC inhibitor U73122 and an inactive control compound, U73343 (Merck Millipore), were used. U73122 is known to inhibit GPCR-induced activation of PLC, ablating the production of IP_3 and release of Ca^{2+} from intracellular stores into the cytoplasm (Bleasdale and Fisher 1993). As shown in figure 3.8 A, treatment of cells with 5 µM of the PLC inhibitor U73122 stimulated basal shedding 2-fold. Additionally, C_{230}-A TG2 induced GPR56 activity was further elevated to 3-fold above solvent control. In contrast, U73343 did not affect *p*-NPP hydrolysis rates and they were equal to DMSO solvent control (Fig. 3.8 A).

The non-competitive IP_3-receptor antagonist, 2-aminoethoxydiphenyl borate (2-APB), was used to look at effects of abolishing the release of intracellular

Ca^{2+}. 2-APB inhibits the release of Ca^{2+} from intracellular stores such as the ER, without affecting binding of IP_3 to its receptors (Maruyama et al., 1997). Treatment of GPR56-expressing cells with 5 µM 2-APB had no effect on GPR56-dependent AP-AR shedding and was comparable to DMSO solvent control (Fig. 3.8 B).

The PKCα/β inhibitor, the indolocarbazole Gö6976 (Merck), was used in order to investigate whether PKC activity was involved in GPR56-induced AP-AR shedding. Gö6976 was reported to interfere with the Ca^{2+}-dependent PKC isozymes α and β1, whereas it does not inhibit any of the Ca^{2+}-independent PKC subtypes (δ, ε, ζ) even at high concentrations (Martiny-Baron et al. 1993). Figure 3.8 C shows that treatment with 1 µM Gö6976 stimulated basal GPR56-activity leading to shedding of AP-AR. However, the TG2 response was ablated.

In summary, interfering with the PKC/PLC-signalling pathway did not inhibit basal GPR56-induced shedding of AP-AR by ADAM17. However, treatment with the PKC-inhibitor Gö6976 abolished TG2 stimulation.

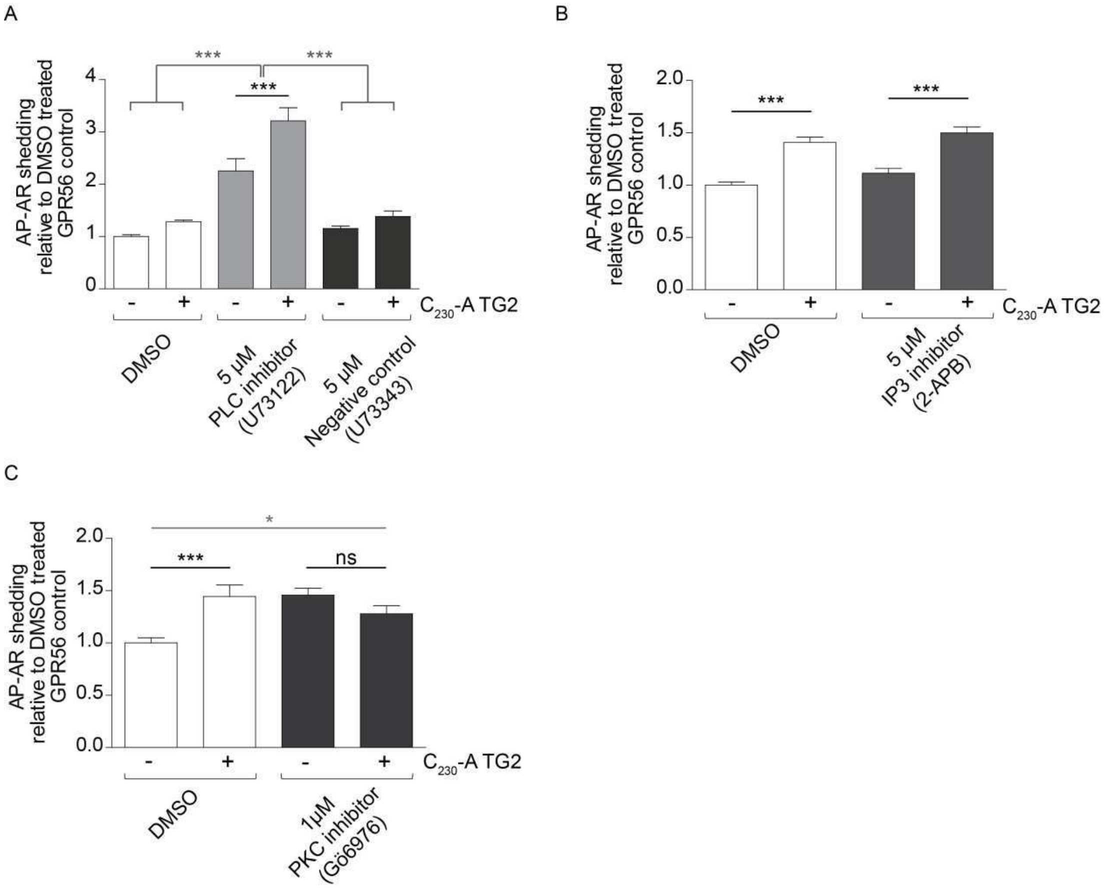

Figure 3.8 Inhibition of the PKC/PLC signalling pathway does not block basal GPR56-induced shedding of AP-AR by ADAM17.

Two days post-transfection, GPR56 and AP-AR co-transfected cells were serum starved for 1 h in the presence of DMSO solvent control or (A) 5 µM PLC inhibitor U73122 or 5 µM negative control U73343, (B) 5 µM IP_3-receptor antagonist 2-APB or (C) 1 µM PKCα/β inhibitor Gö6976. Cells were treated with 20 µg/ml C_{230}-A TG2 for 1 h in the presence of DMSO solvent control or the same compounds.

Data presented show mean of 3 independent experiments with 3 to 4 repeats each +/- SEM (n=10 to 12). Statistical significance denoted as follows: ***, p<0.001; *, p < 0.05; ns, non-significant.

In order to investigate whether the stimulating effect of PLC inhibition on GPR56-dependent AP-AR shedding was due to increased GPR56 surface expression levels, an experiment using confocal microscopy was performed to assess cell surface expression levels of GPR56 (Fig. 3.9). Cells were transfected with SNAP-GPR56 and 48 h post-transfection serum starved. SNAP-GPR56 (shown in red) was stained using SNAP-surface substrate 647 (NEB) at 4 °C for 15 mins. Cells were stimulated with C_{230}-A TG2 in the presence of U73343 negative control compound (Fig. 3.9 A) or U73122 PLC inhibitor (Fig. 3.9 B) for 1 h. As shown in figure 3.9, SNAP-GPR56 was internalised to the same amount in the presence of both compounds, indicating that the PLC inhibitor U73122 did not block internalisation of GPR56 (the SNAP-tag technology and its application in experiments using confocal microscopy is explained in detail in Chapter 6).

Therefore, the stimulating effect of U73122 regarding GPR56-dependent AP-AR shedding cannot be explained with elevated GPR56 cell surface levels.

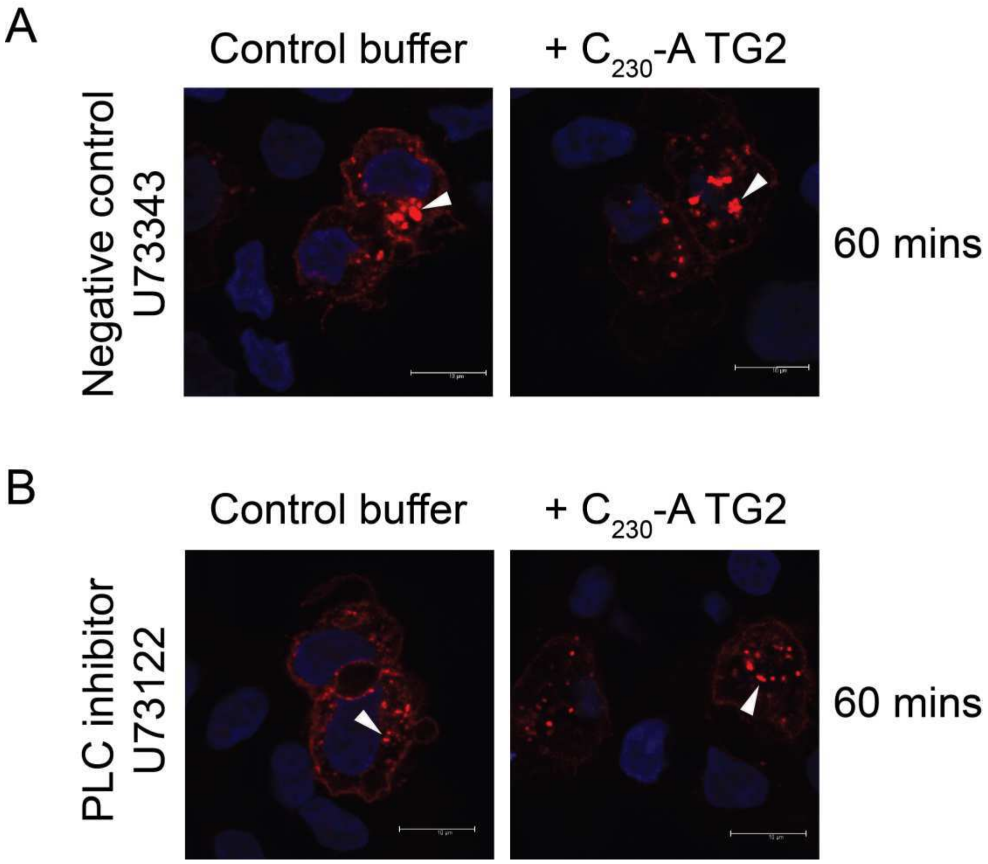
A
Control buffer
+ C230-A TG2
Negative control U73343
60 mins
B
Control buffer
+ C230-A TG2
PLC inhibitor U73122
60 mins

Figure 3.9 The PLC inhibitor U73122 does not stabilise cell surface expression levels of GPR56.

Cells were seeded onto poly-L-lysine coated glass coverslips and the next day transfected with SNAP-GPR56. Two days later, cells were serum starved for 1 h. SNAP-GPR56 (shown in red) was stained at 4 °C for 15 mins using SNAP-surface substrate 647 (NEB). Cells were treated with control buffer or 20 µg/ml C_{230}-A TG2 for 1 h in (A) 5 µM U73343 or (B) 5 µM U73122 containing medium.

White arrow heads, internalised GPR56 stained with SNAP-surface substrate 647 (red).

3.2.4.2 Inhibition of the RhoA signalling mechanism

The following experiments were performed to investigate whether stimulation of GPR56 with C_{230}-A TG2 leads to activation of RhoA. For this purpose, the Rho-associated protein kinase (ROCK) inhibitor Y-27632 (Sigma-Aldrich) was used in the shedding assay. GPR56 and AP-AR co-transfected cells were serum starved and treated with C_{230}-A TG2 in the presence or absence of 2 µM Y-27632. Figure 3.10 shows that treatment with the ROCK inhibitor reduced basal GPR56-activity, leading to loss of basal AP-AR shedding to almost half of the value of untreated control. Stimulation of GPR56 with C_{230}-A TG2 did not lead to a significant increase of *p*-NPP hydrolysis rates in the presence of the inhibitor, when compared to the buffer control.

These data demonstrated that stimulation of GPR56 with C_{230}-A activated RhoA and that this signalling pathway must be involved in GPR56-dependent shedding of AP-AR.

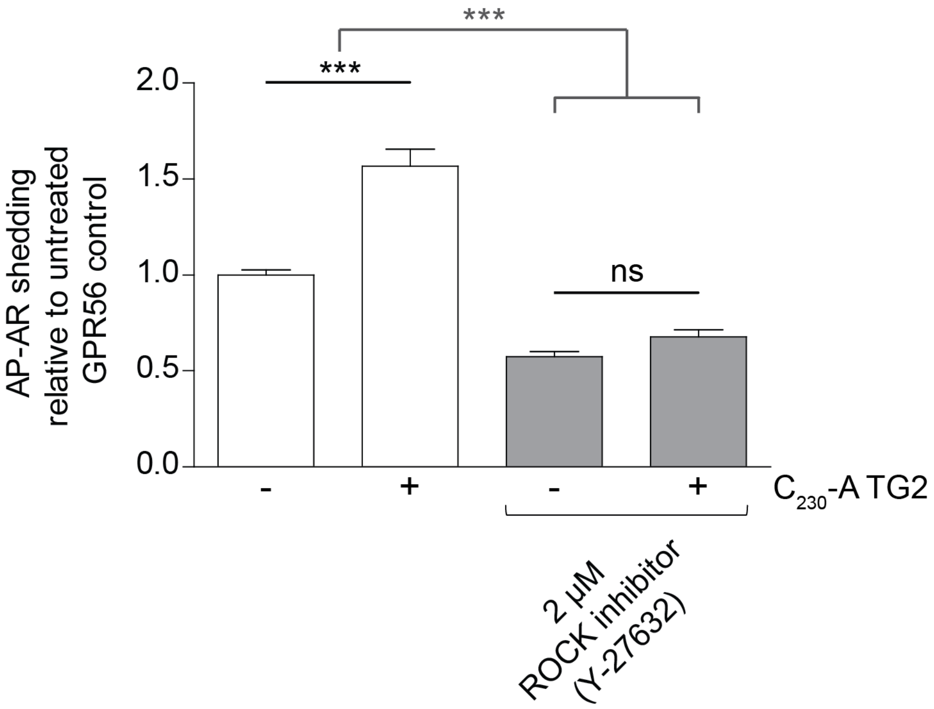

Figure 3.10 The ROCK inhibitor Y-27632 blocks GPR56-dependent shedding of AP-AR and ablates stimulation of GPR56 with C_{230}-A TG2.

Cells were transfected with GPR56 and AP-AR and 48 h later serum starved for 1 h in the presence of 2 µM ROCK inhibitor Y-27632 or serum-free medium control. Cells were then treated with 20 µg/ml C_{230}-A TG2 for 1 h in the presence or absence of the same inhibitor.

Data presented show mean of 3 independent experiments with 4 repeats each +/- SEM (n=12). Statistical significance denoted as follows: ***, $p<0.001$; ns, non-significant.

3.2.4.3 Inhibition of the epidermal growth factor receptor (EGFR)

Previous results demonstrated that activation of GPR56 led to shedding of the EGFR-ligand amphiregulin by ADAM17. In order to test whether EGFR itself was involved directly or indirectly in GPR56-dependent AP-AR shedding, the EGFR inhibitor AG1478 was used in the shedding assay. AG1478 inhibits the intrinsic tyrosine kinase activity of EGFR and prevents the induction of EGFR-dependent downstream signalling.

GPR56 and AP-AR co-transfected cells were first serum starved, then stimulated with C_{230}-A TG2 in the presence of 5 µM AG1478 or DMSO solvent control. Treatment with AG1478 decreased basal GPR56 activity compared to DMSO solvent control (Fig. 3.11). However, the presence of the EGFR inhibitor did not influence the stimulating effect of C_{230}-A TG2 on AP-AR shedding. This result indicated that AG1478 does not block the TG2 response significantly.

The data implied that the activity of EGFR is important for the cross-talk between GPR56 and EGFR, thus GPR56-dependent shedding of AP-AR.

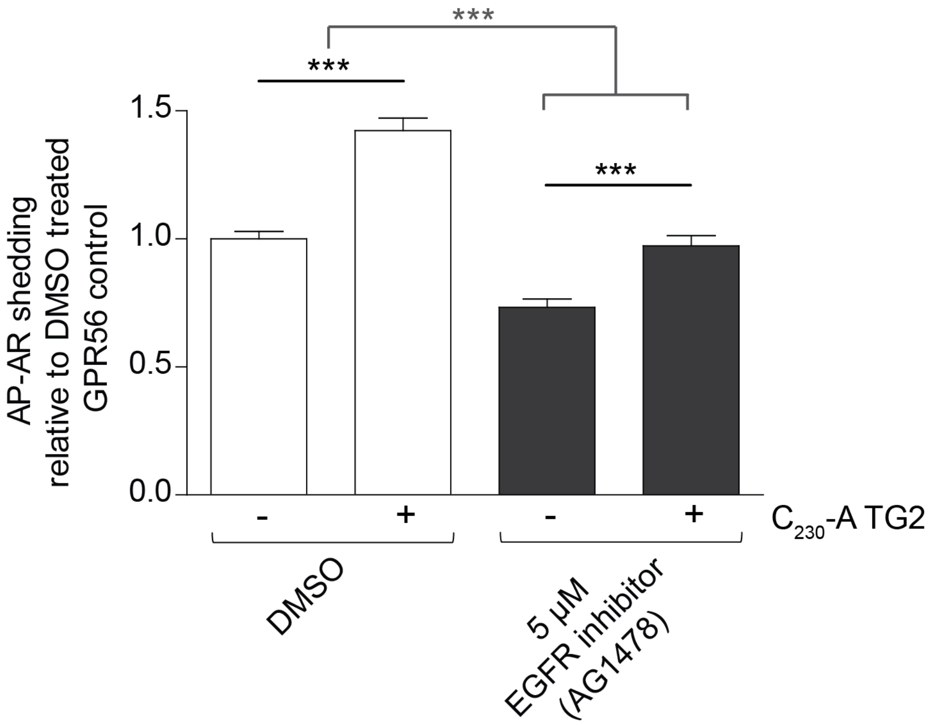

Figure 3.11 Basal GPR56-dependent AP-AR shedding is reduced in the presence of the EGFR inhibitor AG1478.

48 h post-transfection, GPR56 and AP-AR transfected cells were serum starved for 1 h in the presence of 5 µM EGFR inhibitor AG1478 or DMSO solvent control, followed by treatment with 20 µg/ml C_{230}-A TG2 for 1 h in the presence or absence of 5 µM AG1478.

Data presented show mean of 3 independent experiments with 4 repeats each +/- SEM (n=12). Statistical significance denoted as follows: ***, p<0.001.

3.3 Discussion

This chapter introduced a sensitive shedding assay, representing a tool to assess GPCR activation, as shown by others (Inoue et al. 2012). In order to define the signalling activity of GPR56, the assay described by Inoue et al. (2012) was modified regarding the ADAM substrate used. Instead of AP-TGF-α, AP-tagged amphiregulin was used in this project as an example for an EGF-like ligand (Fig. 3.1 A), as substrate depletion was reached much faster with AP-TGF-α than with AP-AR when cells were co-transfected with GPR56 (data not shown).

Using this assay, it was demonstrated that GPR56 had a high ligand-independent, basal activity indicating constitutive activation of the receptor (Fig. 3.1 & 3.2). This phenomenon was described for other GPCRs like the histamine H_1 receptor (H_1R) using the TGF-α shedding assay (Inoue et al. 2012) and GPR56 specifically, using reporter assays as well as RhoA pulldown assays (Shashidhar et al. 2005; Iguchi et al. 2008; Kim et al. 2010).

Moreover, work performed in this project demonstrated for the first time an agonistic TG2-GPR56 relationship, since AP-AR shedding was further increased by treatment with C_{230}-A TG2 (Fig. 3.2). This finding is in contrast to a report from Chiang et al. (2011), who claimed that human TG2 was not an endogenous binding partner. However, experiments performed by Andreas Heil in the Aeschlimann laboratory clearly showed an interaction between human N-GPR56-Fc and human TG2 in solution (data not shown). In addition, Yang et al. (2014) just recently confirmed our results by co-IP experiments using MC-1 human melanoma cells overexpressing GPR56, as well as experiments demonstrating pulldown of hTG2-GST with $hGPR56^N$-Fc.

Western blot analysis of the cells used in the shedding assays confirmed that HEK293 cells were negative for endogenous GPR56 and TG2 expression, therefore these cells are a good choice to evaluate signalling by GPR56 (Fig. 3.3). Western blot analysis for N-GPR56 revealed a typical banding pattern for wild type GPR56, consisting of the major bands running between ~60 and

75 kDa, representing differentially glycosylated N-GPR56 forms, as well as full-length receptor, respectively (Fig. 3.3 A). The banding pattern is in line with several reports from the literature (Jin et al. 2007; Chiang et al. 2011; Luo et al. 2011; Paavola et al. 2011), however the detected bands do not correspond to the predicted size for N-GPR56, which should be much smaller (~40 kDa). As shown by Jin et al. (2007) and Chiang et al. (2011), N-GPR56 carries 7 N-glycosylations and 5-15 moieties of sialic acid. Therefore, the protein ladder between 60 kDa to 75 kDa likely corresponds to N-GPR56 decorated with carbohydrate chains added in ER and golgi. In general, N-glycosylations are important for proper protein folding, as well as trafficking, cell surface expression and secretion. As a result, mutations within GPR56, affecting proper glycosylation and cell surface expression, were shown to cause the brain malformation BFPP (Jin et al. 2007).

Due to a lack of GPR56 antibodies, the V5-epitope tag was used to detect the C-GPR56 domain, consisting of the 7TM-domain and the cytoplasmic tail. Western blot analysis using anti-V5 antibody showed a banding pattern for wild type GPR56 consisting of bands running at ~27 kDa (monomer), 50 kDa (dimer) and 75 kDa (Fig. 3.3 B), the latter most likely representing full-length GPR56, as this band was also recognised with the anti-N-GPR56 antibody. Others speculated that this might be a trimeric C-terminal receptor form (Chiang et al. 2011). In general, the banding pattern is in good agreement with other reports (Jin et al. 2007; Xu et al. 2006; Paavola et al. 2011). However, the band for monomeric C-GPR56 (~27 kDa) is smaller than its predicted size, likely due to the hydrophobic nature of the C-terminal fragment which includes the 7TM-region (Jin et al. 2007). Interestingly, the only difference between control buffer and C_{230}-A TG2 treatment was a reduction in the expression level of the dimeric receptor form, running at ~50 kDa following TG2-treatment. This finding points toward increased receptor internalisation and probably degradation, as investigated in Chapter 6. In addition, it indicates that the dimer is the receptor form mainly expressed at the cell surface, as shown by others for GPR56 using a surface biotinylation approach (Paavola et al. 2011) and for different GPCRs (Terrillon and Bouvier 2004; Milligan 2004).

In conditioned media, secreted GPR56-ECD was only found in N-GPR56 transfected cells, but not in medium from wild type GPR56-transfected cells (Fig. 3.3 D). This is in contrast to observations by Chiang and colleagues (2011) who detected secreted N-GPR56 in medium of cells transfected with wild type GPR56 and several receptor mutants carrying missense mutations in the N-terminal domain and ECLs. They demonstrated that there must be an additional cleavage event independent of GPS proteolysis, mediated by MMPs or ADAMs, as release was abolished by the metalloproteinase inhibitor GM6001 (Chiang et al. 2011). In addition, Jin and colleagues (2007) could also detect wild type N-GPR56 in conditioned medium. It must be noted that conditioned media were tested for GPR56 expression after 1 h incubation in this project, whereas Jin and colleagues (2007) left cells for 48 h. Thus, there may be small amounts of GPR56 present in the medium after 1 h, which is below detectable levels.

Using the shedding assay, it was shown that TG2 and C_{230}-A TG2 activate GPR56-dependent AP-AR shedding. This result was validated by showing the same degree of receptor activation with an agonistic anti-N-GPR56 antibody (Fig. 3.4). These findings expand the understanding of TG2-GPR56 interactions, as they upgrade TG2 from a binding partner (Xu et al. 2006) to an agonistic ligand for GPR56.

A receptor-ligand response was previously shown for collagen III and GPR56, whereas collagen III negatively regulated neural progenitor migration through stimulation of GPR56-dependent Rho activation (Luo et al. 2011). The results presented in this chapter showed that collagen III did not activate GPR56. However, it must be noted that Luo et al. (2012) mentioned variations regarding the biological function of different collagen III batches (Abcam), which they tested before performing their experiments. It is likely that the collagen III used in my project was inactive due to fibril formation and thus did not activate GPR56.

In this project, ADAM17 was identified as a mediator of GPR56 signalling, which is involved in GPR56-dependent and TG2-induced cleavage of AP-AR

(Fig. 3.7). In the past, Gschwind et al. (2003) demonstrated the involvement of ADAM17 in GPCR-dependent shedding of amphiregulin and subsequent EGFR activation in squamous cell carcinoma. Moreover, Inoue et al. (2012) identified ADAM17 as the main ADAM involved in GPCR-dependent cleavage of TGFα, as siRNA-mediated knockdown of ADAM17 abolished GPCR-induced shedding for almost all receptors tested. This thesis is the first report showing activation of ADAM17 by GPR56 or an adhesion GPCR.

In order to investigate potential downstream signalling pathways induced by GPR56, inhibitors were tested that interfere with the PLC/PKC signalling pathway, which is downstream of GPCRs coupling to $G\alpha_q$-proteins (Rebecchi and Pentyala 2000; Inoue et al. 2012). GPR56 itself was shown to bind to $G\alpha_{q/11}$ (Little et al. 2004). Moreover, using PKC inhibitors as well as a dominant negative mutant of PKCα, Yang et al. (2011) demonstrated that the inhibitory effect of GPR56 on melanoma growth and angiogenesis is mediated by PKCα.

Active PLC generates two second messengers, diacylglyerol (DAG) and inositol triphosphate (IP_3). DAG activates PKC, which in turn phosphorylates a variety of proteins. IP_3 binds to receptors located in the membrane of the ER, leading to release of intracellular Ca^{2+}, which itself controls multiple cellular processes (Bootman et al. 2001).

Treatment with the PLC inhibitor U73122 led to a significant increase in basal shedding of AP-AR (Fig. 3.8 A). $G\alpha_q$-PLC-PKC signalling might compete with other pathways induced by different Gα-proteins, thus inhibiting PLC could promote the initiation of other signalling pathways leading to AP-AR shedding. A similar effect was described by Inoue et al. (2012) as “shunting of Gα coupling”, since they observed increased TGFα shedding for some GPCRs due to increased $G\alpha_q$-/$G\alpha_{12/13}$-signalling when they inhibited $G\alpha_s$ and $G\alpha_i$. However, they could not observe this effect with the same PLC inhibitor used in my project.

On the other hand, U73122 was shown to have opposing, unspecific effects such as increasing the release of intracellular Ca^{2+} (Mogami et al. 1997), including IP_3-mediated release of Ca^{2+}. Interestingly, coupling of the agonist-

activated AT_1-receptor to G_q was shown to activate PLC, leading to mobilisation of Ca^{2+} and production of reactive oxygen species (ROS), which promotes ADAM17-dependent shedding of HB-EGF (Mifune et al. 2005). Thus, a direct effect of elevated Ca^{2+} levels on ADAM17 activity due to U73122 treatment, resulting in increased basal shedding cannot be excluded. A good example for a direct effect of compounds on ADAM17 activity are the results obtained with the ADAM10/17 inhibitor and the inhibitory ADAM17 antibody (Fig. 3.7), resulting in decreased AP-AR shedding.
The normal TG2 response in the presence of the PLC inhibitor, however, can be explained by the GPR56-dependent activation of ADAM17, as observed with DMSO solvent control (Fig. 3.8 A).

Treatment with the PKC inhibitor Gö6976 significantly increased basal shedding when compared to DMSO control (Fig. 3.8 C). PKC activates GPCR kinase 2 (GRK2) by phosphorylation, resulting in binding of GRK2 to GPCRs, followed by their internalisation (Winstel et al. 1996). In addition, PKC was also shown to directly phosphorylate GPCRs, leading to their internalisation and attenuation of G protein signalling (García-Sáinz et al. 2000). Thus, inhibition of PKC by Gö6976 could inhibit internalisation of GPR56, leading to enhanced cell surface levels of GPR56, resulting in increased basal shedding of AP-AR. As discussed above, treatment with the PLC inhibitor U73122 also increased basal shedding dramatically, when compared to cells treated with the negative control U73343 (Fig. 3.8 A). Since PKC is activated downstream of PLC, inhibition of PLC would also impair PKC activity, which might result in inhibition of GPR56 internalisation. Therefore, it was tested whether the PLC-inhibitor elevated GPR56 cell surface expression levels. Confocal analysis of cells treated with U73122 did not indicate elevated cell surface expression levels of GPR56 (Fig. 3.9). Nonetheless, it must be noted that approaches like flow cytometry or biotinylation of cell surface proteins represent better tools to quantify GPR56 present in the cell membrane. Thus, it cannot entirely be excluded that the increase in basal shedding observed in the presence of the PLC and PKC inhibitors is due to elevated cell surface expression levels of GPR56.

On the other hand, PKC inhibition by Gö6976 could also directly interfere with ADAM17 activity, independent of GPR56. It was demonstrated by Ghosh et al. (2004) that inhibition of PKC by Gö6976 stimulates extracellular signal-regulated kinase (ERK)-phosphorylation. Activated ERK, in turn, phosphorylates ADAM17, leading to trafficking of ADAM17 to the cell surface and induction of its catalytic shedding activity (Fan and Derynck 1999; Soond et al. 2005; Bell and Gööz 2010).

In addition, PKC is known to directly activate ADAM17 resulting in increased substrate shedding, as shown for TGF-α (Dang et al. 2011; Kveiborg et al. 2011). Thus, inhibition of PKC could directly interfere with ADAM17 activation, which may explain the fact that TG2 addition did not lead to a stimulation of AP-AR shedding in wells treated with PKC inhibitor.

Experiments using the IP_3-receptor inhibitor 2-APB showed that inhibition of Ca^{2+}-release from the ER had no effect on basal and TG2-induced AP-AR shedding (Fig. 3.8 B). The results implicate that Ca^{2+} does not play a role for shedding of AP-AR, which is supported by the finding that ADAM10, but not ADAM17 is activated by Ca^{2+}-flux, inducing TGF-α and AR shedding (Horiuchi et al. 2007). In addition, the result indicates that GPR56' constitutive and TG2-stimulated activity do not induce Ca^{2+}-flux, thus GPR56 likely does not signal via G_q. Using luciferase reporter assays looking at GPR56-dependent signalling, Dr. Vera Knäuper could show that GPR56 does not couple G_q (data not shown). These findings are in line with a report from Inoue et al. (2012) demonstrating that not only $G\alpha_q$-, but especially $G\alpha_{12/13}$-dependent pathways were involved in TGFα shedding, which may also account for GPR56-dependent shedding of AP-AR.

Data presented in this project show that Rho-signalling is activated by GPR56 and that ROCK-activity is required for GPR56-induced shedding by ADAM17 (Fig. 3.10). These findings confirm previous reports, demonstrating RhoA activation by GPR56 overexpression (Iguchi et al. 2008; Luo et al. 2011; Kim et al. 2010). In addition, Luo et al. (2011) showed elevated RhoA signalling following collagen III treatment, resulting in inhibition of migratory signals observed in their neurosphere assays. Using a ROCK inhibitor, it was demonstrated for the first time that GPR56-induced Rho signalling is also stimulated by TG2. RhoA is usually associated with G$\alpha_{12/13}$- and in a few cases with G_q-coupled receptors (Chikumi et al. 2002). Kim and colleagues (2010) used the same ROCK inhibitor Y-27632 and demonstrated that GPR56-dependent SRE-activity was mediated through G$\alpha_{12/13}$ and Rho, pointing toward an involvement of G$\alpha_{12/13}$ in GPR56-dependent shedding of AP-AR.

Another GPCR signalling mechanism that plays a critical role for cell proliferation and migration, is the transactivation of epidermal growth factor receptors (EGFR) (Daub et al. 1996; Prenzel et al. 1999). GPCR-dependent cleavage of EGF-like ligands by metalloproteinases leads to activation of EGFRs. G_q-, G_i- and G_{13}-proteins were reported to be involved in this signalling pathway (Daub et al. 1997; Gohla et al. 1998; Gohla et al. 1999), as well as β-arrestins (Noma and Lemaire 2007). The shedding assay used to measure GPR56 activity in this project is an indicator for GPR56-dependent EGFR transactivation, as amphiregulin is one of the known EGFR ligands. Activation of the EGFR leads to EGFR dimerization and phosphorylation, resulting in the activation of several downstream mediator proteins like mitogen-activated protein kinases (MAPKs) (Daub et al. 1997).
Experiments using the EGFR inhibitor AG1478 showed that basal AP-AR shedding was decreased in the presence of inhibitor (Fig. 3.11). This result indicates that there might be a positive feedback loop from downstream signalling pathways activated by EGFR to ADAM17. ERK is phosphorylated downstream of EGFR and was shown to activate ADAM17, as discussed above (Fan and Derynck 1999; Soond et al. 2005; Bell and Gööz 2010). Thus, inhibiting EGFR activation may result in decreased ADAM17 shedding activity, independent of GPR56. In addition, the result could also reflect a direct interaction between GPR56 and EGFR, as shown for somatostatin receptors 1 and 5 with EGFR (Watt et al. 2009), leading to activation of ADAM17. However, stimulation of shedding by TG2 was not affected in the

presence of the AG1478, indicating that GPR56-dependent ADAM17 activation was not inhibited.

In summary, results presented in this chapter showed that GPR56 activation can be measured by ADAM17-mediated AP-AR shedding. GPR56 has a high constitutive activity and is further activated by its agonist human TG2 or an agonistic anti-N-GPR56 antibody. The signalling mechanism is likely to be $G\alpha_{12/13}$-dependent, requiring ROCK activity. Figure 3.12 summarises the discussion of this chapter.

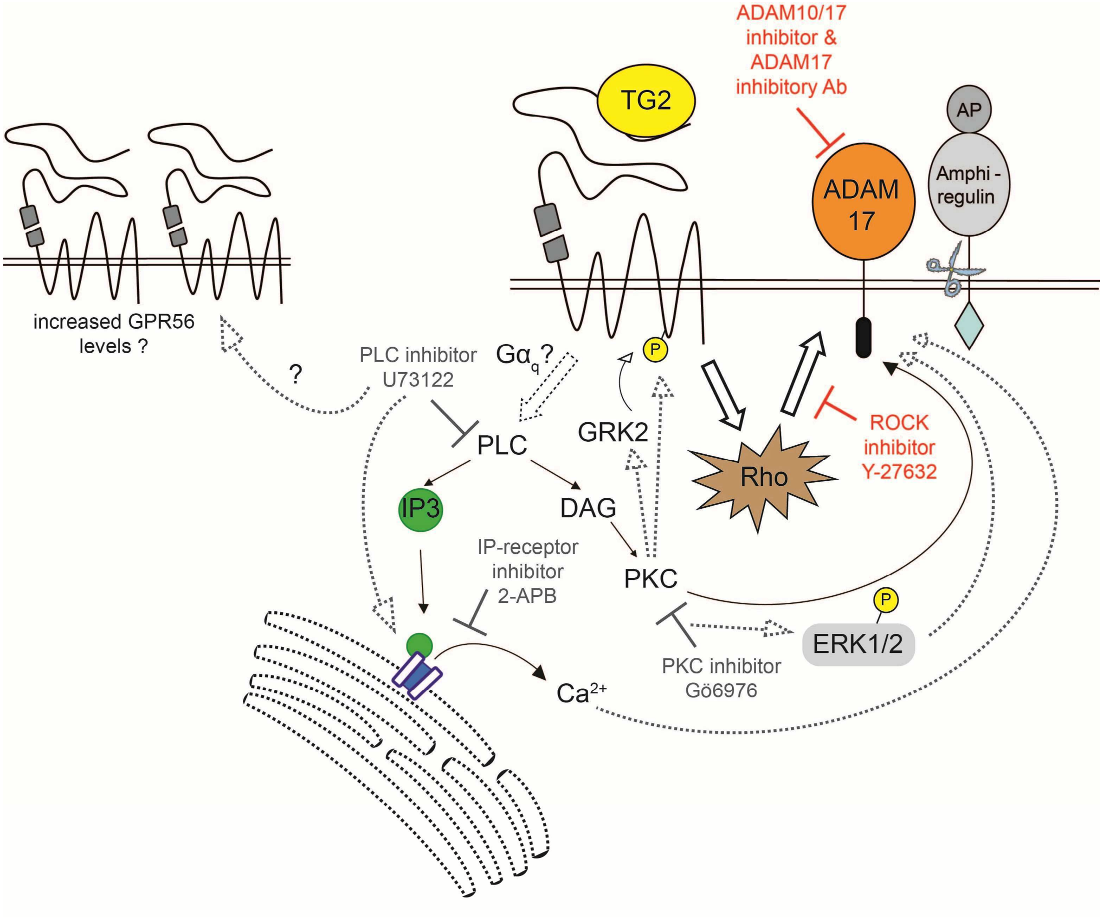
ADAM10/17 inhibitor & ADAM17 inhibitory Ab
TG2
AP
Amphi - regulin
ADAM 17
increased GPR56 levels ?
?
PLC inhibitor U73122
Gα$_q$?
P
GRK2
PLC
Rho
ROCK inhibitor Y-27632
IP3
DAG
IP-receptor inhibitor 2-APB
PKC
P
ERK1/2
PKC inhibitor Gö6976
Ca^{2+}

Figure 3.12 Potential downstream signalling pathways involved in GPR56-dependent ADAM17-activation.

Constitutive and TG2-induced GPR56 activity leads to RhoA and ROCK activation, which induces ADAM17-dependent shedding of AP-AR shedding, as shown by treatments with ADAM17 and ROCK inhibitors. Experiments using inhibitors for PLC, PKC, IP_3-receptors and EGFR could not entirely exclude an involvement of PKC-, calcium- and ERK1/2-signalling in GPR56-dependent ADAM17 activation, which needs further evaluation.

CHAPTER 4:

Characterisation of GPR56-TG interactions

4 Characterisation of GPR56-TG interactions

4.1 Introduction

Having established that TG2 activated GPR56, the next step was to characterise sequence and domain requirements of TG2 involved in receptor activation.

TG2 consists of 4 main domains: the N-terminal β-sandwich, a catalytic core and two C-terminal β-barrels. Regarding the interaction with GPR56, Xu et al. (2006) demonstrated that the β-barrel domain was indispensable for binding of GPR56. Their findings indicated that the two β-barrels alone would be sufficient to bind and potentially activate GPR56. However, activation of GPR56 by TG2 or its β-barrels was not demonstrated in their study.

The best studied catalytic function of TGs is the post-translational modification of proteins by crosslinking of a glutamine to a lysine residue. The reaction is highly Ca^{2+}-dependent and can be inhibited by guanine nucleotides (Király et al. 2011; Pinkas et al. 2007). It is unclear whether the catalytic activity of TG2 is required for GPR56 activation. Moreover, non-enzymatic functions of extracellular TG2, including direct interactions with ECM components and cell surface proteins, were associated with cellular processes like cell adhesion, migration and signalling (Nurminskaya and Belkin 2012). Thus, it is likely that the catalytic activity of TG2 is not essential for the activation of GPR56. This hypothesis was tested by using two catalytically inactive TG2 variants.

The C_{277}-S TG2 mutant lacks transglutaminase activity such as crosslinking, as it carries a mutation in the catalytic triad (Cys_{277}-His_{335}-Asp_{358}) located within the core domain of TG2, essential for its catalytic activity (Lee et al. 1993).

Open Conformation-TG2 (OC-TG2, Open-TG2) is stabilized in an extended conformation by an irreversible inhibitor that binds to the catalytic site cysteine, making the TG2 active site inaccessible for substrates and forcing the inactivation of the enzyme. Due to the conformational change of inhibitor-bound Open-TG2, usually buried residues are accessible for potential interacting partners and the catalytic site is exposed (Pinkas et al. 2007).

In order to identify critical structural domains for GPR56-activation, the related TG, human Factor XIII (FXIII) lacking the two C-terminal β-barrels, was tested. FXIII can be found intracellularly as well as extracellularly in the plasma, where it functions in the blood coagulation system by stabilising fibrin clots (Mehta and Eckert 2005).

Moreover, TG6 and TG7 were used in order to address the question whether other TGs activate GPR56.

TG6 is expressed in the central nervous system, testis and lung, but its main function and whether it causes disease is unknown (Mehta and Eckert 2005). However, TG6 autoantibodies were associated with the development of coeliac disease with epilepsy and cerebral calcifications (CEC) (Johnson et al. 2013). Neuronal transglutaminase represents an interesting candidate for a GPR56 ligand, as GPR56 ablation leads to the developmental brain disease BFPP (Piao et al. 2004).

TG7 is ubiquitously, but predominantly expressed in testis and lung, however its physiological function and potential role in disease remains elusive (Grenard et al. 2001). Like TG6, TG7 is closely related to TG2 and sequence alignments showed a high level of sequence identity regarding the core domain (~50%) (Grenard et al. 2001).

4.1.1 Aims of the chapter

- To investigate whether the enzymatic activity of TG2 is required for the activation of GPR56.

- To identify specific domains within TGs required for the interaction and activation of GPR56.

- To identify new GPR56 ligands using the shedding assay.

4.2 Results

4.2.1 GPR56 activation by TG2 is independent of transglutaminase activity

Results of the previous chapter showed that TG2, C_{230}-A TG2 and an anti-N-GPR56 antibody stimulate GPR56-dependent AP-AR shedding. Wild type and C_{230}-A TG2 are both catalytically active under the experimental conditions as evaluated using a real-time fluorescence assay which measures TG-dependent isopeptidase activity (Adamczyk 2013; and data not shown).
In order to test whether the catalytic activity of TG2 was needed to activate GPR56, two catalytically inactive TG2 variants, C_{277}-S TG2 and Open-TG2, were tested using the shedding assay.

Figure 4.1 shows the analysis of *p*-NPP hydrolysis of GPR56 and AP-AR co-transfected cells treated with C_{277}-S TG2 and OC-TG2 (purchased from Zedira GmbH, Darmstadt) or C_{230}-A TG2. Treatment with C_{277}-S TG2 activated GPR56 by >30 % compared to buffer control. Treatment with Open-TG2 led to an increase in GPR56 activity of about ~37 % above controls. Thus, both catalytically inactive TG2 variants activated GPR56 to a similar extend as active C_{230}-A TG2 (Fig. 4.1).

These data showed that the catalytic activity of TG2 is dispensable for the stimulation of GPR56-mediated signalling.

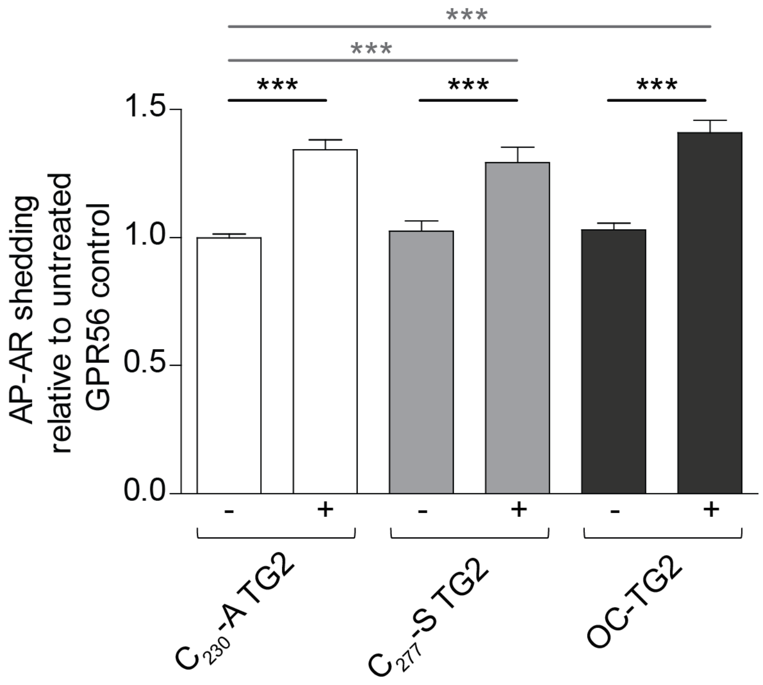

Figure 4.1 Catalytically inactive tissue transglutaminases activate GPR56.

Cells were transfected with GPR56 and AP-AR. Two days post-transfection, cells were serum starved for 1 h, followed by treatment with 20 µg/ml C_{230}-A TG2, C_{277}-S TG2 or Open-TG2 for 1 h.

Data presented show mean of 4 to 7 independent experiments with 4 repeats each +/- SEM (n=16-28). Statistical significance denoted as follows: ***, p<0.001.

4.2.2 Other TG isoenzymes

Previous results showed that TG2, C_{230}-A TG2 as well as two catalytically inactive TG2 variants, C_{277}-S TG2 and OC-TG2, activated GPR56-mediated shedding. Next, other members of the TG family were tested in order to identify novel potential GPR56 ligands.

4.2.2.1 Neuronal transglutaminase (TG6, TG_Y) induces GPR56-dependent AP-AR shedding

To test TG6 as a potential ligand for GPR56, GPR56 and AP-AR co-transfected cells were treated with TG6 or C_{230}-A TG2 for comparison (Fig. 4.2). Treatment with TG6 led to an increase in *p*-NPP hydrolysis of ~30 % compared to buffer control. Treatment with TG6 buffer alone resulted in a 35 % increase when compared to the C_{230}-A TG2 buffer control. Thus, the TG6 buffer had a similar stimulating effect as treatment with C_{230}-A TG2. This was most likely caused by the presence of 10 mg/ml sucrose in the TG6 buffer. In contrast to TG2, TG6 tends to aggregate and precipitate, which is prevented by the addition of sucrose to the buffer (personal communication with Zedira GmbH, Darmstadt). Sucrose is known to inhibit receptor internalisation and could therefore enhance the cell surface expression levels of GPR56, facilitating shedding of AP-AR. TG6 and C_{230}-A TG2 both stimulated GPR56-dependent shedding when compared to their buffer controls.

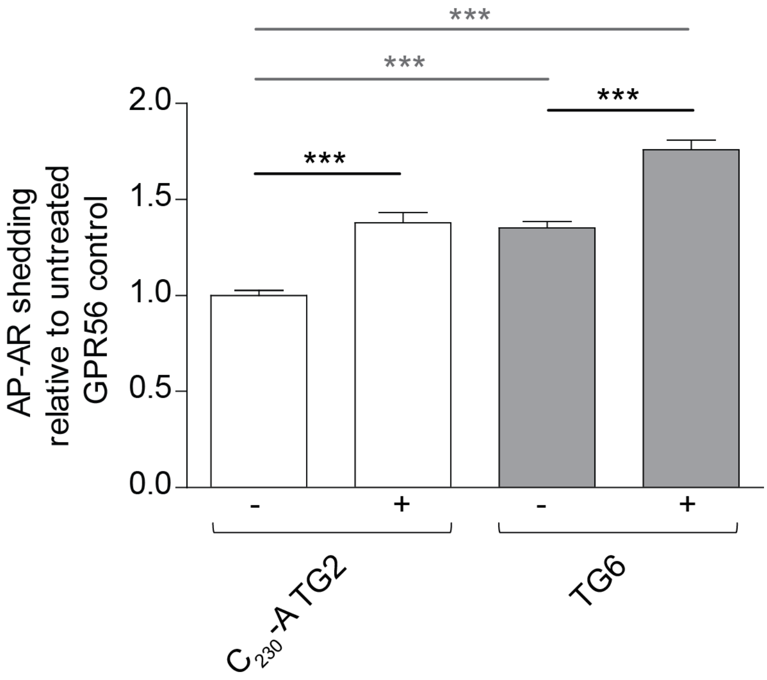

Figure 4.2 TG6 activates GPR56-induced shedding of AP-AR.

Cells were transfected with GPR56 and AP-AR. 48 h post-transfection, cells were serum starved for 1 h, followed by treatment with 20 µg/ml C_{230}-A TG2 or TG6 for 1 h.

Data presented show mean of 4 independent experiments with 4 repeats each +/- SEM (n=16). Statistical significance denoted as follows: ***, p<0.001.

4.2.2.2 Transglutaminase 7 (TG7, TG_Z) activates GPR56

The next member of the transglutaminase family tested was TG7. Cells co-transfected with GPR56 and AP-AR where treated with TG7 or C_{230}-A TG2 and AP activity was analysed in the medium (Fig. 4.3). Treatment with TG7 caused an increase of ~30 % when compared to buffer control. The stimulating effect of TG7 was therefore comparable to that of C_{230}-A TG2. The presence of reduced glutathione in the TG7 buffer did not influence GPR56-dependent shedding of AP-AR.

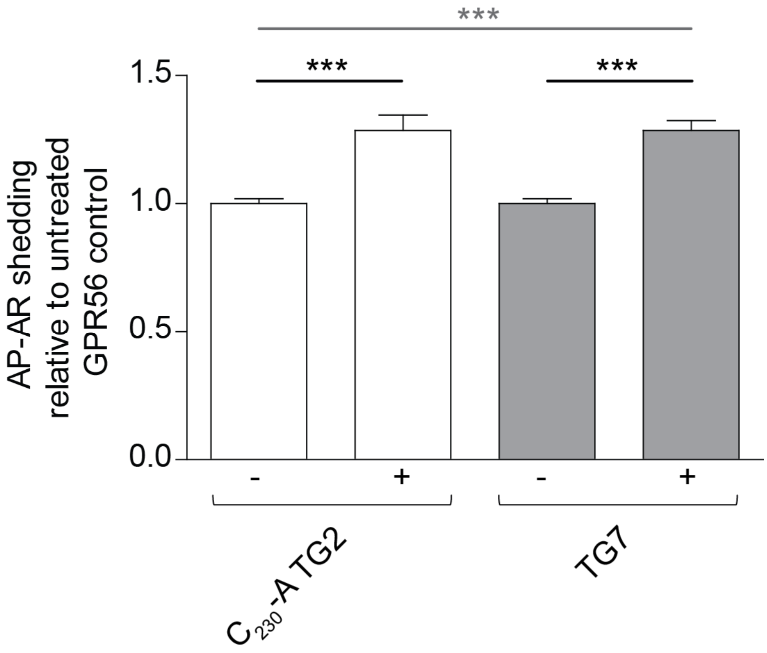

Figure 4.3 TG7 activates GPR56-dependent AP-AR shedding.

Cells were transfected with GPR56 and AP-AR. Two days after transfection, cells were serum starved for 1 h, followed by treatment with 20 µg/ml C_{230}-A TG2 or TG7 for 1 h.

Data presented show mean of 4 independent experiments with 4 repeats each +/- SEM (n=16). Statistical significance denoted as follows: ***, p<0.001.

4.2.2.3 A transglutaminase lacking the β-barrel domains fails to activate GPR56

Next, the involvement of the TG2 β-barrels in GPR56 signalling was tested, as these domains were shown to mediate binding to N-GPR56 (Xu et al. 2006). Unfortunately, a TG2 mutant lacking those domains was not available for the study, but a mutant isoform of the related TG, human factor XIII, solely consisting of the β-sandwich and core domain (ΔFXIII; purchased from Zedira GmbH, Darmstadt) was used to investigate whether the two C-terminal β-barrels of TGs were required to activate GPR56.

GPR56 and AP-AR co-transfected cells were treated with ΔFXIII or C_{230}-A TG2 and AP-activity was analysed in the medium (Fig. 4.4). In contrast to C_{230}-A TG2, treatment with ΔFXIII did not significantly increase *p*-NPP hydrolysis when compared to the buffer controls. Unfortunately, full-length FXIII was not available for control experiments in order to evaluate its ability to activate GPR56.

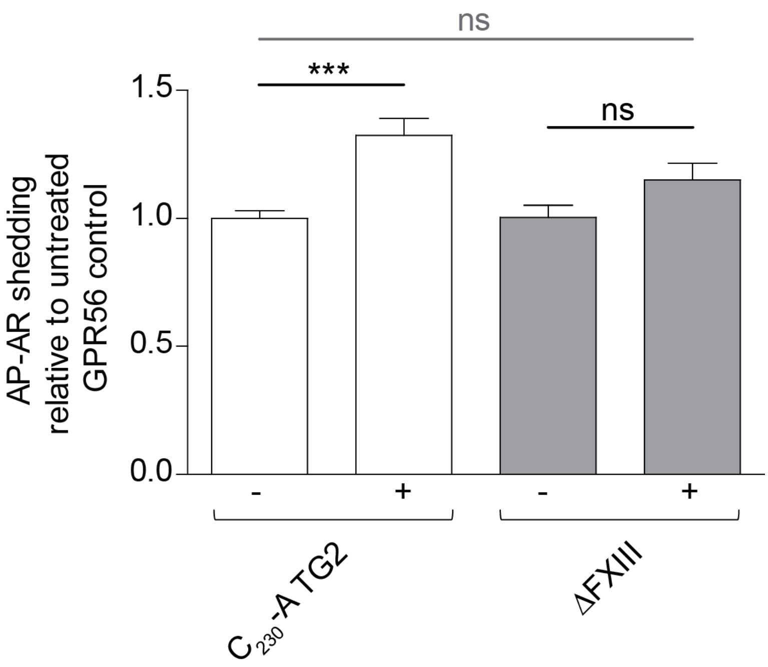

Figure 4.4 Truncated ∆FXIII does not activate GPR56-dependent AP-AR shedding.

Cells were transfected with GPR56 and AP-AR. 48 h post-transfection, cells were serum starved for 1 h, followed by treatment with 20 µg/ml C_{230}-A TG2 or ∆FXIII for 1 h.

Data presented show mean of 3 independent experiments with 4 repeats each +/- SEM (n=12). Statistical significance denoted as follows: ***, p<0.001; ns, non-significant.

4.2.2.4 The β-barrel domains of TG2 are sufficient to activate GPR56

Cells transfected with GPR56 and AP-AR were treated with the β-barrels of TG2 or full-length C_{230}-A TG2 and AP activity was analysed in conditioned medium (Fig. 4.5). Treatment of cells with the β-barrels increased AP-AR shedding significantly when compared to buffer control. However, the stimulation was not as effective as with full-length C_{230}-A TG2.

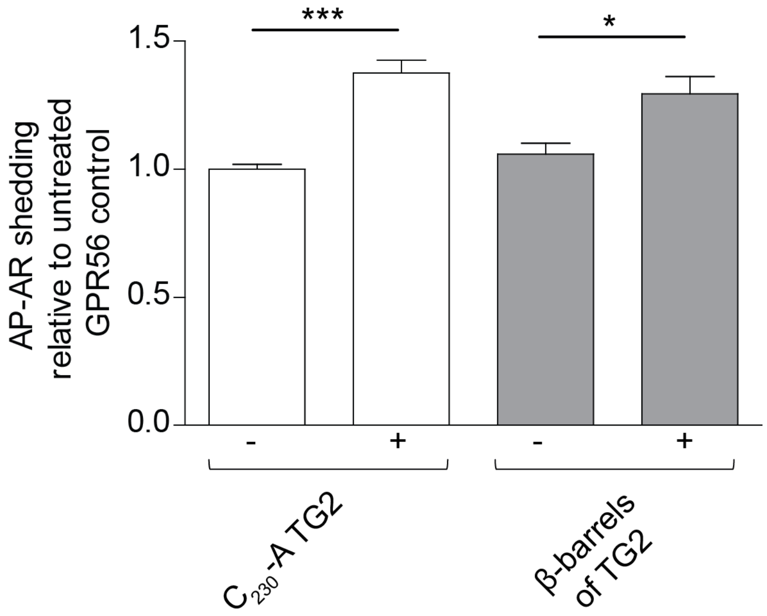

Figure 4.5 The β-barrel domains of TG2 activate GPR56.

Cells were transfected with GPR56 and AP-AR. 48 h post-transfection, cells were serum starved for 1 h, followed by treatment with 20 µg/ml C230-A TG2 or β-barrels of TG2 for 1 h.

Data presented show mean of 6 independent experiments with 4 repeats each +/- SEM (n=24). Statistical significance denoted as follows: ***, $p<0.001$; *, $p<0.05$.

4.3 Discussion

The results presented in this chapter demonstrated that the transglutaminase activity of TG2 is dispensable for activating GPR56. Two catalytically inactive isoforms of TG2, C_{277}-S TG2 and Open-TG2 were used in the shedding assay and both activated GPR56 (Fig. 4.1).

The catalytic site of TG2, crucial for transglutaminase activities including crosslinking, is present in the core domain. This domain is located between the N-terminal β-sandwich and the two C-terminal β-barrels (Fig. 4.6). The catalytic triad within the core domain consists of $cysteine_{277}$ (mutated in C_{277}-S TG2), a histidine and an aspartate, as well as a conserved tryptophan that stabilizes the transition state of TG2, in which the enzyme is catalytically active (Iismaa et al. 2009).

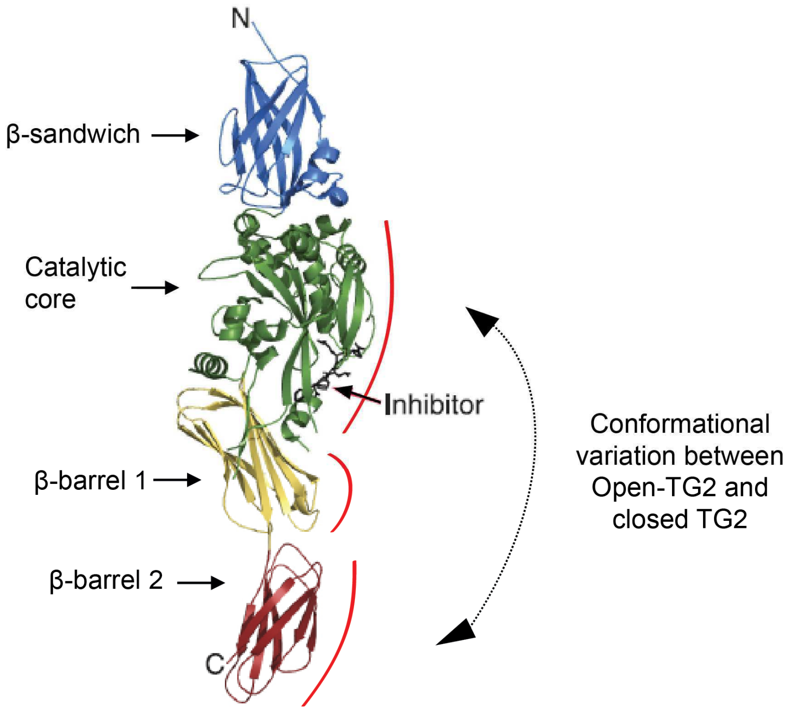
N
β-sandwich
Catalytic core
Inhibitor
β-barrel 1
β-barrel 2
C
Conformational variation between Open-TG2 and closed TG2

Figure 4.6 Crystal structure of Open-TG2.

Expanded form of enzymatically inactive, irreversible peptide inhibitor-bound TG2. Motifs additionally accessible for GPR56-binding in the extended conformation are marked in red.

Taken from Iismaa et al. (2009), modified.

Catalytically active TG2 is known to crosslink itself to ECM proteins like fibronectin, to form intramolecular cross-links stabilizing proteins and intermolecular isopeptide bonds, resulting in the formation of dimers and polymers, as shown for several ECM proteins (Belkin 2011). Thus, it was speculated that TG2 could also crosslink GPR56 intra- or intermolecularly, resulting in conformational changes or the formation of receptor dimers, respectively. A similar phenomenon was observed for FXIIIa, which crosslinks agonist-occupied AT_1 receptors on the cell surface of monocytes from hypertensive patients. Crosslinking of AT_1 resulted in enhanced receptor signalling promoting monocyte adhesion (Abdalla et al. 2004). Moreover, emerging evidence indicates that GPCRs function as oligomers in the cell membrane rather than as monomers (Terrillon and Bouvier 2004; Milligan 2004). However, results shown in figure 4.1 using catalytically inactive C_{277}-S TG2, as well as western blot analysis shown in the previous chapter (3.2.2.1) demonstrated that the transglutaminase activity was not crucial for receptor activation and we were unable to detect crosslinking of GPR56 by TG2. Therefore, TG2 might just act as a ligand for GPR56, by inducing conformational changes and signalling through the receptor.

Experiments using Open-TG2 confirmed the observations made with C_{277}-S TG2, indicating the dispensability of its catalytic activity for activation of GPR56-dependent AP-AR shedding (Fig. 4.1). Open-TG2 remains in an extended conformational state, containing a covalently bound peptide inhibitor that occupies the catalytic site (Fig. 4.6). This prevents conformational changes and Open-TG2 is enzymatically inactive (Pinkas et al. 2007). The β-barrel domains that were proposed to be important for GPR56 binding (Xu et al. 2006) are accessible in Open-TG2. Moreover, there are additional structural motifs accessible in the core domain, as well as in the β-barrels. These motifs are normally buried when TG2 is in the closed conformation and could contribute to receptor binding (Fig. 4.6).

Generally, it is not well understood whether the conformational state of inhibitor-bound Open-TG2 reflects the structure of catalytically active, Ca^{2+}-bound TG2, due to the lack of x-ray structural data (Pinkas et al. 2007; Király et al. 2011). It is still unclear how the enzymatic activity of TG2 is regulated outside the cell (Pinkas et al. 2007). The extracellular milieu is high in Ca^{2+}, which should activate TG2, however, TG2 is inactive under normal physiological conditions. It was speculated that TG2 remains in a closed, catalytically inactive conformation upon secretion (Pinkas et al. 2007), or alternatively that it is inactivated due to oxidation and disulphide formation (Stamnaes et al. 2010). Extracellular TG2 induces cell adhesion and migration independent of its enzymatic activities (Zemskov et al. 2006). Since GPR56 belongs to the family of adhesion GPCRs, regulating neural progenitor cell migration (Iguchi et al. 2008; Luo et al. 2011), these cellular processes might be induced through activation of GPR56 by catalytically inactive TG2.

In order to gain additional information about conformational requirements regarding GPR56 activation, closed TG2 could be tested as a GPR56 ligand. Closed TG2 lacks transglutaminase activity, as the catalytic site is buried in this conformation. It is the predominant isoform of TG2 in the cytoplasm, where Ca^{2+}-levels are low and GTP-levels high. TG2 adopts the closed conformation by binding GTP/GDP and acts as a G protein intracellularly (Achyuthans and Greenberg 1987; Nakaoka et al. 1994). However, in cell culture medium containing 1.8 mM Ca^{2+}, the closed conformation is unstable and can unfold. In order to preserve a closed conformation in the assay, an alternative experimental approach would be employed. A stable TG2-$GTP_{\gamma}S$ complex formed by addition of a non-hydrolysable form of GTP to TG2, would allow to experimentally test this scenario.

Results shown in this chapter also identified two new potential ligands for GPR56, TG6 and TG7 (Fig. 4.2 & Fig. 4.3). Little information is available about TG6 and TG7, but interestingly TG6 was shown to be predominantly expressed in a subset of neurons (Grenard et al. 2001; Aeschlimann and Grenard 2006). GPR56 is involved in early brain development and mutations in GPR56 cause the developmental brain disease BFPP (Piao et al. 2004), thus TG6 might represent a physiological GPR56 ligand in the CNS. TG6 shows close homology to TG2, and TG6 autoantibodies were associated with the development of neurological disorders, such as gluten ataxia (Hadjivassiliou and Aeschlimann 2008). Autoantibodies interacting with TG6 would lead to a TG6 null situation in ataxia patients. If TG6 represents a physiologically relevant ligand for GPR56 in the brain, then depletion of TG6 would also affect GPR56 signalling. This, in turn could contribute to the development of the neurological disorders mentioned above.

The function of TG7 remains elusive, but in addition to the high expression in testis and lung, high transcript levels were found in breast cancer cells (Mehta and Eckert 2005). This finding implicates an involvement in cancer development, which could provide the link to GPR56, which itself was suggested to play a potential role in diverse cancers. GPR56 functions as a tumour suppressor in metastatic melanoma, where its overexpression inhibits tumour growth and metastasis (Xu et al. 2006; Yang et al. 2011) and reduced GPR56 protein levels are associated with pancreatic cancer (Huang et al. 2008). Opposing findings showed that GPR56 down-regulation is associated with the inhibition of melanoma progression, presenting GPR56 as a tumour promoter (Ke et al. 2007; Yang et al. 2014). Moreover, GPR56 mRNA was shown to be up-regulated in diverse cancers like pancreatic, lung, esophageal squamous cell carcinoma and breast cancer, where TG7 could be a putative ligand (Ke et al. 2007; Sud et al. 2006). GPR56 protein is also overexpressed in glioblastoma, where it is potentially involved in adhesion signalling (Shashidhar et al. 2005).

Xu et al. (2006) demonstrated that the β-barrels of TG2 bind GPR56. However, the importance of these domains for receptor activation was demonstrated for the first time in my project. Experiments using truncated ∆FXIII missing the two C-terminal β-barrels indicated that the two domains were indispensable for GPR56 activation (Fig. 4.4). However, it was not tested whether full-length FXIII activates GPR56.

In addition, experiments using the β-barrel domains of TG2 as a ligand for GPR56 showed that they were sufficient to induce GPR56-dependent AP-AR shedding (Fig. 4.5). However, stimulation was not as pronounced as with full-length TG2. Thus, data presented in this project may support a model of GPR56 activation by TGs that requires the presence of full-length TGs. In this model, the C-terminal β-barrels interact with N-GPR56 and the N-terminal domain of TG2, containing the catalytic core, potentially contributes by additional interactions with the 7TM-domain of C-GPR56 (Fig. 4.7). This hypothesis, however, requires further experimental verification. In order to investigate whether C-GPR56 interacts with TG2, a C-GPR56-Fc probe could be used to pulldown TG2. In addition, an N-terminally truncated form of GPR56 was tested in the AP-AR shedding assay and it was shown that this form, lacking the N-terminal TG2 binding domain, was not activated upon TG2 treatment (see Chapter 5).

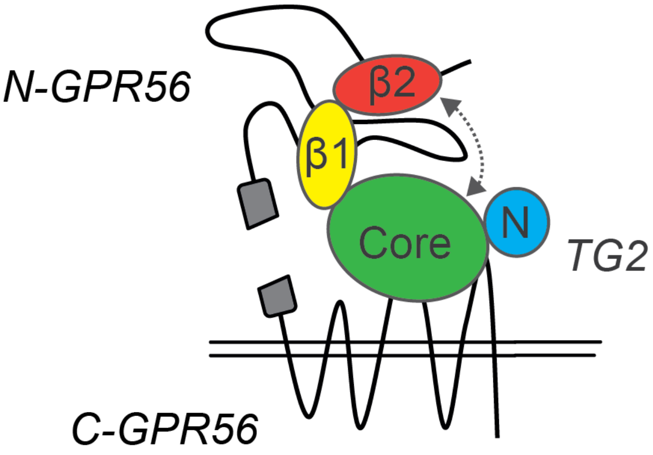

Figure 4.7 Model of potential TG2-GPR56 interactions.

Experiments using the β-barrels of TG2 showed that GPR56 is activated only submaximal when compared to the induction of GPR56-dependent shedding of AP-AR in response to treatments with full-length TG2. Therefore, it was speculated that interactions of the core and the β-sandwich domains of TG2 with the 7TM-domain of GPR56 are required in addition to the interaction between the TG2 β-barrels with N-GPR56 in order to achieve full receptor activation.

In summary, results in this chapter showed that the catalytic activity of TG2 is not required for activation of GPR56-dependent AP-AR shedding. Two new potential ligands, TG6 and TG7 activated GPR56. The experiments also indicated that the β-barrels of TGs are essential for GPR56 interaction and activation.

CHAPTER 5:

Identifying GPR56 structural domains involved in downstream signalling

5 Identifying GPR56 structural domains involved in downstream signalling

5.1 Introduction

Most studies looking at GPR56 functions focus on mutations causing the cobblestone-like brain malformation BFPP (Piao et al. 2004), which is associated with overmigrating neural progenitors through a defective pial BM in the forebrain and the rostral cerebellum. 25 BFPP-associated GPR56 mutations, including missense, splicing and frameshift mutations were identified in human (Piao et al. 2004; Quattrocchi et al. 2013; Singer et al. 2012; Fujii et al. 2013). All of the missense mutations studied in more detail impair receptor trafficking and cell surface expression, indicating that BFPP is caused by the absence of functional GPR56 at the cell surface. This is in line with the finding that GPR56 plays an important role in early brain development and reflected by analysis of *Gpr56*$^{-/-}$ mice, showing a similar cobblestone-like brain malformation (Piao 2004; Li 2008; Koirala 2009).

Several other studies focussed on the putative role of N-GPR56 for receptor signalling, specifically regarding its ligand binding ability and its potential role as an endogenous ligand. The TG2 binding site was identified within aa108-177 and the collagen III-interaction site within aa27-160 of N-GPR56 (Luo et al. 2012; Yang et al. 2011). Deletion of the TG2 binding site or removal of the entire N-terminal domain increased the basal activity of GPR56, indicating an inhibitory role of N-GPR56 in GPR56 activation (Yang et al. 2011; Paavola et al. 2011). In contrast, natural splice variants of GPR56 lacking huge parts of N-GPR56 showed reduced activities in luciferase reporter assays, indicating that truncation of the N-terminus does not always result in constitutive activation of GPR56 (Kim et al. 2010).

Regarding a specific role of the N-terminus, latrophilin-1, another aGPCR was investigated in more detail. Prömel et al. (2012) showed that the null allele *lat-1*(ok1465) of the *C.elegans* latrophilin homolog *lat-1* results in development and fertility phenotypes characterised by a high lethality rate or infertility in surviving individuals, respectively. By expressing certain transgenic *lat-1* proteins in *lat-1*(ok1465) animals both phenotypes could be rescued, which was highly dependent on the presence of the latrophilin-1 N-terminus in the expressed transgene. At the same time, a construct with an intact GPS-site lacking the 7TM-domain ("ΔTM2-7") still rescued the fertility phenotype, which was independent of the presence of specific sequences in the remaining TM1. Therefore, the authors concluded that the receptor had 7TM-independent functions that were not mediated by interactions of the N-terminus and the 7TM-domain of another receptor ("split personality receptor model"), as observed before for the N-terminus of latrophilin-1 and C-GPR56 (Silva et al. 2009). In contrast, Prömel et al. (2012) demonstrated that ΔTM2-7 latrophilin-1 mutants, in addition deficient in GPS-cleavage, rescued both phenotypes if co-expressed with another mutant latrophilin-1 contributing a wild type C-terminus, although the defective C-terminus of ΔTM2-7 was inaccessible for replacement. The authors further showed that the presence, but not the cleavability of the GPS-domain was essential for latrophilin-1 surface expression and signalling, indicating that the GPS-domain served as an endogenous ligand during latrophilin-1 activation that interacted with the homologous 7TM-domain. It was hypothesized that receptor dimerization occurs, in which homodimers are formed (7TM-dependent) due to the interaction of latrophilin-1 N-termini. Another model suggested that *cis*-interactions with co-receptors like teneurin take place, which are mediated through the GPS-domain of latrophilin-1 and do not require activation of the latrophilin-1 7TM-domain.

Much attention was spent on investigating the role of N-GPR56, however the C-terminus of GPCRs also plays a very important role, as it represents a docking site for intracellular proteins facilitating signalling. Expression of the natural splice variant Δ_{430-35}-GPR56 was shown to result in increased transcriptional activities when compared to wild type GPR56, indicating that the six amino acid deletion in ICL1 affects receptor signalling (Kim et al. 2010). Since GPCRs are known to mostly signal via different types of G proteins (Lefkowitz 2000), it is likely that a deletion within ICL1 affects G protein binding or may facilitate the interaction with other signalling mediators like β-arrestins. For a long time, β-arrestins were only known to desensitize GPCRs by physically interrupting G protein-mediated signalling and moreover to promote internalisation via clathrin-coated pits (Shenoy and Lefkowitz 2003). Within seconds of GPCR activation and interaction with G proteins, kinases (GRKs) phosphorylate the GPCR on its cytoplasmic tail or ICL3, promoting the binding of β-arrestins (Lefkowitz 2007). More recently, however, β-arrestins were also found to represent signalling mediator proteins on their own (Lefkowitz and Shenoy 2005).

5.1.1 Aims of the chapter

- To investigate the role of specific domains within GPR56 such as the ligand-binding domain, the entire N-terminus, the C-terminus and potential C-terminal phosphorylation sites, for GPR56 activity and stimulation by TG2.

- To investigate the signalling capacity of a naturally occurring splice variant and a BFPP-causing GPR56 mutant.

5.2 Results

5.2.1 Cloning of the C-terminal tail phosphorylation site mutants ΔS-A-GPR56, T_{688}A-GPR56, ΔS/T-A GPR56

The aim of the following experiments was to generate three new GPR56 mutants with several serine and/or threonine to alanine mutations in the C-terminal tail region between residues 684 to 691. Phosphorylation site prediction within ICL3 and the cytoplasmic tail of GPR56 using NetPhos 2.0 revealed the presence of several residues likely to be phosphorylated (Fig. 5.1). Six serines at position 684, 685, 687, 689, 690, 691 and one threonine at position 688, all located within the cytoplasmic tail, were selected for PCR mutagenesis.

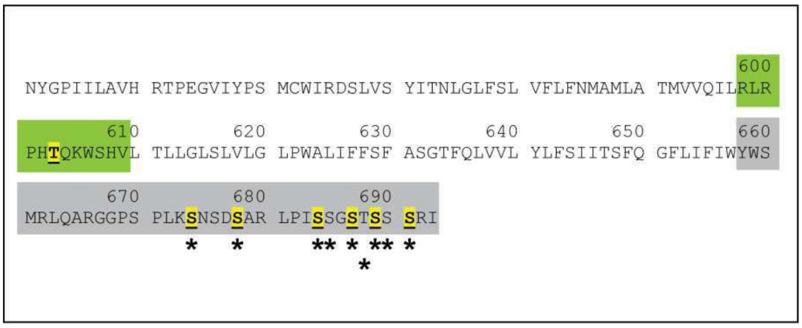
600
NYGPIILAVH RTPEGVIYPS MCWIRDSLVS YITNLGLFSL VFLFNMAMLA TMVVQILRLR
610 620 630 640 650 660
PHTQKWSHVL TLLGLSLVLG LPWALIFFSF ASGTFQLVVL YLFSIITSFQ GFLIFIWYWS
670 680 690
MRLQARGGPS PLKSNSDSAR LPISSGSTSS SRI
* * ** * ** *
*

Amino acid position	Score
S674	0.992
S678	0.796
S684*	0.832
S685*	0.332
S687*	0.976
S689*	0.977
S690*	0.140
S691*	0.521
T603	0.787
T688*	0.207
Y658	0.007

Figure 5.1 Prediction for serine, threonine and tyrosine phosphorylation sites and residues mutated to generate the three phosphorylation site mutants. Phosphorylation sites were predicted for ICL3 and the cytoplasmic tail of GPR56 using NetPhos 2.0 (Center for Biological Sequence Analysis, CBS).

**, mutated residue; yellow marked, residues likely to be phosphorylated (score > 0.5); green box, ICL3 (aa598-609); grey box, cytoplasmic tail (aa658-693).*

The first step was to create an intermediate expression vector carrying C-terminally truncated *Gpr56* (*Gpr56*^{f}), lacking the last ~400 bp (Fig. 5.2 A-B). Meanwhile, the three mutated C-terminal tail fragments were generated by PCR mutagenesis and ligated into *Gpr56*^{f} in pcDNA4-GPR56^{f}/V5-His (Fig. 5.2 B-C). This allowed the creation of three new GPR56 mutant expression vectors, pcDNA4-ΔS-A-GPR56/V5-His ("ΔS-A-GPR56"), pcDNA4-T_{688}A-GPR56/V5-His ("T_{688}A-GPR56") and pcDNA4-ΔS/T-A-GPR56/V5-His ("ΔS/T-A-GPR56") (Fig. 5.2 C). The complete coding sequence of one bacterial clone for each expression construct was sent for dideoxy sequencing (MWG Operon). The sequencing analysis (Fig. 5.3) showed that the T_{688}A-GPR56 mutant carried the threonine to alanine mutation at position 688, as designed. DNA sequencing also revealed that the ΔS-A-GPR56 and ΔS/T-A-GPR56 mutants had all the serine and threonine to alanine mutations except of one serine at position 684, which was replaced by glycine. A check-up of the primers used for the PCR mutagenesis reaction showed that the error was introduced by the primer sequence. As glycine is the smallest natural occurring amino acid and structurally very similar to alanine, the expression constructs were used to assess the contribution of the serine residues in the GPR56 tail towards shedding of AP-AR.

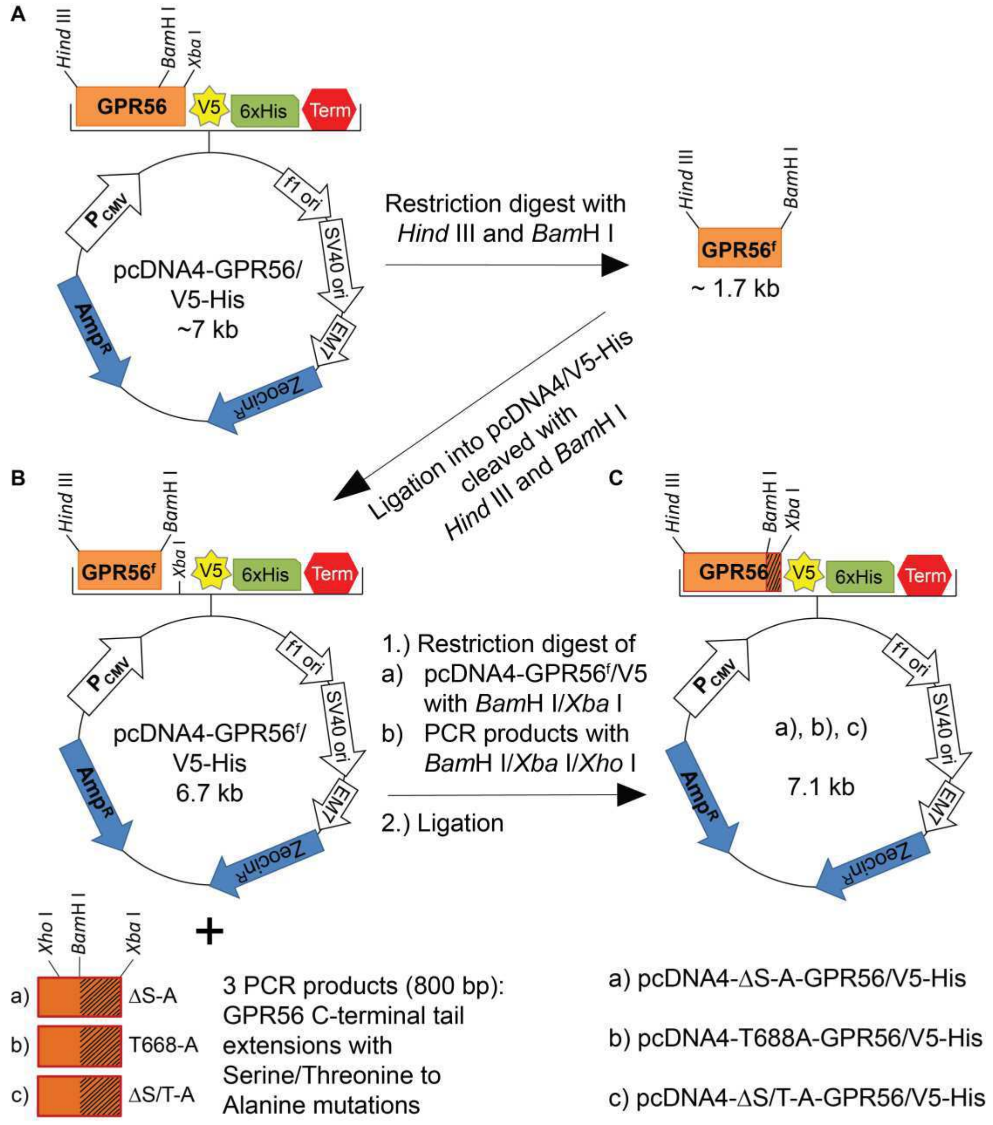
A
Hind III
BamH I
Xba I
GPR56
V5
6xHis
Term
P CMV
f1 ori
SV40 ori
EM7
ZeocinR
AmpR
pcDNA4-GPR56/
V5-His
~7 kb
Restriction digest with
Hind III and BamH I
Hind III
BamH I
GPR56f
~ 1.7 kb
Ligation into pcDNA4/V5-His
cleaved with
Hind III and BamH I
B
Hind III
BamH I
Xba I
GPR56f
V5
6xHis
Term
P CMV
f1 ori
SV40 ori
EM7
ZeocinR
AmpR
pcDNA4-GPR56f/
V5-His
6.7 kb
1.) Restriction digest of
a) pcDNA4-GPR56f/V5
with BamH I/Xba I
b) PCR products with
BamH I/Xba I/Xho I
2.) Ligation
C
Hind III
BamH I
Xba I
GPR56
V5
6xHis
Term
P CMV
f1 ori
SV40 ori
EM7
ZeocinR
AmpR
a), b), c)
7.1 kb
+
Xho I
BamH I
Xba I
a)
b)
c)
ΔS-A
T668-A
ΔS/T-A
3 PCR products (800 bp):
GPR56 C-terminal tail
extensions with
Serine/Threonine to
Alanine mutations
a) pcDNA4-ΔS-A-GPR56/V5-His
b) pcDNA4-T688A-GPR56/V5-His
c) pcDNA4-ΔS/T-A-GPR56/V5-His

Figure 5.2 Cloning of three GPR56 C-terminal tail serine/threonine phosphorylation mutants.

(A) The full-length coding sequence of GPR56 was cleaved with *Hind* III and *Bam*H I to generate a truncated GPR56^{f} fragment. GPR56^{f} was ligated into pcDNA4/V5-His linearized by cleavage with the same restriction enzymes.

(B) The obtained intermediate expression vector pcDNA4-GPR56^{f}/V5-His was digested with *Bam*H I/*Xba* I and the PCR products with *Bam*H I/*Xba* I/*Xho* I. The 400 bp long PCR fragments resulting from *Bam*H I/*Xba* I cleavage were isolated and ligated into linearized pcDNA4-GPR56^{f}/V5-His, respectively.

(C) The final cloning products pcDNA4-ΔS-A-GPR56/V5-His, pcDNA4-ΔS/T-A-GPR56/V5-His and pcDNA4-T$_{688}$A-GPR56/V5-His were used to transform *E.coli.* Positive clones were selected by ampicillin resistance, DNA was amplified and sent for dideoxy sequencing.

pcDNA4-∆S-A-GPR56/V5-His:

∆S-A *658* YWSMRLQARGGPSPLKSNSDSARLPI**GA**G**A**T**AAA**RI *693*
YWSMRLQARGGPSPLKSNSDSARLPI..G.T...RI
GPR56 *658* YWSMRLQARGGPSPLKSNSDSARLPISSGSTSSSRI *693*

pcDNA4-∆S/T-A-GPR56/V5-His:

S/T-A *658* YWSMRLQARGGPSPLKSNSDSARLPI**GA**G**AAAAA**RI *693*
YWSMRLQARGGPSPLKSNSDSARLPI..G.....RI
GPR56 *658* YWSMRLQARGGPSPLKSNSDSARLPISSGSTSSSRI *693*

pcDNA4-T688A-GPR56/V5-His:

T688A *658* YWSMRLQARGGPSPLKSNSDSARLPISSGS**A**SSSRI *693*
YWSMRLQARGGPSPLKSNSDSARLPISSGS.SSSRI
GPR56 *658* YWSMRLQARGGPSPLKSNSDSARLPISSGSTSSSRI *693*

Figure 5.3 Sequencing analysis of GPR56 phosphorylation site mutants.

The results of the dideoxy sequencing (MWG operon) were used to generate sequence alignments of the C-terminal tail region (aa 658-693) of full-length GPR56 and the three phosphorylation site mutants. The full amino acid sequence of wild type GPR56 is included in Appendix V.

5.2.2 Analysis of wild type and mutant GPR56 expression levels in transiently transfected HEK293 cells

Besides the three C-terminal phosphorylation site mutants ΔS-A-GPR56, T_{688}A-GPR56 and ΔS/T-A-GPR56 described above, five mutants were cloned by Dr. Vera Knäuper: The ligand interaction site deletion mutant ΔSTP-GPR56 lacking the TG2- and collagen III-binding sites (Δ93-143), the N-terminal domain deletion mutant ΔN-GPR56 (Δ1-342), a C-terminal ΔTail-GPR56 mutant missing the last 23 residues (Δ671-693), the natural splice variant $\Delta_{430\text{-}35}$-GPR56 carrying a six amino acid deletion in ICL1, the BFPP-mutant R_{565}W-GPR56 with the mutation in ECL2 and N-GPR56 consisting of the N-terminal domain only (Δ383-693).

Figure 5.4 illustrates all of the GPR56 constructs used in this study.

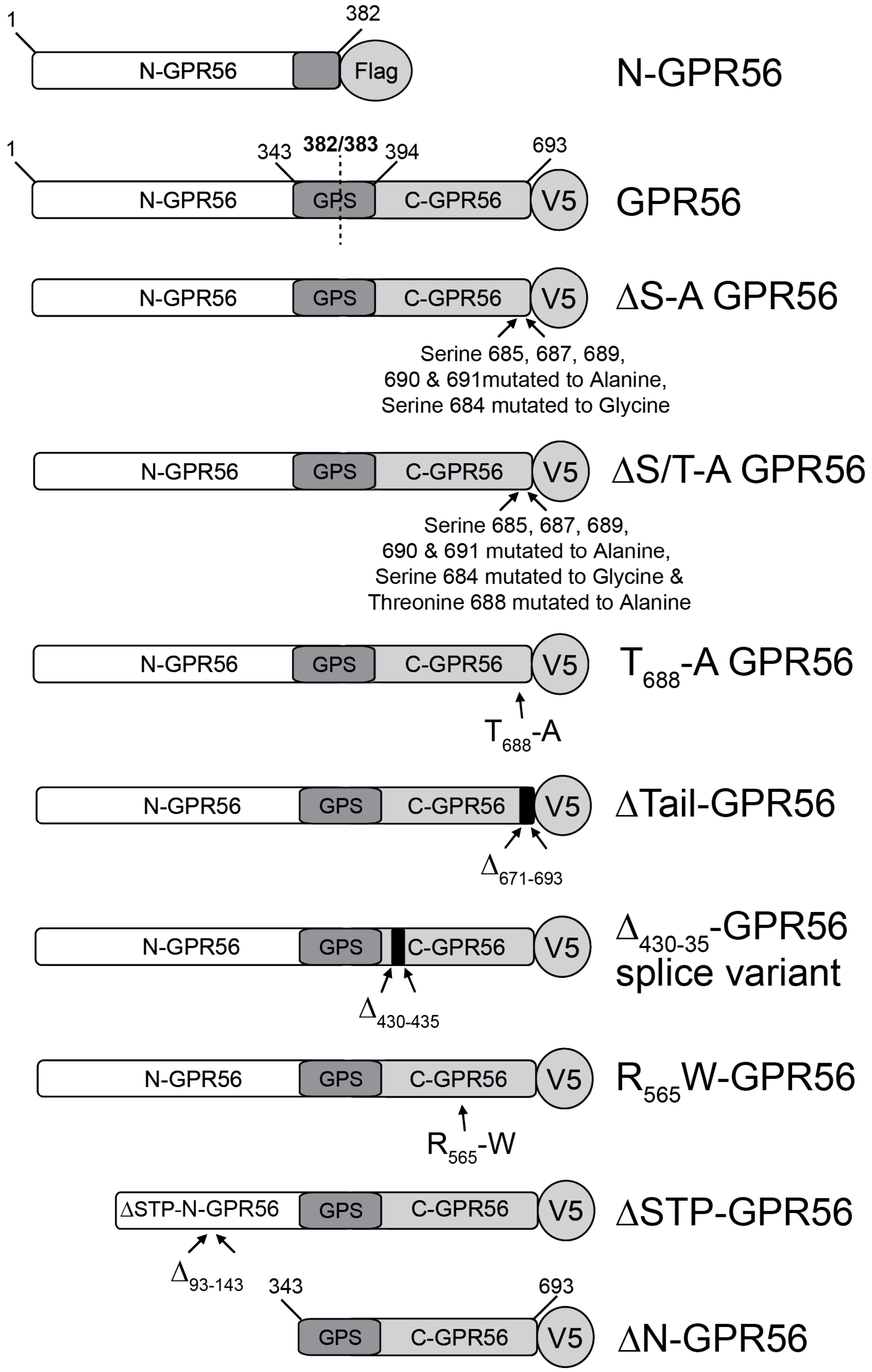
1
382
N-GPR56
Flag
N-GPR56
1
343
382/383
394
693
N-GPR56
GPS
C-GPR56
V5
GPR56
N-GPR56
GPS
C-GPR56
V5
ΔS-A GPR56
Serine 685, 687, 689,
690 & 691mutated to Alanine,
Serine 684 mutated to Glycine
N-GPR56
GPS
C-GPR56
V5
ΔS/T-A GPR56
Serine 685, 687, 689,
690 & 691 mutated to Alanine,
Serine 684 mutated to Glycine &
Threonine 688 mutated to Alanine
N-GPR56
GPS
C-GPR56
V5
T688-A GPR56
T688-A
N-GPR56
GPS
C-GPR56
V5
ΔTail-GPR56
Δ671-693
N-GPR56
GPS
C-GPR56
V5
Δ430-35-GPR56
splice variant
Δ430-435
N-GPR56
GPS
C-GPR56
V5
R565W-GPR56
R565-W
ΔSTP-N-GPR56
GPS
C-GPR56
V5
ΔSTP-GPR56
Δ93-143
343
693
GPS
C-GPR56
V5
ΔN-GPR56

Figure 5.4 Schematic representation of GPR56 expression constructs.

N-GPR56, N-terminal domain of GPR56; C-GPR56, C-terminal domain of GPR56; GPS, GPCR proteolytic site; V5, V5-epitope tag; Flag, Flag-epitope tag; STP, serine/threonine/proline-rich sequence motif within N-GPR56.

Firstly, immunocytochemical analysis of cell surface expression and localisation of the GPR56 mutants was performed in transiently transfected HEK293 cells using confocal microscopy. In figure 5.5 and 5.6, cells transiently transfected with wild type GPR56 or GPR56 mutants are shown. For cell surface staining, cells were fixed and stained with anti-N-GPR56 antibody without permeabilising cells, as shown in figure 5.5. The C-terminus of GPR56 was stained in permeabilised cells with anti-V5 antibody, as shown in figure 5.6 A.

The C-terminal phosphorylation site mutants ΔS-A-GPR56, T_{688}A-GPR56 and ΔS/T-A GPR56, as well as ΔTail-GPR56, the natural splice variant $\Delta_{430\text{-}35}$-GPR56 and wild type GPR56 showed high cell surface and cytoplasmic expression levels (Fig. 5.5 & 5.6). The ligand interaction site deletion mutant ΔSTP-GPR56 showed very little cell surface staining and was mostly located in the perinuclear region, implicating folding and/or trafficking problems. The same was observed for the BFPP-mutant R_{565}W-GPR56, which is in good agreement with a previous report from the literature (Chiang et al. 2011). The N-terminal domain deletion mutant ΔN-GPR56 showed normal cell surface localisation (Fig. 5.6 A).

Cells expressing N-GPR56 were also probed with anti-N-GPR56 antibody for cell surface staining (Fig. 5.5), but an anti-Flag antibody was used to stain N-GPR56 in permeabilised cells, as it contains a C-terminal Flag-epitope tag (Fig. 5.6 B). Although there is no membrane anchor keeping N-GPR56 at the cell membrane, it showed some cell surface localisation indicating binding to cell surface proteins, confirming previous findings by others (Paavola et al. 2011).

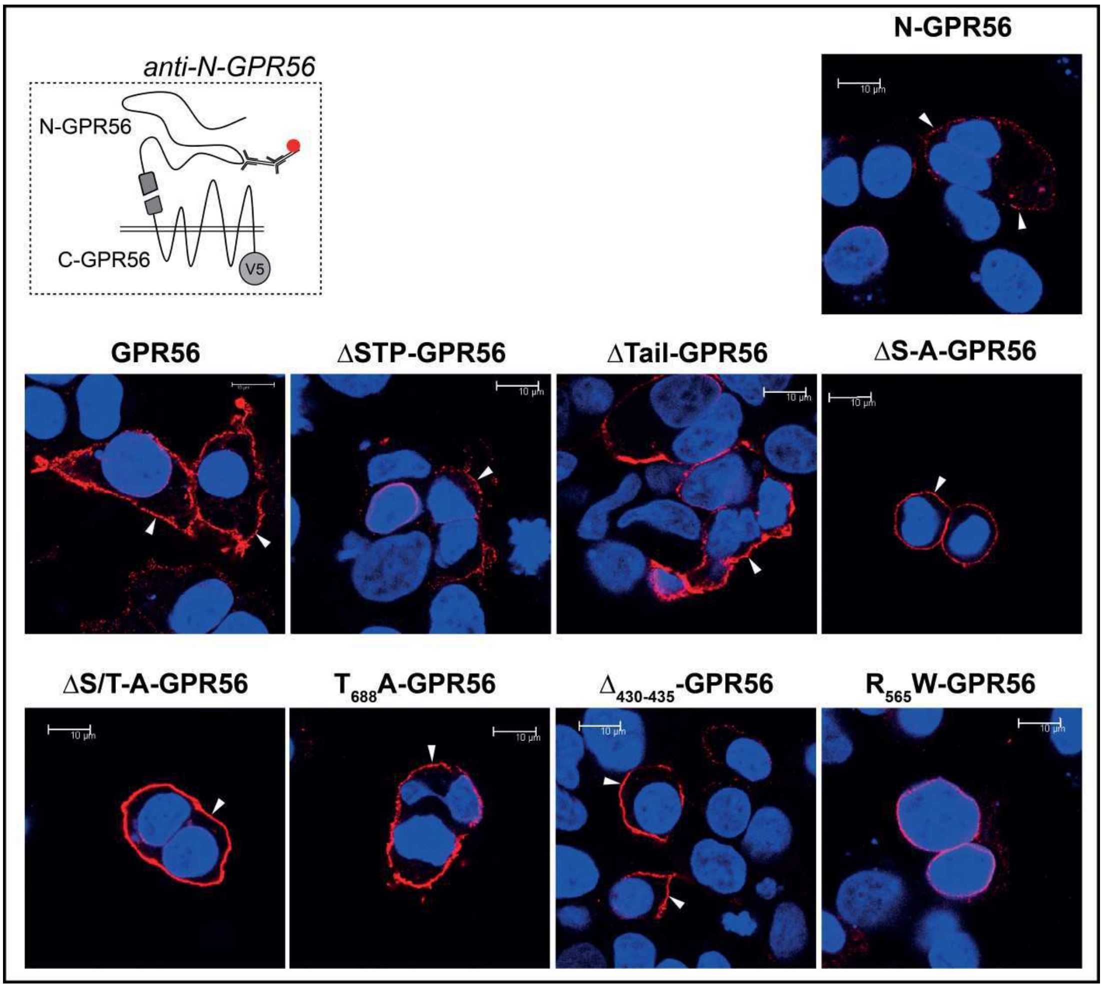
anti-N-GPR56
N-GPR56
C-GPR56
V5
N-GPR56
GPR56
ΔSTP-GPR56
ΔTail-GPR56
ΔS-A-GPR56
ΔS/T-A-GPR56
T688A-GPR56
Δ430-435-GPR56
R565W-GPR56
10 µm

Figure 5.5 Cell surface staining of wild type and mutant GPR56 in transiently transfected HEK293.

Cells were seeded onto poly-L-lysine glass coverslips and transfected with GPR56 or one of the mutant GPR56 expression constructs. Two days post-transfection, cells were fixed and stained with anti-N-GPR56 (R&D Systems) and secondary anti-sheep Alexa549 (Jackson ImmunoResearch) antibodies (red).

White arrow heads, GPR56 cell surface expression (red); scale bar, 10 µm.

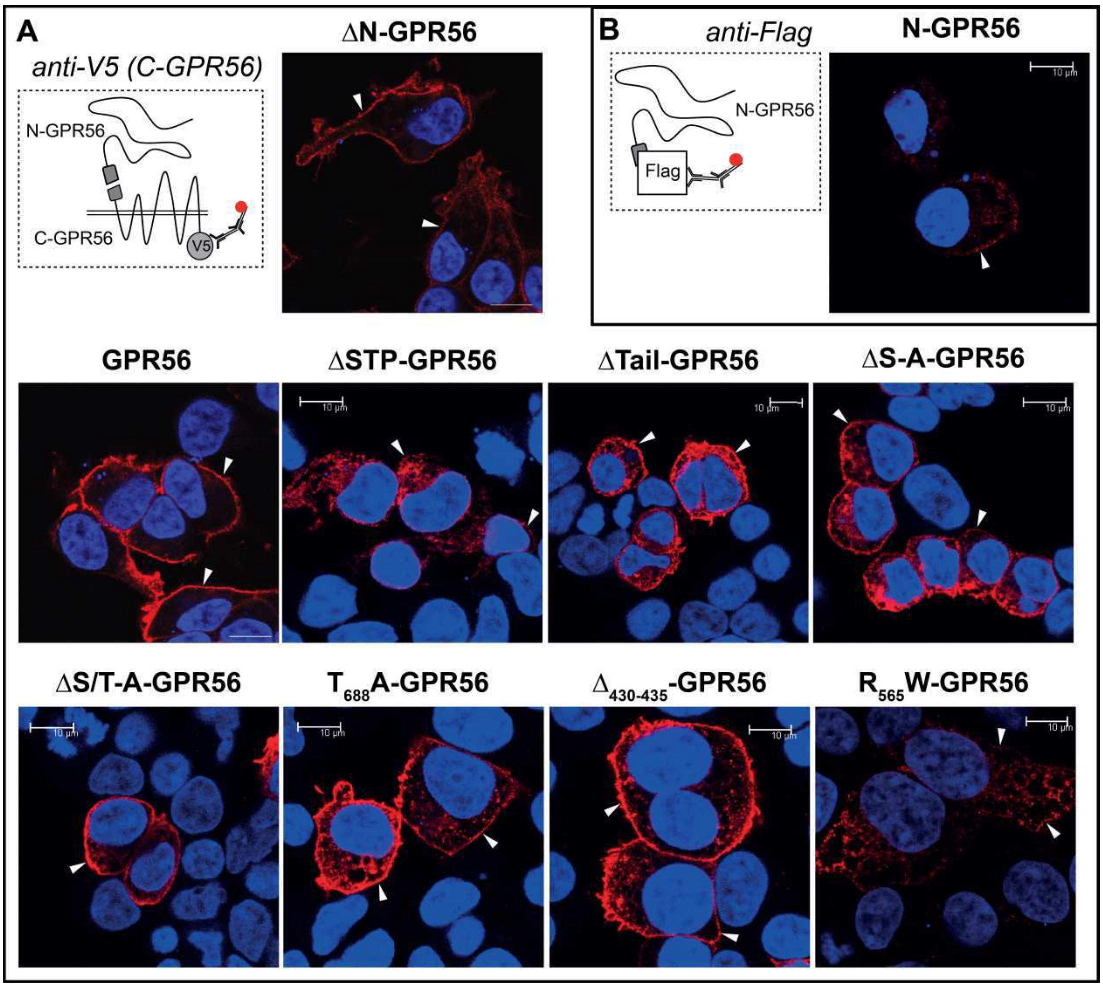
A
anti-V5 (C-GPR56)
N-GPR56
C-GPR56
V5
ΔN-GPR56
B
anti-Flag
N-GPR56
Flag
N-GPR56
10 µm
GPR56
ΔSTP-GPR56
ΔTail-GPR56
ΔS-A-GPR56
ΔS/T-A-GPR56
T688A-GPR56
Δ430-435-GPR56
R565W-GPR56

Figure 5.6 Immunolocalisation of wild type and mutant GPR56 in transiently transfected HEK293 cells under permeabilising conditions.

Cells were seeded onto poly-L-lysine glass coverslips and transfected with GPR56 or one of the mutant GPR56 expression constructs. Two days post-transfection, cells were fixed and permeabilised.

(A) For detection of the GPR56 C-terminal domain via the V5-epitope tag, cells were stained with mouse anti-V5 (Invitrogen) and anti-mouse Alexa594 (Jackson ImmunoResearch) antibodies (red).

(B) To detect the C-terminal Flag-epitope tag of N-GPR56-Flag, cells were stained with mouse anti-Flag (Sigma-Aldrich) and secondary anti-mouse Alexa594 (Jackson ImmunoResearch) antibodies (red).

White arrow heads, GPR56 cell surface expression (red); scale bar, 10 µm.

5.2.3 GPR56 mutants in the AP-AR shedding assay

5.2.3.1 Basal- and C_{230}-A TG2-induced AP-AR shedding is impaired in the BFPP-mutant R_{565}W-GPR56 and the natural splice variant $\Delta_{430\text{-}35}$-GPR56

Confocal microscopy of cells stained with anti-N-GPR56 and anti-V5 antibodies (Fig. 5.5 & 5.6) indicated reduced cell surface expression of the R_{565}W-GPR56 mutant when compared to wild type GPR56. In contrast to the BFPP-mutant, the splice variant $\Delta_{430\text{-}35}$-GPR56 showed strong surface expression (Fig. 5.5 & 5.6).

In order to test the activity of both GPR56 mutants, R_{565}W-GPR56 and $\Delta_{430\text{-}35}$-GPR56 were compared to wild type GPR56 in shedding assays (Fig. 5.7). *p*-NPP hydrolysis was significantly decreased in cells co-expressing the R_{565}W-GPR56 BFPP-mutant in non-stimulated conditions (Fig. 5.7 A), demonstrating some loss of constitutive activity which may be due to impaired cell surface expression. The mutant was not activated by C_{230}-A TG2, which again can be explained by the diminished cell surface expression of R_{565}W-GPR56 shown in figures 5.5 & 5.6.

The splice variant $\Delta_{430\text{-}35}$-GPR56 behaved similar to R_{565}W-GPR56 showing impaired *p*-NPP hydrolysis in non-stimulated conditions and lack of stimulation by C_{230}-A TG2 (Fig. 5.7 B). The six residue deletion in ICL1 might influence the interaction with intracellular binding partners such as G proteins, altering the signalling ability of the splice variant and signalling pathways activated.

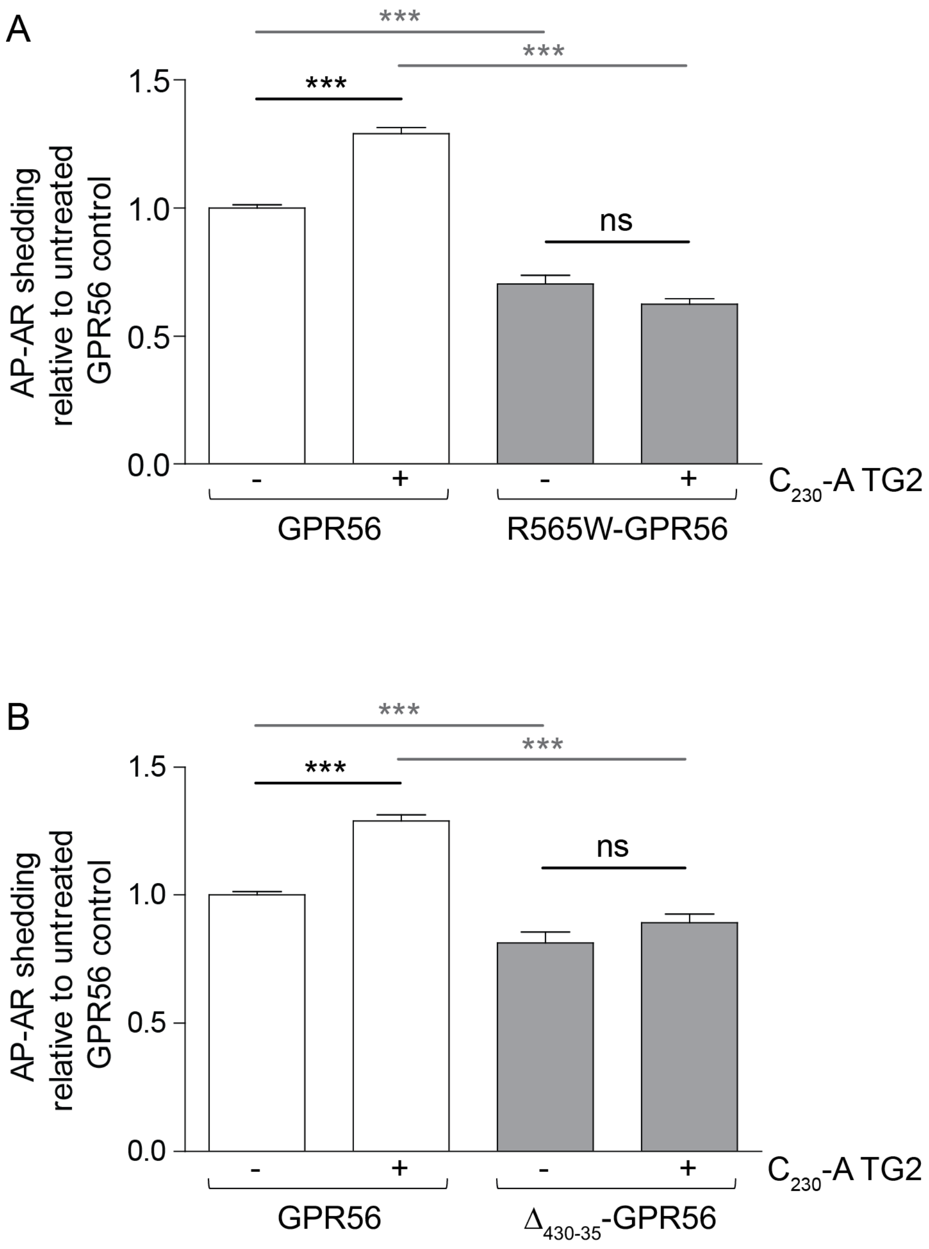

Figure 5.7 The BFPP-mutant R_{565}W-GPR56 and the splice variant Δ_{430-35}-GPR56 show a significant decrease in basal- and C_{230}-A TG2-induced AP-AR shedding.

Cells were co-transfected with (A) GPR56 and AP-AR or R_{565}W-GPR56 and AP-AR, or (B) Δ_{430-35}-GPR56 and AP-AR or GPR56 and AP-AR. 48 h later, cells were serum starved for 1 h, followed by 1 h treatment in control buffer or 20 µg/ml C_{230}-A TG2. Data presented show mean of 5 to 18 independent experiments with 4 repeats each +/- SEM (n=20-72). Statistical significance denoted as follows: ***, p<0.001; ns, non-significant.

In order to analyse overall expression levels of the different GPR56 mutants, cell lysates were prepared and analysed by western blotting. Figure 5.8 shows the analysis of total lysates from cells expressing GPR56, Δ_{430-35}-GPR56 and R_{565}W-GPR56 using anti-N-GPR56 antibody (Fig. 5.8 A) or anti-V5 antibody (Fig. 5.8 B). Western Blot analysis revealed high expression levels for GPR56 and Δ_{430-35}-GPR56 using the anti-N-GPR56 antibody (Fig. 5.8 A), showing the typical banding pattern of four main bands at ~60, 65, 70 and 75 kDa.

In contrast, the R_{565}W-GPR56 mutant showed one prominent band at the lower molecular size of ~58 kDa (Fig. 5.8 A), indicating problems with N-glycosylation, as shown by others (Jin et al. 2007; Chiang et al. 2011). A band running above 245 kDa was detected in lysates of R_{565}W-GPR56 only, likely representing poly-ubiquitinated or multimeric protein.

Staining of lysates from cells expressing GPR56 or Δ_{430-35}-GPR56 with the anti-V5 antibody (Fig. 5.8 B) showed strong bands running at ~27, 50 and 75 kDa, most likely reflecting monomeric, dimeric and full-length receptor. For Δ_{430-35}-GPR56, elevated band intensities for monomeric C-GPR56 were detected. The signal intensity of full-length receptor running at 75 kDa was comparable to wild type GPR56, whereas intensities of dimeric C-GPR56 running at 50 kDa were reduced.

The R_{565}W-GPR56 showed reduced expression levels for all bands corresponding to the C-GPR56 domain detected with the anti-V5 antibody, but the receptor was processed, as shown by the presence of dimeric and monomeric C-GPR56 (Fig. 5.8 B). Therefore, the R_{565}W-mutation does not influence GPS-cleavage, as shown by others (Jin et al. 2007; Chiang et al. 2011). As seen in figure 5.8 B, a high molecular weight band running at 245 kDa was detected with anti-V5 antibody in lysates of R_{565}W-GPR56 only, indicating protein aggregation (Chiang et al. 2011).

Moreover, decreased expression levels of dimeric C-GPR56 in response to C_{230}-A TG2 were only observed in cells expressing GPR56. The protein ladder between monomeric and dimeric C-GPR56 in Δ_{430-35}-GPR56 could represent degraded protein.

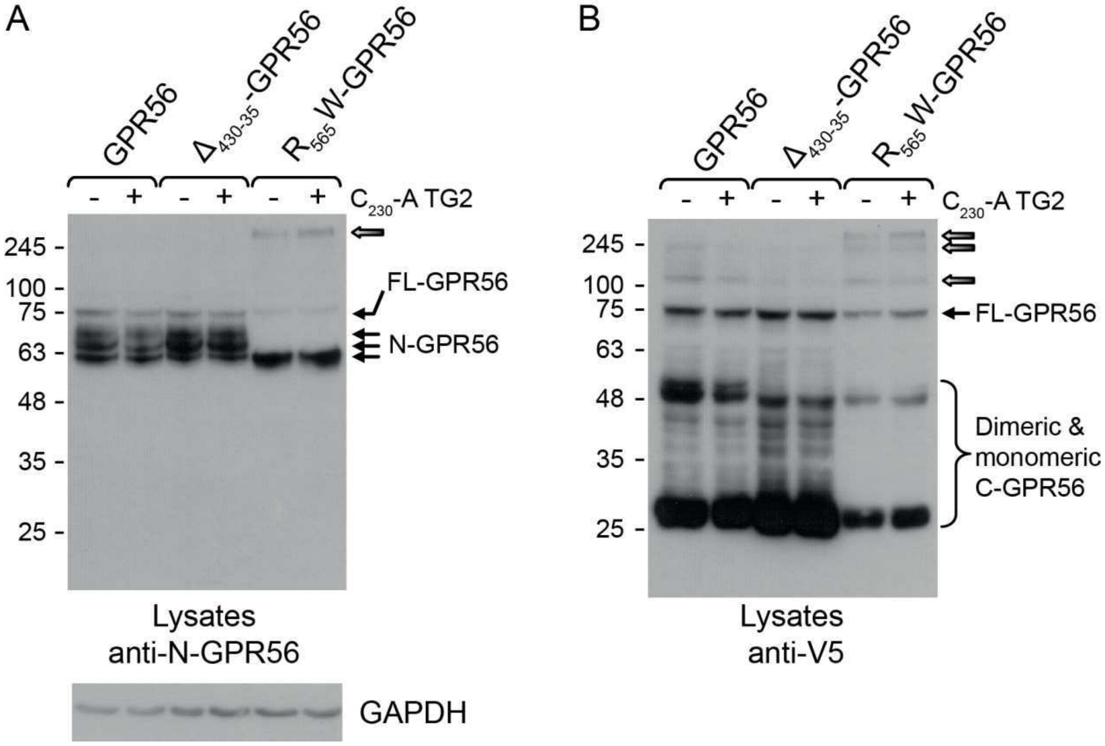
A
GPR56
Δ430-35-GPR56
R565W-GPR56
- + - + - +
C230-A TG2
245
100
75
63
48
35
25
FL-GPR56
N-GPR56
Lysates
anti-N-GPR56
GAPDH
B
GPR56
Δ430-35-GPR56
R565W-GPR56
- + - + - +
C230-A TG2
245
100
75
63
48
35
25
FL-GPR56
Dimeric &
monomeric
C-GPR56
Lysates
anti-V5

Figure 5.8 Western Blot analysis of total lysates from cells expressing GPR56, $\Delta_{430\text{-}35}$-GPR56 or R_{565}W-GPR56 used in the AP-AR shedding assay.

Total cell lysates were prepared, separated in a 10% resolving gel and blotted onto PVDF-membrane, which was stained with (A) anti-N-GPR56 antibody or (B) anti-V5 antibody. Anti-GAPDH staining was used as loading control. Data are representative for 5 independent experiments.

For all following western blots 10% resolving gels were used if not otherwise stated.

5.2.3.2 TG2-stimulated GPR56-dependent AP-AR shedding requires the N-terminal domain of the receptor

5.2.3.2.1 The ligand interaction site deletion mutant ∆STP-GPR56

Using overlap extension mutagenesis, 51 amino acids (∆93-143) of a serine, threonine, proline (STP)-rich region within N-GPR56 were removed (by Dr. Vera Knäuper). Thus, ∆STP-GPR56 lacks parts of both binding motifs for TG2 and collagen III, which partially overlap (Luo et al. 2012; Yang et al. 2011; Li et al. 2008).

Analysis by confocal microscopy revealed that ∆STP-GPR56 had a folding or trafficking defect, as there was only very little protein present at the cell surface (Fig. 5.5 & 5.6). To test the hypothesis that low surface expression would be reflected in loss of signalling, ∆STP-GPR56 and GPR56 were compared in shedding assays (Fig. 5.9 A). Co-expression of ∆STP-GPR56 led to significantly reduced AP-activities when compared to GPR56 in non-stimulated conditions. C_{230}-A TG2 treatment failed to stimulate GPR56-dependent shedding in cells co-expressing ∆STP-GPR56, indicating loss of receptor activation.

Western Blot analysis using anti-N-GPR56 antibody (Fig. 5.9 B) showed an intense band at 70 kDa in cells expressing ∆STP-GPR56, likely representing full-length protein (FL-∆STP-GPR56). The mutant isoform was ~5 kDa smaller than FL-GPR56, which is in accordance to the deletion of 51 amino acids (Li et al. 2008). The band corresponding to FL-∆STP-GPR56 was very pronounced, indicating reduced processing of mutant receptor. However, a band of smaller molecular size was detected at ~52 kDa, likely representing cleaved ∆STP-N-GPR56. High molecular weight bands running around 245 kDa were detected with anti-V5 antibody in lysates of ∆STP-GPR56, indicating protein aggregation.

Staining with anti-V5 antibody (Fig. 5.9 C) showed similar band intensities for monomeric C-GPR56 at 27 kDa for ∆STP-GPR56, but reduced intensities for the dimeric 50 kDa bands when compared to lysates of GPR56 expressing cells treated with control buffer. The FL-ΔSTP-GPR56 was also detected with the anti-V5 antibody and higher molecular weight bands, representing ubiquitinated or multimeric receptor forms, were detected in lysates of ΔSTP-GPR56 only.

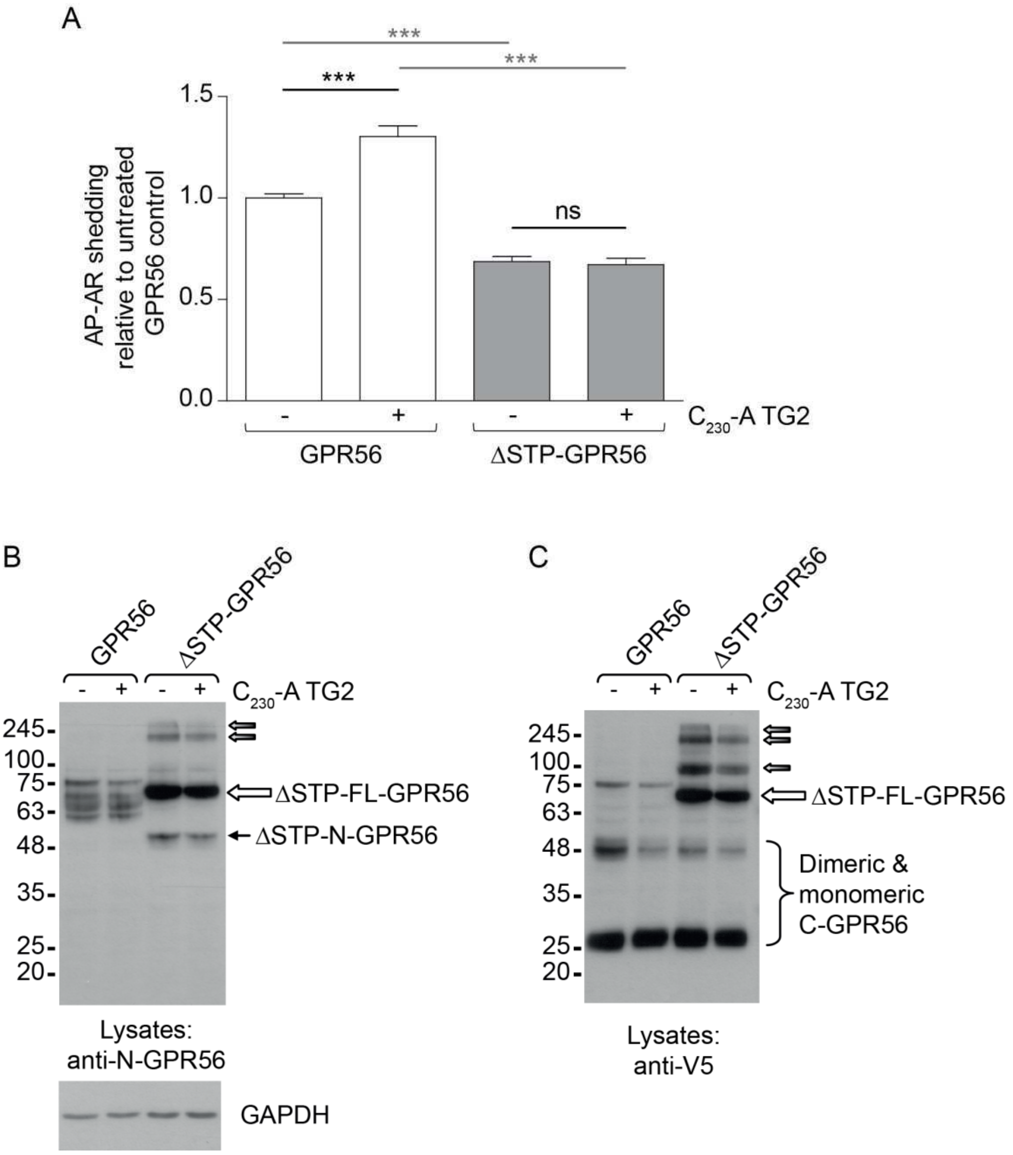

Figure 5.9 Deletion of 51 residues within N-GPR56 results in a significant decrease of basal- and C_{230}-A TG2 induced AP-AR shedding and less processing of the receptor.

(A) Cells were transfected with ΔSTP-GPR56 and AP-AR or GPR56 and AP-AR for comparison. 48 h later, cells were serum starved for 1 h, followed by treatment with control buffer or 20 µg/ml C_{230}-A TG2 for 1 h. Data presented show mean of 3 independent experiments with 4 repeats each +/- SEM (n=12). Statistical significance denoted as follows: ***, p<0.001, ns, non-significant.

(B)&(C) Western Blot analysis of the cells used for the shedding assay in (A). Total cell lysates were prepared and analysed using (B) anti-N-GPR56 antibody and (C) anti-V5 antibody. Anti-GAPDH labelling was used as loading control. Data are representative for 3 independent experiments.

5.2.3.2.2 The N-terminal domain deletion mutant ∆N-GPR56

In order to test the activity of ∆N-GPR56 (∆1-342) lacking the N-terminal domain up to the GPS domain, GPR56 and ∆N-GPR56 were tested in the shedding assay (Fig. 5.10 A). When compared to GPR56, *p*-NPP hydrolysis was slightly elevated in ∆N-GPR56 expressing cells in non-stimulated conditions, indicating enhanced constitutive activity. This is in line with observations made by Paavola et al. (2011), who used the same mutant.
∆N-GPR56 did not respond to C_{230}-A TG2 stimulation, as the ligand binding site was missing. Analysis by confocal microscopy using anti-V5 antibody showed normal cell surface localisation for ∆N-GPR56 (Fig. 5.6 A).

Western Blot analysis using anti-N-GPR56 antibody confirmed the absence of the N-terminal domain in ∆N -GPR56 (Fig. 5.10 B).
Staining with anti-V5 antibody (Fig. 5.10 C) showed reduced band intensities for ∆N-GPR56 when compared to the corresponding domain of wild type GPR56. The bands for monomeric and dimeric C-GPR56 ran slightly higher in cells expressing ∆N-GPR56 when compared to wild type GPR56. This is interesting, as wild type C-GPR56 and ∆N-GPR56 should have the same size and differences might be due to ubiquitination and require further analysis.

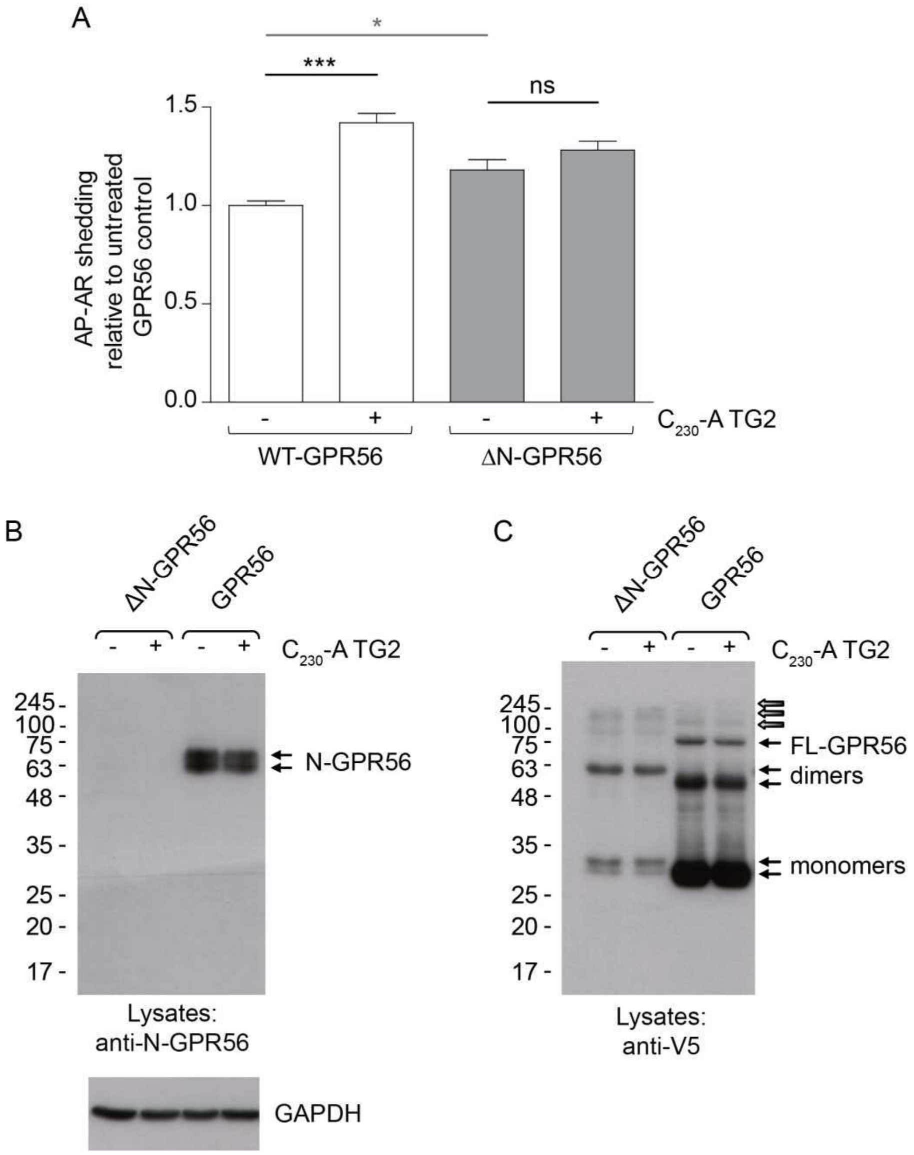

Figure 5.10 Deletion of the N-terminal domain enhances basal AP-AR shedding activity and ablates stimulation by TG2.

(A) Cells were transfected with ΔN-GPR56 and AP-AR or GPR56 and AP-AR. 48 h post-transfection, cells were serum starved for 1 h and treated with control buffer or 20 µg/ml C_{230}-A TG2 for 1 h. Data presented show mean of 3 independent experiments with 4 repeats each +/- SEM (n=12). Statistical significance denoted as follows: ***, p<0.001; *, p<0.05; ns, non-significant.

(B)&(C) Western Blot analysis of cells expressing GPR56 or ΔN-GPR56. Total lysates were separated in a 12.5% resolving gel and blotted onto a PVDF-membrane that was stained with (B) anti-N-GPR56 antibody or (C) anti-V5 antibody. GAPDH loading control is shown. Data are representative for 3 independent experiments.

5.2.3.3 Multiple mutations of six serine residues alone or in conjunction with threonine-688 in the C-terminal tail of GPR56 do not affect receptor-induced signalling

Several serine and threonine residues located within the C-terminal tail of GPR56 represent potential ligand-induced phosphorylation sites (Fig. 5.1). The next step was to test whether mutation of these residues would influence GPR56-dependent AP-AR shedding. The effect of losing six to seven potential phosphorylation sites in the C-terminal tail was tested by comparing ∆S-A-GPR56 with GPR56, or ∆S/T-A-GPR56 with GPR56 in AP-AR shedding assays (Fig. 5.11 A&B). The mutation of six serine residues alone (Fig. 5.11 A) or in conjunction with threonine-688 (Fig. 5.11 B) did not significantly alter GPR56-dependent shedding in the absence or presence of C_{230}-A TG2 when compared to GPR56.

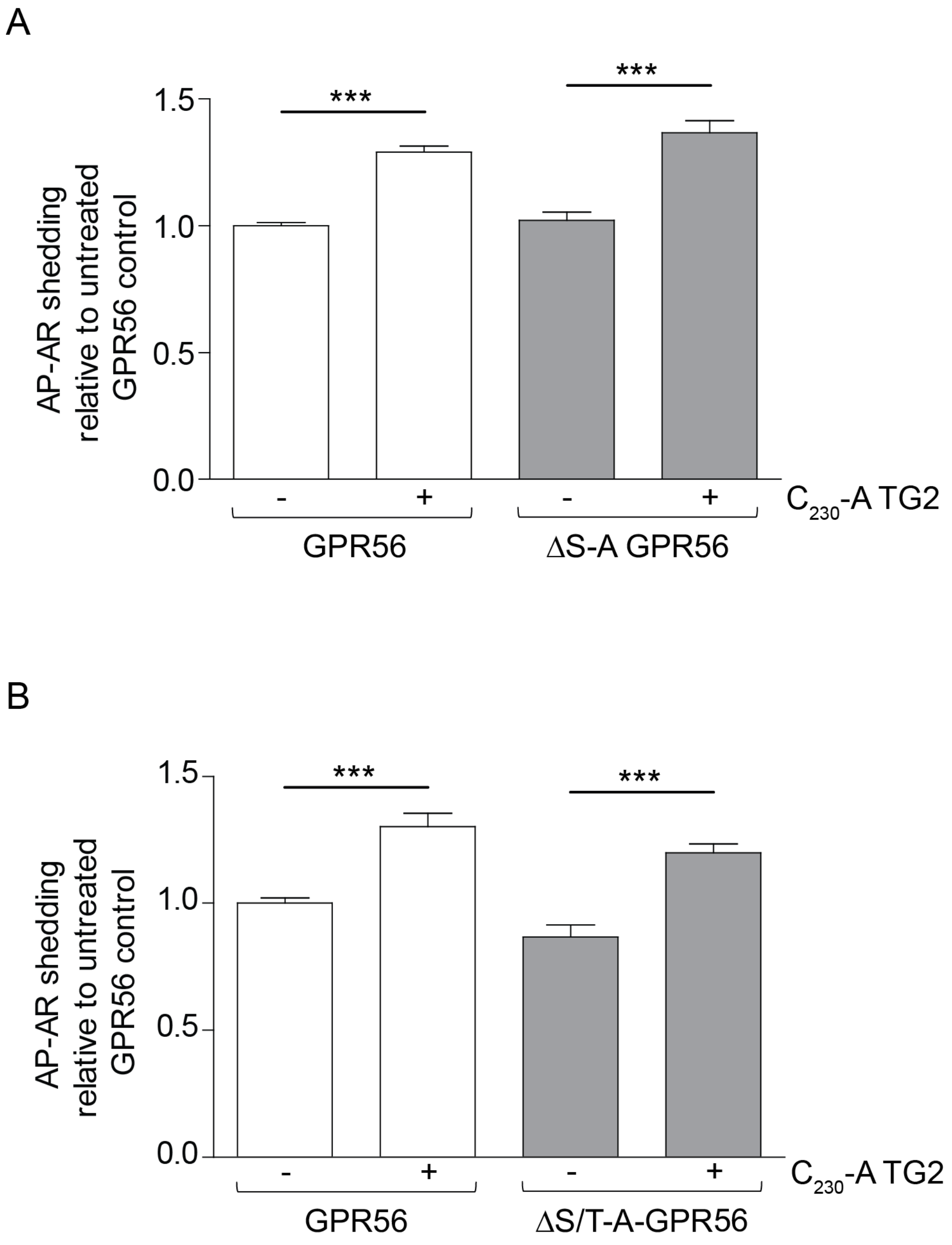

Figure 5.11 Multiple serine mutations alone or in conjunction with threonine-688 to alanine in the C-terminal tail do not impair GPR56-dependent AP-AR shedding.

Cells were transfected with (A) ΔS-A-GPR56 and AP-AR or GPR56 and AP-AR or (B) ΔS/T-A-GPR56 and AP-AR or GPR56 and AP-AR. Two days post-transfection, cells were serum starved for 1 h, followed by treatment with control buffer or 20 µg/ml C_{230}-A TG2 for 1 h. Data presented show mean of 3 to 18 independent experiments with 4 repeats each +/- SEM (n=12-72). Statistical significance denoted as follows: ***, $p<0.001$.

Total cell lysates were prepared and analysed by western blotting using anti-N-GPR56 (Fig. 5.12 A&C) and anti-V5 antibodies (Fig. 5.12 B&D). Staining with anti-N-GPR56 antibody showed similar band intensities, as well as the same banding pattern for wild type GPR56, ΔS-A-GPR56 and ΔS/T-A-GPR56, indicating normal processing of receptors (Fig. 5.12 A&C).

Analysis using the anti-V5 antibody showed the expected bands for monomeric, dimeric and full-length receptor for GPR56, ΔS-A-GPR56 and ΔS/T-A GPR56 (Fig. 5.12 B&D). However, the signal reduction of dimeric C-GPR56 following C_{230}-A TG2 treatment was only present in GPR56 expressing cells, while the phosphorylation site mutants were not affected.

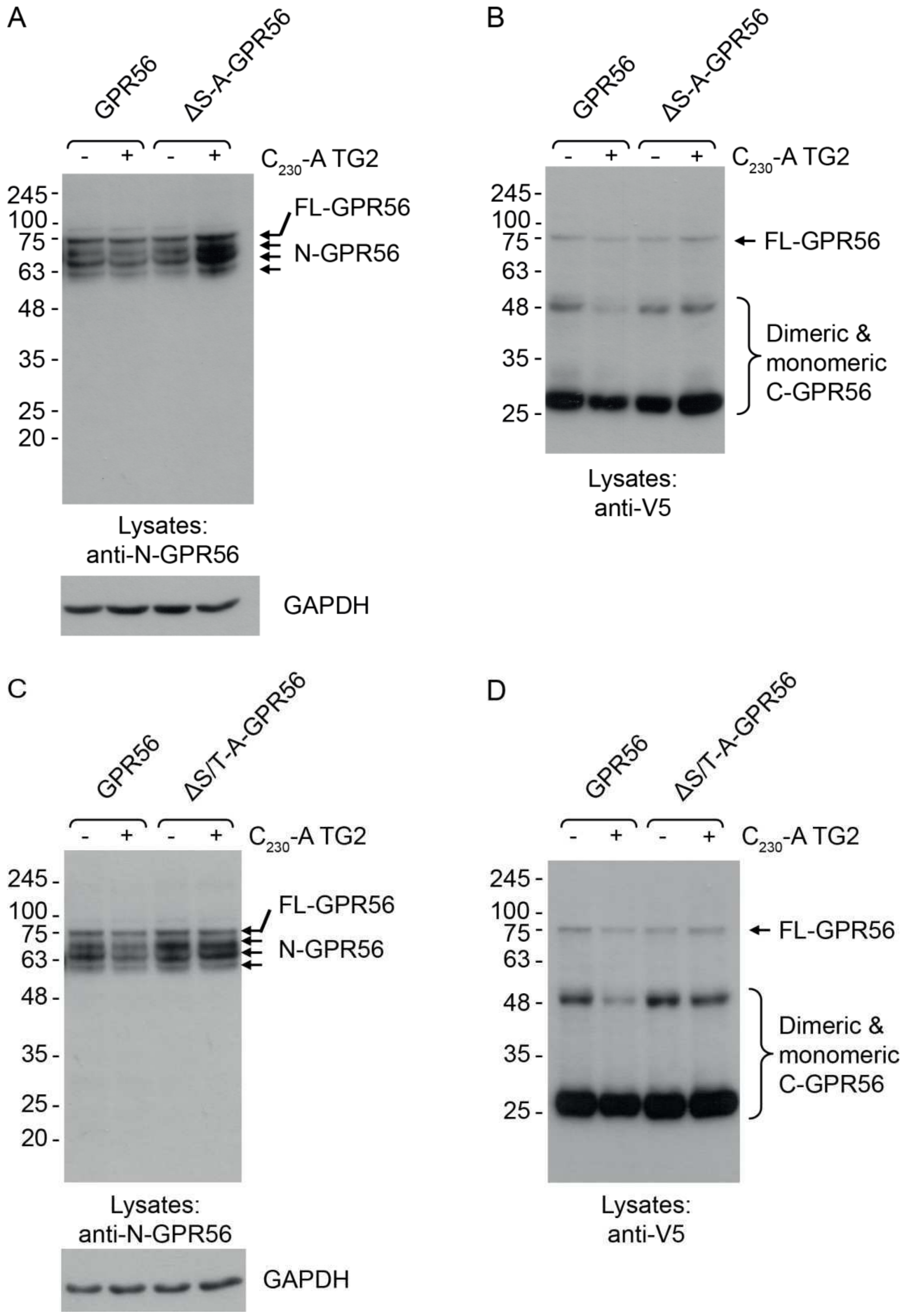
A
GPR56
ΔS-A-GPR56
- + - +
C230-A TG2
245
100
75
63
48
35
25
20
FL-GPR56
N-GPR56
Lysates:
anti-N-GPR56
GAPDH
B
GPR56
ΔS-A-GPR56
- + - +
C230-A TG2
245
100
75
63
48
35
25
FL-GPR56
Dimeric &
monomeric
C-GPR56
Lysates:
anti-V5
C
GPR56
ΔS/T-A-GPR56
- + - +
C230-A TG2
245
100
75
63
48
35
25
20
FL-GPR56
N-GPR56
Lysates:
anti-N-GPR56
GAPDH
D
GPR56
ΔS/T-A-GPR56
- + - +
C230-A TG2
245
100
75
63
48
35
25
FL-GPR56
Dimeric &
monomeric
C-GPR56
Lysates:
anti-V5

Figure 5.12 Western Blot analysis of total lysates from cells expressing GPR56, ∆S-A-GPR56 or ∆S/T-A-GPR56 used in the AP-AR shedding assay.

Total cell lysates of cells used in the shedding assays were analysed by western blotting. Membranes were stained with (A)&(C) anti-N-GPR56 antibody or (B)&(D) anti-V5 antibody. GAPDH was stained for loading control. Data are representative for 3 independent experiments.

The last C-terminal phosphorylation site mutant that was compared to GPR56 in the shedding assays was T_{688}-A GPR56 (Fig. 5.13 A). The threonine-688 to alanine mutation alone did not cause a significant change in GPR56-dependent basal or C_{230}-A TG2 induced shedding of AP-AR.

When total lysates of the same cells were analysed by western blotting and stained with anti-N-GPR56 antibody (Fig. 5.13 B), a banding pattern comparable to that of wild type GPR56 was found. Signal intensities were slightly elevated in lysates of cells expressing T_{688}-A GPR56.

Analysis using the anti-V5 antibody (Fig. 5.13 C) showed identical banding patterns for T_{688}-A GPR56 and GPR56. T_{688}-A GPR56 expression levels were slightly higher than GPR56. These results indicated that the threonine-688 to alanine mutant was normally processed.

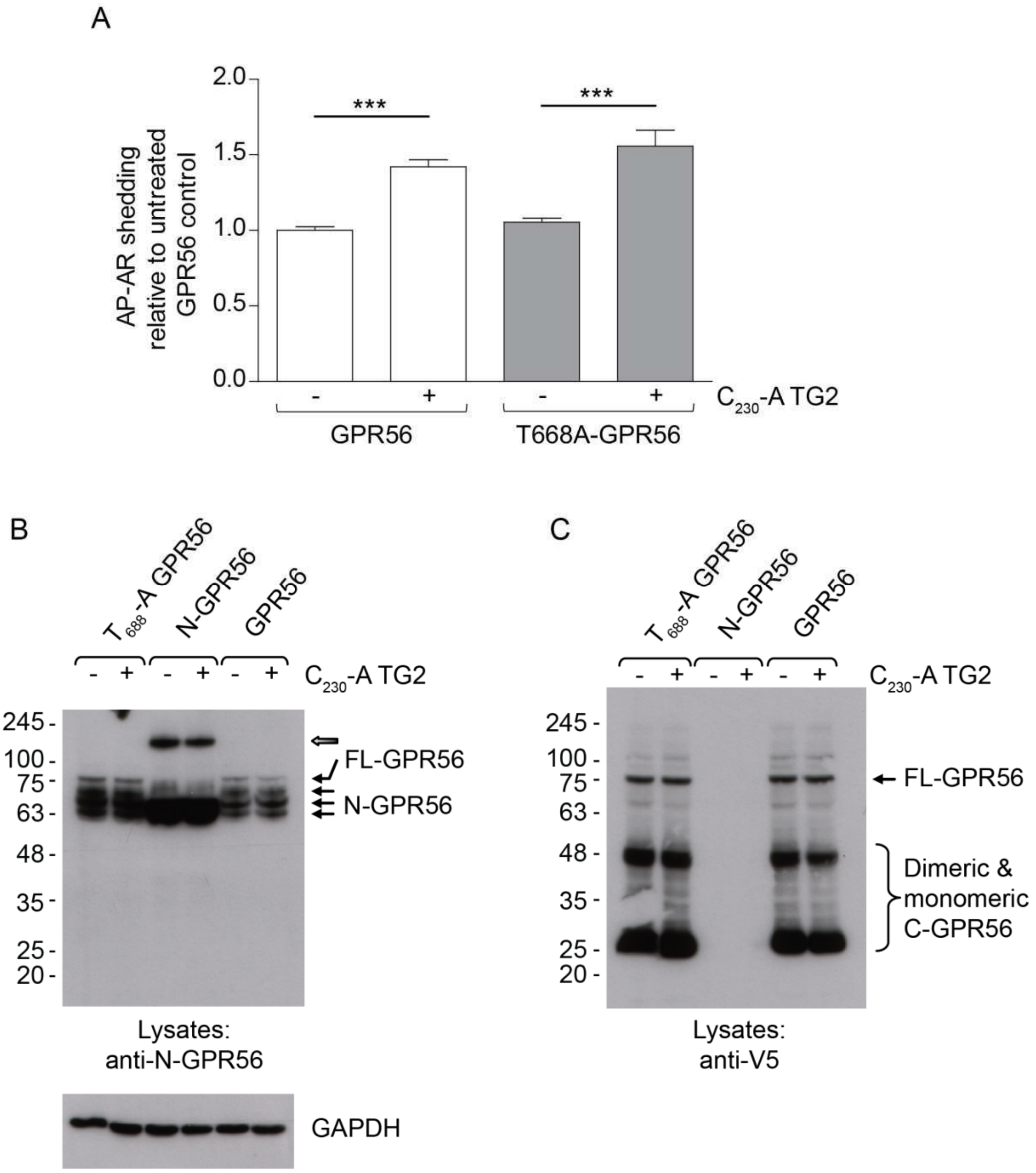

Figure 5.13 The mutation of threonine-688 to alanine does not alter GPR56-dependent shedding, nor expression patterns.

(A) Cells were transfected with T_{688}-A-GPR56 and AP-AR or GPR56 and AP-AR. 48 h later, cells were serum starved for 1 h and treated with control buffer or 20 µg/ml C_{230}-A TG2 for 1 h. Data presented show mean of 3 independent experiments with 4 repeats each +/- SEM (n=12). Statistical significance denoted as follows: ***, p<0.001.

(B)&(C) Lysates of cells used in the shedding assay were analysed using western blotting. Membranes were stained with (B) anti-N-GPR56 antibody or (C) anti-V5 antibody. GAPDH staining served as loading control. Data are representative for 3 independent experiments.

5.2.3.4 The GPR56 C-terminal tail regulates basal, but not TG2-induced AP-AR shedding

Finally, the contribution of the C-terminal tail on GPR56-dependent AP-AR shedding was investigated by comparing ∆Tail-GPR56 (∆671-693) to GPR56 in shedding assays (Fig. 5.14 A). In non-stimulated conditions, AP-AR shedding was reduced in ∆Tail-GPR56 expressing cells when compared to GPR56. However, both GPR56 and ∆Tail-GPR56 responded to C_{230}-A TG2 treatment with an increase in *p*-NPP hydrolysis, indicating that the GPR56 C-terminal tail region contributes to basal, but not TG2-inducing shedding activity of receptor.

Western blot analysis of total lysates from cells co-transfected with ∆Tail-GPR56 using anti-N-GPR56 antibody (Fig. 5.14 B) showed elevated expression levels for N-GPR56 and full-length ∆Tail-GPR56 compared to GPR56. High molecular weight bands running at ~180 to 245 kDa were detected for ∆Tail-GPR56 only.

Staining of lysates with anti-V5 antibody (Fig. 5.14 C) showed monomeric and dimeric C-GPR56 bands in lysates of cells transfected with ∆Tail-GPR56, running at smaller molecular sizes around ~25 and 45 kDa, as expected. Again, expression levels were elevated for ∆Tail-GPR56 when compared to GPR56 and higher molecular weight bands were detectable for ∆Tail-GPR56 only.

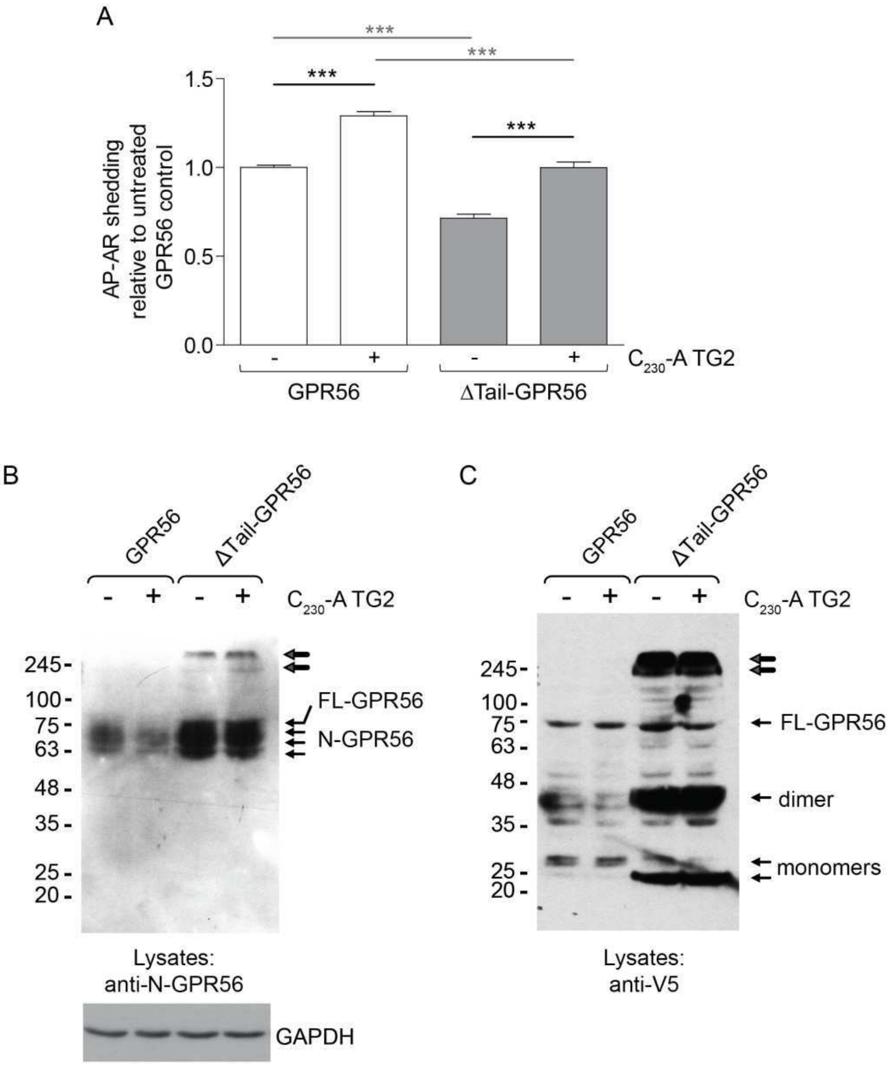

Figure 5.14 Deletion of a 23 residues long GPR56 C-terminal tail region reduces basal AP-AR shedding activity and results in elevated expression levels of the receptor.

(A) Cells were transfected with ΔTail-GPR56 and AP-AR or GPR56 and AP-AR. Two days later, cells were serum starved for 1 h and treated with control buffer or 20 µg/ml C_{230}-A TG2 for 1 h. Data presented show mean of 5 independent experiments with 4 repeats each +/- SEM (n=20). Statistical significance denoted as follows: ***, $p<0.001$.

(B)&(C) Western Blot analysis of cells expressing GPR56 or ΔTail-GPR56. Total lysates were analysed by staining the membrane with (B) anti-N-GPR56 antibody or (C) anti-V5 antibody. GAPDH loading control is shown. Data are representative for 5 independent experiments. *Western blot shown was performed by Tim Wanger and Andreas Heil.*

5.3 Discussion

In order to gain information about the relation of structural domains and signalling properties of GPR56, different GPR56 mutants were analysed for their ability to induce AP-AR shedding in non-stimulated and C_{230}-A TG2-stimulated conditions. This enabled a comparison of basal and TG2-induced activity of mutant to wild type GPR56.

The BFPP-causing GPR56 mutant R_{565}W-GPR56 showed a very low activity and did not respond to C_{230}-A TG2 stimulation (Fig. 5.7 A). This might be explained by the reduced cell surface expression level and its localisation in the perinuclear region (Fig. 5.5 & 5.6 A). These results confirm impaired surface expression, due to the mutant accumulating in the ER, indicating a trafficking defect (Chiang et al. 2011). In addition, Jin et al. (2007) failed to detect C-GPR56 at the cell surface of cells expressing R_{565}W-GPR56, which was in contrast to wild type GPR56.
The molecular mass of the N-terminal domain of R_{565}W-GPR56 was reduced, albeit processed at the GPS site as shown by normal staining for C-GPR56 (Fig. 5.8 B), whilst confocal microscopy showed perinuclear staining (Fig. 5.5 & 5.6 A). Data presented in this project show incorrect trafficking as well as lack of N-gylcosylation as seen by others (Chiang et al. 2011; Luo, Yang, et al. 2011). Using Endoclycosidase H treatment, Chiang and colleagues (2011) demonstrated that in contrast to wild type GPR56, R_{565}W-GPR56 carried only high mannose oligosaccharides added in the ER, indicating that the mutation would interfere with the correct trafficking of N-GPR56 into Golgi. Additionally, high molecular weight protein aggregates were found in lysates of cells expressing R_{565}W-GPR56 potentially indicating misfolding, as shown in figure 5.8. Chiang et al. (2011) looked at the distribution of N- and C-GPR56 to distinct membrane subdomains and found that wild type N-GPR56 was localized solely in non-raft fractions, whereas C-GPR56 was evenly distributed to non-raft and lipid raft fractions. Lipid rafts are important for intracellular signalling, confirming the importance of C-GPR56 for the

transduction of an extracellular signal to a cellular response. However, the C-terminal domain of R_{565}W-GPR56 formed aggregates and was mostly located in non-raft fractions like N-GPR56. This indicated conformational changes in C-GPR56 induced by the mutation in ECL2 leading to aggregation (Chiang et al. 2011).

The splice variant $\Delta_{430\text{-}35}$-GPR56 showed a reduced basal shedding activity and was not stimulated by C_{230}-A TG2 (Fig. 5.7 B). This result cannot be explained easily, as cell surface expression levels of $\Delta_{430\text{-}35}$-GPR56 and wild type GPR56 were comparable (Fig. 5.5 & 5.6 A). However, the insertion of six amino acids into wild type GPR56 could potentially lead to changes in intracellular binding partners leading to a different signalling response upon ligand treatment. This is potentially supported by Kim et al.'s (2010) previous work demonstrating increased SRE-activation upon $\Delta_{430\text{-}35}$-GPR56 overexpression when compared to wild type GPR56. The deletion of six residues within ICL1 could directly interfere with proteins mediating GPCR signalling, like G proteins or β-arrestins. Several reports demonstrated that activation by a ligand caused conformational changes, affecting the relative orientations of TM helices 3 and 6 in rhodopsin. These changes in turn affected the conformation of ICLs interacting with G proteins and β-arrestins uncovering previously buried interaction sites. However, in case of rhodopsin, interactions sites for Gα were identified in ICL2 and 3 and for Gβγ in α-helix 8 (previously designated ICL4), but not in ICL1 (Farrens et al. 1996; Franke et al. 1990; Ernst 2000; Hamm 2001). More recently, 10 residues present in ICL2 that are highly conserved within the rhodopsin family GPCRs were shown to regulate β-arrestin binding (Marion et al. 2006), 2006), although these are not the sole determinants, as ICL1 and 3 were also implicated in arrestin-binding (Krupnick et al. 1994; Raman et al. 2003). The deletion of six residues within ICL1 of GPR56 could also induce conformational changes indirectly affecting the conformation of the entire 7TM-domain, thus interactions with intracellular proteins.

Experiments using the ligand interaction site deletion mutant ΔSTP-GPR56 and the N-terminally truncated mutant ΔN-GPR56 revealed that the presence of an intact N-terminal domain is required for C_{230}-A TG2 induced GPR56-dependent AP-AR shedding (Fig. 5.9 A and 5.10 A), which is in line with predictions for the location of the ligand interaction sites made by others (Li et al. 2008; Yang et al. 2011; Luo et al. 2012).

∆STP-GPR56 was almost inactive in the shedding assay, likely due to impaired receptor processing, as indicated by a pronounced band for full-length ∆STP-GPR56 (Fig. 5.9 B&C). GPS-cleavage was not entirely abolished, as ∆STP-N-GPR56, as well as monomeric and dimeric ∆STP-C-GPR56 were detected.

In contrast, a similar mutant lacking the TG2 interaction site (∆108-177) was shown to be auto-active and induced VEGF synthesis in a PKCα-dependent manner. Yang et al. (2011) concluded that the N-terminal domain inhibits the receptor, although ligand activation studies were not performed and thus their experiments measure ligand independent receptor activities. In contrast to their report (Yang et al. 2011), data presented here demonstrated impaired cell surface expression of ∆STP-GPR56 with most of the receptor located in the perinuclear region (Fig. 5.5 & 5.6 A), explaining reduced receptor activities. The data were corroborated by experiments performed with ∆N-GPR56, lacking the complete ligand binding domain, which clearly demonstrated that the N-terminal domain is required for GPR56 activation by TG2 (Fig. 5.10 A). The enhanced basal activity observed with ∆N-GPR56, on the other hand, indicated increased constitutive activation of the receptor due to deletion of the N-terminal domain. This is in line with observations made by Yang et al. (2011) and Paavola et al. (2011). The decreased expression levels for ∆N-GPR56 observed with western blot analysis (Fig. 5.10 C) might be explained by elevated internalisation and degradation of mutant receptor, which was indicated by previous findings demonstrating increased co-localisation with β-arrestin-2 and receptor poly-ubiquitination (Paavola et al. 2011). High molecular weight bands indicating ubiquitination were also observed in this project, using anti-V5 antibody staining (Fig. 5.10 C). However, stimulation of AP-AR shedding by C_{230}-A TG2 was abolished in case of ∆N-GPR56, confirming that the N-terminal domain is required for ligand-dependent receptor activation.

It was shown for several GPCRs that β-arrestin-binding to agonist-activated receptors requires phosphorylation of serine and threonine residues located in ICL3 and the C-terminal tail (Oakley et al. 2001; Luttrell and Lefkowitz 2002). Some GPCRs, such as the β2-adrenergic receptor (β_2AR), quickly dissociate from β-arrestin near the cell membrane, whereas others like the vasopressin receptor-2 (V_2R) remain tightly associated with β-arrestin and internalise into endocytic vesicles as a complex (Oakley et al. 1999; Oakley et al. 2000). Oakley et al. (2001) showed that phosphorylation of several residues by GRKs dramatically enhances the affinity of β-arrestins to GPCRs, leading to the formation of stable β-arrestin-receptor complexes. In case of the β_2AR, GRK-phosphorylation enhanced β-arrestin binding 10-30 fold. Therefore, it was speculated that mutation of several potential phosphorylation sites within the C-terminal tail of GPR56 might influence receptor activity or activation by C_{230}-A TG2. However, experiments with the three phosphorylation site mutants ∆S-A-, ∆S/T-A- and T_{688}-A-GPR56 did not result in an alteration of AP-AR shedding activity (Fig. 5.11 and 5.13 A), indicating that the signalling pathway is not mediated by β-arrestins. However, it was also speculated that the agonist-induced conformational change of receptors is more important for β-arrestin-binding than GRK-phosphorylation (Marion et al. 2006), thus an involvement of β-arrestins in GPR56-dependent ADAM17-activation cannot be entirely excluded by ablating phosphorylation sites. Moreover, it remains unclear whether receptor internalisation that is promoted by association of β-arrestins to GPCRs is required for GPR56-dependent AP-AR shedding. In addition, GPR56 internalisation may be β-arrestin-independent as shown for other GPCRs (Bhatnagar et al. 2001; Koppen and Jakobs 2004).

Experiments with ∆Tail-GPR56 showed that deletion of a huge part of the cytoplasmic tail does not affect C_{230}-A TG2-stimulated AP-AR shedding (Fig. 5.14 A). This is in line with the findings made using the phosphorylation site mutants discussed above, indicating that GPR56-dependent ADAM17 activation is not mediated through β-arrestins. However, western blot analysis showed that expression levels of ∆Tail-GPR56 were elevated when compared to wild type GPR56 (Fig. 5.14 B&C), which might result from impaired internalisation and endocytosis mediated through β-arrestins. However, Cen et al. (2001) showed that C-terminal truncation of δ-opioid receptor (DOR) only partially impaired the interaction with β-arrestins, as this was compensated by the presence of ICL3, which is sufficient for β-arrestin binding. Moreover, it was shown that the interactions of ICL3 and the C-terminus of DOR with the β-arrestins were additive and that both domains bound to different sites of β-arrestins. A similar effect might be observed with ΔTail-GPR56, as its overall activity was reduced when compared to wild type GPR56, thus the presence of ICL3 might compensate the loss of the C-terminal tail resulting in impaired, but still detectable receptor activity and significant activation by its ligand TG2.

Taken together, this chapter showed that mutation or deletion of several domains within GPR56 results in altered receptor activities. Loss of TG2-dependent GPR56 activation was observed for R_{565}W-GPR56 and ΔSTP-GPR56, which likely resulted from folding/trafficking defects as reflected by impaired cell surface expression levels. Loss of TG2-activation of $\Delta_{430\text{-}35}$-GPR56 might be a result of alterations in interaction sites required for signal transduction, although we currently have no evidence for that. In contrast, ablation of potential C-terminal phosphorylation sites (ΔS-A-, ΔS/T-A-, T_{688}A-GPR56) or deletion of the cytoplasmic tail (ΔTail-GPR56) did not influence C_{230}-A TG2 induced receptor activation. This potentially indicates that GPR56-dependent activation of ADAM17-mediated AP-AR shedding was independent of β-arrestins, although experimental evidence for this conclusion needs to be collected. Moreover, the hypothesis of N-GPR56 inhibiting C-GPR56 was confirmed by experiments using N-terminally truncated ΔN-GPR56 showing enhanced constitutive activity. The results also demonstrated that the N-terminal domain was required for TG2-interaction, as stimulation with C_{230}- TG2 did not activate ΔN-GPR56.

CHAPTER 6:

Exploring the mechanism of GPR56-dependent internalisation of TG2 using confocal microscopy

6 Exploring the mechanism of GPR56-dependent internalisation of TG2 using confocal microscopy

6.1 Introduction

GPCR internalisation requires either clathrin-dependent or clathrin-independent routes. The formation of clathrin-coated vesicles is initiated by the invagination of membrane structures, called pits, which is promoted by the recruitment of adaptor proteins like AP-2 to the plasma membrane. The size of clathrin-coated pits depends on their cargo, e.g. a GPCR, but their size is limited to 200 nm (McMahon and Boucrot 2011)
Clathrin-dependent internalisation was established by monitoring the uptake of transferrin (Tf) in erythropoietic cells (Harding et al. 1983). At the cell surface, transferrin receptors (TRs) bind Tf to import iron from the serum (Collawn et al. 1990). TRs are constitutively internalised via clathrin-coated pits and Tf-uptake was found to be temperature-dependent, i.e. TRs bind Tf at 4 °C and internalise at 37 °C (Harding et al. 1983). Once the internalised TR-Tf complex reaches the endosome, Tf does not dissociate from its receptor. At pH 5, the ligand-receptor pair remains associated in endosomes, whereas iron is removed from Tf. The iron-free TR-Tf complex recycles back to the cell surface, where iron-free Tf dissociates at neutral pH. New iron-loaded Tf binds the receptor for another round of clathrin-dependent endocytosis (Goldstein et al. 1985).

The best characterised, clathrin-independent mechanism of GPCR internalisation is the caveolae-dependent pathway. Lipid rafts/caveolae do not only play a role for vesicular transport processes (endocytosis/exocytosis), but are also involved in sorting of lipids, protein trafficking and signal transduction (Sprong et al. 2001; Johannes and Lamaze 2002; Chini and Parenti 2004). Besides GPCRs, receptor tyrosine kinases (e.g. EGFR), ion channels, transporters, Src family kinases, G proteins and others are located in membrane rafts like caveolae (Patel et al. 2008). Some GPCRs naturally assemble in these membrane structures, others might move their upon ligand stimulation before internalisation. Thus there must be targeting signals determining the localisation of the receptors within the cell membrane (Chini and Parenti 2004; Patel et al. 2008). It was speculated that cholesterol, present in caveolae, might influence the localisation of GPCRs in rafts by interacting with their 7TM-domain. Re-arrangements of the 7TM-region following agonist-activation or oligomerisation of GPCRs could affect the affinity to cholesterol, leading to raft localisation. Additionally, the ECD, ICLs and the cytoplasmic tail of GPCRs may also be involved. The ECD could interact with proteins or lipids on the outer leaflet of the membrane and palmitoylation (lipid modification on Cys residues) or phosphorylation of the cytoplasmic tail and ICLs may act as a target-signal for localisation of GPCRs in rafts (Chini and Parenti 2004).

The flask-shaped caveolae were first identified using electron microscopy (Palade 1953). Confocal imaging, however, represents a very useful tool to visualise GPCR endocytosis via caveolae by staining typical marker proteins such as caveolin-1 (cav-1) (Chini and Parenti 2004). Interestingly, GPR56 is partially located in lipid raft fractions positive for cav-1 expression (Chiang et al. 2011).

Independent of the endocytotic machinery, the internalised vesicles fuse with early endosomes and the GPCR is either recycled back to the cell surface (resensitisation) or degraded (signal termination) (Hanyaloglu and von Zastrow 2008).

6.1.1 Aims of the chapter

- To investigate whether the interaction of GPR56 and TG2 triggers internalisation.

- To identify the mechanism of endocytosis (clathrin-dependent or -independent).

- To shed some light on the fate of receptor and ligand (i.e. recycling or degradation).

6.2 Results

6.2.1 Interaction of GPR56 and TG2 in stably transfected HEK293 cells

The aim of the experiments was to confirm the specific interaction between GPR56 and TG2 using an additional experimental approach to the shedding assay. Therefore, it was investigated whether GPR56 is internalised upon prolonged stimulation with its ligand TG2.

For this purpose, a stable HEK293 cell line inducibly expressing GPR56 was used. Firstly, conditions were established to induce GPR56 expression using 10 µg/ml doxycycline-containing medium, which was compared to control medium at the 48 h time point. Total cell lysates were prepared and analysed for GPR56 and TG2 expression (Fig. 6.1). In order to show that the stable HEK293 cell line was negative for TG2 expression, stably transfected HCA2 fibroblasts overexpressing TG2 cDNA in either sense (S) or antisense (As) orientation were cultured for 72 h and cell lysates were analysed next to those of the stable HEK293 cell line. Figure 6.1 A shows that doxycycline treatment for two days efficiently induced GPR56 expression in stably transfected HEK293 cells, whereas HCA2 fibroblasts as well as non-treated, stably transfected HEK293 cells were completely negative for GPR56 expression. In contrast to HCA2 TG2 sense cells, stable HEK293 cells were negative for TG2 expression, independent of GPR56 expression levels (Fig. 6.1 B).

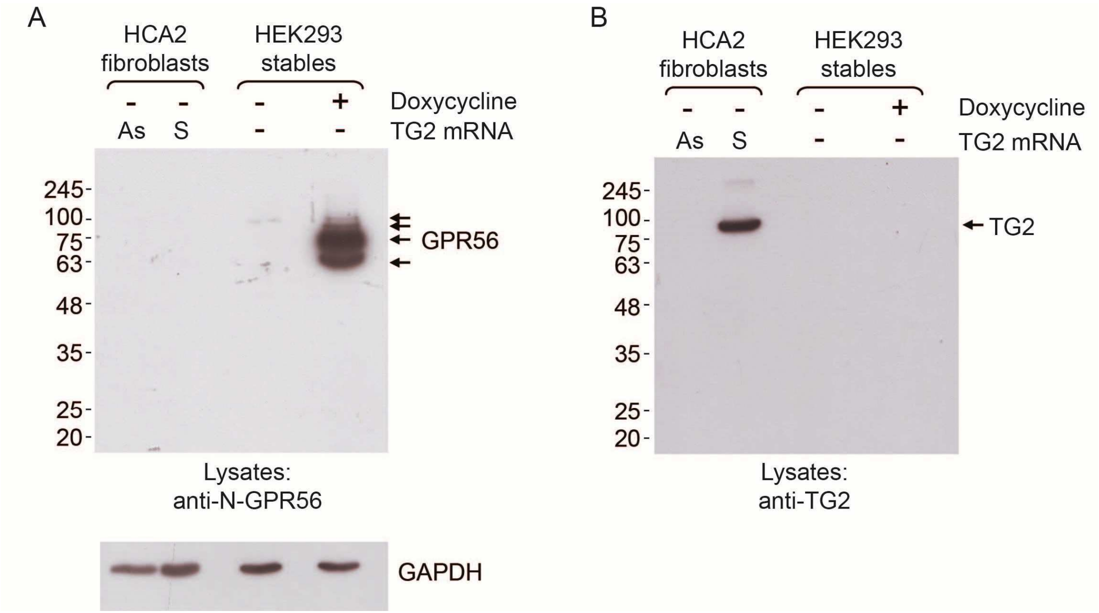
A
HCA2 fibroblasts
HEK293 stables
- - - +
Doxycycline
As S - -
TG2 mRNA
245-
100-
75-
63-
48-
35-
25-
20-
GPR56
Lysates: anti-N-GPR56
GAPDH
B
HCA2 fibroblasts
HEK293 stables
- - - +
Doxycycline
As S - -
TG2 mRNA
245-
100-
75-
63-
48-
35-
25-
20-
TG2
Lysates: anti-TG2

Figure 6.1 GPR56 and TG2 expression in stably transfected HEK293 cells. Western Blot analysis of total lysates from HCA2 fibroblasts stably expressing TG2 sense (S) or antisense (As) cDNA and the stable HEK293 cell line inducibly expressing GPR56. Transfected HCA2 cells were grown for 72 h before lysates were prepared. HEK293 cells were cultured in doxycycline-free medium (control cells) or 10 µg/ml doxycycline containing medium for 48 h prior to production of total cell lysates. Lysates were separated using a 10% resolving gel, blotted onto a PVDF-membrane and stained with (A) anti-N-GPR56 antibody and (B) anti-TG2 antibody. GAPDH staining served as the loading control.

To exclude an effect of TG2 on GPR56 expression levels or crosslinking of GPR56 by TG2, cell lysates of stable HEK293 control cells and doxycycline-induced cells were analysed following control buffer or C_{230}-A TG2 treatment for 1 h. Figure 6.2 shows the western blot analysis of total cell lysates using anti-N-GPR56 antibody, confirming that control cells were negative for GPR56 expression and that C_{230}-A TG2 treatment did not alter the N-GPR56 banding pattern or intensity in doxycycline-induced cells at the 1 h treatment point.

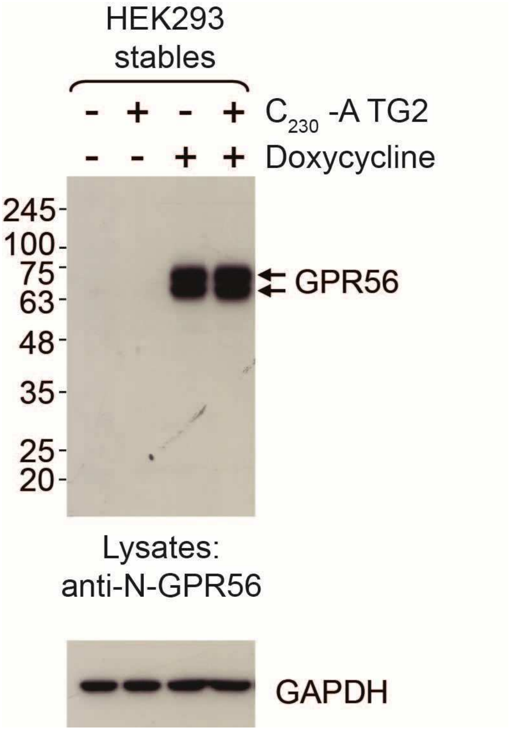

Figure 6.2 GPR56 expression in stably transfected HEK293 cells.

For GPR56 expression, stably transfected HEK293 cells were incubated in 10 µg/ml doxycycline-containing medium or control cells in doxycycline-free medium for 48 h. Cells were serum starved for 1 h, followed by treatment with 20 µg/ml C_{230}-A TG2 or control buffer for 1 h. Lysates were prepared, separated using a 10% resolving gel and blotted onto a PVDF-membrane. Anti-N-GPR56 and anti-GAPDH antibodies were used to stain the membrane.

For confocal microscopy, stable HEK293 cells were incubated in doxycycline-containing medium for 48 h to induce GPR56 expression and control cells in doxycycline-free medium. Cells were serum starved, followed by treatments with control buffer or 20 µg/ml C_{230}-A TG2 for 5 sec, 15 mins or 30 mins. Cells were fixed and permeabilised and GPR56 and C_{230}-A TG2 were stained using anti-N-GPR56 and anti-TG2 antibodies, which were detected with appropriate secondary antibodies leading to GPR56 staining in red and TG2 staining in green.

Figure 6.3 shows doxycycline pre-treated cells expressing GPR56 at the cell surface and in intracellular compartments. Non-induced control cells were GPR56 and TG2 negative and are shown in Appendix VI.

GPR56 was present at the cell surface in doxycycline-induced cells treated with control buffer (Fig. 6.3 A, white arrow heads) or C_{230}-A TG2 (Fig. 6.3 B, white arrow heads) after 5 sec treatment. Some GPR56 was found intracellularly throughout the entire experiment and slightly more after 15 or 30 mins of incubation (Fig. 6.3 A&B, white arrow heads), which may represent internalised or newly synthesised GPR56, which cannot be distinguished using this labelling technique.

TG2 staining was absent in buffer control treated cells (Fig. 6.3 A), however, cell surface TG2 staining was detected in GPR56 positive cells within 5 sec of treatment and partially overlapped with GPR56 staining (Fig. 6.3 B, black arrow heads). This indicated a fast and specific interaction between the receptor and its ligand. Following C_{230}-A TG2 treatment for 15 mins, some TG2 was located intracellularly (Fig. 6.3 B, white arrows) and some remained at the cell surface. After 30 mins treatment, even more C_{230}-A TG2 was present in intracellular vesicles, demonstrating GPR56-dependent endocytosis of TG2 (Fig. 6.3 B, white arrows). There was very little co-localisation between GPR56 and internalised TG2 in intracellular vesicles.

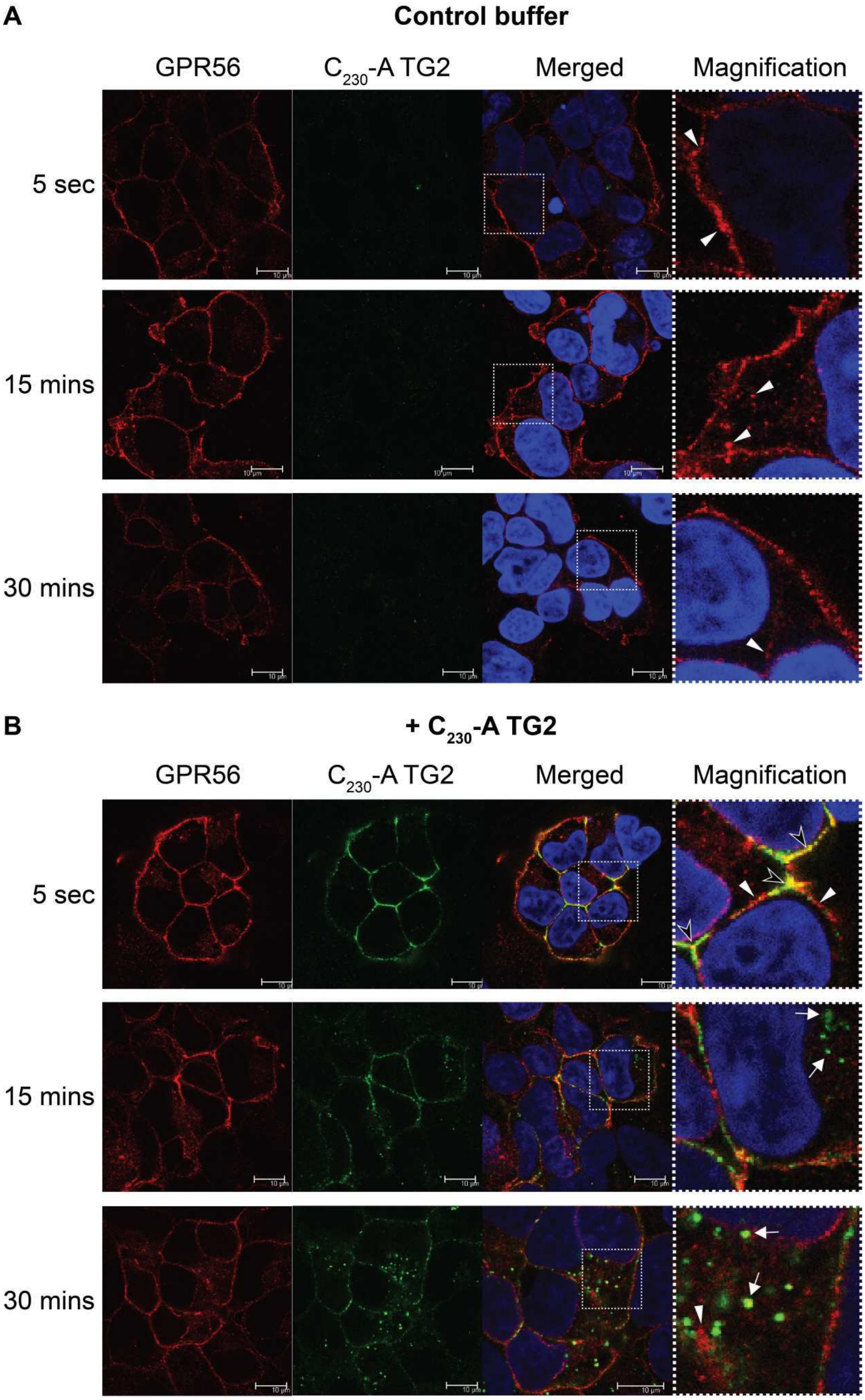
A
Control buffer
GPR56
C_{230}-A TG2
Merged
Magnification
5 sec
15 mins
30 mins
10 µm
B
+ C_{230}-A TG2
GPR56
C_{230}-A TG2
Merged
Magnification
5 sec
15 mins
30 mins
10 µm

Figure 6.3 Internalisation of GPR56 and TG2 in stably transfected HEK293 cells.

The GPR56 inducible cell line was seeded onto poly-L-lysine coated glass coverslips and GPR56 expression was induced with 10 µg/ml doxycycline for 48 h prior to 1 h serum starvation. Cells were then treated for 5 sec, 15 mins or 30 mins with (A) control buffer or (B) 20 µg/ml C_{230}-A TG2. Cells were fixed and permeabilised and GPR56 was stained with anti-N-GPR56 (red; R&D Systems) and anti-sheep Alexa568 antibodies (Jackson ImmunoResearch). C_{230}-A TG2 was stained with monoclonal anti-TG2 (green; Thermo Scientific) and anti-mouse Alexa488 antibodies (Jackson ImmunoResearch).

(A) After treatment with control buffer for 5 sec, GPR56 was present at the cell surface. Some GPR56 was detectable intracellularly throughout the experiment, which was slightly more pronounced after 15 mins and 30 mins. Cells were always negative for TG2 staining.

(B) Cells treated with C_{230}-A TG2 for 5 sec were positive for GPR56 and TG2 cell membrane staining, which partially overlapped. After 15 mins, GPR56 and TG2 staining were still apparent at the cell surface and some internalisation of TG2 was observed. After 30 mins, more TG2 was found in intracellular vesicles of GPR56-positive cells. Some GPR56 was found intracellularly, however, most of it was still apparent at the cell surface after 30 mins. The degree of co-localisation between internalised TG2 and intracellular GPR56 was very low.

White arrow heads, GPR56 staining (red); white arrows, C_{230}-A TG2 staining (green); black arrow heads, co-localisation of GPR56 and C_{230}-A TG2 (yellow); scale bar, 10 µm.

6.2.2 Internalisation of GPR56 and TG2 in HEK293 cells transiently expressing SNAP-tagged GPR56

In figure 6.3, binding of TG2 to GPR56 and GPR56-dependent endocytosis of TG2 using immunocytochemistry was demonstrated. In contrast, GPR56 remained at the cell surface. Since immunocytochemistry is unable to distinguish between internalised, recycling and newly synthesised receptor, this methodology was not amendable to investigate endocytosis of GPR56. Prestaining of GPR56 with anti-N-GPR56 antibody was not an option, as data presented in Chapter 3 demonstrated that the antibody has agonistic activity. Therefore, the SNAP-tag technology (NEB) was explored.

The SNAP-tag is a 20 kDa mutant O^6-alkylguanine-DNA alkyltransferase that can be covalently labelled by adding specific benzylguanine substrates fused to fluorescent dyes. SNAP-GPR56 carrying an extracellular, N-terminal SNAP-tag was cloned by Dr. Vera Knäuper and cell surface GPR56 was fluorescently labelled prior to addition of C_{230}-A TG2. In that way, the fate of the receptor-ligand pair was followed. In most experiments, SNAP-tag staining preceded immunocytochemical detection of TG2 and/or vesicle marker proteins such as LAMPs.

6.2.2.1 Optimisation of SNAP-GPR56 staining and comparison to the SNAP-β_2-adrenergic receptor

Firstly, expression of SNAP-GPR56 was compared to GPR56 using transiently transfected HEK293 cells, which were treated with control buffer or C_{230}-A TG2. Cell lysates were prepared and analysed by western blotting using anti-N-GPR56 antibody (Fig. 6.4). Two major bands running at ~80 and ~95 kDa were detected for SNAP-GPR56, representing SNAP-tagged N-GPR56 and full-length SNAP-GPR56. The detected bands correlate well with the predicted sizes for SNAP-GPR56.

Additionally, preliminary data revealed that SNAP-GPR56 is active in the AP-AR shedding assay (data not shown).

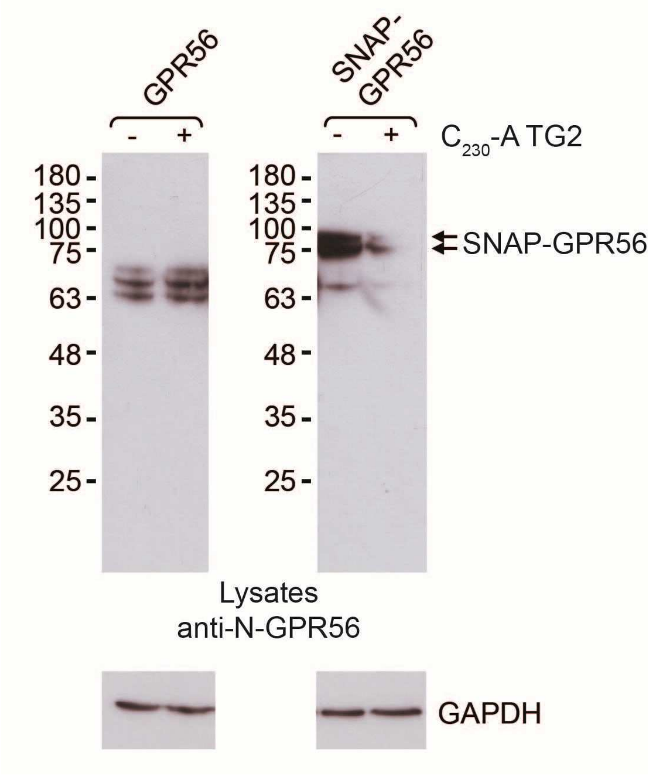

Figure 6.4 Expression of SNAP-GPR56 in HEK293 cells. Cells were transfected with GPR56 or SNAP-GPR56. Two days post-transection, cells were serum starved for 1 h, followed by treatment with 20 µg/ml C_{230}-A TG2 or control buffer for 1 h. Lysates were prepared, separated in a 10% resolving gel and blotted onto a PVDF-membrane. Anti-N-GPR56 antibody was used to stain the membrane, GAPDH served as loading control.

In order to test SNAP-tag staining of GPR56, HEK293 cells were transiently transfected with SNAP-GPR56 or the control vector provided by New England Biolabs (NEB), encoding SNAP-β_2-adrenergic receptor (SNAP-β_2AR). Staining of the two receptors was compared using confocal microscopy (Fig. 6.5).

All cells shown in figure 6.5 were grown for 48 h following transfection and were serum starved for 1 h prior to SNAP-surface staining. In figure 6.5 A, cells were incubated with SNAP-surface substrate 488 or 549 for 15 mins at 37 °C prior to fixation. Due to the incubation with the SNAP-substrates at 37 °C for 15 mins, some receptor internalisation occurred in the absence of ligand addition (Fig. 6.5 A, white arrow heads indicating internalised receptors stained with SNAP-substrate 549 (red); white arrows indicating internalised receptors stained with SNAP-substrate 488 (green)). Endocytosis was much more pronounced in cells expressing SNAP-GPR56 (Fig. 6.5 A, right panels) when compared to SNAP-β_2AR (Fig. 6.5 A, left panels), indicating different kinetics of constitutive internalisation between GPR56 and β_2AR.

Next, the specific interaction between GPR56 and TG2 was demonstrated using a combination of SNAP-tag staining and immunocytochemistry. Following SNAP-tag staining with SNAP-substrate 549 or 488, SNAP-GPR56 (right panels) or SNAP-β_2AR (left panels) transfected cells were treated with C_{230}-A TG2 for 5 sec and fixed immediately (Fig. 6.5 B&C). TG2 was stained using anti-TG2 antibody and secondary Alexa488- or Alexa594-labelled antibodies, depending on the colour of the SNAP-surface substrate used to stain the receptors. Some receptor internalisation, especially in SNAP-GPR56-expressing cells (Fig. 6.5 B&C, white arrow heads and white arrows), was apparent. In contrast, TG2 staining at the 5 sec time point was only detectable at the cell surface of SNAP-GPR56 expressing cells, with staining partially overlapping with GPR56 (Fig. 6.5 B&C, right panels, black arrow heads). This confirmed the highly specific interaction between GPR56 and TG2, as SNAP-β_2AR positive cells did not bind C_{230}-A TG2 (Fig. 6.5 B&C, left panels). Moreover, the results demonstrated that SNAP-tag staining was a good method to allow cell surface receptor staining, which was further optimised by performing the SNAP-tag labelling step at 4 °C, a temperature that blocked ligand independent receptor internalisation. Therefore, internalisation studies with this technique were combined with immunocytochemistry to assess receptor internalisation in response to ligand.

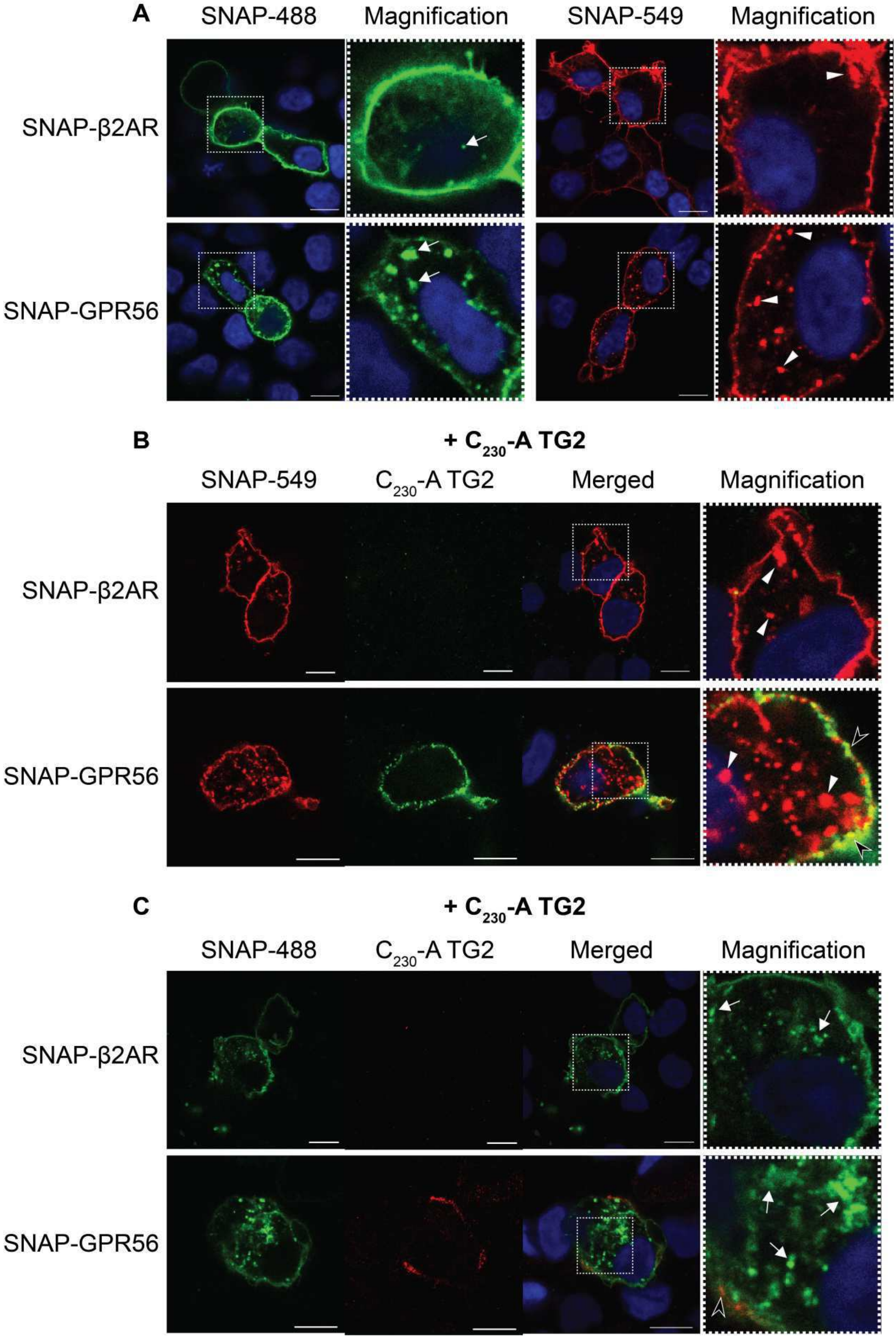
A
SNAP-488
Magnification
SNAP-549
Magnification
SNAP-β2AR
SNAP-GPR56
B
+ C_{230}-A TG2
SNAP-549
C_{230}-A TG2
Merged
Magnification
SNAP-β2AR
SNAP-GPR56
C
+ C_{230}-A TG2
SNAP-488
C_{230}-A TG2
Merged
Magnification
SNAP-β2AR
SNAP-GPR56

Figure 6.5 SNAP-tag staining of SNAP-GPR56 and SNAP-β_2AR in transiently transfected HEK293 cells.

Cells were seeded onto poly-L-lysine coated glass coverslips and the next day transfected with SNAP-GPR56 or SNAP-β_2AR. 48 h post-transfection, cells were serum starved for 1 h. SNAP-tags were stained at 37 °C for 15 mins using SNAP-surface substrates 488 (green receptor staining; NEB) or 549 (red receptor staining; NEB).

(A) Cells were fixed immediately following SNAP-tag staining. SNAP-GPR56 (right panels) and SNAP-β_2AR (left panels) were present at the cell surface and some receptor was found in intracellular vesicles, which was much more pronounced in case of SNAP-GPR56.

(B) Cells were stained with SNAP-substrate 549 (red), treated with C_{230}-A TG2 for 5 sec, fixed and stained for TG2 (green) with anti-TG2 (Thermo Scientific) and anti-mouse Alexa488 antibodies (Jackson ImmunoResearch). Cells showed positive surface staining for SNAP-GPR56 (right panels) and SNAP-β_2AR (left panels) and there was more internalised SNAP-GPR56 than SNAP-β_2AR. C_{230}-A TG2 cell surface staining was only present in SNAP-GPR56-expressing cells, where it partially overlapped with GPR56 staining.

(C) Same as in (B), but cells were stained with SNAP-substrate 488 (green) and TG2 (red) was stained using anti-TG2 antibody (Thermo Scientific) in combination with anti-mouse Alexa594 antibody (Jackson ImmunoResearch).

White arrow heads, internalised receptors stained with SNAP-surface substrate 549 (red); white arrows, internalised receptors stained with SNAP-surface substrate 488 (green); black arrow heads, cell surface co-localisation of SNAP-GPR56 and C_{230}*-A TG2 (yellow); scale bar, 10 µm.*

6.2.2.2 Co-internalisation of SNAP-GPR56 and TG2

The results shown above introduced an alternative way to specifically stain cell surface GPR56 via an N-terminal SNAP-tag and demonstrated that this method could be used to follow receptor internalisation in living cells.

Next, the GPR56-TG2 internalisation study presented in 6.2.1 was modified using a combination of SNAP-tag staining for GPR56 and immunostaining for TG2. Figure 6.6 shows cells that were transfected with SNAP-GPR56. SNAP-surface substrate 647 (shown in green) was used to stain GPR56 for 15 mins at 4 °C, in order to prevent internalisation prior to TG2 treatment. Cells were pulse-treated with 20 µg/ml C_{230}-A TG2 or control buffer for 5 sec, followed by direct fixation or incubation in serum-free medium for up to 60 mins (the chase), as indicated. Pulse-chase experiments were performed in order to follow the fate of receptor-ligand pairs that initially formed at the cell surface after 5 sec of treatment with C_{230}-A TG2. Finally, cells were fixed and permeabilised, followed by antibody staining of TG2 (red).

Cells treated with control buffer (Fig. 6.6 A) showed cell surface localisation of SNAP-GPR56, particularly after 5 sec (upper panels, white arrows) and lacked TG2 staining at any time point tested. Internalisation of SNAP-GPR56 was detectable after 15 mins and the amount of internalised receptor increased over time, with little SNAP-GPR56 left at the cell surface after 60 mins (white arrows indicating internalised receptor).

SNAP-GPR56 cells treated for 5 sec with TG2 (Fig. 6.6 B) showed surface staining for GPR56 (upper panels, white arrows) and partial co-localisation of receptor and ligand (upper panels, black arrow heads), indicating specific binding of C_{230}-A TG2 to the receptor. After 15 mins of incubation, intracellular vesicles stained positive for SNAP-GPR56 (white arrows indicating internalised receptor) and TG2 positive vesicles were also positive for SNAP-GPR56 (yellow; black arrow heads), indicating that internalisation of C_{230}-A TG2 was highly GPR56-dependent. At the 30 mins and 60 mins time points, increasing numbers of vesicles were positive for SNAP-GPR56 alone (white arrows), although some vesicles remained positive for both receptor and ligand (yellow; black arrow heads). Little SNAP-GPR56 and even less C_{230}-A TG2 was left at the cell surface after 60 mins incubation. Over the 60 mins time period receptor or ligand recycling to the cell membrane was not evident.

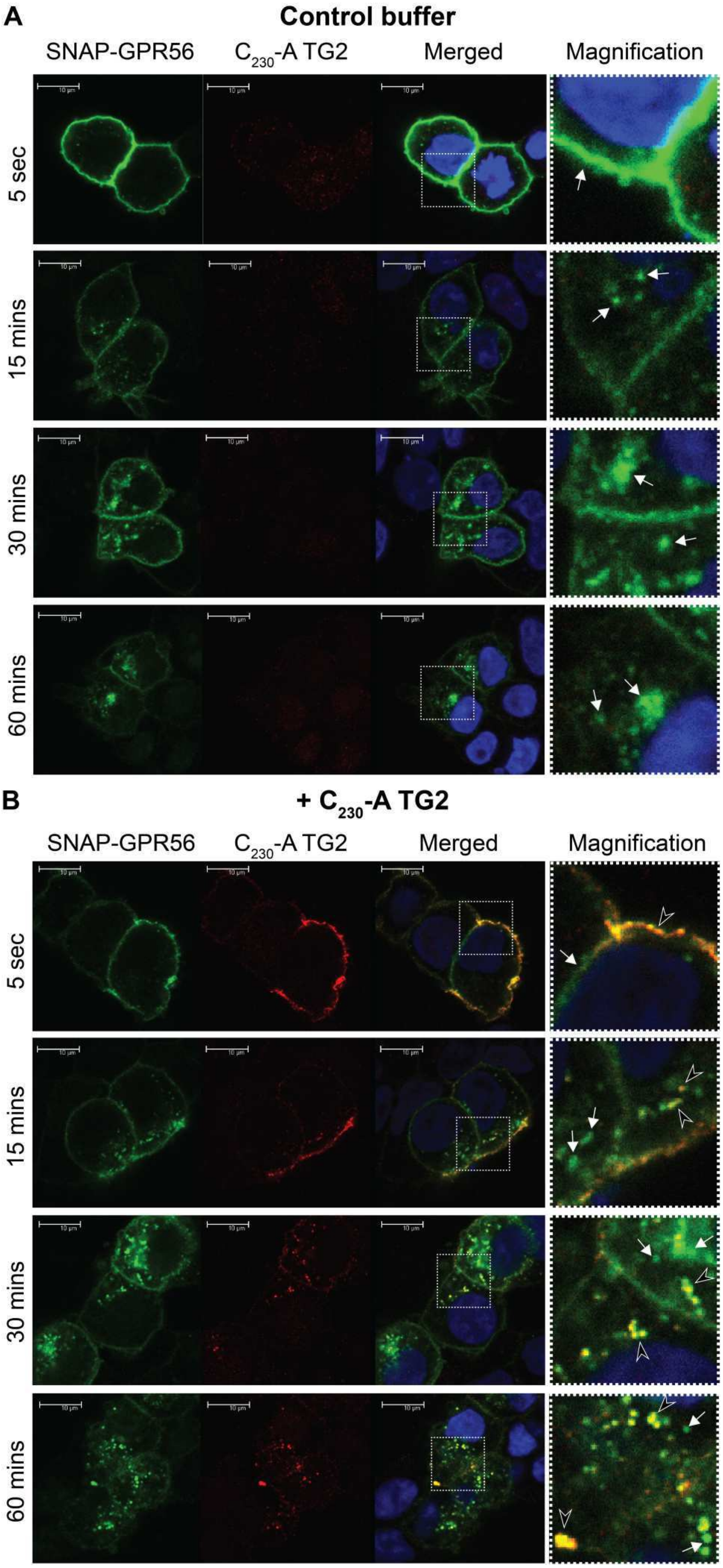
A
Control buffer
SNAP-GPR56
C_{230}-A TG2
Merged
Magnification
5 sec
15 mins
30 mins
60 mins
10 µm
B
+ C_{230}-A TG2
SNAP-GPR56
C_{230}-A TG2
Merged
Magnification
5 sec
15 mins
30 mins
60 mins

Figure 6.6 SNAP-GPR56 and C_{230}-A TG2 internalise simultaneously in transiently transfected HEK293 cells.

Cells were seeded onto poly-L-lysine coated glass coverslips, transfected with SNAP-GPR56 and two days later serum starved for 1 h. SNAP-GPR56 was stained at 4 °C for 15 mins using SNAP-surface substrate 647 (shown in green; NEB). Cells were treated with (A) control buffer or (B) 20 µg/ml C_{230}-A TG2 for 5 sec, followed by immediate fixation or incubation in serum-free medium for 15, 30 or 60 mins prior to fixation. Cells were permeabilised and TG2 (red) was stained using anti-TG2 (Thermo Scientific) and secondary anti-mouse Alexa594 antibodies (Jackson ImmunoResearch).

(A) Control buffer treated cells showed cell surface staining for SNAP-GPR56, with increasing amounts of internalised SNAP-GPR56 over time, beginning after 15 mins. Little SNAP-GPR56 was left at the cell surface after 60 mins. Cells were negative for TG2 staining.

(B) In cells treated with C_{230}-A TG2 for 5 sec, SNAP-GPR56 surface and intracellular staining looked similar to staining in cells treated with control buffer over the entire time. Cells were positive for C_{230}-A TG2 surface staining and internalised TG2 was detectable after 15 mins in a highly GPR56-dependent manner. SNAP-GPR56 positive, as well as SNAP-GPR56 and C_{230}-A TG2-positive vesicles were found, with very little C_{230}-A TG2 and little SNAP-GPR56 left at the cell surface after 60 mins.

White arrows, SNAP-GPR56 staining (green); black arrow heads, co-localisation of SNAP-GPR56 and C_{230}-A TG2 (yellow); scale bar, 10 µm.

6.2.2.3 Internalisation of GPR56 and TG2 is clathrin-dependent

Following the interaction of GPR56 and TG2 over time in SNAP-GPR56 transfected cells showed that both the receptor and its ligand ended up intracellularly, where they partially co-localised in the same intracellular vesicles. A well described mechanism of GPCR internalisation is clathrin-dependent endocytosis and experiments presented in this chapter set out to investigate whether GPR56-internalisation was mediated by clathrin-coated pit formation.

6.2.2.3.1 The clathrin-inhibitor sucrose prevents internalisation

Treatment of cells with hypertonic medium (0.45 M sucrose) is known to prevent the interaction of clathrin and the AP-2 adaptor protein, inhibiting clathrin-dependent receptor internalisation (Hansen et al. 1993).

In the following experiments, cells were transfected with SNAP-GPR56. 48 h later, cells were serum starved for 30 mins in serum-free medium containing 0.45 M sucrose. SNAP-GPR56 (shown in green) was stained with SNAP-surface substrate 647 at 4 °C for 15 mins, followed by pulse-treatment with control buffer or C_{230}-A TG2 for 5 sec. Cells were either fixed directly or incubated for 30 mins in serum-free medium in the presence or absence of 0.45 M sucrose prior to fixation. TG2 (red) was immunocytochemically stained as outlined before.

In figure 6.7 A, cells were fixed immediately after the 5 sec pulse treatment with control buffer (left panels) or C_{230}-A TG2 (right panels). As observed before (Fig. 6.6), cell surfaces stained positive for SNAP-GPR56 (white arrows), partially overlapping with TG2 staining in those cells treated with C_{230}-A TG2 (yellow; black arrow heads).

Following incubation in the absence of sucrose for 30 mins (Fig. 6.7 B), SNAP-GPR56 was found in intracellular vesicles (white arrows) and only little receptor was left at the cell surface in either control or TG2 treated cells. In cells treated with C_{230}-A TG2, some intracellular vesicles were positive for both SNAP-GPR56 and TG2 (yellow; black arrow heads) after 30 mins, as described before. This indicated that 30 mins pre-incubation in 0.45 M sucrose medium was insufficient to prevent receptor internalisation.

In contrast, incubation in hyperosmotic sucrose medium for 30 mins following pulse treatment with buffer control or C_{230}-A TG2 completely abolished receptor and ligand internalisation in all cells (Fig. 6.7 C). Staining was similar to what was observed in cells fixed immediately (Fig. 6.7 A). Both SNAP-GPR56 (white arrows) and TG2 were present at the cell surface, where they partially co-localised (yellow; black arrow heads). All cells lacked intracellular vesicles after 30 mins incubation in 0.45M sucrose, indicating that both internalisation of GPR56 and GPR56-mediated endocytosis of TG2 were clathrin-dependent.

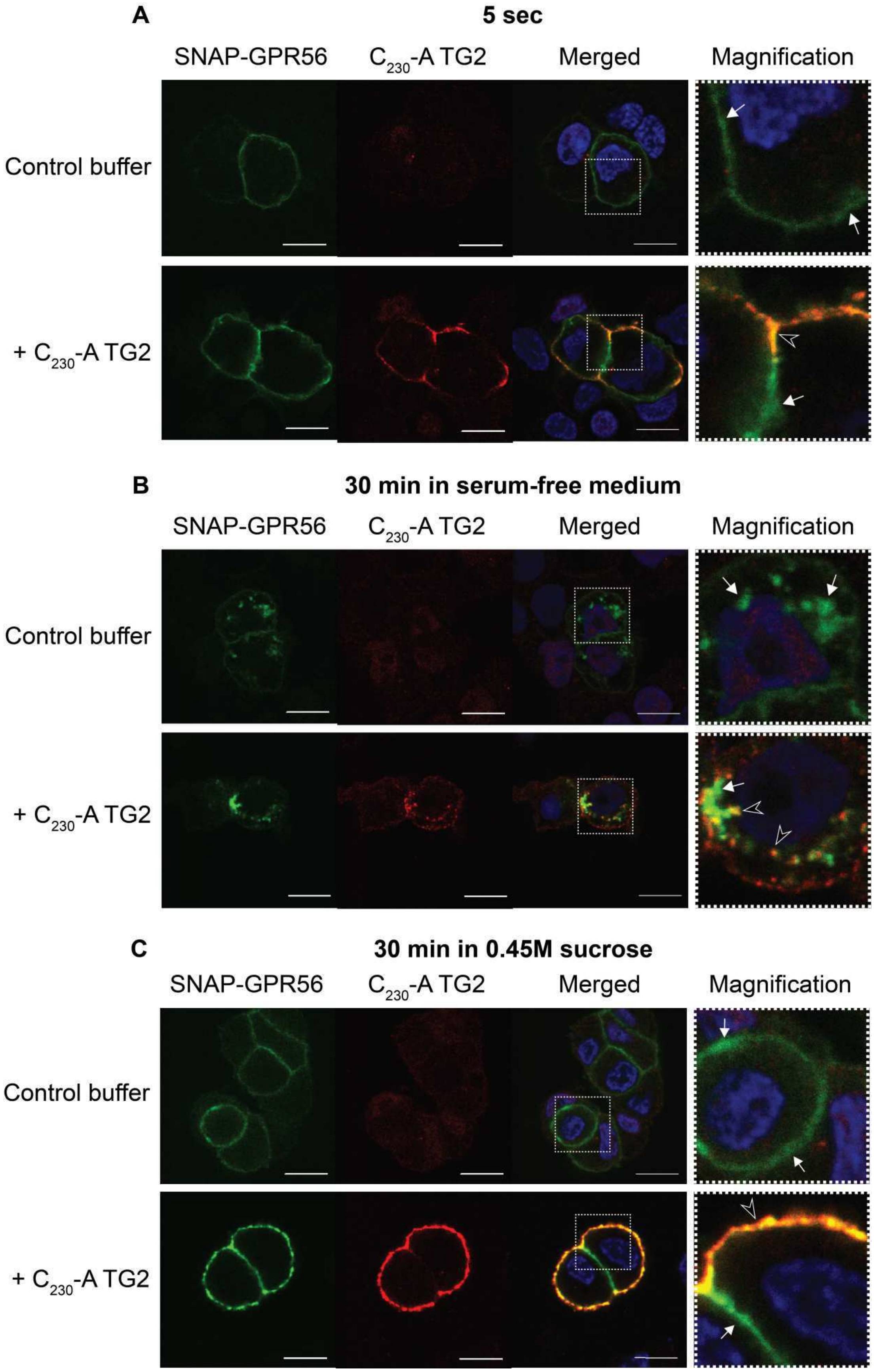
A
5 sec
SNAP-GPR56
C230-A TG2
Merged
Magnification
Control buffer
+ C230-A TG2
B
30 min in serum-free medium
SNAP-GPR56
C230-A TG2
Merged
Magnification
Control buffer
+ C230-A TG2
C
30 min in 0.45M sucrose
SNAP-GPR56
C230-A TG2
Merged
Magnification
Control buffer
+ C230-A TG2

Figure 6.7 Sucrose treatment abolishes internalisation of GPR56 and TG2 in SNAP-GPR56 transfected HEK293 cells.

Cells were seeded onto poly-L-lysine coated glass coverslips and transfected with SNAP-GPR56. Two days post-transfection, cells were serum starved for 30 mins in 0.45 M sucrose-containing medium, followed by staining of SNAP-GPR56 with SNAP-surface substrate 647 (shown in green; NEB) for 15 mins at 4 °C. Cells were treated with buffer control or 20 µg/ml C_{230}-A TG2 for 5 sec and (A) fixed immediately, (B) incubated in serum free medium for 30 mins or (C) incubated in hyperosmotic medium (0.45 M sucrose) for 30 mins pior to fixation. Following permeabilisation, TG2 (red) was stained using monoclonal anti-TG2 (Thermo Scientific) and anti-mouse Alexa594 antibodies (Jackson ImmunoResearch).

(A) Control buffer treated cells that were fixed directly, showed cell surface staining for SNAP-GPR56 (left panels). C_{230}-A TG2 treated cells (right panels) showed SNAP-GPR56 and TG2 surface staining, partially overlapping (yellow).

(B) Following incubation in serum-free medium for 30 mins, SNAP-GPR56 was found in intracellular vesicles, with little receptor left at the cell surface. In cells treated with C_{230}-A TG2 (right panels), intracellular vesicles were partially positive for both SNAP-GPR56 and TG2 staining. Little C_{230}-A TG2 was left at the cell surface.

(C) SNAP-GPR56 and C_{230}-A TG2 internalisation was prevented by incubation in 0.45 M sucrose for 30 mins following treatment with buffer control (left panels) or C_{230}-A TG2 (right panels) for 5 sec.

White arrows, SNAP-GPR56 staining (green); black arrow heads, co-localisation of SNAP-GPR56 and C_{230}-A TG2 (yellow); scale bar, 10 µm.

In addition to analysing the effect of sucrose treatment on GPR56 internalisation by confocal microscopy, GPR56-dependent shedding of AP-AR in the presence of sucrose was investigated using the shedding assay. GPR56 and AP-AR co-transfected cells were treated with 20 µg/ml C_{230}-A TG2 in the absence or presence of 0.45 M sucrose for 1 h. As shown in figure 6.8, the presence of sucrose during the treatment led to a massive increase in *p*-NPP hydrolysis that was ~12-13 fold higher compared to medium without sucrose. Thus, AP-activity probably reached a maximum, as there was no further increase in *p*-NPP hydrolysis due to the addition of C_{230}-A TG2. The increase in AP-AR shedding could be explained by the inhibition of GPR56 internalisation. Due to the accumulation of receptor at the cell surface, more AP-AR was shed by ADAM17, leading to a higher AP-activity in the medium. The result also demonstrated that GPR56 endocytosis attenuates receptor signalling normally inducing ADAM activation.

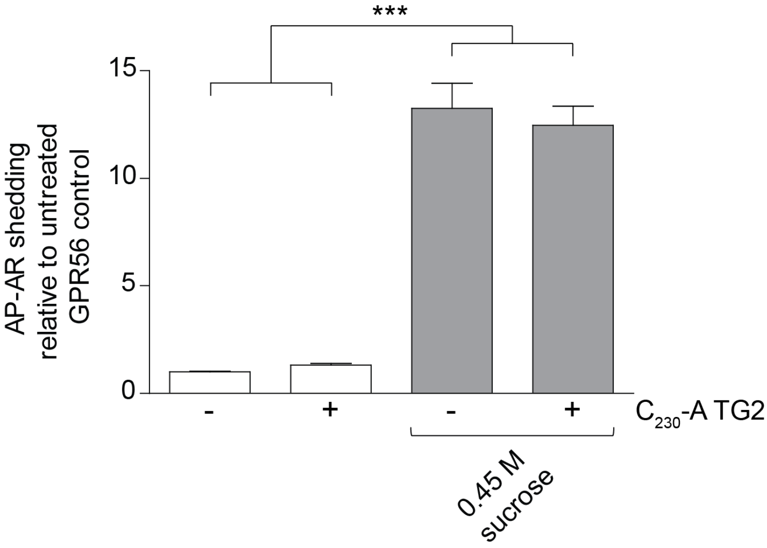

Figure 6.8 Shedding of AP-AR is potentiated in the presence of sucrose.

Cells were transfected with GPR56 and AP-AR. Two days later, cells were serum starved for 1 h and treated with control buffer or 20 µg/ml C_{230}-A TG2 for 1 h in the presence or absence of 0.45 M sucrose.

Data presented show mean of 3 independent experiments with 4 repeats each +/- SEM (n=12). Statistical significance denoted as follows: ***, $p<0.001$.

6.2.2.3.2 SNAP-GPR56 internalises with transferrin receptors

Treatment with sucrose inhibited GPR56 internalisation, as well as GPR56-dependent endocytosis of TG2, indicating clathrin-dependency of these events. The next step was to confirm that endocytosis of GPR56 is clathrin-dependent by co-staining for transferrin receptors (TR) using fluorescent-labelled transferrin (Tf).

In the following experiments, TR and GPR56 endocytosis were observed over time in order to investigate whether both receptors would internalise in the same way. In figure 6.9, SNAP-GPR56 transfected cells were incubated with Alexa488-labelled Tf (green, Tf-488) at 4 °C for 30 mins to prevent preliminary Tf-uptake (Harding et al. 1983). SNAP-GPR56 (shown in red) was then stained with SNAP-surface substrate 647 at 4 °C for 15 mins. Cells were pulse-treated with 20 µg/ml C_{230}-A TG2 or control buffer for 5 sec and fixed immediately or incubated in serum-free medium for 15 min prior to fixation.

Cells that were fixed directly after treatment showed cell surface staining for SNAP-GPR56 (white arrow heads) and staining for Tf-488 (white arrows), which appeared slightly below the cell surface (Fig. 6.9 A). It was first tried to co-label the TR and SNAP-GPR56 simultaneously at 4 °C. This approach, however, was not amendable due to lack of TR staining (data not shown). Therefore, TR-Tf complexes were established first, prior to SNAP-GPR56 labelling. Remarkably, the degree of co-localisation (yellow; black arrow heads) between the two proteins was low at 5 sec, as TR-Tf complexes had already started to internalise (Fig. 6.9 A). This probably occurred because of the timely separated staining for SNAP-GPR56 and TR. Labelling in the presence of sucrose was also evaluated, which should prevent receptor internalisation and increase the amount of TR at the cell surface, but was not successful (data not shown). It is likely that a component present in the SNAP-substrate prevents Tf-488 to bind to TR, however, the exact composition of the solution is unknown (NEB). Since the SNAP-substrate is dissolved in DMSO, I also tested labelling of TR with Tf-488 in the presence of DMSO, which did not interfere with TR-Tf complex formation (data not shown).

Following incubation in serum-free medium for 15 mins (Fig. 6.9 B), SNAP-GPR56 and TR-Tf complexes appeared in the same intracellular vesicles (yellow; black arrow heads). Only a few intracellular vesicles were positive solely for SNAP-GPR56 (white arrow heads) or Tf-488 (white arrows). Some SNAP-GPR56, but very little Tf-488 was left at the cell surface after 15 mins. The staining pattern of SNAP-GPR56 and TR-Tf complexes looked similar in cells treated with control buffer (left panels) and C_{230}-A TG2 (right panels).

Incubation for 30 mins and longer resulted in a complete loss of TR-Tf complexes in the cells (data not shown). It is likely that Tf-488 was already recycled back to the cell surface and dissociated, since this process takes ~20-30 mins (Harding et al. 1983; Goldstein et al. 1985). This might explain why TR-Tf complexes were not detectable in cells at later time points.

Although it was difficult to demonstrate cell surface co-localisation of GPR56 and TR initially, the high amount of co-staining in intracellular vesicles after 15 mins (black arrow heads) indicated co-internalisation. Therefore, the experiments confirmed the clathrin-dependent endocytosis of GPR56.

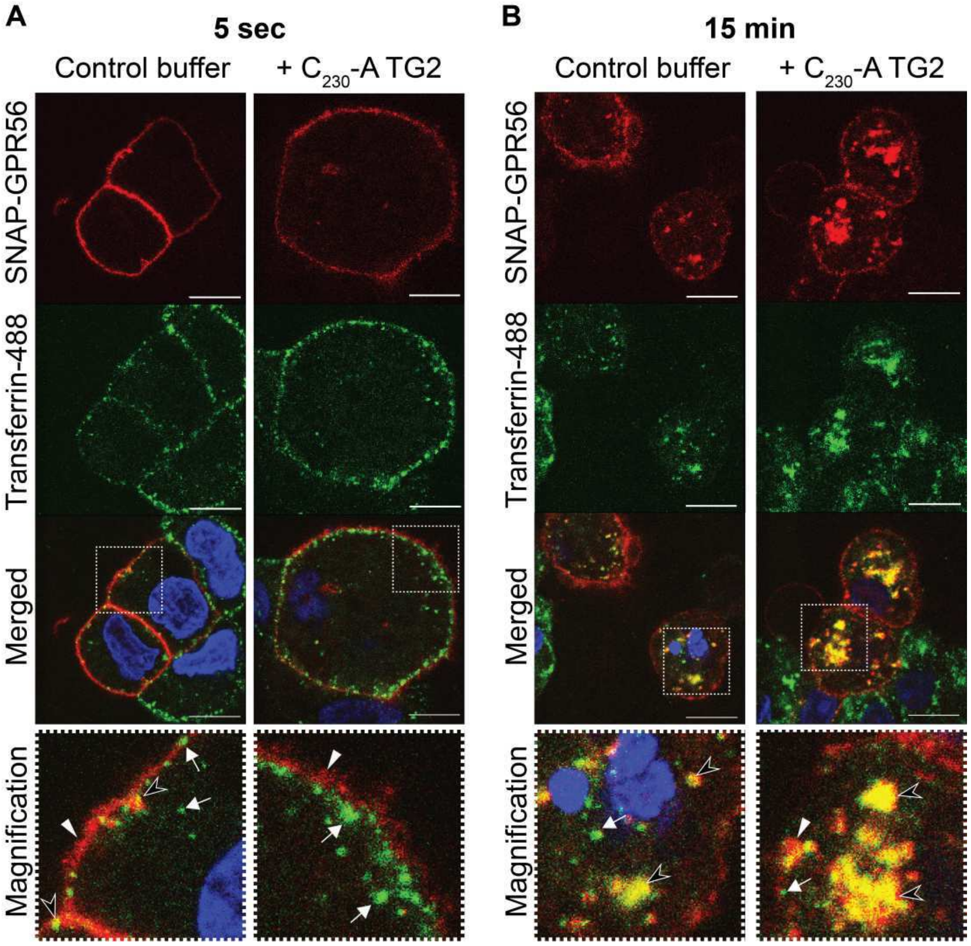

Figure 6.9 Transferrin-receptors co-localise with SNAP-GPR56 following endocytosis.

Cells were seeded onto poly-L-lysine coated glass coverslips and transfected with SNAP-GPR56. Two days later, cells were serum starved for 1 h, followed by incubation with 10 µg/ml transferrin-488 solution (green, Tf-488; Molecular Probes) for 30 mins at 4 °C. SNAP-GPR56 (shown in red) was stained with SNAP-surface substrate 647 (NEB) for 15 mins at 4°C. Cells were treated with control buffer (left panels) or 20 µg/ml C_{230}-A TG2 (right panels) for 5 sec, followed by (A) direct fixation or (B) incubation in serum-free medium for 15 mins prior to fixation.

(A) Initially, cells were positive for SNAP-GPR56 surface staining. Tf-488 appeared slightly below the cell surface, indicating beginning of TR internalisation.

(B) After 15 mins incubation, little SNAP-GPR56 and even less Tf-488 was left at the cell surface. Intracellular vesicles, mostly positive for both SNAP-GPR56 and Tf-TR complexes (yellow), were detectable.

White arrow heads, SNAP-GPR56 staining (red); white arrows, Tf-488 staining (green); black arrow heads, co-localisation of SNAP-GPR56 and Tf-488 (yellow); scale bar, 10 µm.

6.2.2.3.3 Endocytosis of SNAP-GPR56 is caveolae-independent

The results presented above indicated that GPR56 endocytosis was dependent on the formation of clathrin-coated pits. Internalisation by caveolae (“little caves”), a clathrin-independent pathway, is also known for GPCRs (Chini and Parenti 2004). In order to investigate non-clathrin-internalisation, one of the main structural proteins of caveolae, caveolin-1 (cav-1), was co-stained in cells expressing SNAP-GPR56. The expression of the ~20 kDa protein cav-1 is necessary and sufficient for the formation of caveolae, thus cav-1 represents a good marker for caveolae-staining (Fra et al. 1995).

SNAP-GPR56 transfected cells (shown in red) were stained with SNAP-surface substrate 647 for 15 mins at 4 °C and treated with buffer control or 20 µg/ml C_{230}-A TG2 for 5 sec. Cells were either fixed immediately or incubated in serum-free medium for up to 60 mins prior to fixation and permeabilisation. A polyclonal anti-cav-1 antibody was used to stain caveolae (green).

At 5 sec (Fig. 6.10 A), cells treated with control buffer (left panels) or C_{230}-A TG2 (right panels) showed cell surface staining for SNAP-GPR56 (white arrow heads), which partially overlapped with cav-1 (yellow; black arrow heads). Additionally, cav-1 was also located intracellularly at this stage (white arrows), since caveolae endocytose several proteins.

After 15 mins of incubation in serum-free medium (Fig. 6.10 B), intracellular vesicles positively staining for SNAP-GPR56 (white arrow heads) were found in all cells. After 60 mins (Fig. 6.10 C), the amount of internalised SNAP-GPR56 increased, with little left at the cell surface.

The overall pattern of cav-1 staining remained similar for all time points and conditions investigated, showing some surface staining and some staining of vesicles (white arrows). There was very little co-localisation of cav-1 and SNAP-GPR56 in the intracellular vesicles (yellow; black arrow heads).

These results indicated that GPR56 internalisation was independent of caveolae, confirming the idea of clathrin-mediated endocytosis.

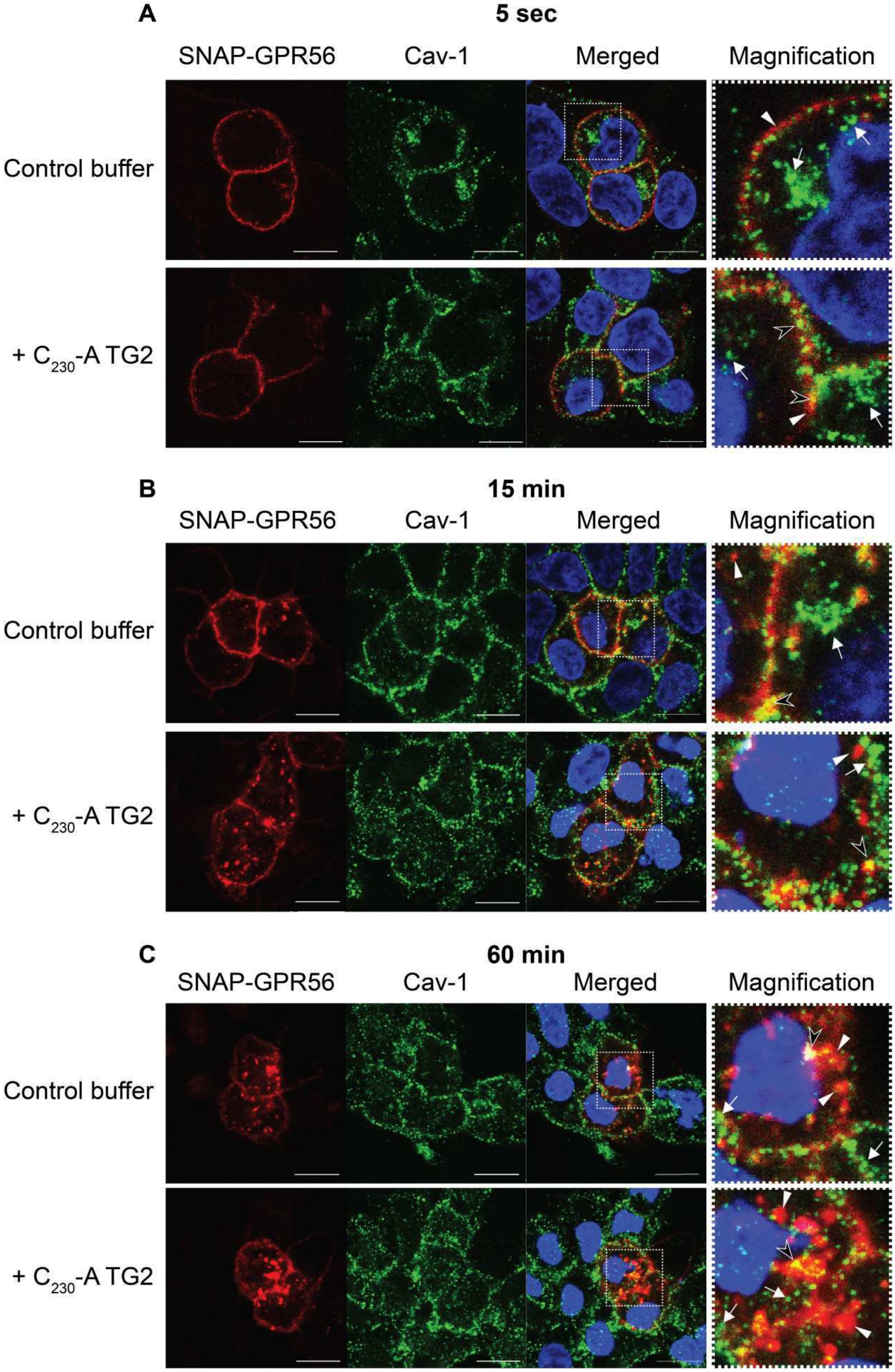
A
5 sec
SNAP-GPR56
Cav-1
Merged
Magnification
Control buffer
+ C230-A TG2
B
15 min
SNAP-GPR56
Cav-1
Merged
Magnification
Control buffer
+ C230-A TG2
C
60 min
SNAP-GPR56
Cav-1
Merged
Magnification
Control buffer
+ C230-A TG2

Figure 6.10 Internalisation of SNAP-GPR56 is not mediated by caveolae.

Cells were seeded onto poly-L-lysine glass coverslips and transfected with SNAP-GPR56. 48 h post-transfection, cells were serum starved for 1 h, followed by SNAP-GPR56 staining (shown in red) with SNAP-surface substrate 647 (NEB) for 15 mins at 4 °C. Cells were treated with control buffer (left panels) or 20 µg/ml C_{230}-A TG2 (right panels), followed by (A) direct fixation or incubation in serum-free medium for (B) 15 mins or (C) 60 mins prior to fixation and permeabilisation. Caveolae (green) were stained using anti-cav-1 (Abcam) and anti-rabbit Alexa488 antibodies (Jackson ImmunoResearch).

(A) After 5 sec, the cell surface was positive for SNAP-GPR56 staining, partially overlapping with cav-1 (yellow). Cav-1 staining was also present intracellularly.

(B) After 15 mins, some internalisation of SNAP-GPR56 occurred, but there was little intracellular co-localisation with cav-1 positive vesicles (yellow).

(C) Following 60 mins of incubation in serum-free medium, the amount of SNAP-GPR56-positive vesicles increased, still there was little co-localisation with cav-1 intracellularly, indicating caveolae-independent internalisation of GPR56.

White arrow heads, SNAP-GPR56 staining (red); white arrows, cav-1 staining (green); black arrow heads, co-localisation of SNAP-GPR56 and cav-1 (yellow); scale bar, 10 µm.

6.2.2.4 Internalised GPR56 and TG2 do not co-localise in lysosomes

So far, the interaction between GPR56 and TG2 resulted in simultaneous internalisation of both proteins, which was most likely mediated by clathrin. The results indicated that recycling of GPR56 within the 1 h time window investigated was slow and that TG2 did not traffic back to the cell surface. Thus, the fate of receptor and ligand following endocytosis was still unclear and was investigated further.

In addition to recycling via early endosomes, a likely event following internalisation of transmembrane proteins and their ligands is degradation, which usually occurs in lysosomes carrying proteolytic enzymes (Sorkin and von Zastrow 2009). In order to investigate whether GPR56 and TG2 were sorted into lysosomes, co-staining for lysosome-associated membrane proteins LAMP1 and LAMP2 was performed.

Cells were transfected with SNAP-GPR56 (shown in red) stained with SNAP-surface substrate 647 at 4 °C for 15 mins. Cells were pulse-treated with control buffer or 20 µg/ml C_{230}-A TG2, followed by incubation in serum-free medium for up to 6 h prior to fixation and permeabilisation. Cells were then co-stained for TG2 (shown in cyan) and the lysosomal marker LAMP1 (green).

Cytoplasmic staining for lysosomes was present over the entire incubation time in both buffer treated (A) and C_{230}-A TG2 treated (B) cells (Fig. 6.11, white arrows).

In control buffer treated cells (Fig. 6.11 A), SNAP-GPR56 was present at the cell surface after 5 sec and in endocytic vesicles (white arrow heads), which were apparent after 30 mins and increased over 60 mins with very little SNAP-GPR56 left at the cell surface. There was very little co-localisation between internalised SNAP-GPR56 and LAMP1-positive lysosomes (black arrow heads) after 30 mins or 60 mins in control buffer treated cells.

Fig. 6.11 B shows that SNAP-GPR56 and TG2 partially co-localised at the cell surface of C_{230}-A TG2 treated cells after 5 sec and in endocytic vesicles (white; black arrows) that were detectable after 30 mins and increased over

60 mins, with little SNAP-GPR56 and TG2 left in the plasma membrane. There was little to no colocalisation between LAMP1-positive lysosomes and the endocytosed receptor-ligand pair. Strikingly, the amount of intracellular TG2 dramatically decreased after the 60 mins time point, with almost nothing left after 6 h (Fig. 6.11 B). However, even at the 3 h time point, the remaining TG2 did not co-localise with LAMP1. This finding and the fact that TG2 is not recycled back to the cell surface could indicate degradation via a different pathway, e.g. proteasomal degradation.

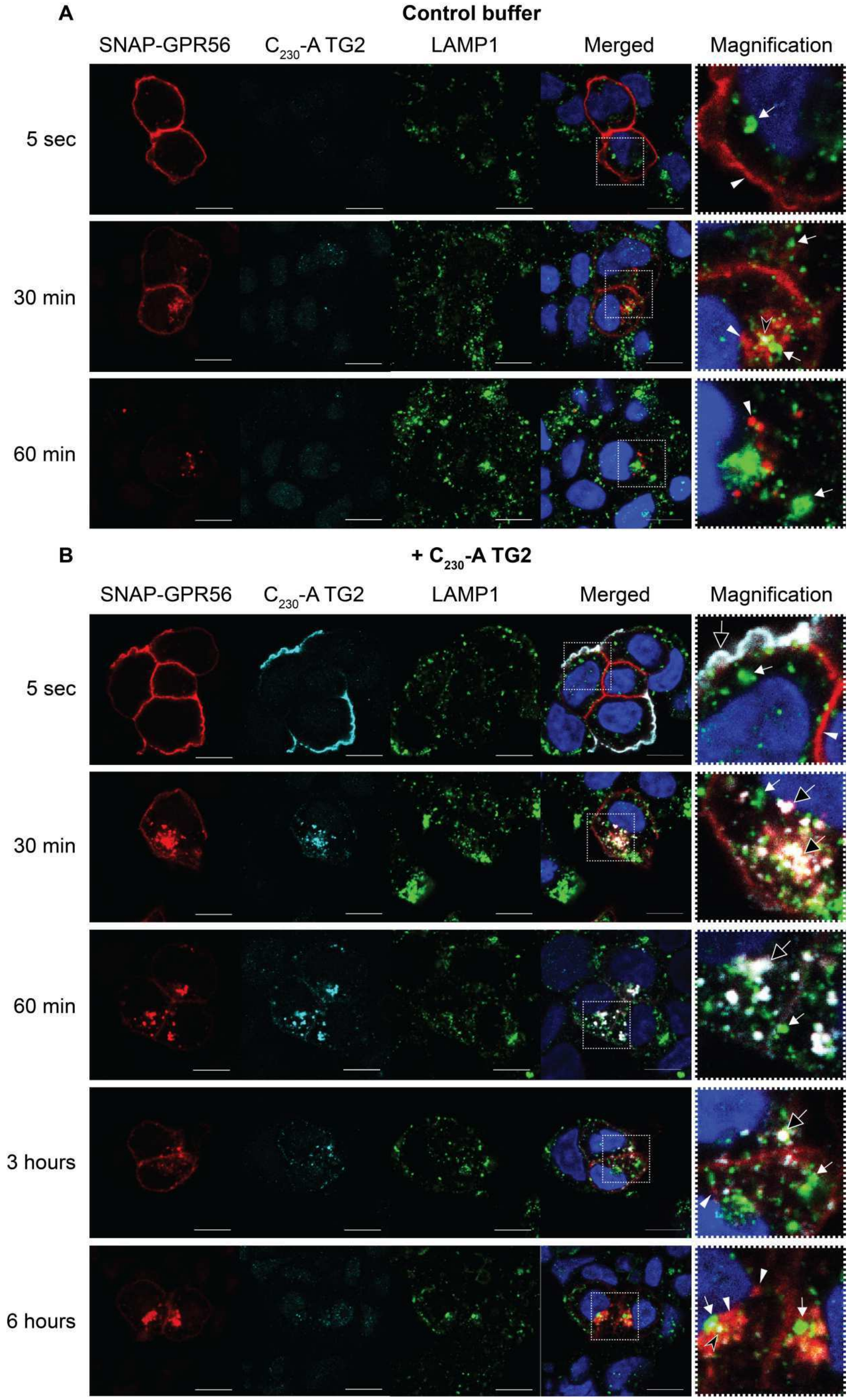
A
Control buffer
SNAP-GPR56
C_{230}-A TG2
LAMP1
Merged
Magnification
5 sec
30 min
60 min
B
+ C_{230}-A TG2
SNAP-GPR56
C_{230}-A TG2
LAMP1
Merged
Magnification
5 sec
30 min
60 min
3 hours
6 hours

Figure 6.11 Internalised SNAP-GPR56 and C_{230}-A TG2 are not targeted to LAMP1-positive lysosomes.

Cells growing on poly-L-lysine coated glass coverslips were transfected with SNAP-GPR56 and 48 h serum starved for 1 h. SNAP-surface substrate 647 (NEB) was used to stain SNAP-GPR56 (shown in red) for 15 mins at 4 °C. Cells were treated with (A) control buffer or (B) 20 µg/ml C_{230}-A TG2, followed by immediate fixation or incubation in serum-free medium for 30 mins, 60 mins, 3 h or 6 h prior to fixation and permeabilisation. C_{230}-A TG2 (shown in cyan) was stained with mouse anti-TG2 (Thermo Scientific) and anti-mouse Alexa594 antibodies (Jackson ImmunoResearch). Late endosomes/early lysosomes (green) were stained using anti-LAMP1 (Sigma-Aldrich) and anti-rabbit Alexa488 antibodies (Jackson ImmunoResearch).

(A) Control buffer treated cells were negative for TG2 staining at any time. SNAP-GPR56 (red) was internalised as observed before, with little receptor left at the cell surface after 1 h incubation in serum free medium. There was very little co-localisation of GPR56 and LAMP1-positive lysosomes intracellularly (yellow).

(B) After 5 sec incubation, SNAP-GPR56 and TG2 showed overlapping cell surface staining (white). Over time, the ligand-receptor pair internalised simultaneously (15 mins to 3 h time points). After 6 h, GPR56 was only found intracellularly with very little left at the cell surface and no TG2 present in the cells, indicating degradation that was not LAMP1-dependent.

White arrow heads, SNAP-GPR56 staining (red); white arrows, LAMP1 staining (green); black arrow heads, co-localisation of LAMP1 and SNAP-GPR56 (yellow); Black arrows, co-localisation of SNAP-GPR56 and TG2 staining (white); scale bar, 10 µm.

Next, LAMP2 was tested as a second lysosomal marker in experiments using immunocytochemistry. Figure 6.12 shows SNAP-GPR56 (shown in red) expressing cells that were treated with control buffer (A) or C_{230}-A TG2 (B), followed by fixation, permeabilisation and co-staining with mouse anti-LAMP2 antibody (green). In comparison to LAMP1, LAMP2 staining seemed more prominent (white arrows). Regarding co-localisation with SNAP-GPR56, there was no difference between LAMP1 and LAMP2 staining. SNAP-GPR56 was apparent at the cell surface after 5 sec and was partially internalised after 30 mins, with little left at the cell surface after 60 mins (Fig. 6.12 A & B, white arrow heads). The majority of intracellular vesicles containing SNAP-GPR56 were negative for LAMP2 staining, indicating that GPR56 was not targeted to lysosomes once it entered the cell. Again there was no evidence for degradation of GPR56 in lysosomes.

Taken together, experiments using SNAP-tagged GPR56 presented in this chapter demonstrated that SNAP-tag staining is a good method to follow N-terminal domain receptor internalisation that can be combined with immunocytochemistry to stain other proteins, or ligand. In contrast to pure antibody staining of GPR56 and TG2 (6.2.1), SNAP-tag staining enabled the analysis of GPR56-dependent TG2-internalisation, as well as it revealed the clathrin-dependency of this event. The question of the receptor-ligand fate inside the cell could not entirely be answered, but experiments performed excluded lysosome-dependent degradation.

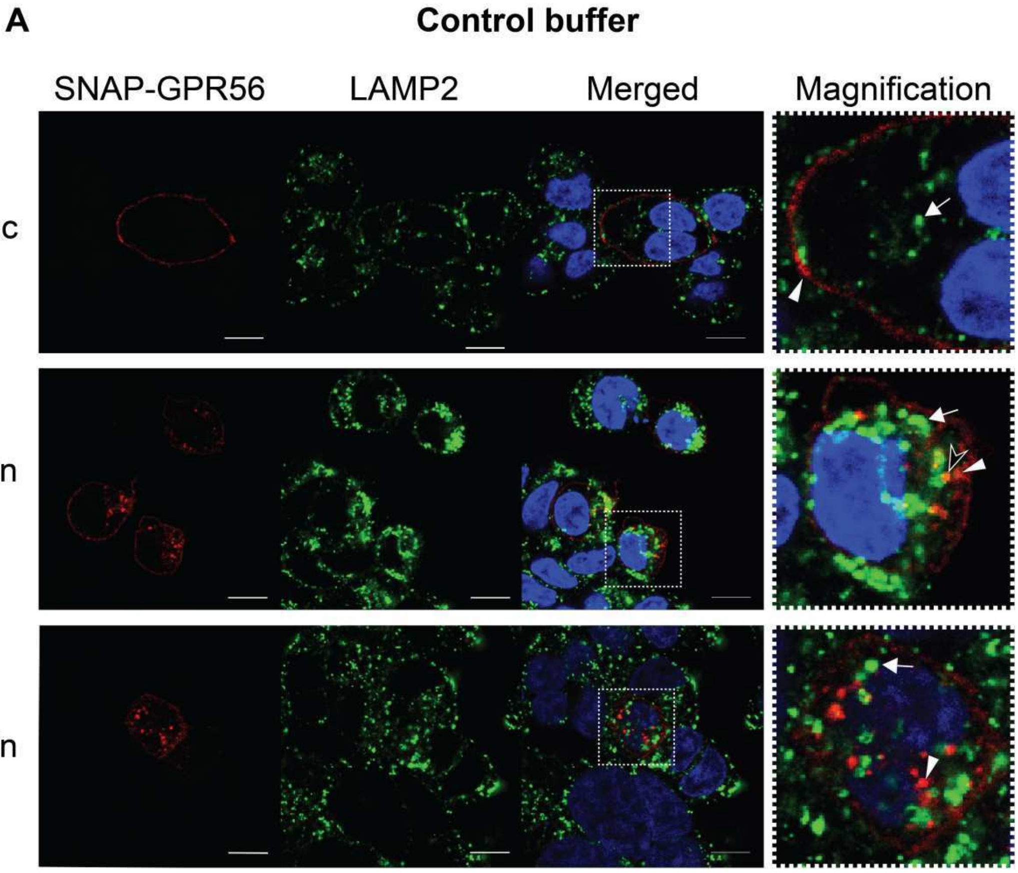
A
Control buffer
SNAP-GPR56
LAMP2
Merged
Magnification
5 sec
30 min
60 min

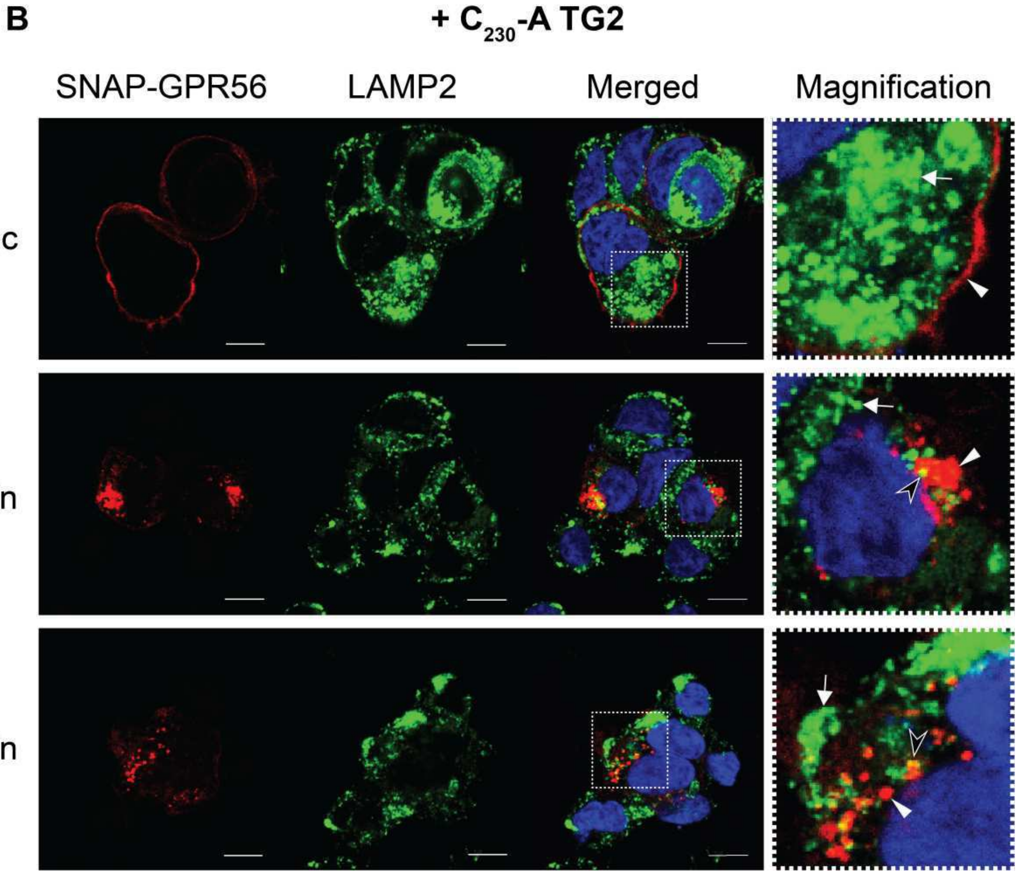
B
+ C_{230}-A TG2
SNAP-GPR56
LAMP2
Merged
Magnification
5 sec
30 min
60 min

Figure 6.12 Internalised SNAP-GPR56 and C_{230}-A TG2 do not co-localise with LAMP2-positive lysosomes.

Cells growing on poly-L-lysine coated glass coverslips were transfected with SNAP-GPR56 and 48 h later serum starved for 1 h. SNAP-surface substrate 647 (NEB) was used to stain SNAP-GPR56 (shown in red) for 15 mins at 4 °C. Cells were treated with (A) control buffer or (B) 20 µg/ml C_{230}-A TG2, followed by immediate fixation or incubation in serum-free medium for 30 mins or 60 mins prior to fixation and permeabilisation. Late endosomes/early lysosomes (green) were stained using mouse anti-LAMP2 (DHSB) and anti-mouse Alexa488 antibodies (Jackson ImmunoResearch).

White arrow heads, SNAP-GPR56 staining (red); white arrows, LAMP2 staining (green); black arrow heads, co-localisation of LAMP2 and SNAP-GPR56 (yellow); Scale bar, 10 µm.

6.3 Discussion

In this chapter, confocal microscopy was used to investigate whether GPR56 is internalised constitutively and/or upon TG2-stimulation. Confocal microscopy cannot be used to identify membrane invaginations or lipid rafts, as they are too small and dynamic, but it is very useful to study intracellular trafficking of GPCRs in combination with markers for clathrin-dependent and -independent endocytosis or intracellular compartments like endosomes (Chini and Parenti 2004).

The first attempt to follow the fate of the receptor-ligand pair, antibody staining against GPR56 and TG2 was used on fixed and permeabilised HEK293 cells inducibly expressing GPR56 (Fig. 6.3). Using this approach, it was shown that C_{230}-A TG2 exclusively bound to cells expressing GPR56. Moreover, as a result of the receptor-ligand interaction, TG2 was internalised in a GPR56-dependent manner. These findings confirm the conclusion drawn from the previous chapters, illustrating TG2 as a *bona fide* ligand for GPR56.

Zemskov et al. (2007) showed that TG2 binds to the lipoprotein-receptor related protein-1 (LRP1) at the cell surface and undergoes endocytosis and lysosomal degradation upon prolonged incubation (> 90 mins). LRP1-dependent constitutive internalisation of TG2 was shown to occur via both clathrin- and caveolae-dependent pathways. HEK293 cells are negative in LRP-1 expression (Montel et al. 2007) and thus represent a very good cell model to investigate GPR56-dependent and LRP1-independent TG2 internalisation.

Immunostaining of GPR56 was not feasible to follow endocytosis of GPR56, since the antibody stains all N-GPR56 present in the cell, so that it is impossible to distinguish between maturing and endocytosed GPR56. Additionally, the degree of co-localisation between GRP56 and internalised TG2 was very low. This might be explained by sterical hindrance between the GPR56 and TG2 antibodies, preventing the GPR56 antibody or the secondary antibody to bind. However, this did not account for the initial time point, showing co-localisation between GPR56 and TG2 at the cell surface prior to internalisation. Therefore, epitopes of N-GPR56 that are accessible at the cell surface may be non-accessible upon endocytosis due to conformational changes. Moreover, prolonged agonist stimulation, as performed here with TG2 treatments for up to 60 mins, can influence the fate of the endocytosed receptor, leading to down-regulation of the GPCRs by degradation, a phenomenon that is implicated in the development of drug resistance (von Zastrow 2001).

Therefore, another biochemical approach was used for further experiments. Using HEK293 cells transiently transfected with SNAP-tagged GPR56, it was possible to follow receptor internalisation, as this method only stains receptor initially present at the cell surface. Western blot and confocal analyses of cells expressing SNAP-GPR56 showed that the receptor was normally processed (Fig. 6.4) and that receptor trafficking to the cell surface was not influenced by the presence of the SNAP-tag (Fig. 6.5 & 6.6). A comparison of SNAP-GPR56 and SNAP-β_2AR, the control receptor, showed that the SNAP-tag did not influence C_{230}-A TG2 binding to GPR56. In addition, the results confirmed the specific interaction of the ligand-receptor pair, as SNAP-β_2AR did not bind TG2 (Fig. 6.5 B&C).

A comparison of ligand-independent internalisation of GPR56 and β_2AR showed that there was a lot of GPR56 endocytosed after 15 mins at 37 °C, whereas there was little β_2AR present in intracellular vesicles (Fig. 6.5 A). This may indicate a faster recycling of β_2AR. The β_2AR belongs to class A GPCRs that only weakly interact with β-arrestin and recycle rapidly (Oakley et al. 2001). GPR56 associates with β-arrestin2 (Paavola et al. 2011) and might belong to the family of class B receptors that associate tightly with β-arrestin and recycle slowly back to the cell surface. However, in order to confirm this speculation, β-arrestin and SNAP-GPR56 stainings should be combined.

On the other hand, the β_2AR was described to be relatively stable at the cell surface for up to 1 h in HEK293 cells under ligand-free conditions (von Zastrow and Kobilka 1994). This explains the low amount of internalised β_2AR observed in our experiment and indicates a higher degree of constitutive internalisation of GPR56 as a result of a high basal activity, as observed for the melanocortin MC4 receptor (Mohammad et al. 2007).

In order to investigate whether TG2 and GPR56 internalise together, SNAP-GPR56 expressing cells were treated with C_{230}-A TG2 for 5 sec (the pulse), followed by incubation in TG2-free medium for up to 1 h (the chase) (Fig. 6.6). GPR56 and TG2 co-localised at the cell surface, and simultaneous endocytosis was detected after 15 mins. GPR56-TG2 complexes accumulated in intracellular vesicles, with little GPR56 and even less TG2 left at the cell surface at 60 mins, indicating degradation and slow recycling. GPR56 also rapidly internalised constitutively in the absence of TG2. The results potentially show a higher degree of internalisation in the presence of TG2, however, the experiments were not analysed quantitatively and conclusions in this direction cannot be drawn.

The next step was to shed some light on the mechanism of GPR56 internalisation. GPCRs can switch the mode of endocytosis upon agonist-activation. In HeLa cells, the β_2AR and the M3 acetylcholine muscarinic receptors switch from a clathrin-independent mechanism of constitutive internalisation to clathrin-dependent endocytosis upon agonist stimulation (Scarselli and Donaldson 2009). Sucrose is a non-toxic clathrin inhibitor (McMahon and Boucrot 2011) that is cheap and easy to handle, thus SNAP-GPR56 expressing cells were pulse-treated with C_{230}-A TG2, followed by incubation in 0.45 M sucrose-containing medium for 30 mins (Fig. 6.7 C). The treatment with sucrose completely prevented constitutive as well as TG2-induced endocytosis of GPR56, therefore constitutive internalisation of GPR56 and GPR56-dependent internalisation of TG2 are both dependent on clathrin.

In order to confirm that endocytosed GPR56 was present in clathrin-coated vesicles, the transferrin-receptor (TR) was co-localised (Fig. 6.9). In the beginning of the experiment, Tf-488 and GPR56 were present at the cell surface. However, the degree of co-localisation between the two proteins was low, as Tf-uptake had already started. This was probably due to the experimental procedure, as the cells were first incubated with Tf-488 prior to SNAP-tag staining. However, simultaneous incubation with Tf-488 and SNAP-substrate abolished staining of TR, which might be due to the presence of a component in the SNAP-substrate solution that interferes with TR-Tf complex formation. The SNAP-substrates themselves, benzylguanine derivatives, are probably too small to sterically interfere with Tf-488 or TR. Nonetheless, Tf-488 and GPR56 co-localised in the same endocytic vesicles after 15 mins of incubation in serum-free medium at 37 °C (Fig. 6.9), again indicating that GPR56 internalisation was mediated by clathrin-coated pits.

In order to exclude a contribution of caveolae in GPR56 endocytosis, a cav-1 antibody was used to co-stain SNAP-GPR56 expressing cells pulse-treated with C_{230}-A TG2 (Fig. 6.10). Cav-1 staining was pronounced at the cell surface, but also present intracellularly, since caveolae are formed in the ER and cav-1 also plays a role as a molecular chaperone (Cohen et al. 2003). Following incubation for up to 1 h, GPR56 internalised, as observed in previous experiments. The distribution of cav-1, however, did not change significantly over time and the degree of co-localisation between cav-1 and the GPR56 was very low. These results indicate that internalisation of GPR56 is not mediated by caveolae. In addition, the pattern of GPR56 endocytosis was the same in the absence or presence of TG2, as also observed with labelled Tf-488 (Fig. 6.9), again indicating that constitutive and ligand-induced internalisation of GPR56 are mediated by clathrin.

Zhang et al. 1996 showed that some receptors switch to clathrin-independent endocytosis when a mediator for clathrin-dependent endocytosis like β-arrestin is inhibited. In order to exclude the possibility that GPR56 could internalise via clathrin-independent mechanisms, the same experiment could be repeated in Cos-7 cells, which show low endogenous β-arrestin levels (Zhang et al. 1996). Moreover, depending on the cell type, some GPCRs use different mechanisms of endocytosis. The β_2AR for example internalises via clathrin-dependent endocytosis in HEK293 cells, whereas it uses caveolae for internalisation in A431 epithelial carcinoma cells (von Zastrow 2001).

Thus, the mechanism of endocytosis seems to be dependent on the GPCR, the presence of agonist and the cell type.

Finally, experiments using lysosomal markers were performed in order to investigate the fate of endocytosed GPR56 and TG2. At 60 mins, plasma membrane levels for GPR56 and TG2 were low, with most of the receptor-ligand pair present in endocytic vesicles. After 3 h and 6 h, GPR56 was still present in endocytic vesicles, whereas most of intracellular TG2 staining was lost, indicating degradation. Lysosomal degradation is an important function of endocytosis and many cells use it to regulate the composition of their plasma membrane and to attenuate signal transduction (von Zastrow 2001). Co-staining of the lysosomal integral membrane proteins LAMP1 and LAMP2 did not indicate co-localisation with GPR56 or TG2. Results recently presented by Yang et al. (2014) indicated GPR56-dependent internalisation of TG2, followed by lysosomal degradation of TG2 after 60 mins. Treatment of GPR56-expressing MC-1 melanoma cells with the lysosomal inhibitors chloroquine and NH_4Cl increased the amount of TG2 present in the ECM. Additionally, the results showed accumulation of N-GPR56 in the ECM, raising questions about potential exocytosis of the N-terminus. However, these experiments were performed in a completely different cell system and the endocytic machinery as well as the receptor/ligand fate upon internalisation can vary between different cell types for the same receptor (von Zastrow 2001). In contrast to the TG2 pulse treatments (5 sec) performed in my experiments, Yang et al. (2014) treated their cells for prolonged times (up to 60 mins) with TG2, an important difference that potentially influences the outcome for the internalised receptor-ligand pair.

In order to further investigate whether TG2 is degraded in GPR56-expressing HEK293 cells upon endocytosis, cells could be pulse treated with C_{230}-A TG2 for 5 sec, then incubated in serum-free medium for 60 mins and longer, followed by analysis of cell lysates for TG2 degradation products using western blot analysis. This experiment could clarify whether TG2 is degraded, but not how this might happen.

Experiments presented in this chapter may indicate that GPR56 and TG2 are degraded by another, non-lysosomal mechanism in HEK293 cells, such as the 26S proteasome, the megaprotease complex degrading most cellular proteins. However, endocytosis via clathrin-coated pits is generally believed to be associated with receptor ubiquitination and lysosomal degradation, as shown for the β_2AR and δ-opioid receptors in HEK293 cells (Shenoy et al. 2008; Tsao and von Zastrow 2000; Keith et al. 1996). The β_2AR is mainly recycled, but can be detected in lysosomes after >6 h of prolonged agonist stimulation. The δ-opioid receptors are mainly degraded and detected in lysosomes ~60 mins after endocytosis (Moore et al. 1999; Tsao and von Zastrow 2000). In addition, the δ-opioid receptor was shown to undergo substantial proteloytic degradation even after the removal of agonist (pulse treatment) (Tsao and von Zastrow 2000). However, another report demonstrated basal and agonist-induced proteasomal degradation of δ-opioid receptors in HEK293 cells following polyubiquitination of the receptors (Chaturvedi et al. 2001). Proteolysis of the receptors was apparent 2-4 h after agonist stimulation and it was suggested that the ubiquitin/proteasome-pathway operates upstream of lysosomes. A similar observation was made with the platelet-derived growth factor that is degraded by the proteasome, but remaining peptide fragments are further degraded in lysosomes (Mori et al. 1995). Thus, GPR56 might behave similar to the δ-opioid receptors, i.e. it is internalised via clathrin-coated pits, followed by polyubiquitination and degradation in the proteasome. This hypothesis would support my finding that GPR56 and TG2 are not detected in lysosomes within the timeframe of the performed experiments.

In order to further investigate how GPR56 and TG2 are degraded, their fate could be chased in the presence of lysosomal protease inhibitors or proteasomal inhibitors (Chaturvedi et al. 2001). If intracellular TG2 or GPR56 levels remained constantly high over time in the presence of one of the inhibitors, this would point towards degradation in the respective compartment.

Additionally, it must be noted that co-localisation of C-GPR56 with LAMP-positive lysosomes cannot be excluded, as SNAP-surface staining does only follow the fate of N-GPR56. N-GPR56 mainly localises in non-raft fractions, whereas C-GPR56 is partially found in lipid rafts (Chiang et al. 2011). Therefore, it is possible that their endocytic routes differ and it cannot be excluded that C-GPR56 is internalised via a clathrin-independent mechanism. Experiments setting out to follow the fate of the C-GPR56 domain were performed, in which HEK293 cells were transfected with a SNAP-GPR56-mCherry expression construct. The N-terminal SNAP-tag was stained with SNAP-surface substrate 488 in order to monitor potential co-localisation of SNAP-N-GPR56 and C-GPR56-mCherry at the cell surface or in endocytic vesicles upon internalisation (data not shown). However, analysis using confocal microscopy and western blotting revealed that mCherry is cleaved from the C-terminal tail and localised in huge intracellular vesicles independently of the localisation of N-GPR56, thus this methodology was not useful to follow the fate of C-GPR56.

Taken together, data presented in this chapter indicate that GPR56 is internalised via clathrin-coated pits in HEK293 cells under ligand-free and TG2-stimulated conditions. GPR56 internalises rapidly (detected after 15 mins), but seems to recycle slowly. Moreover, neither receptor nor ligand seem to be degraded by lysosomes.

CHAPTER 7:

Generation and preliminary characterisation of stable GPR56 knockdown glioblastoma cells

7 Generation and preliminary characterisation of stable GPR56 knockdown glioblastoma cells

7.1 Introduction

Glioblastoma multiforme (GBM) is a grade IV astrocytoma and the most aggressive type of brain cancer in humans. One of the hallmarks of GBM is its invasive behaviour due to cell subpopulations within the tumours that migrate into the normal brain tissue, but rarely metastasise outside the brain. The highly invasive potential of these glioblastoma cells often leads to tumour recurrences, despite surgery and chemo- or radiation therapies. In most cases, the cells have already invaded the surrounding healthy areas of the brain at the time of surgery (Angers-Loustau et al. 2004; Demuth and Berens 2004). The process of motility is out of control in cancer cells, enabling them to migrate and invade healthy tissue (Demuth and Berens 2004). Invasion is a complex process including cell shape modifications, cell polarisation, interactions with adjacent cells and the ECM, as well as degradation of the ECM (Belkin et al. 2001). Cell invasion is a balance between cell adhesion and detachment, in which cell adhesion receptors and their ligands play important roles (Shashidhar et al. 2005).

GPR56, an adhesion GPCR, is involved in cell adhesion and migration since members of the adhesion GPCR family mainly facilitate cell-cell and cell-ECM contacts (Araç, Aust, et al. 2012). GPR56 was identified as a neural stem cell marker (Terskikh et al. 2001; Bai et al. 2009) and as a regulator of neural progenitor cell migration (Iguchi et al. 2008; Luo et al. 2011). Gliomas arise from astrocytes and their precursors, as well as from transformation of normal stem cells (Berger et al. 2004; Shashidhar et al. 2005). GPR56 mRNA and protein levels in normal adult brain are very low (Shashidhar et al. 2005). However, GPR56 protein expression is significantly up-regulated in the tested glioblastoma cell lines U87, G122 and D566, as well as in glioblastoma tumour tissue. Moreover, immunohistochemical analysis of GPR56 expression revealed that GPR56 was specifically up-regulated in astrocytic tumours, whereas other brain tumours showed low expression levels. Thus, GPR56 seems to play a role for the development of astrocytomas (Shashidhar et al. 2005). GPR56 co-localised with α-actinin in extended membrane structures and focal adhesion complexes in U87 cells, indicating a role of the receptor in cell adhesion and migration. Luciferase reporter assays performed in HEK293 cells transiently transfected with GPR56 revealed that GPR56 activated PAI-1, TCF and NF-κB responsive elements. PAI-1 and TCF are implicated in processes such as cell invasion, metastasis, adhesion and progression, thus involved in tumourigenesis (Shashidhar et al. 2005).

A good way to investigate the role of GPR56 in cancer is its down-regulation in specific cell types. So far, shRNA approaches were used to knockdown GPR56 in neural progenitor cells (NPCs) (Iguchi et al. 2008), NIH/3T3 cells (Luo et al. 2011), rostral granule cells (Koirala et al. 2009), acute myeloid leukemia (AML) cells (Saito et al. 2013) and melanoma cell lines (Yang et al. 2014; Ke et al. 2007), but not in glioblastoma cells. NPCs and AML cells failed to activate RhoA upon GPR56 knockdown, resulting in decreased cellular adhesion (Luo et al. 2011; Saito et al. 2013). A similar result was observed in the GPR56-knockdown granule cells that showed decreased adherence to fibronectin or laminin-1 (Koirala et al. 2009), confirming a role of GPR56 in cell adhesion. In addition, loss of GPR56 expression or mutations affecting GPR56 cell surface expression are associated with overmigration of neurons through a defective pial basement membrane, leading to the brain malformation observed in BFPP patients (Li et al. 2008; Luo et al. 2012; Piao et al. 2004).

7.1.1 Aims of the chapter

- To generate GPR56-silenced glioblastoma cell lines by using shRNA.

- To characterise the GPR56 knockdown cells.

7.2 Results

7.2.1 Hygromycin dose-response

The first step in order to generate GPR56-silenced U373 cells using stable transfection with shRNA targeting plasmids was to determine the effective hygromycin B concentration to kill all non-transfected cells. Parental U373 cells were seeded in hygromycin-free or in hygromycin-supplemented growth medium containing concentrations ranging from 100 to 800 µg/ml. Figure 7.1 shows that 200 µg/ml hygromycin was sufficient to kill most cells. Further improvement in the killing effectiveness at higher hygromycin doses could not be achieved, thus 200 µg/ml hygromycin was used to establish the stable shGPR56 cell lines.

Three different shRNAs, two targeting *Gpr56* at two different sites of the gene (shGPR56.2 and shGPR56.4) and a non-coding control shRNA (shRNA.NC) were used to transfect U373 cells. Following transfection, cells were cultured in the selection medium containing 200 µg/ml hygromycin and single cell clones were isolated. In case of shGPR56.2 transfected cells, eight single cells clones and one pooled population were isolated. For shGPR56.4, only one pooled population could be isolated, as well as one single clone for the non-coding shRNA.

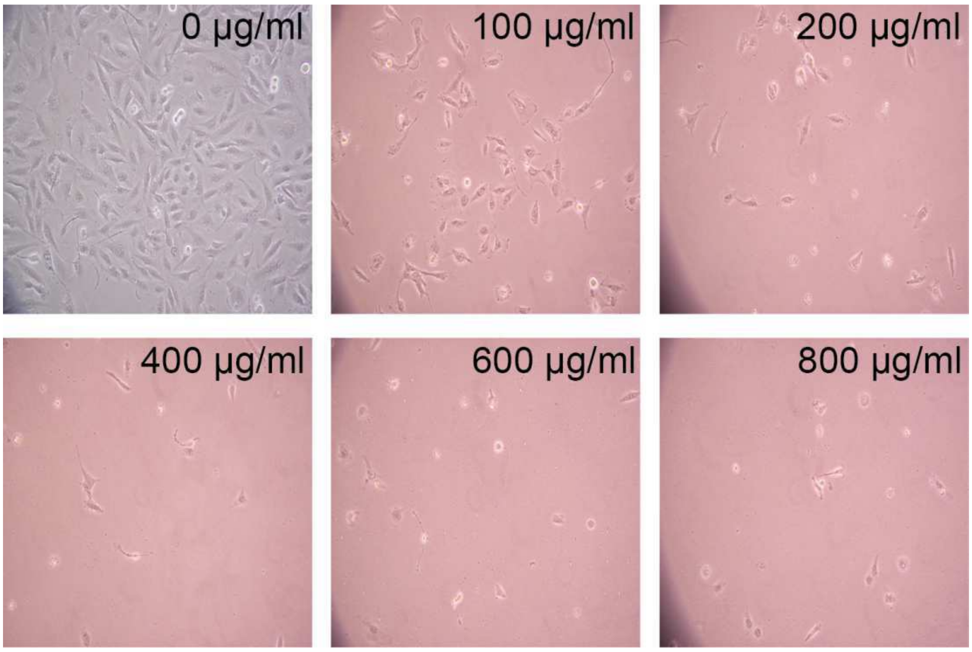

Figure 7.1 Hygromycin kill curve of U373 cells.

Non-transfected U373 cells were seeded at 10% confluence in a 6-well plate containing growth medium that was hygromycin B free or supplemented with 100-800 µg/ml hygromycin B. Medium was changed every other day and cells were cultured until cells in the hygromycin-free medium reached confluence. The effective hygromycin concentration killing all non-transfected cells was determined at 200 µg/ml hygromycin.

7.2.1.1 GPR56 expression levels and pattern

In order to characterise the GPR56 knockdown cells, total cell lysates were analysed for GPR56 expression using western blotting. Figure 7.2 shows that the overall degree of GPR56 down-regulation was not very high among the isolated cell clones transfected with shGPR56.2, as this depends on the site of integration in the cellular genome. Only one pooled population consisting of several small single colonies could be rescued for shGPR56.4 transfected cells. Although single clones were tentatively isolated, they did not survive the expansion step.

Of the nine polyclonal or clonal cell populations expressing shGPR56.2, only the single clones #3 and #4 showed a significant decrease in GPR56 expression (Fig. 7.2 A). However, the pattern of GPR56 expression in the two cell clones looked different, since clone #3 showed a prominent reduction in expression for the band likely representing full-length GPR56, whereas clone #4 mainly showed a reduction for the bands likely representing N-GPR56.

Preliminary data of a cell growth curve experiment indicated that there are no differences in cell proliferation between the parental U373 cells and several shRNA-transfected cell populations under serum-containing conditions (data not shown). However, these experiments would need to be expanded and performed in serum-free medium.

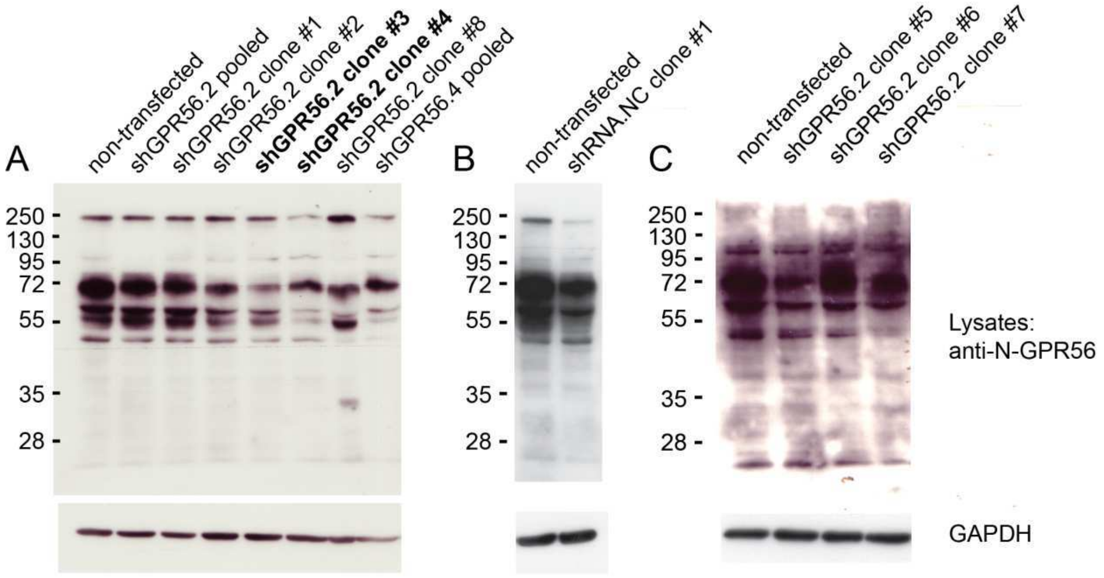
A
non-transfected
shGPR56.2 pooled
shGPR56.2 clone #1
shGPR56.2 clone #2
shGPR56.2 clone #3
shGPR56.2 clone #4
shGPR56.2 clone #8
shGPR56.4 pooled
B
non-transfected
shRNA.NC clone #1
C
non-transfected
shGPR56.2 clone #5
shGPR56.2 clone #6
shGPR56.2 clone #7
250
130
95
72
55
35
28
Lysates:
anti-N-GPR56
GAPDH

Figure 7.2 GPR56 expression in GPR56-silenced U373 cell clones.

Two shRNAs targeting *Gpr56* (shGPR56.2 and shGPR56.4) and one non-coding control shRNA (shRNA.NC) were used for stable transfection of U373 cells. Following selection of stably transfected cells in 200 µg/ml hygromycin-containing selection medium, single cell clones were isolated and grown until confluent. Total cell lysates of non-transfected U373 cells and U373 cells stably transfected with shRNA were prepared and analysed using western blotting. Cell lysates were separated in a 10% resolving gel, followed by blotting onto a PVDF-membrane and immunostaining using anti-N-GPR56 antibody (R&D Systems). GAPDH was stained as a loading control.

(A) Clone #3 and clone #4 of cells transfected with shGPR56.2 showed the best down-regulation of GPR56 expression.

(B) Non-transfected U373 cells and cell clone #1 of U373 cells transfected with shRNA.2 show high GPR56 expression levels.

(C) Non-transfected U373 cells and cell clones #5, #6 and #7 derived from U373 cells transfected with shGPR56.2, which show a low degree of GPR56 down-regulation.

In order to further evaluate cellular localisation of remaining GPR56 in the two shGPR56 clones with the highest degree of knockdown, confocal microscopy was performed using anti-N-GPR56 staining, which was compared to staining of the parental U373 cell line. Parental U373 cells were polarised, with N-GPR56 staining at the leading edge (Fig. 7.3 A). In contrast, upon GPR56 knockdown both shGPR56.2 clones investigated adopted a more round morphology and showed loss of GPR56 staining at the cell surface (Fig. 7.3 B & C). Due to a lack of a C-terminal GPR56 antibody, the localisation of this domain could not be investigated.

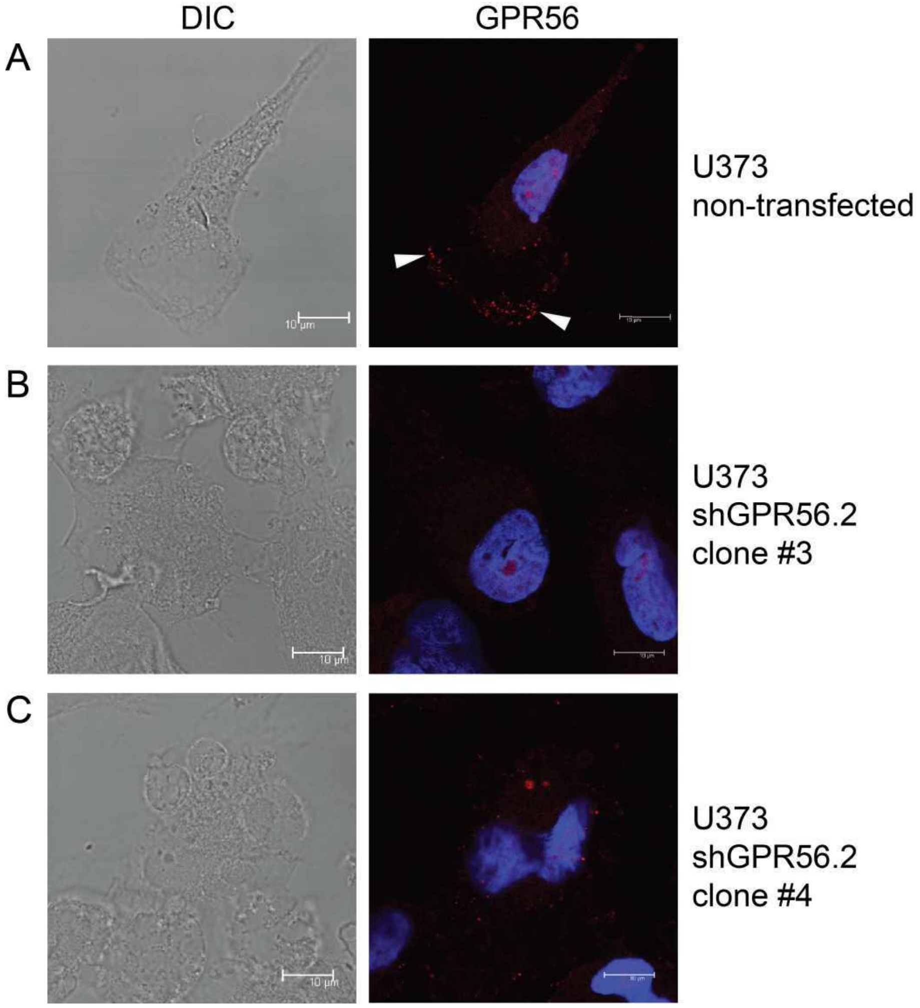

Figure 7.3 GPR56 expression in U373 non-transfected and GPR56 knockdown cells.

(A) Parental U373 cells, (B) cells of clone #3 stably transfected with shGPR56.2 and (C) cells of clone #4 stably transfected with shGPR56.2 were seeded onto poly-L-lysine coated glass coverslips and grown for 72 h. Cells were fixed and GPR56 expression detected using anti-N-GPR56 (red; R&D Systems) and secondary anti-sheep Alexa568 antibodies (Jackson ImmunoResearch).

White arrow heads, GPR56 staining.

7.3 Discussion

This is the first report demonstrating GPR56 knockdown in a glioblastoma cell line by stable transfection with shRNA. Two shRNAs targeting *Gpr56* were used to transfect U373 glioblastoma cells, followed by isolation of several stably transfected cell clones. Western Blot analysis using anti-N-GPR56 antibody showed high expression levels of GPR56 in non-transfected U373 cells (Fig. 7.2), confirming GPR56 as a biomarker for GBM (Shashidhar et al. 2005). GPR56 knockdown in the isolated cell clones was incomplete, which may indicate the importance of GPR56 expression for the survival of the glioblastoma cells. It was shown that re-expression of GPR56 in highly metastatic melanoma cells, in which GPR56 is down-regulated, leads to inhibition of tumour growth and metastasis (Xu et al. 2006). Thus, it could be the other way around in glioblastoma cells, in which GPR56 is normally highly expressed and GPR56 down-regulation may be lethal. As shown with the contradictory reports about GPR56 as a tumour suppressor or promoter, GPR56 seems to play varying roles in tumour development and progression, depending on the cancer type and stage (Xu et al. 2006; Shashidhar et al. 2005; Ke et al. 2007; Xu et al. 2010; Yang et al. 2011; Yang et al. 2014).

ShRNAs are inserted randomly into the genome and there are regions within the genomic DNA that are transcribed more efficiently than others, which may explain the differences in the degree of GPR56 down-regulation among the isolated U373 cell clones. Nonetheless, two clones of cells transfected with shGPR56.2, clone #3 and #4, showed significant down-regulation of GPR56 protein and were chosen for further analysis using confocal microscopy (Fig. 7.3). A comparison of the two clones with the parental cell line indicated that GPR56 was located at the cell front in non-transfected cells, which is in good agreement with the report from Shashidhar et al. (2005). In their study, the authors demonstrated that GPR56 was located at the leading edge of extending cell membrane structures of migrating cells, co-localising with α-actinin. I showed that GPR56 expression was missing in shGPR56.2 transfected cells, reflecting shRNA-mediated down-regulation. In addition, the cell shape of the transfected cells looked different to the shape of the parental cells, indicating loss of cell polarisation.

Cell polarisation is a very important, initial step in the process of cell migration, which can be induced by extracellular factors like chemokines, hormones, growth factors or ECM molecules (Ridley et al. 2003). GPCRs are associated with cell polarisation, since they sense these extracellular stimuli and are activated. This leads to the activation of different signalling cascades resulting in the remodelling of the actin cytoskeleton via small GTPases of the Rho family, including Cdc42, Rac and Rho (Cotton and Claing 2009). Membrane protrusions at the leading front, such as lamellipodia or filopodia, are formed by actin polymerisation, mediated by Cdc42 and Rac. Rho activity on the other hand is inhibited at the front, but present at the rear of the cell inducing the formation of contractile actin:myosin filaments. These actin:myosin bundles are crosslinked by α-actinin and anchored to focal adhesions that connect the actin cytoskeleton to the ECM (Ridley et al. 2003). The small GTPases involved in cell polarisation can be activated by several GPCRs, usually signalling via $G_{12/13}$ or G_q, but it was also shown for G_i-coupled GPCRs in some cell types (Cotton and Claing 2009). Overexpression of GPR56 in HEK293 cells, neural progenitors and NIH/3T3 fibroblasts or treatment of NIH/3T3 cells with collagen III results in activation of RhoA via $G\alpha_{12/13}$ (Iguchi et al. 2008; Luo, Jeong, et al. 2011). RhoA activation led to actin reorganisation and inhibition of migration. RhoA was reported to suppresses the activity of Rac1, thus limiting the number of membrane protrusions and inhibiting cancer cell invasion (Legg 2011; Vega et al. 2011; Simpson et al. 2004). It is possible that in glioblastoma cells the down-regulation of GPR56 affects the activities of small GTPases like RhoA, resulting in the observed changes of cell morphology. However, it is unclear as to which role GPR56 potentially plays in glioblastoma cells, in which it is overexpressed. Taking into account that GPR56 was demonstrated to activate signalling pathways involved in the regulation of cell adhesion and oncogenesis, it likely plays a role as an oncogene in these cells (Shashidhar et al. 2005). Additionally, GPR56 seems to have some tumour-promoting functions in melanoma, since only a complete knockdown of TG2 and

GPR56 ablates tumour growth, whereas GPR56-positive melanomas still grow in a TG2-depleted environment (Yang et al. 2014). However, further investigations will be necessary to confirm my preliminary data and to elucidate the functions of GPR56 in the development and progression of glioblastoma.

CHAPTER 8:

General discussion and future experiments

8 General discussion and future experiments

8.1 Summary of the results

The results presented in this thesis demonstrate for the first time that TG2 activates GPR56, which requires the presence of the N-terminal domain of GPR56. Activation of GPR56 by TG2 results in activation of ADAM17-dependent shedding of the membrane-tethered EGFR-ligand amphiregulin and involves RhoA/ROCK signalling in HEK293 cells. This signalling mechanism might be involved in glioblastoma development and progression, since GPR56 is overexpressed in glioma cells and down-regulation of GPR56 induces changes in cell morphology that might be caused by impaired Rho signalling. Moreover, GPR56-dependent internalisation of TG2 is mediated by clathrin in HEK293 cells. The fate of the receptor-ligand pair largely remains elusive, since results indicated that they are not recycled back to the cell surface within the investigated time frame and are not degraded in lysosomes.

Figure 8.1 schematically summarises the findings of this thesis.

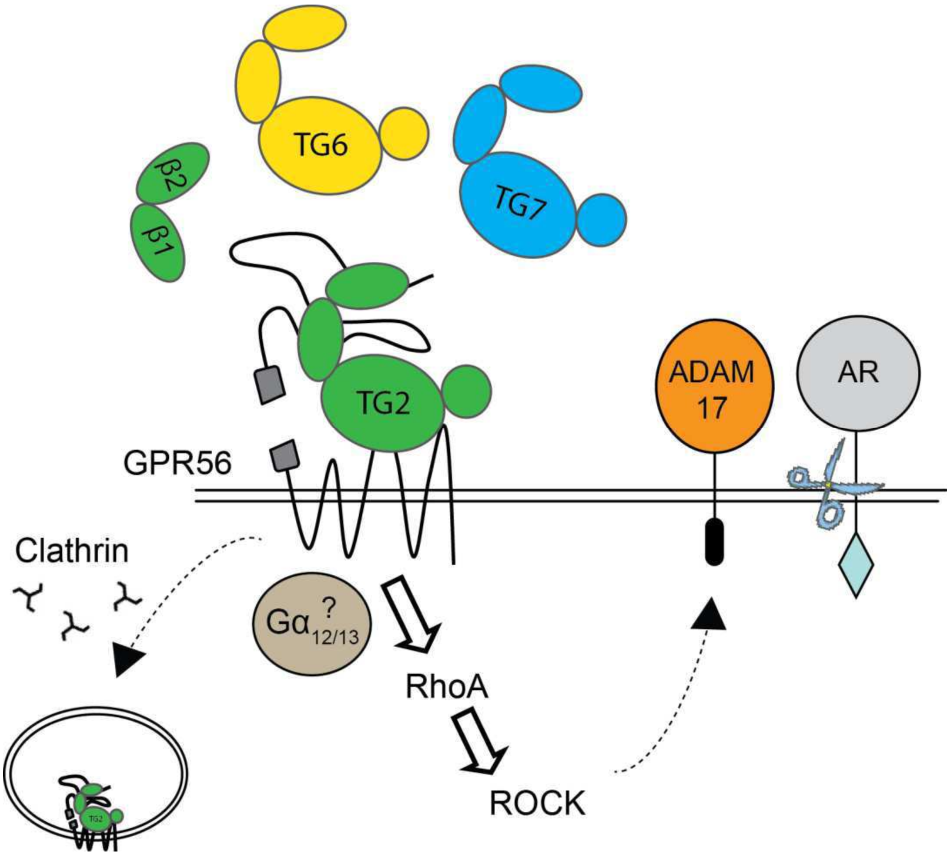
TG6
TG7
β2
β1
TG2
GPR56
ADAM 17
AR
Clathrin
Gα ? 12/13
RhoA
ROCK
TG2

Figure 8.1 Summary of the main findings of this thesis.

GPR56 is activated by TG2, the β-barrels of TG2, TG6 and TG7. Activation of GPR56 induces signalling via RhoA and ROCK, which is potentially mediated by G$\alpha_{12/13}$ and leads to shedding of amphiregulin by ADAM17.

Activation of GPR56 by TG2 furthermore induces clathrin-dependent internalisation of the GPR56-TG2 pair.

8.2 Conclusions

8.2.1 TG2 stimulates GPR56-dependent activation of ADAM17

Previous work by Edwards (2010) in the Aeschlimann laboratory had shown that keratinocytes placed on TG2-containing ECM were able to activate ADAM17, leading to EGFR ligand release into the medium. It was shown that the keratinocytes expressed GPR56 and at the same time a paper by Xu et al. (2006) described a direct interaction between TG2 and GPR56. Thus, the hypothesis was developed that TG2-dependent GPR56 signalling may represent the missing link leading to ADAM17 activation and subsequent EGFR ligand release in keratinocytes.

Thus, a sensitive, cell-based shedding assay was established in order to investigate GPR56-induced, ADAM-dependent cleavage of the membrane-tethered proform of the alkaline phosphatase-tagged EGFR ligand amphiregulin (AP-AR) in response to TG2 treatment. Inoue et al. (2012) recently showed that a similar assay, measuring GPCR activity as ectodomain shedding of AP-TGF-α, is a very useful tool to investigate signalling through $G\alpha_{12/13}$- and $G\alpha_q$-coupled receptors.

Data presented in this project demonstrate that overexpression of GPR56 in HEK293 cells activates ADAM17, leading to cleavage of AP-AR (Chapter 3). Activation of ADAMs by GPCRs leading to transactivation of the EGFR was demonstrated for G_q-, G_i- and G_{13}-coupled GPCRs (Faure et al. 1994; Gschwind et al. 2001; Gohla et al. 1998). The role of the G protein that is likely involved in GPR56-dependent ADAM17 activation will be discussed in more detail in section 8.2.3.

Activation of ADAM17 by GPR56 overexpression in the absence of ligand indicates that the receptor is auto-active. This was shown by others for GPR56, using Rho pulldown and luciferase reporter assays (Iguchi et al. 2008; Kim et al. 2010; Shashidhar et al. 2005). Inoue et al. (2012) demonstrated ADAM17 activation by several constitutively active GPCRs, inducing shedding of TGF-α. Many GPCRs exhibit some basal (constitutive) activity, which is defined by the equilibrium of inactive and active GPCR conformations in the absence of a ligand (Kobilka 2007).

The nature of the GPR56-TG2 interaction has been discussed controversially, since no GPR56-dependent cellular signalling response to TG2 treatment was demonstrated before. It remains elusive whether TG2 acts as a GPR56 ligand inducing downstream signalling. Adhesion GPCRs are supposed to play dual roles in signalling and adhesion (Yona et al. 2008; Araç, Aust, et al. 2012), therefore TG2 might form a complex with GPR56 in the ECM, mediating cell-ECM contacts.

Using the shedding assay, data presented in this thesis demonstrated for the first time GPR56-dependent signalling in response to TG2. Treatment with exogenous TG2 activates GPR56-dependent AP-AR shedding, demonstrating TG2 as a *bona fide* ligand for GPR56 (Chapter 3).

8.2.2 TG2-dependent GPR56 signalling is independent of TG2 crosslinking activity

Extracellular TG2 is localised on the cell surface and in the ECM and some of its functions require its catalytic activity. Crosslinking of ECM-components such as fibrin(ogen), collagen or fibronectin (FN) stabilises the ECM and promotes cell-ECM adhesion (Akimov et al. 2000; Belkin et al. 2005). However, extracellular TG2 is mostly inactive, but can be activated by high Ca^{2+}-levels and may be stabilised by cell surface/ECM proteins in an activate conformation. However, the exact mechanism of activation is still under investigation (Nurminskaya and Belkin 2012; Király et al. 2011; Pinkas et al. 2007). Independent of its catalytic activity, cell surface TG2 interacts with fibronectin (FN) and β1/β3/β5-integrins. Cell surface TG2 mediates the association of FN with integrins, acting as a co-receptor for FN (Akimov et al. 2000). The integrin co-receptor function of extracellular TG2 was demonstrated in normal and transformed cells and potentiates integrin-signalling, which is important for cell adhesion, migration, spreading, survival and differentiation (Belkin 2011; Zemskov et al. 2006). Since these and other functions of extracellular TG2 are independent of its enzymatic activity, it was investigated whether transglutaminase activity was required for activation of GPR56 signalling. The enzymatically inactive, inhibitor-bound Open-TG2 and the C_{277}-S TG2 mutant lacking transglutaminase activity activated GPR56 signalling to comparable levels as wild type or the oxidation-resistant C_{230}-A TG2 mutant (Chapter 4). Additionally, western blot analysis did not detect crosslinked GPR56 products when incubated with catalytically active TG2. Finally, the two β-barrel domains of TG2 also activated GPR56. The data presented in this project show activation of signalling by the β-barrels, while Xu et al. (2006) had shown that these domains were sufficient for the interaction with N-GPR56. However, activation was less pronounced, which indicates that the other domains of TG2 such as the core and the N-terminal β-sandwich domains might also be involved in GPR56 activation. This could be further investigated by testing a C-terminally truncated TG2 mutant lacking the β-barrels or by using an N-terminally truncated C-GPR56-Fc probe for pulldown experiments with TG2.

In summary, the results obtained with the shedding assay indicated that TG2 acts as an agonist for GPR56, independently of its crosslinking activity, leading to downstream signalling. This is in contrast to the tumour promoting functions of TG2 demonstrated in melanoma, which requires its crosslinking function. Experiments using a xenograft tumour model showed that only the injection of GPR56-depleted MC-1 melanoma cells overexpressing enzymatically active, wild-type TG2 into mice reduced tumour growth (Yang et al. 2014). Expression of the enzymatically inactive TG2 mutants C_{277}-S and W_{241}-A TG2 in the MC-1 cells did not affect melanoma growth. However, these experiments were performed using GPR56-independent conditions and thus cannot reflect GPR56 activation by extracellular TG2.

8.2.3 GPR56 downstream signalling

8.2.3.1 GPR56 activates RhoA signalling

The signal transduction pathways downstream of GPR56 where investigated in this project and it was shown that RhoA is involved in ADAM17-dependent shedding of AP-AR. Experiments using an inhibitor of Rho-associated protein kinase (ROCK) demonstrated for the first time that RhoA, which functions upstream of ROCK, is activated by GPR56 in response to TG2 stimulation (Chapter 3).

Interestingly, the natural splice variant $\Delta_{430\text{-}35}$-GPR56 was not activated by TG2 (Chapter 5), although this mutant was demonstrated to be more active than GPR56 and induced Rho-dependent, SRE-mediated transcription (Kim et al. 2010). However, the authors compared the activities of wild type and $\Delta_{430\text{-}35}$-GPR56 using ligand-free conditions. TG2 binding likely induces a conformational change of GPR56, similar to other GPCR ligands (Deupi and Kobilka 2007), which affects the affinity for a particular G protein, in this case likely $G\alpha_{12/13}$. Since the splice variant lacks six amino acids within ICL1, it might not be able to adjust an active confirmation upon TG2 binding like wild type receptor, thus it is not stimulated by TG2.

On the one hand, ROCK activity is associated with increased cell migration and tumour cell invasion (Bourguignon et al. 1999; Riento and Ridley 2003). GPCR-dependent signalling through $G\alpha_{12/13}$ and RhoA is associated with migratory and invasive phenotypes (Ridley 2004). RhoA activates endothelial cell invasion through regulation of MMP-9 expression and also regulates the expression of MT1-MMP in glioma cells (Meriane et al. 2006; Annabi et al. 2005). Shedding of EGF-like ligands by ADAM17 leads to activation of the EGFR, which activates downstream signalling pathways such as Ras-Raf-MAPK or PI3K signalling that induce cell proliferation, growth, survival and migration (Fischer et al. 2003). Therefore, GPR56-dependent activation of ROCK and ADAM17 could induce pro-survival and pro-migratory signalling responses, which may also be involved in tumour development and progression, since TG2 likely represents the ligand for GPR56 in the tumour microenvironment (Xu et al. 2006; Yang et al. 2011; Yang et al. 2014). These data would agree with previous findings observed by Edwards (2010), where TG2-containing ECM supported increased migration of keratinocytes due to ADAM17-dependent shedding of EGFR ligands.

On the other hand, excessive Rho activation is associated with the inhibition of cell migration (Riento and Ridley 2003). GPR56 constitutively activates RhoA in a $G\alpha_{12/13}$-dependent way (Iguchi et al. 2008; Luo et al. 2011; Shashidhar et al. 2005), which is further elevated by treatment with collagen III, the GPR56 ligand in the developing brain, leading to inhibition of neural progenitor migration (Luo et al. 2011; Iguchi et al. 2008). This signalling mechanism is likely involved in early brain development, since GPR56 mutations that affect cell surface expression such as R_{565}W-GPR56 (Chapter 3), or loss of GPR56 expression, cause the developmental brain disease bilateral frontoparietal polymicrogyria (BFPP). *Gpr56*$^{-/-}$ mice and BFPP patients develop a cobblestone-like cortex that is characterised by a defective pial basement membrane (BM), through which neurons and radial glial cells migrate, leading to the formation of neural ectopias at the cortex surface (Piao et al. 2004; Li et al. 2008; Koirala et al. 2009). Histological analysis of mouse brain slices revealed that the pial BM of *Gpr56*$^{-/-}$ mice appears normal during early embryonic development, suggesting that GPR56 is dispensable for the initial BM assembly. Around embryonic day 12.8, however, breaches in the pial BM are detected. It was suggested that the ECM polymer assembly is instable in the absence of GPR56, thus cannot sustain the tension generated by the expanding cortex. Additionally, loss of GPR56 expression might cause up-regulation of enzymes that degrade the pial BM, resulting in BM breaches through which the neural progenitors migrate, leading to the brain malformation (Li et al. 2008).

In conclusion, neurons and their precursors express GPR56 that binds collagen III in the pial BM, activating RhoA. This interaction is required to arrest neural migration, a process implicated in early brain development and cortical patterning (Fig. 8.2).

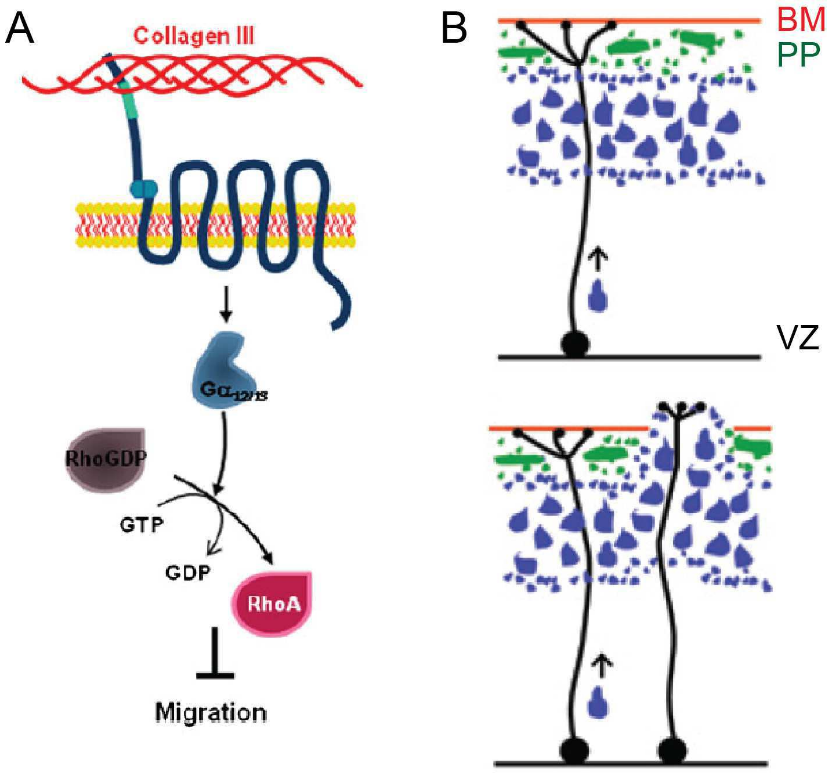

Figure 8.2 Collagen III-induced signalling through GPR56 and its role in early brain development.

A) Collagen III activates GPR56 that couples to G$\alpha_{12/13}$, inducing RhoA signalling, whcih contributes to inhibition of neural progenitor cell migration.

B) Top: in normal brain, the preplate neurons (PP, green) and the end feet of the radial glial cells (black), which extend from the ventricular zone (VZ), are in direct contact with an intact pial BM (red). Postmitotic neurons (blue) migrate along radial glial processes to their respective layer, eventually forming the six-layered cortex found in adult brain; Bottom: *Gpr56*$^{-/-}$ or *Col3a1*$^{-/-}$ brains show a cobblestone-like cortex that is characterised by a defective pial BM in combination with overmigrating neurons and radial glial cells that place their end feet beyond the breaches in the pial BM.

Taken from Singer et al. (2012) and Strokes & Piao (2010), modified.

The Rho-family GTPases Cdc42, Rac and Rho regulate the assembly and re-organisation of the actin cytoskeleton, which is involved in the regulation of cell migration (Riento and Ridley 2003). Rho is especially active at the rear of the cell body and activates its downstream effector ROCK, enhancing actin-myosin contractility and tail retraction, which promotes cell movement. Actin-myosin contractility also leads to the assembly of focal adhesions and dysregulation or excessive activity of Rho can inhibit migration due to the formation of strong focal adhesion complexes (Riento and Ridley 2003). This is likely the case in the neural progenitor cells with high GPR56 expression. Interestingly, genetic deletion of the G$\alpha_{12/13}$ genes in the CNS also result in a cobblestone-like malformation, similar to BFPP, indicating a link between GPR56 and G$\alpha_{12/13}$ in brain development (Moers et al. 2008).

8.2.3.2 GPR56-mediated ADAM17-activation is independent of G_q-signalling

In order to exclude an involvement of G_q in GPR56-dependent ADAM17-activation, experiments using inhibitors of PLC/PKC-signalling were performed (Chapter 3). GPR56 was shown to exist in a complex with the tetraspanins CD81/9 and G_q (Little et al. 2004). The activation of G_{q}-coupled AT_1R induces ADAM17-dependent HB-EGF shedding via PLC-signalling and mobilisation of Ca^{2+} (Mifune et al. 2005). Therefore, this signalling mechanism could also be involved in GPR56-dependent ADAM17 activation. The results obtained using different inhibitors targeting PLC, PKC and IP_3-receptors (Ca^{2+}-flux) require cautious evaluation. The shedding assay used to investigate GPR56 downstream signalling does not always allow a distinction between inhibition of GPR56-dependent signalling leading to ADAM17 activation, or direct inhibition of ADAM17 activity, independent of GPR56. ADAM17 has some constitutive shedding activity that is independent of GPR56, as seen with co-expression of N-GPR56. PKC phosphorylates and activates ADAM17 (Dang et al. 2011; Kveiborg et al. 2011), thus the data could measure ADAM17-activity independent of GPR56. Inhibition of PKC ablated the TG2-induced shedding response, indicating that PKC may be activated downstream of GPR56. In contrast, inhibition of PLC, which is active upstream of PKC, did not affect TG2-induced shedding. However, PLC-inhibition increased basal AP-AR shedding dramatically, an effect that was also observed to a lesser extent with the PKC-inhibitor. It was speculated that this could be explained by elevated cell surface expression levels of GPR56, but this was not confirmed by confocal analysis. However, the PLC-inhibitor has non-specific side effects leading to an increase of intracellular Ca^{2+}-levels, which might activate ADAM17 (Mifune et al. 2005). This hypothesis, however, is not supported by experiments blocking the release of intracellular Ca^{2+}, which did not affect ADAM17 activation. Additionally, luciferase reporter assays indicated that GPR56 does not couple G_q (Dr. Vera Knäuper) and Iguchi et al. (2008) demonstrated that Ca^{2+}-signalling was not activated upon treatment of GPR56-expressing cells with an agonistic anti-N-GPR56 antibody.

Together with the results presented by Shashidhar et al. (2005) and Iguchi et al. (2008), showing GPR56-dependent activation of $G\alpha_{12/13}$ and RhoA, results presented in this project point towards an involvement of $G\alpha_{12/13}$- and not G_q-signalling in GPR56-dependent activation of ADAM17. Future experiments should further address which G protein is involved, by co-expressing dominant-negative G_q and $G_{12/13}$ proteins together with GPR56 and AP-AR or specific inhibitors for G proteins could be applied. In order to identify the G proteins involved in GPCR-dependent TGF-α shedding, Inoue et al. (2012) used siRNAs targeting $G\alpha_{12/13}$, as well as chimeric G proteins. In these chimeric Gα proteins, six amino acids within the C-terminus, critical for GPCR binding, are replaced by residues from another Gα protein. For example, chimeric $G\alpha_{q/s}$ consists of a G_q backbone with a G_s C-terminus, thus binds to $G\alpha_s$-coupled GPCRs and activates $G\alpha_q$-downstream signalling. A similar approach could be used to further investigate whether $G\alpha_{12/13}$ or $G\alpha_q$ is required for GPR56-dependent shedding of AP-AR by ADAM17.

8.2.3.3 A role for β-arrestins in GPR56-dependent signalling?

An involvement of β-arrestin in GPR56-dependent activation of ADAM17, similar to a report showing that β_1AR activates an unidentified MMP (Noma and Lemaire 2007), cannot entirely be excluded. Interactions with β-arrestins were not investigated in this thesis. In future experiments, fluorescently labelled β-arrestins could be co-expressed with GPR56 and their potential interaction upon TG2 treatment analysed by confocal microscopy. Additionally, truncated β-arrestins lacking GPCR interaction sites might be co-expressed in cells and analysed using the shedding assay. Interestingly, investigations of GPR56 and TG2 internalisation showed that this mechanism was clathrin-dependent (Chapter 6). Clathrin-dependent internalisation of GPCRs is usually mediated by β-arrestins that desensitise G protein-dependent signalling and recruit components of the clathrin-endocytosis machinery (Zhang et al. 1996). Therefore, β-arrestin could well play a role in GPR56-dependent activation of ADAM17. On the other hand, GPR56 mutants lacking potential serine and threonine phosphorylation sites in the tail region that could contribute to GRK phosphorylation and subsequent β-arrestin binding, as well a C-terminal tail truncation mutant, showed TG2-dependent GPR56 activation. These results point towards G protein-dependent signalling, although it is not clear whether the particular residues or the entire C-terminal tail of GPR56 are required for β-arrestin interactions, which could be investigated using immunoprecipitation approaches.

8.2.4 Novel GPR56 ligands

In order to investigate the hypothesis that other TGs expressed in brain are able to activate GPR56, TG6 and TG7 were tested using the shedding assay for a signalling response (Chapter 4). The functions of TG6 and TG7 remain elusive, however, they are close TG2 homologues and the residues of the catalytic triad are conserved among these members of the TG family (Grenard et al. 2001) and both TG6 (Thomas et al. 2013) and TG7 (Zedira GmbH, Darmstadt) are catalytically active. TG7 is expressed ubiquitously in human and TG7 mRNA was detected in breast cancer cells (Mehta and Eckert 2005). GPR56 mRNA is also up-regulated in breast cancer (Ke et al. 2007), therefore TG7 could represent a ligand for GPR56 in these cells.

However, to date studies evaluating GPR56 and TG7 in breast cancer have not been presented.

TG6 is expressed abundantly in the CNS, where it could act as a ligand for GPR56 in neurons (Aeschlimann and Grenard 2006; Thomas et al. 2013). Although there is no proof for any physiological role of TG6, TG6 gene mutations were recently associated with autosomal dominant ataxia (Wang et al. 2010) and TG6 autoantibodies were associated with the development of gluten ataxia (GA) (Hadjivassiliou et al. 2008). GA is a neurological disorder that involves the cerebellum. GA is a manifestation of gluten sensitivity, an autoimmune disorder that was originally described in patients with coeliac disease (CD). CD is caused by the development of antibodies against TG2-deamidated peptides present in gliadin, a major component of wheat gluten protein, in combination with TG2-autoantibodies. This causes an autoimmune reaction involving specific human leucocyte antigen (HLA) alleles, resulting in damage to the small intestine. Patients with GA are usually free of the gastrointestinal symptoms observed in CD patients, including diarrhea, bloating or abdominal pain. However, GA can be treated with a gluten-free diet, similar to CD. In addition, GA patients also develop autoantibodies against TG6, which is primarily expressed in neural tissue and represents the targeted auto-antigen in the CNS. The immune-mediated damage and shrinkage of the cerebellum cause ataxia in GA patients, which is manifested by impaired muscle coordination, resulting in problems with balance, gait or vision (Hadjivassiliou et al. 2008). These results indicate an important role for TG6 in motor neurons.

GA patients are usually diagnosed at the age of 40-50. GA does not develop during embryogenesis and is caused by gluten consumption. GPR56 expression levels are known to be very low in the adult brain, thus it is unlikely that the interaction of GPR56 with TG6 is involved in the pathogenesis of GA. Nonetheless, GPR56 is expressed in neurons and their progenitors in the developing cortex and TG6 could represent a physiological ligand for GPR56 in the developing brain, as TG6 expression was recently associated with neurogenesis in mice (Thomas et al. 2013). Analysis of the phenotype of *TG6*$^{-/-}$ mice, which may show similarities to *Gpr56*$^{-/-}$ mice, could help to address this issue in the future.

8.2.5 Internalisation of GPR56

In this project, internalisation of TG2 in a GPR56-dependent way was demonstrated (Chapter 6) and information about the mechanism of endocytosis was provided. GPR56-dependent internalisation of extracellular TG2 was apparent after 15 mins and TG2 was not internalised in control cells lacking GPR56 expression. Internalisation of GPCRs is a common mechanism used by cells to dampen receptor signalling and can result in receptor recycling or degradation, but can also be the cause of biased intracellular signalling (Ferguson 2001; Lefkowitz and Shenoy 2005). GPCR endocytosis was originally observed for agonist-bound receptors, however, constitutively active receptors also internalise, as seen for GPR56 in the absence of TG2, as well as β_2AR. Constitutive internalisation rates for β_2AR were slower than for GPR56, as the number of GPR56-positive vesicles under ligand-free conditions was higher.

Co-staining of the lysosomal-associated markers LAMP1 and LAMP2 did not indicate that GPR56 or TG2 co-localise in lysosomes upon internalisation in HEK293 cells. A time frame of up to 6 h was investigated and recycling of TG2 and GPR56 was not detectable. However, the signal intensity of intracellular TG2 staining decreased over time. There are additional pathways leading to receptor/ligand degradation and it is possible that GPR56 and its ligand TG2 are targeted to the proteasome, where they are degraded as observed for δ-opoid receptors (Chaturvedi et al. 2001). It is also possible that TG2 dissociates from N-GPR56 and that only TG2 is then degraded in the proteasome. Western blot analysis of GPR56 indicated that the expression of the GPR56 dimer is reduced following stimulation with TG2 for 1 h, which potentially indicates that this is the receptor form interacting with TG2 at the cell surface, leading to its degradation. Yang et al. (2014) demonstrated GPR56-dependent internalisation of Alexa488-labelled TG2 in

MC-1 melanoma cells. Confocal and western blot analysis showed a decrease of TG2 after treating GPR56-expressing cells with TG2 for 1 h, indicating its degradation. The use of lysosomal inhibitors over a time frame of 1h blocked degradation of TG2 in GPR56-expressing cells and resulted in ECM-deposition of TG2 and N-GPR56 (Yang et al. 2014).

To further address the question of the GPR56 fate, markers of recycling endosomes, such as members of the Rab family could be stained using confocal analysis (Griffiths and Gruenberg 1991). Moreover, lysosomal and proteasomal inhibitors could be used during the experiments, in order to distinguish between the two mechanisms (Chaturvedi et al. 2001).

Internalisation of GPR56 and GPR56-dependent TG2 internalisation is mediated by clathrin-coated pits, as shown by sucrose treatments and staining for transferrin receptors and caveolae (Chapter 6). Endocytosis via clathrin is the prototypical mechanism of GPCR endocytosis (McMahon and Boucrot 2011; Doherty and McMahon 2009). Sucrose, which inhibits the association of clathrin and AP-2 adaptor protein (Hansen et al. 1993), ablates GPR56 internalisation, as shown by confocal analysis. In addition, sucrose treatments dramatically increase ADAM17-dependent shedding of AP-AR, as observed in the shedding assay. This result may indicate that GPR56-dependent activation of ADAM17 is not a result of signalling by internalised GPR56 from endocytic vesicles.

8.2.6 Controversial roles of GPR56 in cancer

GPR56 is up- or down-regulated in several human cancers and its role in tumour development and progression is controversial. Studies focussing on the role of GPR56 in melanoma progression provided information about potential interactions between GPR56 and TG2 *in vitro* and *in vivo*. GPR56 mRNA and protein are down-regulated in highly metastatic melanoma cells (Zendman et al. 1999; Xu et al. 2006). In a xenograft cancer model, overexpression of GPR56 in highly metastatic MC-1 melanoma cells inhibits tumour growth and metastasis, when cells are injected into immunodeficient mice (Xu et al. 2006). However, GPR56 expression does not alter melanoma cell progression *in vitro.* It was speculated that TG2, present in the tumour microenvironment, modulates the inhibitory function of GPR56 (Xu et al. 2006).

Tumours derived from melanoma cells transfected with GPR56 show significantly fewer blood vessels than control cells (Yang et al. 2011). However, N-terminally truncated C-GPR56 or a TG2-interaction site deletion mutant of GPR56 fail to inhibit melanoma tumour growth and angiogenesis *in vivo* and induce vascular epidermal growth factor (VEGF) production, which requires PKCα activity (Yang et al. 2011). Addition of N-GPR56-Fc to C-GPR56 expressing cells results in a significant reduction of VEGF production, thus recovering the tumour inhibiting functions of GPR56 (Fig. 8.3).

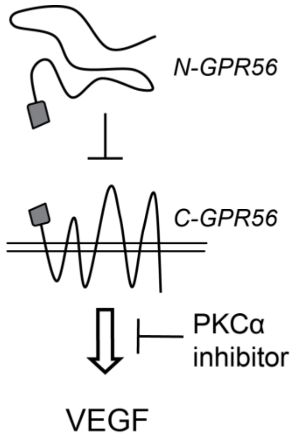

Figure 8.3 C-GPR56-dependent induction of VEGF production requires PKCα activity and is inhibited by N-GPR56. ***After Yang et al. (2011).***

These results indicated that N-GPR56 inhibits C-GPR56 and that removal of N-GPR56 constitutively activates the receptor, inducing VEGF production. It was proposed that TG2 might mediate the inhibiting effect of N-GPR56, since deletion of the TG2-binding domain inactivates N-GPR56. This is in line with results presented in this thesis, demonstrating that the entire N-terminus of

GPR56 is required for receptor activation by TG2, since N-terminal deletion mutants are not activated by TG2 (Chapter 5).

Further investigations using a xenograft tumour model revealed that TG2 promotes melanoma growth and metastasis. A complete ablation of TG2 in the recipient mice and the injected melanoma cells reduces tumour weight and the number of lung metastasis. The data demonstrate that extracellular TG2, present in tumour stroma, promotes melanoma metastasis (Yang et al. 2014). Overexpression of GPR56 in the injected melanoma cells inhibits tumour growth. GPR56 antagonises the tumour promoting effects of TG2 by internalisation, likely leading to its degradation. However, GPR56 itself has some tumour promoting functions independent of TG2 and a combined knockdown of GPR56 and TG2 entirely ablates tumour growth (Fig. 8.4) (Yang et al. 2014).

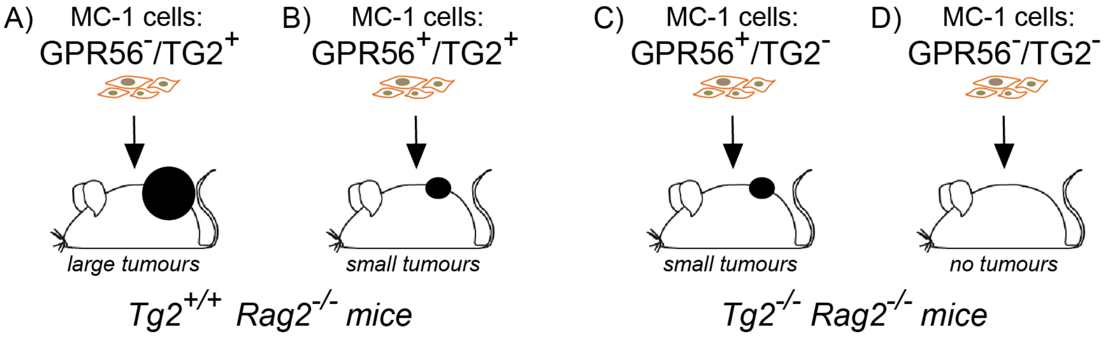

Figure 8.4 Summary of mouse experiments performed by Yang et al. (2014), investigating the role of GPR56 and TG2 in melanoma tumour growth.

A) Melanoma cells, ablated in GPR56 expression and endogenously expressing TG2, grow large melanoma tumours in TG2-positive, immunodeficient mice;

B) Melanoma cells, overexpressing GPR56 and endogenous levels of TG2, grow only small tumours in TG2-positive mice. The results indicate that GPR56 antagonises the tumour promoting effects of TG2.

C) Melanoma cells, overexpressing GPR56 and ablated in TG2 expression, grow small melanoma tumours in TG2-knockout, immunodeficient mice;

D) Melanoma cells, ablated in both GPR56 and TG2 expression, do not grow tumours in TG2-knockout mice, indicating that GPR56 itself has some tumour promoting functions.

Mouse illustrations taken from Kühn & Wurst (2009), modified.

It must be noted that MC-1 cells were transfected with empty vector as a control for GPR56 overexpression in the study by Yang et al. (2014). Overexpression of GPR56 results in reduced tumour growth, which might also be induced by cellular stress, independently of GPR56 function. Therefore, expression of an inactive GPR56 mutant, for example a BFPP-mutant with impaired membrane trafficking ability, would represent a better control than empty vector transfections in order to show that the reduction in tumour growth is induced by cell-surface GPR56 and not caused by a cellular stress reaction such as apoptosis.

Moreover, a critical control experiment, in which TG2-depleted MC-1 cells overexpressing GPR56 are injected into TG2-expressing mice, was not performed in their study (Yang et al. 2014). This experiment would yield results for many cancer cells, where GPR56 is overexpressed and might interact with extracellular TG2 in the microenvironment. This experiment would also reproduce the *in vitro* experiments described in this thesis.

Analysis of endogenous cancer progression in *Gpr56*$^{-/-}$ mice using a transgenic cancer model indicated that GPR56 has no effect on endogenous melanoma progression (Xu et al. 2010). Thus, GPR56 might have different effects on tumour progression in xenograft models compared to endogenous tumour progression or the results might be explained by different genetic backgrounds of the mice used.

Data presented in this project rather point to a tumour promoting function of GPR56, since the activation of ADAMs and the shedding of EGF-like ligands is connected to the activation of EGFR signalling, promoting cell survival and tumour progression. However, it is not clear whether GPR56 signals via this mechanism in tumour cells, as this was only investigated in HEK293 cells and downstream signalling caused by GPR56 activation could potentially vary between different cell populations.

GPR56 mRNA levels are up-regulated in esophageal squamous cell carcinoma and many other cancers, such as breast, ovarian, colon, lung and brain, suggesting a general role in cell transformation and tumorigenesis

(Sud et al. 2006; Ke et al. 2007). In addition, GPR56 protein is highly expressed in glioblastoma (Shashidhar et al. 2005), which was confirmed by analysis of U373 glioblastoma cells (Chapter 7). This is the first report demonstrating knockdown of GPR56 in glioblastoma cells using stable shRNA transfection. GPR56 knockdown was incomplete in U373 cells, which may be explained by a lethal effect of GPR56 depletion in these cells. Nonetheless, confocal analysis of GPR56 expression in parental U373 cells and two cell clones that showed the highest GPR56 knockdown, indicate changes in the cell morphology upon GPR56 down-regulation. GPR56 was expressed at the migrating front of normal U373 cells, confirming results of U87 glioblastoma cells, in which GPR56 is localised at the leading edge of membrane protrusions, where it co-localises with α-actinin (Shashidhar et al. 2005). In GPR56-silenced U373 cells, however, GPR56 is absent at the cell surface and in addition, the cells acquire a different shape, indicating loss of cell polarity. Induction of cell polarity is important for cell motility and involves the activities of the small GTPases Cdc42, Rac and Rho (Cotton and Claing 2009). The effect of Rho and ROCK activation in glioblastoma is controversial. Several studies have shown that activation of this pathway inhibits glioblastoma migration and that inhibition of Rho and ROCK increases cell motility (Tabu et al. 2007; Salhia et al. 2005). Another study, however, showed that inhibition of ROCK suppresses glioblatoma cell migration. ROCK inhibition also affected glioblastoma proliferation and a link to ERK signalling was established (Zohrabian et al. 2009). The different results may be explained by different inhibitors or varying inhibitor concentrations applied, as well as genetic alterations between the glioblastoma cell lines used. GPR56 is up-regulated in glioblastoma cells, therefore it is possible that GPR56-dependent activation of RhoA contributes to the invasive behaviour of glioblastoma cells, as observed for other cell systems (Iguchi et al. 2008; Luo et al. 2011). Further experiments are required to address these questions. Firstly, experiments such as detailed analysis of cytoskeletal rearrangements in GPR56-silenced U373 cells compared to parental cells using cytoskeletal markers and confocal microscopy might be considered. Cell growth curves and Rho pulldown assays should be performed. In addition, the effect of extracellular TG2 on glioblastoma proliferation and migration should be addressed, since TG2 might represent the ligand for GPR56 in the glioma microenvironment. TG2 activity is increased in glioblastomas compared to normal brain tissue and increased amounts of fibronectin co-localise with TG2 in the ECM. Glioblastoma cells secrete high levels of TG2 and application of a TG2 inhibitor blocks the remodelling of fibronectin in the ECM of glioblastomas, increasing apoptosis and sensitising the tumours to chemotherapy (Yuan et al. 2007; Alderton 2006). In order to investigate a link between GPR56-TG2 interaction and cell migration, scratch wound assays could be performed, in which a scratch within a monolayer of glioblastoma cells is performed and the ability of the cells to close the wound is monitored using time lapse microscopy. These experiments can include the addition of TG2 to the medium. Migration experiments according to the protocol by Edwards (2010), in which glioblastoma spheroids are placed on a TG2-containing or TG2-depleted matrix and migration of cells from the spheroids observed over time, also represent an interesting approach to investigate a link between the TG2-GPR56 interaction and cell migration.

8.3 Future outlook

In order to further advance the understanding of signalling mechanisms mediated by GPR56, future experiments should focus on the mediator proteins involved in GPR56-depenent downstream signalling, such as G proteins or β-arrestins. Moreover, the potential link between the GPR56 signalling response to TG2, as observed in HEK293 cells, and glioblastoma cell migration and proliferation should be investigated in detail in order to gain additional information about the role of GPR56 in glioblastoma.

To achieve this, the GPR56-depleted glioblastoma cells generated in this project should be further characterised regarding potential changes in their morphology and in respect of their ability to proliferate and migrate in comparison to control glioblastoma cells expressing high levels of GPR56. If knockdown of GPR56 had a tumour suppressing function in the glioblastoma cells, such as reduced tumour cell growth and migration, GPR56 could represent an attractive drug target. Generally, targeting GPR56 in adult patients should be feasible, as there are no known post-developmental defects resulting from the GPR56 loss-of-function mutations in humans (Ke et al. 2007). This is in contrast to the developmental brain malformation BFPP, which is caused by GPR56 loss-of-function mutations during embryonic development (Piao et al. 2004). In adult human brain, however, GPR56 might not play a crucial role, since GPR56 expression levels are low, which is in contrast to the high expression levels in glioblastoma (Shashidhar et al. 2005). Therefore, GPR56 might represent an interesting candidate for therapeutic intervention in the context of GBM. Nonetheless, further intensive investigations would be necessary to exclude potential risks caused by silencing GPR56 and interfering with its downstream signalling pathways. One important point is the ability of aGPCRs to form heterodimers, as shown for latrophilin-1 and GPR56 (Silva et al. 2009). The ability to form such heterodimers is based on the GPS cleavage of aGPCRs that produces two fragments, the N- and the C-terminus, which are able to act independently in the cell membrane (Volynski et al. 2004). The hybrid receptors described by Silva et al. (2009) consist of a C-terminus from one aGPCR and an N-terminus of another aGPCR. This was shown for N-EMR4 with C-EMR2 (Huang et al. 2012), as well as N-EMR2 with C-latrophilin-1 (Silva et al. 2009). In the same study, N-latrophilin-1 was shown to co-immunoprecipitate with C-GPR56 (Silva et al. 2009). The “split personality receptor model” implicates that ligand binding to one aGPCR N-terminus could induce signalling via the C-terminus of another aGPCR, generating a very complicated signalling network (Silva et al. 2009). Thus, it is possible that signals sensed by latrophilin-1 may induce GPR56-mediated signalling. Latrophilin-1 was associated with a function in the CNS in the light of neurotransmitter release (Davletov et al. 1998). Therefore, the hybrid receptor consisting of N-latrophilin-1 and C-GPR56 might play an important role in the adult human body, which could cause problems when silencing

GPR56 in the context of an anti-glioblastoma therapy. In order to further investigate potential heterodimer formation between GPR56 and other aGPCRs such as latrophilin-1, the bioluminescence resonance energy transfer (BRET) technology could be used, which allows a direct examination of GPCR dimerisation. The BRET technology is based on biosensors including the bioluminescent donor Renilla luciferase (luc) and a variant of green fluorescent protein (GFP) as the fluorescent acceptor (Angers et al. 2000). In order to detect receptor heterodimerisation, it would be feasible to generate GPR56-luc and latrohilin-1-GFP constructs (or any other aGPCR) and investigate their association at the cell surface by measuring BRET signals. These experiments would indicate whether there are any relevant, complex interactions between GPR56 and other aGPCRs that need to be considered when thinking about targeting and silencing GPR56 in regards of anti-cancer therapies.

References

Abdalla, S., Lother, H., Langer, A., Faramawy, Y. and Quitterer, U. 2004. AT 1 Receptor Dimers of Monocytes at the Onset of Atherosclerosis. *Cell* 119, pp. 343–354.

Achyuthans, K.E. and Greenberg, C.S. 1987. Identification of a Guanosine Triphosphate-binding Site on Guinea Pig Liver Transglutaminase. *J. Biol. Chem.* 262(4), pp. 1901–1906.

Adamczyk, M. 2013. Biomarkers for arthritis : Regulation of extracellular transglutaminase activity by non-conventional export. Cardiff University.

Aeschlimann, D. and Grenard, P. 2006. Transglutaminase gene products. *US Patent 7,052,890*.

Aeschlimann, D. and Paulsson, M. 1994. Transglutaminases: protein cross-linking enzymes in tissues and body fluids. *Thromb. Haemost.* 71(4), pp. 402–15.

Aeschlimann, D. and Thomazy, V. 2000. Protein crosslinking in assembly and remodelling of extracellular matrices: the role of transglutaminases. *Connect. Tissue Res.* 41(1), pp. 1–27.

Ai, L., Kim, W.-J., Demircan, B., Dyer, L.M., Bray, K.J., Skehan, R.R., Massoll, N.A. and Brown, K.D. 2008. The transglutaminase 2 gene (TGM2), a potential molecular marker for chemotherapeutic drug sensitivity, is epigenetically silenced in breast cancer. *Carcinogenesis* 29(3), pp. 510–8.

Akimov, S.S. and Belkin, A.M. 2001. Cell-surface transglutaminase promotes fibronectin assembly via interaction with the gelatin-binding domain of fibronectin: a role in TGFbeta-dependent matrix deposition. *J. Cell Sci.* 114(Pt 16), pp. 2989–3000.

Akimov, S.S., Krylov, D., Fleischman, L.F. and Belkin, a M. 2000. Tissue transglutaminase is an integrin-binding adhesion coreceptor for fibronectin. *J. Cell Biol.* 148(4), pp. 825–38.

Alderton, G. 2006. Tumour microenvironment: Remodelling resistance. *Nat. Rev. Cancer* 7(1), pp. 7–7.

Altenbach, C., Klein-Seetharaman, J., Cai, K., Khorana, H.G. and Hubbell, W.L. 2001. Structure and function in rhodopsin: mapping light-dependent changes in distance between residue 316 in helix 8 and residues in the sequence 60-75, covering the cytoplasmic end of helices TM1 and TM2 and their connection loop CL1. *Biochemistry* 40(51), pp. 15493–500.

Angers, S., Salahpour, A., Joly, E., Hilairet, S., Chelsky, D., Dennis, M. and Bouvier, M. 2000. Detection of beta 2-adrenergic receptor dimerization in living cells using bioluminescence resonance energy transfer (BRET). *Proceedings of the National Academy of Sciences of the United States of America* 97(7), pp. 3684–9.

Angers-Loustau, A., Hering, R., Werbowetski, T.E., Kaplan, D.R. and Maestro, R.F. Del 2004. Src Regulates Actin Dynamics and Invasion of Malignant Glial Cells in Three Dimensions. *Mol. Cancer Res.* 2(11), pp. 595–605.

Annabi, B., Bouzeghrane, M., Moumdjian, R., Moghrabi, A. and Béliveau, R. 2005. Probing the infiltrating character of brain tumors: inhibition of RhoA/ROK-mediated CD44 cell surface shedding from glioma cells by the green tea catechin EGCg. *J. Neurochem.* 94(4), pp. 906–16.

Araç, D., Aust, G., Calebiro, D., Engel, F., Formstone, C., Goffinet, A., Hamann, J., Kittel, R., Liebscher, I., Lin, H.-H., Monk, K., Petrenko, A., Piao, X., Prömel, S., Schiöth, H., Schwartz, T., Stacey, M., Ushkaryov, Y., Wobus, M., Wolfrum, U., Xu, L. and Langenhan, T. 2012. Dissecting signaling and functions of adhesion G protein-coupled receptors. *Ann. N. Y. Acad. Sci.* 1276, pp. 1–25.

Araç, D., Boucard, A., Bolliger, M., Nguyen, J., Soltis, S., Südhof, T. and Brunger, A. 2012. A novel evolutionarily conserved domain of cell-adhesion GPCRs mediates autoproteolysis. *EMBO J.* 31(6), pp. 1364–78.

Arcos-Burgos, M., Jain, M., Acosta, M.T., Shively, S., Stanescu, H., Wallis, D., Domené, S., Vélez, J.I., Karkera, J.D., Balog, J., Berg, K., Kleta, R., Gahl, W.A., Roessler, E., Long, R., Lie, J., Pineda, D., Londoño, A.C., Palacio, J.D., Arbelaez, A., Lopera, F., Elia, J., Hakonarson, H., Johansson, S., Knappskog, P.M., Haavik, J., Ribases, M., Cormand, B., Bayes, M., Casas, M., Ramos-Quiroga, J.A., Hervas, A., Maher, B.S., Faraone, S. V, Seitz, C., Freitag, C.M., Palmason, H., Meyer, J., Romanos, M., Walitza, S., Hemminger, U., Warnke, A., Romanos, J., Renner, T., Jacob, C., Lesch, K.-P., Swanson, J., Vortmeyer, A., Bailey-Wilson, J.E., Castellanos, F.X. and Muenke, M. 2010. A common variant of the latrophilin 3 gene, LPHN3, confers susceptibility to ADHD and predicts effectiveness of stimulant medication. *Molecular psychiatry* 15(11), pp. 1053–66.

Attramadal, H., Arriza, J., Aoki, C., Dawson, T., Codina, J., Kwatra, M., Snyder, S., Caron, M. and Lefkowitz, R. 1992. Beta-arrestin2, a novel member of the arrestin/beta-arrestin gene family. *J. Biol. Chem.* 267(25), pp. 17882–17890.

Bachoo, R.M., Maher, E.A., Ligon, K.L., Sharpless, N.E., Chan, S.S., You, M.J., Tang, Y., DeFrances, J., Stover, E., Weissleder, R., Rowitch, D.H., Louis, D.N. and DePinho, R.A. 2002. Epidermal growth factor receptor and Ink4a/Arf: convergent mechanisms governing terminal differentiation and transformation along the neural stem cell to astrocyte axis. *Cancer cell* 1(3), pp. 269–77.

Bahi-Buisson, N., Poirier, K., Boddaert, N., Fallet-Bianco, C., Specchio, N., Bertini, E., Caglayan, O., Lascelles, K., Elie, C., Rambaud, J., Baulac, M., An, I., Dias, P., des Portes, V., Moutard, M.L., Soufflet, C., El Maleh, M., Beldjord, C., Villard, L. and Chelly, J. 2010. GPR56-related bilateral frontoparietal polymicrogyria: further evidence for an overlap with the cobblestone complex. *Brain* 133(11), pp. 3194–209.

Bai, Y., Du, L., Shen, L., Zhang, Y. and Zhang, L. 2009. GPR56 is highly expressed in neural stem cells but downregulated during differentiation. *Neuroreport* 20(10), pp. 918–922.

Ballesteros, J.A. and Weinstein, H. 1995. Integrated methods for the construction of three dimensional models and computational probing of structure-function relations in G-protein coupled receptors. *Methods Neurosci.* 25, pp. 366–428.

Barak, L.S., Tiberi, M., Freedman, N.J., Kwatra, M.M., Lefkowitz, R.J. and Caron, M.G. 1994. A highly conserved tyrosine residue in G protein-coupled receptors is required for agonist-mediated beta 2-adrenergic receptor sequestration. *J. Biol. Chem.* 269(4), pp. 2790–5.

Barnes, R.N., Bungay, P.J., Elliott, B.M., Walton, P.L. and Griffin, M. 1985. Alterations in the distribution and activity of transglutaminase during tumour growth and metastasis. *Carcinogenesis* 6(3), pp. 459–63.

Barnes, W.G., Reiter, E., Violin, J.D., Ren, X.-R., Milligan, G. and Lefkowitz, R.J. 2005. beta-Arrestin 1 and Galphaq/11 coordinately activate RhoA and stress fiber formation following receptor stimulation. *J. Biol. Chem.* 280(9), pp. 8041–50.

Barsigian, C., Fellin, F.M., Jain, A. and Martinez, J. 1988. Dissociation of fibrinogen and fibronectin binding from transglutaminase-mediated cross-linking at the hepatocyte surface. *J. Biol. Chem.* 263(28), pp. 14015–22.

Barsigian, C., Stern, A.M. and Martinez, J. 1991. Tissue (type II) transglutaminase covalently incorporates itself, fibrinogen, or fibronectin into high molecular weight complexes on the extracellular surface of isolated hepatocytes. Use of 2-[(2-oxopropyl)thio] imidazolium derivatives as cellular transg. *J. Biol. Chem.* 266(33), pp. 22501–9.

Belkin, a M., Akimov, S.S., Zaritskaya, L.S., Ratnikov, B.I., Deryugina, E.I. and Strongin, a Y. 2001. Matrix-dependent proteolysis of surface transglutaminase by membrane-type metalloproteinase regulates cancer cell adhesion and locomotion. *J. Biol. Chem.* 276(21), pp. 18415–22.

Belkin, A.M. 2011. Extracellular TG2: emerging functions and regulation. *FEBS J.* 278(24), pp. 4704–16.

Belkin, A.M., Tsurupa, G., Zemskov, E., Veklich, Y., Weisel, J.W. and Medved, L. 2005. Transglutaminase-mediated oligomerization of the fibrin(ogen) alphaC domains promotes integrin-dependent cell adhesion and signaling. *Blood* 105(9), pp. 3561–8.

Belkin, A.M., Zemskov, E.A., Hang, J., Akimov, S.S., Sikora, S. and Strongin, A.Y. 2004. Cell-surface-associated tissue transglutaminase is a target of MMP-2 proteolysis. *Biochemistry* 43(37), pp. 11760–9.

Bell, H.L. and Gööz, M. 2010. ADAM-17 is activated by the mitogenic protein kinase ERK in a model of kidney fibrosis. *Am. J. Med. Sci.* 339(2), pp. 105–7.

Berger, F., Gay, E., Pelletier, L., Tropel, P. and Wion, D. 2004. Development of gliomas: potential role of asymmetrical cell division of neural stem cells. *Lancet Oncol.* 5(8), pp. 511–4.

Bhatnagar, a, Willins, D.L., Gray, J. a, Woods, J., Benovic, J.L. and Roth, B.L. 2001. The dynamin-dependent, arrestin-independent internalization of 5-hydroxytryptamine 2A (5-HT2A) serotonin receptors reveals differential sorting of arrestins and 5-HT2A receptors during endocytosis. *J. Biol. Chem.* 276(11), pp. 8269–77.

Birckbichler, P., Bonner, R. and Hurst, R. 2000. Loss of tissue transglutaminase as a biomarker for prostate adenocarcinoma. *Cancer* 89(2), pp. 412–423.

Bjarnadóttir, T.K., Fredriksson, R., Höglund, P.J., Gloriam, D.E., Lagerström, M.C. and Schiöth, H.B. 2004. The human and mouse repertoire of the adhesion family of G-protein-coupled receptors. *Genomics* 84(1), pp. 23–33.

Black, R.A., Rauch, C.T., Kozlosky, C.J., Peschon, J.J., Slack, J.L., Wolfson, M.F., Castner, B.J., Stocking, K.L., Reddy, P., Srinivasan, S., Nelson, N., Boiani, N., Schooley, K.A., Gerhart, M., Davis, R., Fitzner, J.N., Johnson, R.S., Paxton, R.J., March, C.J. and Cerretti, D.P. 1997. A metalloproteinase disintegrin that releases tumour-necrosis factor-alpha from cells. *Nature* 385(6618), pp. 729–33.

Black, R.A. and White, J.M. 1998. ADAMs: focus on the protease domain. *Curr. Opin. Cell Biol.* 10(5), pp. 654–9.

Bleasdale, J.E. and Fisher, S.K. 1993. Use of U-73122 as an Inhibitor of Phospholipase C-Dependent Processes. *Neuroprotocols* 3(2), pp. 125–133.

Blobel, C.P. 2005. ADAMs: key components in EGFR signalling and development. *Nat. Rev. Mol. Cell Biol.* 6(1), pp. 32–43.

Blobel, C.P., Wolfsberg, T.G., Turck, C.W., Myles, D.G., Primakoff, P. and White, J.M. 1992. A potential fusion peptide and an integrin ligand domain in a protein active in sperm-egg fusion. *Nature* 356(6366), pp. 248–52.

Bootman, M., Rietdorf, K., Hardy, H. and Dautova, Y. 2001. Calcium signalling and regulation of cell function. *eLS*, pp. 1–7.

Bourguignon, L.Y., Zhu, H., Shao, L., Zhu, D. and Chen, Y.W. 1999. Rho-kinase (ROK) promotes CD44v(3,8-10)-ankyrin interaction and tumor cell migration in metastatic breast cancer cells. *Cell Motil. Cytoskeleton* 43(4), pp. 269–87.

Buchanan, F.G., Wang, D., Bargiacchi, F. and DuBois, R.N. 2003. Prostaglandin E2 regulates cell migration via the intracellular activation of the epidermal growth factor receptor. *J. Biol. Chem.* 278(37), pp. 35451–7.

Buxbaum, J.D., Liu, K.N., Luo, Y., Slack, J.L., Stocking, K.L., Peschon, J.J., Johnson, R.S., Castner, B.J., Cerretti, D.P. and Black, R.A. 1998. Evidence that tumor necrosis factor alpha converting enzyme is involved in regulated alpha-secretase cleavage of the Alzheimer amyloid protein precursor. *J. Biol. Chem.* 273(43), pp. 27765–7.

De Camilli, P., Takei, K. and McPherson, P.S. 1995. The function of dynamin in endocytosis. *Curr. Opin. Neurobiol.* 5(5), pp. 559–65.

Cao, L., Petrusca, D.N., Satpathy, M., Nakshatri, H., Petrache, I. and Matei, D. 2008. Tissue transglutaminase protects epithelial ovarian cancer cells from cisplatin-induced apoptosis by promoting cell survival signaling. *Carcinogenesis* 29(10), pp. 1893–900.

Carson-Walter, E.B., Watkins, D.N., Nanda, A., Vogelstein, B., Kinzler, K.W. and St Croix, B. 2001. Cell surface tumor endothelial markers are conserved in mice and humans. *Cancer research* 61(18), pp. 6649–55.

Cen, B., Yu, Q., Guo, J., Wu, Y., Ling, K., Cheng, Z., Ma, L. and Pei, G. 2001. Direct binding of beta-arrestins to two distinct intracellular domains of the delta opioid receptor. *J. Neurochem.* 76(6), pp. 1887–94.

Chaturvedi, K., Bandari, P., Chinen, N. and Howells, R.D. 2001. Proteasome involvement in agonist-induced down-regulation of mu and delta opioid receptors. *J. Biol. Chem.* 276(15), pp. 12345–55.

Chen, G., Gharib, T.G., Huang, C.-C., Thomas, D.G., Shedden, K.A., Taylor, J.M.G., Kardia, S.L.R., Misek, D.E., Giordano, T.J., Iannettoni, M.D., Orringer, M.B., Hanash, S.M. and Beer, D.G. 2002. Proteomic analysis of lung adenocarcinoma: identification of a highly expressed set of proteins in tumors. *Clin. Cancer Res.* 8(7), pp. 2298–305.

Chen, G., Yang, L., Begum, S. and Xu, L. 2010. GPR56 is essential for testis development and male fertility in mice. *Developmental Dynamics* 239(12), pp. 3358–67.

Chen, S., Lin, F., Iismaa, S., Lee, K.N., Birckbichler, P.J. and Graham, R.M. 1996. Alpha1-adrenergic receptor signaling via Gh is subtype specific and independent of its transglutaminase activity. *J. Biol. Chem.* 271(50), pp. 32385–91.

Cheng, Z.-J. 2000. beta -Arrestin Differentially Regulates the Chemokine Receptor CXCR4-mediated Signaling and Receptor Internalization, and This Implicates Multiple Interaction Sites between beta -Arrestin and CXCR4. *J. Biol. Chem.* 275(4), pp. 2479–2485.

Chhabra, A., Verma, A. and Mehta, K. 2009. Tissue transglutaminase promotes or suppresses tumors depending on cell context. *Anticancer research* 29(6), pp. 1909–19.

Chiang, N.-Y., Hsiao, C.-C., Huang, Y.-S., Chen, H.-Y., Hsieh, I.-J., Chang, G.-W. and Lin, H.-H. 2011. Disease-associated GPR56 mutations cause bilateral frontoparietal polymicrogyria via multiple mechanisms. *J. Biol. Chem.* 286(16), pp. 14215–25.

Chiariello, M., Vaqué, J.P., Crespo, P. and Gutkind, J.S. 2010. Activation of Ras and Rho GTPases and MAP kinases by G-protein-coupled receptors. *Methods Mol. Biol.* 661, pp. 137–150.

Della Chiesa, M., Falco, M., Parlonini, S., Bellora, F., Petretto, A., Romeo, E., Balsamo, M., Gambrotti, M., Scordamaglia, F., Tabellini, G., Facchetti, F., Vermi, W., Bottino, C., Moretta, A. and Vitale, M. 2010. GPR56 as a novel marker identifying the CD56dull CD16+ NK cell subset both in blood stream and in inflamed peripheral tissues. *International Immunology* 22(2), pp. 91–100.

Chikumi, H., Vázquez-Prado, J., Servitja, J.-M., Miyazaki, H. and Gutkind, J.S. 2002. Potent activation of RhoA by Galpha q and Gq-coupled receptors. *J. Biol. Chem.* 277(30), pp. 27130–4.

Chini, B. and Parenti, M. 2004. G-protein coupled receptors in lipid rafts and caveolae: how, when and why do they go there? *J. Mol. Endocrinol.* 32(2), pp. 325–38.

Cho, S., Lee, J., Bae, H. and Jeong, E. 2010. Transglutaminase 2 inhibits apoptosis induced by calciumoverload through down-regulation of Bax. *Exp. Mol. Med.* 42(9), pp. 639–650.

Cohen, A.W., Razani, B., Wang, X.B., Combs, T.P., Williams, T.M., Scherer, P.E. and Lisanti, M.P. 2003. Caveolin-1-deficient mice show insulin resistance and defective insulin receptor protein expression in adipose tissue. *Am. J. Physiol. Cell Physiol.* 285(1), pp. C222–35.

Collawn, J., Stangel, M., Kuhn, L. and Esekogwu, V. 1990. Transferrin receptor internalization sequence YXRF implicates a tight turn as the structural recognition motif for endocytosis. *Cell* 63, pp. 1061–1072.

Collighan, R.J. and Griffin, M. 2009. Transglutaminase 2 cross-linking of matrix proteins: biological significance and medical applications. *Amino acids* 36(4), pp. 659–70.

Cotton, M. and Claing, A. 2009. G protein-coupled receptors stimulation and the control of cell migration. *Cell. Signal.* 21(7), pp. 1045–53.

Craft, C.M., Whitmore, D.H. and Wiechmann, A.F. 1994. Cone arrestin identified by targeting expression of a functional family. *J. Biol. Chem.* 269(6), pp. 4613–9.

D’Eletto, M., Farrace, M., Rossin, F., Strappazzon, F., Di Giacomo, G., Cecconi, F., Melino, G., Sepe, S., Moreno, S., Fimia, G., Falasca, L., Nardacci, R. and Piacentini, M. 2012. Type 2 transglutaminase is involved in the autophagy-dependent clearance of ubiquitinated proteins. *Cell Death Differ.* 19, pp. 1228–1238.

Daaka, Y., Luttrell, L.M. and Lefkowitz, R.J. 1997. Switching of the coupling of the beta2-adrenergic receptor to different G proteins by protein kinase A. *Nature* 390(6655), pp. 88–91.

Dang, M., Dubbin, K., D’Aiello, A., Hartmann, M., Lodish, H. and Herrlich, A. 2011. Epidermal growth factor (EGF) ligand release by substrate-specific a disintegrin and metalloproteases (ADAMs) involves different protein kinase C (PKC) isoenzymes depending on the stimulus. *J. Biol. Chem.* 286(20), pp. 17704–13.

Datta, S., Antonyak, M.A. and Cerione, R.A. 2007. GTP-binding-defective forms of tissue transglutaminase trigger cell death. *Biochemistry* 46(51), pp. 14819–29.

Daub, H., Wallasch, C., Lankenau, A., Herrlich, A. and Ullrich, A. 1997. Signal characteristics of G protein-transactivated EGF receptor. *EMBO J.* 16(23), pp. 7032–44.

Daub, H., Weiss, F.U., Wallasch, C. and Ullrich, A. 1996. Role of transactivation of the EGF receptor in signalling by G-protein-coupled receptors. *Nature* 379(6565), pp. 557–60.

Davies, J.Q., Lin, H.-H., Stacey, M., Yona, S., Chang, G.-W., Gordon, S., Hamann, J., Campo, L., Han, C., Chan, P. and Fox, S.B. 2011. Leukocyte adhesion-GPCR EMR2 is aberrantly expressed in human breast carcinomas and is associated with patient survival. *Oncology reports* 25(3), pp. 619–27.

Davletov, B.A., Meunier, F.A., Ashton, A.C., Matsushita, H., Hirst, W.D., Lelianova, V.G., Wilkin, G.P., Dolly, J.O. and Ushkaryov, Y.A. 1998. Vesicle exocytosis stimulated by alpha-latrotoxin is mediated by latrophilin and requires both external and stored Ca2+. *EMBO J.* 17(14), pp. 3909–20.

DeGraff, J.L., Gurevich, V. V and Benovic, J.L. 2002. The third intracellular loop of alpha 2-adrenergic receptors determines subtype specificity of arrestin interaction. *J. Biol. Chem.* 277(45), pp. 43247–52.

Demuth, T. and Berens, M.E. 2004. Molecular mechanisms of glioma cell migration and invasion. *J. Neurooncol.* 70(2), pp. 217–28.

Deupi, X. and Kobilka, B. 2007. Activation of G protein–coupled receptors. *Adv. Protein Chem.* 74(07), pp. 137–166.

Deupi, X. and Standfuss, J. 2011. Structural insights into agonist-induced activation of G-protein-coupled receptors. *Curr. Opin. Struct. Biol.* 21(4), pp. 541–51.

Dixon, R.A., Kobilka, B.K., Strader, D.J., Benovic, J.L., Dohlman, H.G., Frielle, T., Bolanowski, M.A., Bennett, C.D., Rands, E., Diehl, R.E., Mumford, R.A., Slater, E.E., Sigal, I.S., Caron, M.G., Lefkowitz, R.J. and Strader, C.D. 1986. Cloning of the gene and cDNA for mammalian beta-adrenergic receptor and homology with rhodopsin. *Nature* 321(6065), pp. 75–9.

Doherty, G.J. and McMahon, H.T. 2009. Mechanisms of endocytosis. *Annu. Rev. Biochem.* 78(March), pp. 857–902.

Dorsam, R.T. and Gutkind, J.S. 2007. G-protein-coupled receptors and cancer. *Nat. Rev. Cancer* 7(2), pp. 79–94.

Ebermann, I., Wiesen, M.H.J., Zrenner, E., Lopez, I., Pigeon, R., Kohl, S., Löwenheim, H., Koenekoop, R.K. and Bolz, H.J. 2009. GPR98 mutations cause Usher syndrome type 2 in males. *J. Med. Genet.* 46(4), pp. 277–80.

Edwards, D.R., Handsley, M.M. and Pennington, C.J. 2008. The ADAM metalloproteinases. *Mol. Aspects Med.* 29(5), pp. 258–89.

Edwards, J. 2010. Role of Transglutaminases in Signalling that Regulates Epithelial Responses in Wound Healing. Cardiff University.

Ernst, O.P. 2000. Mutation of the Fourth Cytoplasmic Loop of Rhodopsin Affects Binding of Transducin and Peptides Derived from the Carboxyl-terminal Sequences of Transducin alpha and gamma Subunits. *J. Biol. Chem.* 275(3), pp. 1937–1943.

Fan, H. and Derynck, R. 1999. Ectodomain shedding of TGF-alpha and other transmembrane proteins is induced by receptor tyrosine kinase activation and MAP kinase signaling cascades. *EMBO J.* 18(24), pp. 6962–72.

Farrens, D.L., Altenbach, C., Yang, K., Hubbell, W.L. and Khorana, H.G. 1996. Requirement of rigid-body motion of transmembrane helices for light activation of rhodopsin. *Science* 274(5288), pp. 768–70.

Faure, M., Voyno-Yasenetskaya, T. and Bourne, H. 1994. cAMP and beta gamma subunits of heterotrimeric G proteins stimulate the mitogen-activated protein kinase pathway in COS-7 cells. *J. Biol. Chem.* 269(11), pp. 7851–7854.

Ferguson, S.S. 2001. Evolving concepts in G protein-coupled receptor endocytosis: the role in receptor desensitization and signaling. *Pharmacol. Rev.* 53(1), pp. 1–24.

Fischer, O.M., Hart, S., Gschwind, A. and Ullrich, A. 2003. EGFR signal transactivation in cancer cells. *Biochem. Soc. Trans.* 31(Pt 6), pp. 1203–8.

Fra, a M., Williamson, E., Simons, K. and Parton, R.G. 1995. De novo formation of caveolae in lymphocytes by expression of VIP21-caveolin. *Proc. Natl. Acad. Sci. U. S. A.* 92(19), pp. 8655–9.

Franke, R.R., König, B., Sakmar, T.P., Khorana, H.G. and Hofmann, K.P. 1990. Rhodopsin mutants that bind but fail to activate transducin. *Science* 250(4977), pp. 123–5.

Fredriksson, R., Lagerström, M.C., Lundin, L.-G. and Schiöth, H.B. 2003. The G-protein-coupled receptors in the human genome form five main families. Phylogenetic analysis, paralogon groups, and fingerprints. *Mol. Pharmacol.* 63(6), pp. 1256–72.

Fridman, J.S., Caulder, E., Hansbury, M., Liu, X., Yang, G., Wang, Q., Lo, Y., Zhou, B.-B., Pan, M., Thomas, S.M., Grandis, J.R., Zhuo, J., Yao, W., Newton, R.C., Friedman, S.M., Scherle, P.A. and Vaddi, K. 2007. Selective inhibition of ADAM metalloproteases as a novel approach for modulating ErbB pathways in cancer. *Clin. Cancer Res.* 13(6), pp. 1892–902.

Fujii, Y., Ishikawa, N. and Kobayashi, Y. 2013. Compound heterozygosity in GPR56 with bilateral frontoparietal polymicrogyria. *Brain Dev.*

Fung, B.K., Hurley, J.B. and Stryer, L. 1981. Flow of information in the light-triggered cyclic nucleotide cascade of vision. *Proc. Natl. Acad. Sci. U. S. A.* 78(1), pp. 152–6.

Galle, J., Sittig, D., Hanisch, I. and Wobus, M. 2006. Individual cell-based models of tumor-environment interactions: multiple effects of CD97 on tumor invasion. *Am. J. Pathol.* 169(5), pp. 1802–1811.

Gao, H., Sun, Y., Wu, Y., Luan, B., Wang, Y., Qu, B. and Pei, G. 2004. Identification of beta-arrestin2 as a G protein-coupled receptor-stimulated regulator of NF-kappaB pathways. *Mol. Cell* 14(3), pp. 303–17.

García-Sáinz, J. a, Vázquez-Prado, J. and del Carmen Medina, L. 2000. Alpha 1-adrenoceptors: function and phosphorylation. *Eur. J. Pharmacol.* 389(1), pp. 1–12.

Gaultier, A., Cousin, H., Darribère, T. and Alfandari, D. 2002. ADAM13 disintegrin and cysteine-rich domains bind to the second heparin-binding domain of fibronectin. *J. Biol. Chem.* 277(26), pp. 23336–44.

Geevimaan, K. and Babu, P. 2013. Deregulation of cell polarity proteins in gliomagenesis. In: *Evol Mol Biol Brain Tumors Ther. Implic.* pp. 343–353.

Gether, U. 1998. G Protein-coupled Receptors: II. Mechanism of agonist activation. *J. Biol. Chem.* 273(29), pp. 17979–17982.

Ghanouni, P., Gryczynski, Z., Steenhuis, J.J., Lee, T.W., Farrens, D.L., Lakowicz, J.R. and Kobilka, B.K. 2001. Functionally different agonists induce distinct conformations in the G protein coupling domain of the beta 2 adrenergic receptor. *J. Biol. Chem.* 276(27), pp. 24433–6.

Ghanouni, P., Steenhuis, J.J., Farrens, D.L. and Kobilka, B.K. 2001. Agonist-induced conformational changes in the G-protein-coupling domain of the beta 2 adrenergic receptor. *Proc. Natl. Acad. Sci. U. S. A.* 98(11), pp. 5997–6002.

Ghosh, P.M., Bedolla, R., Thomas, C. a and Kreisberg, J.I. 2004. Role of protein kinase C in arginine vasopressin-stimulated ERK and p70S6 kinase phosphorylation. *J. Cell Biol.* 91(6), pp. 1109–29.

Giancotti, F.G. and Ruoslahti, E. 1999. Integrin signaling. *Science* 285(5430), pp. 1028–32.

Gohla, A., Harhammer, R. and Schultz, G. 1998. The G-protein G13 but Not G12 Mediates Signaling from Lysophosphatidic Acid Receptor via Epidermal Growth Factor Receptor to Rho. *J. Biol. Chem.* 273(8), pp. 4653–4659.

Gohla, A., Offermanns, S., Wilkie, T. and Schultz, G. 1999. Differential Involvement of Galpha 12 and Galpha 13 in Receptor-mediated Stress Fiber Formation. *J. Biol. Chem.* 274(25), pp. 17901–17907.

Goldstein, J., Brown, M., Anderson, R., Russel, D. and Schneider, W. 1985. Receptor-mediated endocytosis: concepts emerging from the LDL receptor system. *Annu. Rev. Cell Biol.*, pp. 1–39.

Goodman, O.B., Krupnick, J.G., Gurevich, V. V, Benovic, J.L. and Keen, J.H. 1997. Arrestin/clathrin interaction. Localization of the arrestin binding locus to the clathrin terminal domain. *J. Biol. Chem.* 272(23), pp. 15017–22.

Grenard, P., Bates, M. and Aeschlimann, D. 2001. Evolution of transglutaminase genes: identification of a transglutaminase gene cluster on human chromosome 15q15. *J. Biol. Chem.* 276(35), pp. 33066–78.

Griffiths, G. and Gruenberg, J. 1991. The arguments for pre-existing early and late endosomes. *Trends in cell biology* 1(1), pp. 5–9.

Van Groningen, J.J., Klink, S.L., Bloemers, H.P. and Swart, G.W. 1995. Expression of tissue-type transglutaminase correlates positively with metastatic properties of human melanoma cell lines. *Int. J. Cancer* 60(3), pp. 383–7.

Gschwind, a, Zwick, E., Prenzel, N., Leserer, M. and Ullrich, a 2001. Cell communication networks: epidermal growth factor receptor transactivation as the paradigm for interreceptor signal transmission. *Oncogene* 20(13), pp. 1594–600.

Gschwind, A., Hart, S., Fischer, O.M. and Ullrich, A. 2003. TACE cleavage of proamphiregulin regulates GPCR-induced proliferation and motility of cancer cells. *EMBO J.* 22(10), pp. 2411–21.

Guilluy, C., Rolli-Derkinderen, M., Tharaux, P.-L., Melino, G., Pacaud, P. and Loirand, G. 2007. Transglutaminase-dependent RhoA activation and depletion by serotonin in vascular smooth muscle cells. *J. Biol. Chem.* 282(5), pp. 2918–28.

Gurevich, V. V, Dion, S.B., Onorato, J.J., Ptasienski, J., Kim, C.M., Sterne-Marr, R., Hosey, M.M. and Benovic, J.L. 1995. Arrestin interactions with G protein-coupled receptors. Direct binding studies of wild type and mutant arrestins with rhodopsin, beta 2-adrenergic, and m2 muscarinic cholinergic receptors. *J. Biol. Chem.* 270(2), pp. 720–31.

Hadjipanayis, C.G. and Van Meir, E.G. 2009a. Brain cancer propagating cells: biology, genetics and targeted therapies. *Trends Mol. Med.* 15(11), pp. 519–30.

Hadjipanayis, C.G. and Van Meir, E.G. 2009b. Tumor initiating cells in malignant gliomas: biology and implications for therapy. *J. Mol. Med. (Berl).* 87(4), pp. 363–74.

Hadjivassiliou, M. and Aeschlimann, P. 2008. Autoantibodies in gluten ataxia recognize a novel neuronal transglutaminase. *Ann. Neurol.* 64(3), pp. 332–343.

Hadjivassiliou, M., Aeschlimann, P., Strigun, A., Sanders, D.S., Woodroofe, N. and Aeschlimann, D. 2008. Autoantibodies in gluten ataxia recognize a novel neuronal transglutaminase. *Annals of neurology* 64(3), pp. 332–43.

Hamann, J., Vogel, B., van Schijndel, G. and van Lier, R. 1996. The seven-span transmembrane receptor CD97 has a cellular ligand (CD55, DAF). *J. Exp. Med.* 184, pp. 1185–1189.

Hamm, H.E. 2001. How activated receptors couple to G proteins. *Proc. Natl. Acad. Sci. U. S. A.* 98(9), pp. 4819–21.

Han, J.A. and Park, S.C. 1999. Reduction of transglutaminase 2 expression is associated with an induction of drug sensitivity in the PC-14 human lung cancer cell line. *J. Cancer Res. Clin. Oncol.* 125(2), pp. 89–95.

Hansen, S., Sandvig, K. and Deurs, B. Van 1993. Clathrin and HA2 adaptors: effects of potassium depletion, hypertonic medium, and cytosol acidification. *J. Cell Biol.* 121(1), pp. 61–72.

Hanyaloglu, A.C. and von Zastrow, M. 2008. Regulation of GPCRs by endocytic membrane trafficking and its potential implications. *Annu. Rev. Pharmacol. Toxicol.* 48, pp. 537–68.

Harding, C., Heuser, J. and Stahl, P. 1983. Receptor-mediated Endocytosis of Transferrin and Recycling of the Transferrin Receptor in Rat Reticulocytes Biochemical Approaches to Transferrin. *J. Cell Biol.* 97, pp. 329–339.

Hargrave, P.A., McDowell, J.H., Curtis, D.R., Wang, J.K., Juszczak, E., Fong, S., Mohana Rao, J.K., Argos, P., Mcdowell, H. and Rao, J.K.M. 1983. The structure of bovine rhodopsin. *Biophys. Struct. Mech.* 9(4), pp. 235–244.

Henley, J.R., Krueger, E.W., Oswald, B.J. and McNiven, M.A. 1998. Dynamin-mediated internalization of caveolae. *J. Cell Biol.* 141(1), pp. 85–99.

Hildebrandt, J.D., Sekura, R.D., Codina, J., Iyengar, R., Manclark, C.R. and Birnbaumer, L. 1983. Stimulation and inhibition of adenylyl cyclases mediated by distinct regulatory proteins. *Nature* 302(5910), pp. 706–709.

Hill, S.J. 2006. G-protein-coupled receptors: past, present and future. *Br. J. Pharmacol.* 147 Suppl, pp. S27–37.

Holland, E.C. 2000. Glioblastoma multiforme: the terminator. *Proc. Natl. Acad. Sci. U. S. A.* 97(12), pp. 6242–4.

Hooper, N.M. 1994. Families of zinc metalloproteases. *FEBS letters* 354(1), pp. 1–6.

Horiuchi, K., Le Gall, S., Schulte, M., Yamaguchi, T., Reiss, K., Murphy, G., Toyama, Y., Hartmann, D., Saftig, P. and Blobel, C.P. 2007. Substrate selectivity of epidermal growth factor-receptor ligand sheddases and their regulation by phorbol esters and calcium influx. *Mol. Biol. Cell* 18(1), pp. 176–88.

Huang, Y., Fan, J., Yang, J. and Zhu, G.-Z. 2008. Characterization of GPR56 protein and its suppressed expression in human pancreatic cancer cells. *Mol. Cell. Biochem.* 308(1-2), pp. 133–9.

Huang, Y.-S., Chiang, N.-Y., Hu, C.-H., Hsiao, C.-C., Cheng, K.-F., Tsai, W.-P., Yona, S., Stacey, M., Gordon, S., Chang, G.-W. and Lin, H.-H. 2012. Activation of myeloid cell-specific adhesion class G protein-coupled receptor EMR2 via ligation-induced translocation and interaction of receptor subunits in lipid raft microdomains. *Molecular and cellular biology* 32(8), pp. 1408–20.

Hulpiau, P. and van Roy, F. 2009. Molecular evolution of the cadherin superfamily. *Int. J. Biochem. Cell Biol.* 41(2), pp. 349–69.

Hundhausen, C., Misztela, D., Berkhout, T. a, Broadway, N., Saftig, P., Reiss, K., Hartmann, D., Fahrenholz, F., Postina, R., Matthews, V., Kallen, K.-J., Rose-John, S. and Ludwig, A. 2003. The disintegrin-like metalloproteinase ADAM10 is involved in constitutive cleavage of CX3CL1 (fractalkine) and regulates CX3CL1-mediated cell-cell adhesion. *Blood* 102(4), pp. 1186–95.

Iguchi, T., Sakata, K., Yoshizaki, K., Tago, K., Mizuno, N. and Itoh, H. 2008. Orphan G protein-coupled receptor GPR56 regulates neural progenitor cell migration via a G alpha 12/13 and Rho pathway. *J. Biol. Chem.* 283(21), pp. 14469–78.

Iismaa, S., Begg, G. and Graham, R. 2006. Cross-linking transglutaminases with G protein-coupled receptor signaling. *Sci. Signal.* 2006(353), p. pe34.

Iismaa, S., Mearns, B., Lorand, L. and Graham, R. 2009. Transglutaminases and disease: lessons from genetically engineered mouse models and inherited disorders. *Physiol Rev* 89, pp. 991–1023.

Inoue, A., Ishiguro, J., Kitamura, H., Arima, N., Okutani, M., Shuto, A., Higashiyama, S., Ohwada, T., Arai, H., Makide, K. and Aoki, J. 2012. TGFα shedding assay: an accurate and versatile method for detecting GPCR activation. *Nature methods* 9(10), pp. 1021–9.

Irannejad, R., Tomshine, J.C., Tomshine, J.R., Chevalier, M., Mahoney, J.P., Steyaert, J., Rasmussen, S.G.F., Sunahara, R.K., El-Samad, H., Huang, B. and von Zastrow, M. 2013. Conformational biosensors reveal GPCR signalling from endosomes. *Nature* 495(7442), pp. 534–8.

Jackson, L.F., Qiu, T.H., Sunnarborg, S.W., Chang, A., Zhang, C., Patterson, C. and Lee, D.C. 2003. Defective valvulogenesis in HB-EGF and TACE-null mice is associated with aberrant BMP signaling. *EMBO J.* 22(11), pp. 2704–16.

James, C.D. and Olson, J.J. 1996. Molecular genetics and molecular biology advances in brain tumors. *Curr. Opin. Oncol.* 8(3), pp. 188–95.

Jeong, S., Li, S., Luo, R., Strokes, N. and Piao, X. 2012. Loss of Col3a1, the gene for Ehlers-Danlos syndrome type IV, results in neocortical dyslamination. *PloS one* 7(1), pp. 1–7.

Jeong, S.-J., Luo, R., Singer, K., Giera, S., Kreidberg, J., Kiyozumi, D., Shimono, C., Sekiguchi, K. and Piao, X. 2013. GPR56 Functions Together with α3β1 Integrin in Regulating Cerebral Cortical Development. *PloS one* 8(7), p. e68781.

Jin, Z., Tietjen, I., Bu, L., Liu-Yesucevitz, L., Gaur, S.K., Walsh, C. a and Piao, X. 2007. Disease-associated mutations affect GPR56 protein trafficking and cell surface expression. *Hum. Mol. Genet.* 16(16), pp. 1972–85.

Johannes, L. and Lamaze, C. 2002. Clathrin-dependent or not: is it still the question? *Traffic* 3(7), pp. 443–51.

Johnson, A.M., Dale, R.C., Wienholt, L., Hadjivassiliou, M., Aeschlimann, D. and Lawson, J.A. 2013. Coeliac disease , epilepsy , and cerebral calcifications : association with TG6 autoantibodies. *Dev. Med. child Neurol.* 55, pp. 90–93.

Jones, R.A., Kotsakis, P., Johnson, T.S., Chau, D.Y.S., Ali, S., Melino, G. and Griffin, M. 2006. Matrix changes induced by transglutaminase 2 lead to inhibition of angiogenesis and tumor growth. *Cell death and differentiation* 13(9), pp. 1442–1453.

Kan, Z., Jaiswal, B.S., Stinson, J., Janakiraman, V., Bhatt, D., Stern, H.M., Yue, P., Haverty, P.M., Bourgon, R., Zheng, J., Moorhead, M., Chaudhuri, S., Tomsho, L.P., Peters, B.A., Pujara, K., Cordes, S., Davis, D.P., Carlton, V.E.H., Yuan, W., Li, L., Wang, W., Eigenbrot, C., Kaminker, J.S., Eberhard, D.A., Waring, P., Schuster, S.C., Modrusan, Z., Zhang, Z., Stokoe, D., de Sauvage, F.J., Faham, M. and Seshagiri, S. 2010. Diverse somatic mutation patterns and pathway alterations in human cancers. *Nature* 466(7308), pp. 869–73.

Kang, S.K., Kim, D.K., Damron, D.S., Baek, K.J. and Im, M.-J. 2002. Modulation of intracellular Ca(2+) via alpha(1B)-adrenoreceptor signaling molecules, G alpha(h) (transglutaminase II) and phospholipase C-delta 1. *Biochem. Biophys. Res. Commun.* 293(1), pp. 383–90.

Kang, S.K., Yi, K.S., Kwon, N.S., Park, K.-H., Kim, U.-H., Baek, K.J. and Im, M.-J. 2004. Alpha1B-adrenoceptor signaling and cell motility: GTPase function of Gh/transglutaminase 2 inhibits cell migration through interaction with cytoplasmic tail of integrin alpha subunits. *J. Biol. Chem.* 279(35), pp. 36593–600.

Kaur, B., Brat, D.J., Calkins, C.C. and Van Meir, E.G. 2003. Brain angiogenesis inhibitor 1 is differentially expressed in normal brain and glioblastoma independently of p53 expression. *Am. J. Pathol.* 162(1), pp. 19–27.

Ke, N., Ma, H., Diedrich, G., Chionis, J. and Liu, G. 2008. Biochemical characterization of genetic mutations of GPR56 in patients with bilateral frontoparietal polymicrogyria (BFPP). *Biochem. Biophys. Res. Commun.* 366, pp. 314–320.

Ke, N., Sundaram, R., Liu, G., Chionis, J., Fan, W., Rogers, C., Awad, T., Grifman, M., Yu, D., Wong-Staal, F. and Li, Q.-X. 2007. Orphan G protein-coupled receptor GPR56 plays a role in cell transformation and tumorigenesis involving the cell adhesion pathway. *Mol. Cancer Ther.* 6(6), pp. 1840–50.

Kee, H.J., Ahn, K.Y., Choi, K.C., Won Song, J., Heo, T., Jung, S., Kim, J.-K., Bae, C.S. and Kim, K.K. 2004. Expression of brain-specific angiogenesis inhibitor 3 (BAI3) in normal brain and implications for BAI3 in ischemia-induced brain angiogenesis and malignant glioma. *FEBS letters* 569(1-3), pp. 307–16.

Keith, D.E., Murray, S.R., Zaki, P.A., Chu, P.C., Lissin, D. V., Kang, L., Evans, C.J. and von Zastrow, M. 1996. Morphine Activates Opioid Receptors without Causing Their Rapid Internalization. *J. Biol. Chem.* 271(32), pp. 19021–19024.

Kerbel, R.S., Kobayashi, H. and Graham, C.H. 1994. Intrinsic or acquired drug resistance and metastasis: are they linked phenotypes? *J. Cell Biochem.* 56(1), pp. 37–47.

Kim, J.-E., Han, J.M., Park, C.R., Shin, K.-J., Ahn, C., Seong, J.Y. and Hwang, J.-I. 2010. Splicing variants of the orphan G-protein-coupled receptor GPR56 regulate the activity of transcription factors associated with tumorigenesis. *J. Cancer Res. Clin. Oncol.* 136(1), pp. 47–53.

Király, R., Demény, M. and Fésüs, L. 2011. Protein transamidation by transglutaminase 2 in cells: a disputed Ca2+-dependent action of a multifunctional protein. *FEBS J.* 278(24), pp. 4717–39.

Kiss, A.L. and Botos, E. 2009. Endocytosis via caveolae: alternative pathway with distinct cellular compartments to avoid lysosomal degradation? *J. Cell. Mol. Med.* 13(7), pp. 1228–37.

Kobilka, B. and Deupi, X. 2007. Conformational complexity of G-protein-coupled receptors. *Trends Pharmacol. Sci.* 28(8).

Kobilka, B.K. 2007. G protein coupled receptor structure and activation. *Biochimica et biophysica acta* 1768(4), pp. 794–807.

Kodama, T., Ikeda, E., Okada, A., Ohtsuka, T., Shimoda, M., Shiomi, T., Yoshida, K., Nakada, M., Ohuchi, E. and Okada, Y. 2004. ADAM12 is selectively overexpressed in human glioblastomas and is associated with glioblastoma cell proliferation and shedding of heparin-binding epidermal growth factor. *Am. J. Pathol.* 165(5), pp. 1743–53.

Koh, J.T., Kook, H., Kee, H.J., Seo, Y.-W., Jeong, B.C., Lee, J.H., Kim, M.-Y., Yoon, K.C., Jung, S. and Kim, K.K. 2004. Extracellular fragment of brain-specific angiogenesis inhibitor 1 suppresses endothelial cell proliferation by blocking alphavbeta5 integrin. *Exp. Cell Res.* 294(1), pp. 172–84.

Koh, J.T., Lee, Z.H., Ahn, K.Y., Kim, J.K., Bae, C.S., Kim, H.H., Kee, H.J. and Kim, K.K. 2001. Characterization of mouse brain-specific angiogenesis inhibitor 1 (BAI1) and phytanoyl-CoA alpha-hydroxylase-associated protein 1, a novel BAI1-binding protein. *Brain Res. Mol. Brain Res.* 87(2), pp. 223–37.

Koirala, S., Jin, Z., Piao, X. and Corfas, G. 2009. GPR56-regulated granule cell adhesion is essential for rostral cerebellar development. *J. Neurosci.* 29(23), pp. 7439–49.

Kolakowski, L.F. 1994. GCRDb: a G-protein-coupled receptor database. *Receptors & channels* 2(1), pp. 1–7.

Koppen, C. van and Jakobs, K. 2004. Arrestin-independent internalization of G protein-coupled receptors. *Mol. Pharmacol.* 66(3), pp. 365–367.

Kotsakis, P. and Griffin, M. 2007. Tissue transglutaminase in tumour progression: friend or foe? *Amino acids* 33, pp. 373–384.

Krasnoperov, V., Bittner, M. and Beavis, R. 1997. α-Latrotoxin stimulates exocytosis by the interaction with a neuronal G-protein-coupled receptor. *Neuron* 18, pp. 925–937.

Krasnoperov, V., Bittner, M.A., Holz, R.W., Chepurny, O. and Petrenko, A.G. 1999. Structural requirements for alpha-latrotoxin binding and alpha-latrotoxin-stimulated secretion. A study with calcium-independent receptor of alpha-latrotoxin (CIRL) deletion mutants. *J. Biol. Chem.* 274(6), pp. 3590–6.

Krasnoperov, V., Lu, Y., Buryanovsky, L., Neubert, T. a, Ichtchenko, K. and Petrenko, A.G. 2002. Post-translational proteolytic processing of the calcium-independent receptor of alpha-latrotoxin (CIRL), a natural chimera of the cell adhesion protein and the G protein-coupled receptor. Role of the G protein-coupled receptor proteolysis site (GPS) moti. *J. Biol. Chem.* 277(48), pp. 46518–26.

Krupnick, J., Gurevich, V., Schepers, T., Hamm, H. and Benovic, J. 1994. Arrestin-rhodopsin interaction. Multi-site binding delineated by peptide inhibition. *J. Biol. Chem.* 269(5), pp. 3226–3232.

Kühn, R. and Wurst, W. 2009. Overview on mouse mutagenesis. *Methods Mol. Biol.* 530, pp. 1–12.

Kveiborg, M., Instrell, R., Rowlands, C., Howell, M. and Parker, P.J. 2011. PKCα and PKCδ regulate ADAM17-mediated ectodomain shedding of heparin binding-EGF through separate pathways. *PloS one* 6(2), p. e17168.

Kwakkenbos, M.J., Kop, E.N., Stacey, M., Matmati, M., Gordon, S., Lin, H.-H. and Hamann, J. 2004. The EGF-TM7 family: a postgenomic view. *Immunogenetics* 55(10), pp. 655–66.

Lagerström, M.C., Rabe, N., Haitina, T., Kalnina, I., Hellström, A.R., Klovins, J., Kullander, K. and Schiöth, H.B. 2007. The evolutionary history and tissue mapping of GPR123: specific CNS expression pattern predominantly in thalamic nuclei and regions containing large pyramidal cells. *J. Neurochem.* 100(4), pp. 1129–42.

Lagerström, M.C. and Schiöth, H.B. 2008. Structural diversity of G protein-coupled receptors and significance for drug discovery. *Nat. Rev. Drug Discov.* 7(4), pp. 339–57.

Lai, T.-S., Tucker, T., Burke, J.R., Strittmatter, W.J. and Greenberg, C.S. 2004. Effect of tissue transglutaminase on the solubility of proteins containing expanded polyglutamine repeats. *J. Neurochem.* 88(5), pp. 1253–60.

Langenhan, T., Aust, G. and Hamann, J. 2013. Sticky Signaling--Adhesion Class G Protein-Coupled Receptors Take the Stage. *Sci. Signal.* 6(May).

Langenhan, T., Prömel, S., Mestek, L., Esmaeili, B., Waller-evans, H., Hennig, C., Kohara, Y., Avery, L., Vakonakis, I., Schnabel, R. and Russ, A.P. 2009. Latrophilin Signaling Links Anterior-Posterior Tissue Polarity and Oriented Cell Divisions in the C. elegans Embryo. *Dev. Cell*, pp. 494–504.

Laporte, S.A., Oakley, R.H., Holt, J.A., Barak, L.S. and Caron, M.G. 2000. The interaction of beta-arrestin with the AP-2 adaptor is required for the clustering of beta 2-adrenergic receptor into clathrin-coated pits. *J. Biol. Chem.* 275(30), pp. 23120–6.

Laporte, S.A., Oakley, R.H., Zhang, J., Holt, J.A., Ferguson, S.S., Caron, M.G. and Barak, L.S. 1999. The beta2-adrenergic receptor/betaarrestin complex recruits the clathrin adaptor AP-2 during endocytosis. *Proc. Natl. Acad. Sci. U. S. A.* 96(7), pp. 3712–7.

Lappano, R. and Maggiolini, M. 2011. G protein-coupled receptors: novel targets for drug discovery in cancer. *Nat. Rev. Drug Discov.* 10(1), pp. 47–60.

De Laurenzi, V. and Melino, G. 2001. Gene disruption of tissue transglutaminase. *Mol. Cell. Biol.* 21(1), pp. 148–55.

Lawrence, P.A., Struhl, G. and Casal, J. 2007. Planar cell polarity: one or two pathways? *Nature reviews. Genetics* 8(7), pp. 555–63.

Lebon, G., Warne, T. and Tate, C.G. 2012. Agonist-bound structures of G protein-coupled receptors. *Curr. Opin. Struct. Biol.* 22(4), pp. 482–90.

Lee, K.-H., Lee, N., Lim, S., Jung, H., Ko, Y.-G., Park, H.-Y., Jang, Y., Lee, H. and Hwang, K.-C. 2003. Calreticulin inhibits the MEK1,2-ERK1,2 pathway in alpha 1-adrenergic receptor/Gh-stimulated hypertrophy of neonatal rat cardiomyocytes. *J. Steroid Biochem. Mol. Biol.* 84(1), pp. 101–7.

Lee, K.N., Arnold, S.A., Birkbichler, P.J., Patterson, M.K., Fraij, B.M., Takeuchi, Y. and Carter, H.A. 1993. Site-directed mutagenesis of human tissue transglutaminase: Cys-277 is essential for transglutaminase activity but not for GTPase activity. *Biochim. Biophys. Acta - Protein Struct. Mol. Enzymol.* 1202(1), pp. 1–6.

Leff, P. 1995. The two-state model of receptor activation. *Trends Pharmacol. Sci.* 16(3), pp. 89–97.

Lefkowitz, R. 2007. Seven transmembrane receptors: something old, something new. *Acta physiologica* 190, pp. 9–19.

Lefkowitz, R.J. 2000. The superfamily of heptahelical receptors. *Nature cell biology* 2(7), pp. E133–6.

Lefkowitz, R.J. and Shenoy, S.K. 2005. Transduction of receptor signals by beta-arrestins. *Science* 308(5721), pp. 512–7.

Legg, K. 2011. Cell migration: An ABC of the RHO subfamily. *Nat. Rev. Mol. Cell Biol.* 12(7), p. 403.

Leitinger, B., McDowall, A., Stanley, P. and Hogg, N. 2000. The regulation of integrin function by Ca(2+). *Biochim. Biophys. Acta* 1498(2-3), pp. 91–8.

Lelianova, V.G., Davletov, B.A., Sterling, A., Rahman, M.A., Grishin, E. V, Totty, N.F. and Ushkaryov, Y.A. 1997. Alpha-latrotoxin receptor, latrophilin, is a novel member of the secretin family of G protein-coupled receptors. *J. Biol. Chem.* 272(34), pp. 21504–8.

Leurs, R., Bakker, R. a., Timmerman, H. and de Esch, I.J.P. 2005. The histamine H3 receptor: from gene cloning to H3 receptor drugs. *Nat. Rev. Drug Discov.* 4(2), pp. 107–120.

Levental, K.R., Yu, H., Kass, L., Lakins, J.N., Egeblad, M., Erler, J.T., Fong, S.F.T., Csiszar, K., Giaccia, A., Weninger, W., Yamauchi, M., Gasser, D.L. and Weaver, V.M. 2009. Matrix crosslinking forces tumor progression by enhancing integrin signaling. *Cell* 139(5), pp. 891–906.

Li, S., Jin, Z., Koirala, S., Bu, L., Xu, L., Hynes, R.O., Walsh, C. a, Corfas, G. and Piao, X. 2008. GPR56 regulates pial basement membrane integrity and cortical lamination. *J. Neurosci.* 28(22), pp. 5817–26.

Lin, H., Chang, G., Huang, Y., Hsiao, C., Stacey, M. and Gordon, S. 2009. Multivalent Protein Probes for the Identification and Characterization of Cognate Cellular Ligands for Myeloid Cell Surface Receptors. *Methods Mol. Biol.* 531, pp. 89–101.

Lin, H., Stacey, M. and Chang, G. 2005. Method for selecting and enriching cells expressing low affinity ligands for cell surface receptors. *BioTechniques* 38(5), pp. 696–698.

Lin, H., Stacey, M., Saxby, C. and Knott, V. 2001. Molecular Analysis of the Epidermal Growth Factor-like Short Consensus Repeat Domain-mediated Protein-Protein Interactions. DISSECTION OF THE CD97-CD55. *J. Biol. Chem.* 276(26), pp. 24160–24169.

Little, K.D., Hemler, M.E. and Stipp, C.S. 2004. Dynamic Regulation of a GPCR-Tetraspanin-G Protein Complex on Intact Cells: Central Role of CD81 in Facilitating GPR56-Galphaq/11 association. *Mol. Biol. Cell* 15, pp. 2375–2387.

Liu, M., Parker, R.M., Darby, K., Eyre, H.J., Copeland, N.G., Crawford, J., Gilbert, D.J., Sutherland, G.R., Jenkins, N. a and Herzog, H. 1999. GPR56, a novel secretin-like human G-protein-coupled receptor gene. *Genomics* 55(3), pp. 296–305.

Lorand, L. and Graham, R.M. 2003. Transglutaminases: crosslinking enzymes with pleiotropic functions. *Nat. Rev. Mol. Cell Biol.* 4(2), pp. 140–56.

Ludwig, A., Hundhausen, C., Lambert, M.H., Broadway, N., Andrews, R.C., Bickett, D.M., Leesnitzer, M.A. and Becherer, J.D. 2005. Metalloproteinase inhibitors for the disintegrin-like metalloproteinases ADAM10 and ADAM17 that differentially block constitutive and phorbol ester-inducible shedding of cell surface molecules. *Comb. Chem. High Throughput Screen.* 8(2), pp. 161–71.

Luo, R., Jeong, S.-J., Jin, Z., Strokes, N., Li, S. and Piao, X. 2011. G protein-coupled receptor 56 and collagen III, a receptor-ligand pair, regulates cortical development and lamination. *Proc. Natl. Acad. Sci. U. S. A.* 108(31), pp. 12925–30.

Luo, R., Jin, Z., Deng, Y., Strokes, N. and Piao, X. 2012. Disease-associated mutations prevent GPR56-collagen III interaction. *PloS one* 7(1), p. e29818.

Luo, R., Yang, H.M., Jin, Z., Halley, D.J.J., Chang, B.S., MacPherson, L., Brueton, L. and Piao, X. 2011. A novel GPR56 mutation causes bilateral frontoparietal polymicrogyria. *Pediatric neurology* 45(1), pp. 49–53.

Luttrell, L.M. and Lefkowitz, R.J. 2002. The role of beta-arrestins in the termination and transduction of G-protein-coupled receptor signals. *J. Cell Sci.* 115(Pt 3), pp. 455–65.

MacDonald, M., Ambrose, C., Duyao, M. and Harper, P. 1993. A novel gene containing a trinucleotide repeat that is expanded and unstable on Huntington’s disease chromosomes. The Huntington's Disease Collaborative Research Group. *Cell* 72(6), pp. 971–83.

Mann, A.P., Verma, A., Sethi, G., Manavathi, B., Wang, H., Fok, J.Y., Kunnumakkara, A.B., Kumar, R., Aggarwal, B.B. and Mehta, K. 2006. Overexpression of tissue transglutaminase leads to constitutive activation of nuclear factor-kappaB in cancer cells: delineation of a novel pathway. *Cancer research* 66(17), pp. 8788–95.

Marion, S., Oakley, R.H., Kim, K.-M., Caron, M.G. and Barak, L.S. 2006. A beta-arrestin binding determinant common to the second intracellular loops of rhodopsin family G protein-coupled receptors. *J. Biol. Chem.* 281(5), pp. 2932–8.

Martiny-Baron, G., Kazanietz, M.G., Mischak, H., Blumberg, P.M., Kochs, G., Hug, H., Marmé, D. and Schächtele, C. 1993. Selective inhibition of protein kinase C isozymes by the indolocarbazole Gö 6976. *J. Biol. Chem.* 268(13), pp. 9194–7.

Maruyama, T., Kanaji, T., Nakade, S., Kanno, T. and Mikoshiba, K. 1997. 2APB, 2-Aminoethoxydiphenyl Borate, a Membrane-Penetrable Modulator of Ins(1,4,5)P3-Induced Ca2+ Release. *J. Biol. Chem.* 122(3), pp. 498–505.

Mastroberardino, P.G., Iannicola, C., Nardacci, R., Bernassola, F., De Laurenzi, V., Melino, G., Moreno, S., Pavone, F., Oliverio, S., Fesus, L. and Piacentini, M. 2002. “Tissue” transglutaminase ablation reduces neuronal death and prolongs survival in a mouse model of Huntington’s disease. *Cell Death Differ.* 9(9), pp. 873–80.

Matsushita, H., Lelianova, V.G. and Ushkaryov, Y.A. 1999. The latrophilin family: multiply spliced G protein-coupled receptors with differential tissue distribution. *FEBS letters* 443(3), pp. 348–52.

Maudsley, S., Pierce, K.L., Zamah, a M., Miller, W.E., Ahn, S., Daaka, Y., Lefkowitz, R.J. and Luttrell, L.M. 2000. The beta(2)-adrenergic receptor mediates extracellular signal-regulated kinase activation via assembly of a multi-receptor complex with the epidermal growth factor receptor. *J. Biol. Chem.* 275(13), pp. 9572–80.

McCudden, C.R., Hains, M.D., Kimple, R.J., Siderovski, D.P. and Willard, F.S. 2005. G-protein signaling: back to the future. *Cell. Mol. life Sci.* 62(5), pp. 551–77.

McMahon, H.T. and Boucrot, E. 2011. Molecular mechanism and physiological functions of clathrin-mediated endocytosis. *Nat. Rev. Mol. Cell Biol.* 12(8), pp. 517–33.

McMillan, D.R., Kayes-Wandover, K.M., Richardson, J.A. and White, P.C. 2002. Very large G protein-coupled receptor-1, the largest known cell surface protein, is highly expressed in the developing central nervous system. *J. Biol. Chem.* 277(1), pp. 785–92.

Mehta, K. 1994. High levels of transglutaminase expression in doxorubicin-resistant human breast carcinoma cells. *Int. J. Cancer* 58(3), pp. 400–6.

Mehta, K. and Eckert, R. 2005. Transglutaminases: Family of Enzymes with Diverse Functions. *Prog. Exp. Tumor Res.* 38, pp. 1–253.

Mehta, K., Kumar, A. and Kim, H.I. 2010. Transglutaminase 2: a multi-tasking protein in the complex circuitry of inflammation and cancer. *Biochem. Pharmacol.* 80(12), pp. 1921–9.

Van Meir, E., Hadjipanayis, C.G., Norden, A.D., Shu, H.-K., Wen, P.Y. and Olson, J.J. 2010. Exciting New Advances in Neuro-Oncology: The Avenue to a Cure for Malignant Glioma. *CA. Cancer J. Clin.* 60, pp. 166–193.

Meriane, M., Duhamel, S., Lejeune, L., Galipeau, J. and Annabi, B. 2006. Cooperation of matrix metalloproteinases with the RhoA/Rho kinase and mitogen-activated protein kinase kinase-1/extracellular signal-regulated kinase signaling pathways is required for the sphingosine-1-phosphate-induced mobilization of marrow-derived str. *Stem cells* 24(11), pp. 2557–65.

Mhaouty-Kodja, S. 2004. Ghalpha/tissue transglutaminase 2: an emerging G protein in signal transduction. *Biol. Cell* 96(5), pp. 363–7.

Mifune, M., Ohtsu, H., Suzuki, H., Nakashima, H., Brailoiu, E., Dun, N.J., Frank, G.D., Inagami, T., Higashiyama, S., Thomas, W.G., Eckhart, A.D., Dempsey, P.J., Eguchi, S., Ii, A. and Dempsey, J. 2005. G protein coupling and second messenger generation are indispensable for metalloprotease-dependent, heparin-binding epidermal growth factor shedding through angiotensin II type-1 receptor. *J. Biol. Chem.* 280(28), pp. 26592–9.

Milligan, G. 2004. G protein-coupled receptor dimerization: function and ligand pharmacology. *Mol. Pharmacol.* 66(1), pp. 1–7.

Mizuno, N. and Itoh, H. 2009. Functions and regulatory mechanisms of Gq-signaling pathways. *Neuro-Signals* 17(1), pp. 42–54.

Moers, A., Nürnberg, A., Goebbels, S., Wettschureck, N. and Offermanns, S. 2008. Galpha12/Galpha13 deficiency causes localized overmigration of neurons in the developing cerebral and cerebellar cortices. *Mol. Cell. Biol.* 28(5), pp. 1480–8.

Mogami, H., Lloyd Mills, C. and Gallacher, D. V 1997. Phospholipase C inhibitor, U73122, releases intracellular Ca2+, potentiates Ins(1,4,5)P3-mediated Ca2+ release and directly activates ion channels in mouse pancreatic acinar cells. *Biochem. J.* 324, pp. 645–51.

Mohammad, S., Baldini, G., Granell, S., Narducci, P., Martelli, A.M. and Baldini, G. 2007. Constitutive traffic of melanocortin-4 receptor in Neuro2A cells and immortalized hypothalamic neurons. *J. Biol. Chem.* 282(7), pp. 4963–74.

Montel, V., Gaultier, A., Lester, R.D., Campana, W.M. and Gonias, S.L. 2007. The low-density lipoprotein receptor-related protein regulates cancer cell survival and metastasis development. *Cancer research* 67(20), pp. 9817–24.

Moore, R.H., Tuffaha, A., Millman, E.E., Dai, W., Hall, H.S., Dickey, B.F. and Knoll, B.J. 1999. Agonist-induced sorting of human beta2-adrenergic receptors to lysosomes during downregulation. *J. Cell S* 112(Pt 3), pp. 329–38.

Mori, S., Tanaka, K. and Omura, S. 1995. Degradation Process of Ligand-stimulated Platelet-derived Growth Factor beta-Receptor Involves Ubiquitin-Proteasome Proteolytic Pathway. *J. Biol. Chem.* 270(49), pp. 29447–29452.

Moss, M.L., Sklair-Tavron, L. and Nudelman, R. 2008. Drug insight: tumor necrosis factor-converting enzyme as a pharmaceutical target for rheumatoid arthritis. *Nat. Clin. Pract. Rheumatol.* 4(6), pp. 300–9.

Mundy, D.I., Machleidt, T., Ying, Y., Anderson, R.G.W. and Bloom, G.S. 2002. Dual control of caveolar membrane traffic by microtubules and the actin cytoskeleton. *J. Cell Sci.* 115(Pt 22), pp. 4327–39.

Murphy, G. 2008. The ADAMs: signalling scissors in the tumour microenvironment. *Nat. Rev. Cancer* 8(12), pp. 929–41.

Nagane, M., Lin, H., Cavenee, W.K. and Huang, H.J. 2001. Aberrant receptor signaling in human malignant gliomas: mechanisms and therapeutic implications. *Cancer letters* 162 Suppl, pp. S17–S21.

Nakaoka, H., Perez, D.M., Baek, K.J., Das, T., Husain, A., Misono, K., Im, M.J. and Graham, R.M. 1994. Gh: a GTP-binding protein with transglutaminase activity and receptor signaling function. *Science* 264(5165), pp. 1593–6.

Nanda, N., Iismaa, S.E., Owens, W.A., Husain, A., Mackay, F. and Graham, R.M. 2001. Targeted inactivation of Gh/tissue transglutaminase II. *J. Biol. Chem.* 276(23), pp. 20673–8.

Nathans, J. and Hogness, D.S. 1983. Isolation, sequence analysis, and intron-exon arrangement of the gene encoding bovine rhodopsin. *Cell* 34(3), pp. 807–14.

Nemes, Z., Petrovski, G., Aerts, M., Sergeant, K., Devreese, B. and Fésüs, L. 2009. Transglutaminase-mediated intramolecular cross-linking of membrane-bound alpha-synuclein promotes amyloid formation in Lewy bodies. *J. Biol. Chem.* 284(40), pp. 27252–64.

Nishimori, H., Shiratsuchi, T., Urano, T., Kimura, Y., Kiyono, K., Tatsumi, K., Yoshida, S., Ono, M., Kuwano, M., Nakamura, Y. and Tokino, T. 1997. A novel brain-specific p53-target gene, BAI1, containing thrombospondin type 1 repeats inhibits experimental angiogenesis. *Oncogene* 15(18), pp. 2145–50.

Noma, T. and Lemaire, A. 2007. β-Arrestin–mediated β1-adrenergic receptor transactivation of the EGFR confers cardioprotection. *J. Clin. Invest.* 117(9).

Nurminskaya, M. V and Belkin, A.M. 2012. Cellular functions of tissue transglutaminase. *Int. Rev. Cell Mol. Biol.* 294, pp. 1–97.

Oakley, R.H., Laporte, S. a, Holt, J. a, Barak, L.S. and Caron, M.G. 1999. Association of beta-arrestin with G protein-coupled receptors during clathrin-mediated endocytosis dictates the profile of receptor resensitization. *J. Biol. Chem.* 274(45), pp. 32248–57.

Oakley, R.H., Laporte, S. a, Holt, J. a, Barak, L.S. and Caron, M.G. 2001. Molecular determinants underlying the formation of stable intracellular G protein-coupled receptor-beta-arrestin complexes after receptor endocytosis. *J. Biol. Chem.* 276(22), pp. 19452–60.

Oakley, R.H., Laporte, S. a, Holt, J. a, Caron, M.G. and Barak, L.S. 2000. Differential affinities of visual arrestin, beta arrestin1, and beta arrestin2 for G protein-coupled receptors delineate two major classes of receptors. *J. Biol. Chem.* 275(22), pp. 17201–10.

Oganesian, A., Yarov-Yarovoy, V., Parks, W.C. and Schwinn, D. a 2011. Constitutive coupling of a naturally occurring human alpha1a-adrenergic receptor genetic variant to EGFR transactivation pathway. *Proc. Natl. Acad. Sci. U. S. A.* 108(49), pp. 19796–801.

Ohtsu, H., Dempsey, P.J. and Eguchi, S. 2006. ADAMs as mediators of EGF receptor transactivation by G protein-coupled receptors. *Am. J. Physiol. Cell Physiol.* 291(1), pp. C1–10.

Ostrom, R.S. and Insel, P.A. 2004. The evolving role of lipid rafts and caveolae in G protein-coupled receptor signaling: implications for molecular pharmacology. *Br. J. Pharmacol.* 143(2), pp. 235–45.

Paavola, K.J., Stephenson, J.R., Ritter, S.L., Alter, S.P. and Hall, R. a 2011. The N terminus of the adhesion G protein-coupled receptor GPR56 controls receptor signaling activity. *J. Biol. Chem.* 286(33), pp. 28914–21.

Palade, G. 1953. The fine structure of blood capillaries. *J. Appl. Phys.* 24, pp. 1424–1436.

Palczewski, K., Kumasaka, T., Hori, T., Behnke, C.A., Motoshima, H., Fox, B.A., Le Trong, I., Teller, D.C., Okada, T., Stenkamp, R.E., Yamamoto, M. and Miyano, M. 2000. Crystal Structure of Rhodopsin: A G Protein-Coupled Receptor. *Science* 289(5480), pp. 739–745.

Park, D., Tosello-Trampont, A.-C., Elliott, M.R., Lu, M., Haney, L.B., Ma, Z., Klibanov, A.L., Mandell, J.W. and Ravichandran, K.S. 2007. BAI1 is an engulfment receptor for apoptotic cells upstream of the ELMO/Dock180/Rac module. *Nature* 450(7168), pp. 430–4.

Parton, R.G., Joggerst, B. and Simons, K. 1994. Regulated internalization of caveolae. *J. Cell Biol.* 127(5), pp. 1199–215.

Patel, H.H., Murray, F. and Insel, P. a 2008. Caveolae as organizers of pharmacologically relevant signal transduction molecules. *Annu. Rev. Pharmacol. Toxicol.* 48, pp. 359–91.

Pelkmans, L. and Helenius, A. 2002. Endocytosis Via Caveolae. *Traffic* 3(5), pp. 311–320.

Peng, Y.-M., van de Garde, M.D.B., Cheng, K.-F., Baars, P. a, Remmerswaal, E.B.M., van Lier, R. a W., Mackay, C.R., Lin, H.-H. and Hamann, J. 2011. Specific expression of GPR56 by human cytotoxic lymphocytes. *J. Leukoc. Biol.* 90(4), pp. 735–40.

Peschon, J., Slack, J., Reddy, P., Stocking, K. and Black, R. 1998. An Essential Role for Ectodomain Shedding in Mammalian Development. *Science* 282(5392), pp. 1281–1284.

Piao, X., Chang, B.S., Bodell, A., Woods, K., Benzeev, B., Topcu, M., Guerrini, R., Goldberg-Stern, H., Sztriha, L., Dobyns, W.B., Barkovich, a J. and Walsh, C. a 2005. Genotype-phenotype analysis of human frontoparietal polymicrogyria syndromes. *Annals of neurology* 58(5), pp. 680–7.

Piao, X., Hill, R.S., Bodell, A., Chang, B.S., Basel-Vanagaite, L., Straussberg, R., Dobyns, W.B., Qasrawi, B., Winter, R.M., Innes, a M., Voit, T., Ross, M.E., Michaud, J.L., Déscarie, J.-C., Barkovich, a J. and Walsh, C. a 2004. G protein-coupled receptor-dependent development of human frontal cortex. *Science* 303(5666), pp. 2033–6.

Pierce, K.L., Premont, R.T. and Lefkowitz, R.J. 2002. Seven-transmembrane receptors. *Nat. Rev. Mol. Cell Biol.* 3(9), pp. 639–50.

Pierce, K.L., Tohgo, A., Ahn, S., Field, M.E., Luttrell, L.M. and Lefkowitz, R.J. 2001. Epidermal growth factor (EGF) receptor-dependent ERK activation by G protein-coupled receptors: a co-culture system for identifying intermediates upstream and downstream of heparin-binding EGF shedding. *J. Biol. Chem.* 276(25), pp. 23155–60.

Pinkas, D.M., Strop, P., Brunger, A.T. and Khosla, C. 2007. Transglutaminase 2 undergoes a large conformational change upon activation. *PLoS biology* 5(12), p. e327.

Pitcher, J. a, Freedman, N.J. and Lefkowitz, R.J. 1998. G protein-coupled receptor kinases. *Annual review of biochemistry* 67, pp. 653–92.

Poghosyan, Z., Robbins, S.M., Houslay, M.D., Webster, A., Murphy, G. and Edwards, D.R. 2002. Phosphorylation-dependent interactions between ADAM15 cytoplasmic domain and Src family protein-tyrosine kinases. *J. Biol. Chem.* 277(7), pp. 4999–5007.

Prenzel, N., Zwick, E., Daub, H., Leserer, M., Abraham, R., Wallasch, C. and Ullrich, a 1999. EGF receptor transactivation by G-protein-coupled receptors requires metalloproteinase cleavage of proHB-EGF. *Nature* 402(6764), pp. 884–8.

Prömel, S., Frickenhaus, M., Hughes, S., Mestek, L., Staunton, D., Woollard, A., Vakonakis, I., Schöneberg, T., Schnabel, R., Russ, A.P. and Langenhan, T. 2012. The GPS motif is a molecular switch for bimodal activities of adhesion class G protein-coupled receptors. *Cell reports* 2(2), pp. 321–31.

Qian, F., Boletta, A., Bhunia, A.K., Xu, H., Liu, L., Ahrabi, A.K., Watnick, T.J., Zhou, F. and Germino, G.G. 2002. Cleavage of polycystin-1 requires the receptor for egg jelly domain and is disrupted by human autosomal-dominant polycystic kidney disease 1-associated mutations. *Proc. Natl. Acad. Sci. U. S. A.* 99(26), pp. 16981–6.

Quattrocchi, C.C.C., Zanni, G., Napolitano, A., Longo, D., Cordelli, D.M., Barresi, S., Randisi, F., Valente, E.M., Verdolotti, T., Genovese, E., Specchio, N., Vitiello, G., Spiegel, R., Bertini, E. and Bernardi, B. 2013. Conventional magnetic resonance imaging and diffusion tensor imaging studies in children with novel GPR56 mutations: further delineation of a cobblestone-like phenotype. *Neurogenetics* 14(1), pp. 77–83.

Rahman, M.A., Ashton, A.C., Meunier, F.A., Davletov, B.A., Dolly, J.O. and Ushkaryov, Y.A. 1999. Norepinephrine exocytosis stimulated by alpha-latrotoxin requires both external and stored Ca2+ and is mediated by latrophilin, G proteins and phospholipase C. *Philos. Trans. R. Soc. Lond. B. Biol. Sci.* 354(1381), pp. 379–86.

Rajagopal, S., Rajagopal, K. and Lefkowitz, R.J. 2010. Teaching old receptors new tricks: biasing seven-transmembrane receptors. *Nat. Rev. Drug Discov.* 9(5), pp. 373–86.

Raman, D., Osawa, S., Gurevich, V. V. and Weiss, E.R. 2003. The interaction with the cytoplasmic loops of rhodopsin plays a crucial role in arrestin activation and binding. *J. Neurochem.* 84(5), pp. 1040–1050.

Rebecchi, M. and Pentyala, S. 2000. Structure, function, and control of phosphoinositide-specific phospholipase C. *Physiol. Rev.* 80(4), pp. 1291–1335.

Reiter, E., Ahn, S., Shukla, A.K. and Lefkowitz, R.J. 2012. Molecular mechanism of β-arrestin-biased agonism at seven-transmembrane receptors. *Annu. Rev. Pharmacol. Toxicol.* 52(September), pp. 179–97.

Ridley, A.J. 2004. Rho proteins and cancer. *Breast Cancer Res. Treat.* 84(1), pp. 13–9.

Ridley, A.J., Schwartz, M. a, Burridge, K., Firtel, R. a, Ginsberg, M.H., Borisy, G., Parsons, J.T. and Horwitz, A.R. 2003. Cell migration: integrating signals from front to back. *Science* 302(5651), pp. 1704–9.

Riento, K. and Ridley, A.J. 2003. Rocks: multifunctional kinases in cell behaviour. *Nat. Rev. Mol. Cell Biol.* 4(6), pp. 446–56.

Rocheleau, C.E., Downs, W.D., Lin, R., Wittmann, C., Bei, Y., Cha, Y.H., Ali, M., Priess, J.R. and Mello, C.C. 1997. Wnt signaling and an APC-related gene specify endoderm in early C. elegans embryos. *Cell* 90(4), pp. 707–16.

Rosenbaum, D.M., Rasmussen, S.G.F. and Kobilka, B.K. 2009. The structure and function of G-protein-coupled receptors. *Nature* 459(7245), pp. 356–63.

Ross, E.M. and Gilman, A.G. 1977. Resolution of some components of adenylate cyclase necessary for catalytic activity. *J. Biol. Chem.* 252(20), pp. 6966–9.

Ruan, Q. and Johnson, G.V.W. 2007. Transglutaminase 2 in neurodegenerative disorders. *Front. Biosci.* 12, pp. 891–904.

Rutkowski, M.J., Sughrue, M.E., Kane, A.J., Kim, J.M., Bloch, O. and Parsa, A.T. 2011. Epidermal growth factor module-containing mucin-like receptor 2 is a newly identified adhesion G protein-coupled receptor associated with poor overall survival and an invasive phenotype in glioblastoma. *J. Neurooncol.* 105(2), pp. 165–71.

Sah, V.P., Seasholtz, T.M., Sagi, S.A. and Brown, J.H. 2000. The role of Rho in G protein-coupled receptor signal transduction. *Annu. Rev. Pharmacol. Toxicol.* 40, pp. 459–89.

Sahin, U., Weskamp, G., Kelly, K., Zhou, H.-M., Higashiyama, S., Peschon, J., Hartmann, D., Saftig, P. and Blobel, C.P. 2004. Distinct roles for ADAM10 and ADAM17 in ectodomain shedding of six EGFR ligands. *J. Cell Biol.* 164(5), pp. 769–79.

Saito, Y., Kaneda, K., Suekane, a, Ichihara, E., Nakahata, S., Yamakawa, N., Nagai, K., Mizuno, N., Kogawa, K., Miura, I., Itoh, H. and Morishita, K. 2013. Maintenance of the hematopoietic stem cell pool in bone marrow niches by EVI1-regulated GPR56. *Leukemia* 27(8), pp. 1637–49.

Salcman, M. 2012. Glioblastoma and malignant astrocytoma. *Am. brain tumor Assoc.*

Salhia, B., Rutten, F., Nakada, M., Beaudry, C., Berens, M., Kwan, A. and Rutka, J.T. 2005. Inhibition of Rho-kinase affects astrocytoma morphology, motility, and invasion through activation of Rac1. *Cancer research* 65(19), pp. 8792–800.

Sarkar, N.K., Clarke, D.D. and Waelsch, H. 1957. An enzymically catalyzed incorporation of amines into proteins. *Biochim. Biophys. Acta* 25(2), pp. 451–2.

Satpathy, M., Cao, L., Pincheira, R., Emerson, R., Bigsby, R., Nakshatri, H. and Matei, D. 2007. Enhanced peritoneal ovarian tumor dissemination by tissue transglutaminase. *Cancer research* 67(15), pp. 7194–202.

Scarselli, M. and Donaldson, J.G. 2009. Constitutive internalization of G protein-coupled receptors and G proteins via clathrin-independent endocytosis. *J. Biol. Chem.* 284(6), pp. 3577–85.

Schlesinger, A., Shelton, C.A., Maloof, J.N., Meneghini, M. and Bowerman, B. 1999. Wnt pathway components orient a mitotic spindle in the early Caenorhabditis elegans embryo without requiring gene transcription in the responding cell. *Genes Dev.* 13(15), pp. 2028–38.

Schlöndorff, J. and Blobel, C.P. 1999. Metalloprotease-disintegrins: modular proteins capable of promoting cell-cell interactions and triggering signals by protein-ectodomain shedding. *J. Cell Sci.* 112(Pt 2), pp. 3603–17.

Schwartz, M. 2004. Rho signalling at a glance. *J. Cell Sci.* 5457, pp. 5457–5458.

Schwartz, T.W. 1994. Locating ligand-binding sites in 7tm receptors by protein engineering. *Curr. Opin. Biotechnol.* 5(4), pp. 434–444.

Seals, D.F. and Courtneidge, S.A. 2003. The ADAMs family of metalloproteases: multidomain proteins with multiple functions. *Genes Dev.* 17(1), pp. 7–30.

Sehgal, A. 1998. Molecular changes during the genesis of human gliomas. *Semin. Surg. Oncol.* 14(1), pp. 3–12.

Seta, K. and Sadoshima, J. 2003. Phosphorylation of tyrosine 319 of the angiotensin II type 1 receptor mediates angiotensin II-induced trans-activation of the epidermal growth factor receptor. *J. Biol. Chem.* 278(11), pp. 9019–26.

Shah, B.H., Yesilkaya, A., Olivares-Reyes, J.A., Chen, H.-D., Hunyady, L. and Catt, K.J. 2004. Differential pathways of angiotensin II-induced extracellularly regulated kinase 1/2 phosphorylation in specific cell types: role of heparin-binding epidermal growth factor. *Mol. Endocrinol.* 18(8), pp. 2035–48.

Shashidhar, S., Lorente, G., Nagavarapu, U., Nelson, A., Kuo, J., Cummins, J., Nikolich, K., Urfer, R. and Foehr, E.D. 2005. GPR56 is a GPCR that is overexpressed in gliomas and functions in tumor cell adhesion. *Oncogene* 24(10), pp. 1673–82.

Shenoy, S.K. and Lefkowitz, R.J. 2003. Trafficking patterns of beta-arrestin and G protein-coupled receptors determined by the kinetics of beta-arrestin deubiquitination. *J. Biol. Chem.* 278(16), pp. 14498–506.

Shenoy, S.K., Xiao, K., Venkataramanan, V., Snyder, P.M., Freedman, N.J. and Weissman, A.M. 2008. Nedd4 mediates agonist-dependent ubiquitination, lysosomal targeting, and degradation of the beta2-adrenergic receptor. *J. Biol. Chem.* 283(32), pp. 22166–76.

Shima, Y., Copeland, N.G., Gilbert, D.J., Jenkins, N.A., Chisaka, O., Takeichi, M. and Uemura, T. 2002. Differential expression of the seven-pass transmembrane cadherin genes Celsr1-3 and distribution of the Celsr2 protein during mouse development. *Dev. Dyn.* 223(3), pp. 321–32.

Shima, Y., Kawaguchi, S., Kosaka, K., Nakayama, M., Hoshino, M., Nabeshima, Y., Hirano, T. and Uemura, T. 2007. Opposing roles in neurite growth control by two seven-pass transmembrane cadherins. *Nature neuroscience* 10(8), pp. 963–9.

Shiratsuchi, T., Futamura, M., Oda, K., Nishimori, H., Nakamura, Y. and Tokino, T. 1998. Cloning and characterization of BAI-associated protein 1: a PDZ domain-containing protein that interacts with BAI1. *Biochem. Biophys. Res. Commun.* 247(3), pp. 597–604.

Silva, J., Lelianova, V.G., Ermolyuk, Y.S., Vysokov, N. and Hitchen, P.G. 2011. Latrophilin 1 and its endogenous ligand Lasso / teneurin-2 form a high-affinity transsynaptic receptor pair with signaling capabilities. *Proc. Natl. Acad. Sci. U. S. A.* 108(29), pp. 12113–12118.

Silva, J.-P., Lelianova, V., Volynski, K.E., Hopkins, C. and Ushkaryov, Y. 2009. Functional cross-interaction of the fragments produced by the cleavage of distinct adhesion G-protein-coupled receptors. *J. Biol. Chem.* 284(10), pp. 6495–506.

Simon, M.I., Strathmann, M.P. and Gautam, N. 1991. Diversity of G proteins in signal transduction. *Science* 252(5007), pp. 802–8.

Simpson, K.J., Dugan, A.S. and Mercurio, A.M. 2004. Functional analysis of the contribution of RhoA and RhoC GTPases to invasive breast carcinoma. *Cancer res.* 64(23), pp. 8694–701.

Simundza, J. and Cowin, P. 2013. Adhesion g-protein-coupled receptors: elusive hybrids come of age. *Cell Commun. Adhes.* 20(6), pp. 213–25.

Singer, K., Luo, R., Jeong, S.-J. and Piao, X. 2012. GPR56 and the Developing Cerebral Cortex: Cells, Matrix, and Neuronal Migration. *Mol. Neurobiol.*

Sollid, L.M. 2002. Coeliac disease: dissecting a complex inflammatory disorder. *Nature reviews. Immunology* 2(9), pp. 647–55.

Somsel Rodman, J. and Wandinger-Ness, A. 2000. Rab GTPases coordinate endocytosis. *J. Cell Sci.* 113(2), pp. 183–192.

Soond, S.M., Everson, B., Riches, D.W.H. and Murphy, G. 2005. ERK-mediated phosphorylation of Thr735 in TNFalpha-converting enzyme and its potential role in TACE protein trafficking. *J. Cell Sci.* 118(Pt 11), pp. 2371–80.

Sorkin, A. and von Zastrow, M. 2009. Endocytosis and signalling: intertwining molecular networks. *Nat. Rev. Mol. Cell Biol.* 10(9), pp. 609–22.

Sorkin, A. and Von Zastrow, M. 2002. Signal transduction and endocytosis: close encounters of many kinds. *Nat. Rev. Mol. Cell Biol.* 3(8), pp. 600–14.

Sprong, H., van der Sluijs, P. and van Meer, G. 2001. How proteins move lipids and lipids move proteins. *Nat. Rev. Mol. Cell Biol.* 2(7), pp. 504–13.

Stamnaes, J., Pinkas, D.M., Fleckenstein, B., Khosla, C. and Sollid, L.M. 2010. Redox regulation of transglutaminase 2 activity. *J. Biol. Chem.* 285(33), pp. 25402–9.

Stephens, P., Grenard, P., Aeschlimann, P., Langley, M., Blain, E., Errington, R., Kipling, D., Thomas, D. and Aeschlimann, D. 2004. Crosslinking and G-protein functions of transglutaminase 2 contribute differentially to fibroblast wound healing responses. *J. Cell Sci.* 117(Pt 15), pp. 3389–403.

Sternlicht, M.D., Sunnarborg, S.W., Kouros-Mehr, H., Yu, Y., Lee, D.C. and Werb, Z. 2005. Mammary ductal morphogenesis requires paracrine activation of stromal EGFR via ADAM17-dependent shedding of epithelial amphiregulin. *Development* 132(17), pp. 3923–33.

Strokes, N. and Piao, X. 2010. Adhesion-GPCRs in the CNS. In: Yona, S. and Stacey, M. eds. *Adhesion-GPCRs*. Landes Bioscience and Springer Science+business Media, LLC, pp. 1–11.

Sud, N., Sharma, R., Ray, R., Chattopadhyay, T.K. and Ralhan, R. 2006. Differential expression of G-protein coupled receptor 56 in human esophageal squamous cell carcinoma. *Cancer letters* 233(2), pp. 265–70.

Sullivan, M.L.O., Wit, J. De, Savas, J.N., Comoletti, D., Otto-hitt, S., Iii, J.R.Y. and Ghosh, A. 2012. Report FLRT Proteins Are Endogenous Latrophilin Ligands and Regulate Excitatory Synapse Development. *Neuron* 73(5), pp. 903–910.

Szondy, Z., Sarang, Z., Molnar, P., Nemeth, T., Piacentini, M., Mastroberardino, P.G., Falasca, L., Aeschlimann, D., Kovacs, J., Kiss, I., Szegezdi, E., Lakos, G., Rajnavolgyi, E., Birckbichler, P.J., Melino, G. and Fesus, L. 2003. Transglutaminase 2-/- mice reveal a phagocytosis-associated crosstalk between macrophages and apoptotic cells. *Proc. Natl. Acad. Sci. U. S. A.* 100(13), pp. 7812–7.

Tabu, K., Ohba, Y., Suzuki, T., Makino, Y., Kimura, T., Ohnishi, A., Sakai, M., Watanabe, T., Tanaka, S. and Sawa, H. 2007. Oligodendrocyte lineage transcription factor 2 inhibits the motility of a human glial tumor cell line by activating RhoA. *Mol. Cancer Res.* 5(10), pp. 1099–109.

Tagawa, A., Mezzacasa, A., Hayer, A., Longatti, A., Pelkmans, L. and Helenius, A. 2005. Assembly and trafficking of caveolar domains in the cell: caveolae as stable, cargo-triggered, vesicular transporters. *J. Cell Biol.* 170(5), pp. 769–79.

Telci, D. and Griffin, M. 2006. Tissue transglutaminase (TG2)--a wound response enzyme. *Front. Biosci.* 11, pp. 867–82.

Terrillon, S. and Bouvier, M. 2004. Roles of G-protein-coupled receptor dimerization. *EMBO reports* 5(1), pp. 30–34.

Terskikh, A., Easterday, M., Li, L., Hood, L., Kornblum, H., Geschwind, D. and Weissman, I. 2001. From hematopoiesis to neuropoiesis: evidence of overlapping genetic programs. *Proc. Natl. Acad. Sci. U. S. A.* 98(14), pp. 3–8.

Thomas, H., Beck, K., Adamczyk, M., Aeschlimann, P., Langley, M., Oita, R.C., Thiebach, L., Hils, M. and Aeschlimann, D. 2013. Transglutaminase 6: a protein associated with central nervous system development and motor function. *Amino acids* 44(1), pp. 161–77.

Tsao, P.I. and von Zastrow, M. 2000. Type-specific Sorting of G Protein-coupled Receptors after Endocytosis. *J. Biol. Chem.* 275(15), pp. 11130–11140.

Turner, P.M. and Lorand, L. 1989. Complexation of fibronectin with tissue transglutaminase. *Biochemistry* 28(2), pp. 628–35.

Umata, T., Hirata, M., Takahashi, T., Ryu, F., Shida, S., Takahashi, Y., Tsuneoka, M., Miura, Y., Masuda, M., Horiguchi, Y. and Mekada, E. 2001. A dual signaling cascade that regulates the ectodomain shedding of heparin-binding epidermal growth factor-like growth factor. *J. Biol. Chem.* 276(32), pp. 30475–82.

Vallon, M. and Essler, M. 2006. Proteolytically processed soluble tumor endothelial marker (TEM) 5 mediates endothelial cell survival during angiogenesis by linking integrin alpha(v)beta3 to glycosaminoglycans. *J. Biol. Chem.* 281(45), pp. 34179–88.

Vega, F.M., Fruhwirth, G., Ng, T. and Ridley, A.J. 2011. RhoA and RhoC have distinct roles in migration and invasion by acting through different targets. *J. Cell Biol.* 193(4), pp. 655–65.

Verma, A. and Mehta, K. 2007. Tissue transglutaminase-mediated chemoresistance in cancer cells. *Drug Resist. Updat.* 10(4-5), pp. 144–51.

Volynski, K.E., Silva, J.-P., Lelianova, V.G., Atiqur Rahman, M., Hopkins, C. and Ushkaryov, Y. a 2004. Latrophilin fragments behave as independent proteins that associate and signal on binding of LTX(N4C). *The EMBO journal* 23(22), pp. 4423–33.

Walters, R.W., Shukla, A.K., Kovacs, J.J., Violin, J.D., DeWire, S.M., Lam, C.M., Chen, J.R., Muehlbauer, M.J., Whalen, E.J. and Lefkowitz, R.J. 2009. beta-Arrestin1 mediates nicotinic acid-induced flushing, but not its antilipolytic effect, in mice. *J. Clin. Invest.* 119(5), pp. 1312–21.

Wang, J.L., Yang, X., Xia, K., Hu, Z.M., Weng, L., Jin, X., Jiang, H., Zhang, P., Shen, L., Guo, J.F., Li, N., Li, Y.R., Lei, L.F., Zhou, J., Du, J., Zhou, Y.F., Pan, Q., Wang, J., Wang, J., Li, R.Q. and Tang, B.S. 2010. TGM6 identified as a novel causative gene of spinocerebellar ataxias using exome sequencing. *Brain* 133(Pt 12), pp. 3510–8.

Wang, T., Ward, Y., Tian, L., Lake, R., Guedez, L., Stetler-Stevenson, W.G. and Kelly, K. 2005. CD97, an adhesion receptor on inflammatory cells, stimulates angiogenesis through binding integrin counterreceptors on endothelial cells. *Blood* 105(7), pp. 2836–44.

Wang, Y., Ande, S.R. and Mishra, S. 2012. Phosphorylation of transglutaminase 2 (TG2) at serine-216 has a role in TG2 mediated activation of nuclear factor-kappa B and in the downregulation of PTEN. *BMC cancer* 12(1), p. 277.

Warne, T., Moukhametzianov, R., Baker, J.G., Nehmé, R., Edwards, P.C., Leslie, A.G.W., Schertler, G.F.X. and Tate, C.G. 2011. The structural basis for agonist and partial agonist action on a β(1)-adrenergic receptor. *Nature* 469(7329), pp. 241–4.

Watt, H., Kharmate, G. and Kumar, U. 2009. Somatostatin receptors 1 and 5 heterodimerize with epidermal growth factor receptor: agonist-dependent modulation of the downstream MAPK signalling pathway in. *Cell. Signal.* 21(3), pp. 428–439.

Werb, Z. and Yan, Y. 1998. A cellular striptease act. *Science* 282(5392), pp. 1279–80.

Werry, T.D., Sexton, P.M. and Christopoulos, A. 2005. “Ins and outs” of seven-transmembrane receptor signalling to ERK. *Trends Endocrinol. Metab.* 16(1), pp. 26–33.

Weston, M.D., Luijendijk, M.W.J., Humphrey, K.D., Möller, C. and Kimberling, W.J. 2004. Mutations in the VLGR1 gene implicate G-protein signaling in the pathogenesis of Usher syndrome type II. *Am. J. Hum. Genet.* 74(2), pp. 357–66.

Wetzker, R. and Böhmer, F.-D. 2003. Transactivation joins multiple tracks to the ERK/MAPK cascade. *Nat. Rev. Mol. Cell Biol.* 4(8), pp. 651–7.

Winstel, R., Freund, S., Krasel, C., Hoppe, E. and Lohse, M.J. 1996. Protein kinase cross-talk: membrane targeting of the beta-adrenergic receptor kinase by protein kinase C. *Proc. Natl. Acad. Sci. U. S. A.* 93(5), pp. 2105–9.

Witherow, D.S., Garrison, T.R., Miller, W.E. and Lefkowitz, R.J. 2004. beta-Arrestin inhibits NF-kappaB activity by means of its interaction with the NF-kappaB inhibitor IkappaBalpha. *Proc. Natl. Acad. Sci. U. S. A.* 101(23), pp. 8603–7.

Wolfsberg, T.G., Primakoff, P., Myles, D.G. and White, J.M. 1995. ADAM, a novel family of membrane proteins containing A Disintegrin And Metalloprotease domain: multipotential functions in cell-cell and cell-matrix interactions. *J. Cell Biol.* 131(2), pp. 275–8.

Wu, G., Krupnick, J.G., Benovic, J.L. and Lanier, S.M. 1997. Interaction of arrestins with intracellular domains of muscarinic and alpha2-adrenergic receptors. *J. Biol. Chem.* 272(28), pp. 17836–42.

Wu, J., Liu, S.L., Zhu, J.L., Norton, P.A., Nojiri, S., Hoek, J.B. and Zern, M.A. 2000. Roles of tissue transglutaminase in ethanol-induced inhibition of hepatocyte proliferation and alpha 1-adrenergic signal transduction. *J. Biol. Chem.* 275(29), pp. 22213–9.

Xu, F., Wu, H., Katritch, V., Han, G.W., Jacobson, K.A., Gao, Z.-G., Cherezov, V. and Stevens, R.C. 2011. Structure of an agonist-bound human A2A adenosine receptor. *Science* 332(6027), pp. 322–7.

Xu, L., Begum, S., Barry, M., Crowley, D., Yang, L., Bronson, R.T. and Hynes, R.O. 2010. GPR56 plays varying roles in endogenous cancer progression. *Clin Exp Metastasis* 27(4), pp. 241–9.

Xu, L., Begum, S., Hearn, J.D. and Hynes, R.O. 2006. GPR56, an atypical G protein-coupled receptor, binds tissue transglutaminase, TG2, and inhibits melanoma tumor growth and metastasis. *Proc. Natl. Acad. Sci. U. S. A.* 103(24), pp. 9023–8.

Yang, L., Chen, G., Mohanty, S., Scott, G., Fazal, F., Rahman, A., Begum, S., Hynes, R.O. and Xu, L. 2011. GPR56 Regulates VEGF production and angiogenesis during melanoma progression. *Cancer Res.* 71(16), pp. 5558–68.

Yang, L., Friedland, S., Corson, N. and Xu, L. 2014. GPR56 Inhibits Melanoma Growth by Internalizing and Degrading Its Ligand TG2. *Cancer Res.* 74(4), pp. 1022–1031.

Yao, X., Parnot, C., Deupi, X., Ratnala, V.R.P., Swaminath, G., Farrens, D. and Kobilka, B. 2006. Coupling ligand structure to specific conformational switches in the beta2-adrenoceptor. *Nat. Chem. Biol.* 2(8), pp. 417–22.

Yona, S., Lin, H.-H., Siu, W.O., Gordon, S. and Stacey, M. 2008. Adhesion-GPCRs: emerging roles for novel receptors. *Trends Biochem. Sci.* 33(10), pp. 491–500.

Yona, S. and Stacey, M. 2010. *Adhesion-GPCRs*. Yona, S. and Stacey, M. eds. Boston, MA: Landes Bioscience and Springer Science+business Media, LLC.

Yoshizawa, T. and Wald, G. 1963. Pre-lumirhodopsin and the bleaching of visual pigments. *Nature* 197, pp. 1279–86.

Yuan, L., Siegel, M., Choi, K. and Khosla, C. 2007. Transglutaminase 2 inhibitor, KCC009, disrupts fibronectin assembly in the extracellular matrix and sensitizes orthotopic glioblastomas to chemotherapy. *Oncogene* 26, pp. 2563–2573.

Von Zastrow, M. 2003. Mechanisms regulating membrane trafficking of G protein-coupled receptors in the endocytic pathway. *Life Sciences* 74(2-3), pp. 217–224.

Von Zastrow, M. 2001. Role of endocytosis in signalling and regulation of G-protein-coupled receptors. *Biochem. Soc. Trans.* 29(Pt 4), pp. 500–504.

Von Zastrow, M. and Kobilka, B.K. 1994. Antagonist-dependent and -independent steps in the mechanism of adrenergic receptor internalization. *J. Biol. Chem.* 269(28), pp. 18448–18452.

Zemskov, E. a, Mikhailenko, I., Strickland, D.K. and Belkin, A.M. 2007. Cell-surface transglutaminase undergoes internalization and lysosomal degradation: an essential role for LRP1. *J. Cell Sci.* 120(Pt 18), pp. 3188–99.

Zemskov, E.A., Janiak, A., Hang, J., Waghray, A. and Belkin, A.M. 2006. The role of tissue transglutaminase in cell-matrix interactions. *Front. Biosci.* 11, pp. 1057–76.

Zemskov, E.A., Loukinova, E., Mikhailenko, I., Coleman, R.A., Strickland, D.K. and Belkin, A.M. 2009. Regulation of platelet-derived growth factor receptor function by integrin-associated cell surface transglutaminase. *J. Biol. Chem.* 284(24), pp. 16693–703.

Zendman, A.J.. A., Cornelissen, I.M.H.. I., Weidle, U.H., Ruiter, D.J. and van Muijen, G.N.. 1999. TM7XN1, a novel human EGF-TM7-like cDNA, detected with mRNA differential display using human melanoma cell lines with different metastatic potential. *FEBS Letters* 446(2-3), pp. 292–298.

Zhang, J., Ferguson, S.S., Barak, L.S., Ménard, L. and Caron, M.G. 1996. Dynamin and beta-arrestin reveal distinct mechanisms for G protein-coupled receptor internalization. *J. Biol. Chem.* 271(31), pp. 18302–5.

Zhang, R., Tremblay, T.-L., McDermid, A., Thibault, P. and Stanimirovic, D. 2003. Identification of differentially expressed proteins in human glioblastoma cell lines and tumors. *Glia* 42(2), pp. 194–208.

Zohrabian, V.M., Forzani, B., Chau, Z., Murali, R. and Jhanwar-Uniyal, M. 2009. Rho/ROCK and MAPK signaling pathways are involved in glioblastoma cell migration and proliferation. *Anticancer research* 29(1), pp. 119–23.

Appendix I: Solutions and buffer

Buffer	Recipe
1% agarose gel	1g agarose 99ml TEA buffer 10µl ethidium bromide
4% stacking gel	3.2 ml ddH_20 0.5 ml 40% acrylamide/bis-acrylamide solution, 29:1 (Geneflow) 1.25 ml 0.5M Tris-HCl, pH 6.8 100 µl 10% SDS 100 µl 10% ammonium persulfate 10 µl TEMED
10% resolving gel	4.9 ml ddH_20 2.5 ml 40% acrylamide/bis-acrylamide solution, 29:1 2.5 ml 1.5M Tris-HCl, pH 8.8 100 µl 10% SDS 100 µl 10% ammonium persulfate 10 µl TEMED
Luria-Bertani broth (LB) medium (1L)	10g tryptone 5g yeast extract 10g NaCl
Phosphate buffered saline	10 PBS tablets (OXOID)/1L H_2O
Reducing sample buffer (2x)	3.5 ml dH2O 1.25 ml 0.5M Tris-HCl, pH 6.8 2.5 ml glycerol 2 ml 10% SDS 0.2 ml 0.5% bromophenol blue 0.5 ml β-mercaptoethanol
SDS-PAGE running buffer	25 mM Tris-HCl 190 mM glycine 0.1% SDS
TEA buffer	40 mM Tris acetate 1 mM EDTA
Tris buffered saline (TBS)	50 mM Tris-HCl, pH 8.0 150 mM NaCl
Western blot transfer buffer	25 mM Tris 190mM glycine 20% methanol
Western blot stripping buffer	62.5 mM Tris-HCl pH 6.8 2% SDS 100 mM β-mercaptoethanol

Appendix II: Chemicals

Chemical	**Manufacturer**
Acrylamid / Bisacrylamid-Lösung, 40%, 29:1	National Diagnostics, Hessle, UK
Agar-agar	Fisher Scientific, Loughborough, UK
Agarose	Invitrogen Ltd., Paisley, UK
Ammonium persulfate	Sigma-Aldrich Company Ltd., Gillingham, UK
Benzamidine	Sigma-Aldrich Company Ltd., Gillingham, UK
Bromophenol blue	Sigma-Aldrich Company Ltd., Gillingham, UK
BSA	Promega, Southhampton, UK
β-mercaptoethanol	Sigma-Aldrich Company Ltd., Gillingham, UK
Dimethylsulfoxide (DMSO)	Sigma-Aldrich Company Ltd., Gillingham, UK
dNTPs	Agilent Technologies, Inc., Edingburgh, UK
EDTA	Melford, Chelsworth, UK
Ethanol	Fisher Scientific, Loughborough, UK
Glycerol	Fisher Scientific, Loughborough, UK
Glycine	Fisher Scientific, Loughborough, UK
HCl	Fisher Scientific, Loughborough, UK
HEPES	Fisher Scientific, Loughborough, UK
Isopropanol	Fisher Scientific, Loughborough, UK
Magnesium chloride	Sigma-Aldrich Company Ltd., Gillingham, UK
Methanol	Fisher Scientific, Loughborough, UK
Nonident P-40	Sigma-Aldrich Company Ltd., Gillingham, UK
Paraformaldehyde	Fisher Scientific, Loughborough, UK
Saponin from quillaja bark	Sigma-Aldrich Company Ltd., Gillingham, UK
Skimmed milk powder	Milbona, Lidl, UK
Sodium acetate	Sigma-Aldrich Company Ltd., Gillingham, UK
Sodium chloride	Fisher Scientific, Loughborough, UK
Sodium dodecyl sulphate (SDS)	Sigma-Aldrich Company Ltd., Gillingham, UK
Sodium fluoride	Sigma-Aldrich Company Ltd., Gillingham, UK
Sucrose	Sigma-Aldrich Company Ltd., Gillingham, UK
Tetramethylethylendiamine (TEMED)	Sigma-Aldrich Company Ltd., Gillingham, UK
Tris Base	Fisher Scientific, Loughborough, UK
Trypan blue	Sigma-Aldrich Company Ltd., Gillingham, UK
Tryptone	Fisher Scientific, Loughborough, UK
Tween-20	Sigma-Aldrich Company Ltd., Gillingham, UK
Yeast extract	Fisher Scientific, Loughborough, UK
Vectashield mounting medium	Vector Laboratories, Burlingame, USA

Appendix III: Consumables and laboratory equipment

Consumable	Manufacturer
Developer G153	Agfa, Mortsel, Belgium
Fixer G354	Agfa, Mortsel, Belgium
Cryo vials	Greiner Bio-One Ltd., Stonehouse, UK
Pipette tips (10, 100, 200, 1000 µl)	Elkay Laboratory Products (UK) Limited, Hampshire, UK
Foams	Bio-Rad Laboratories Ltd., Hertfordshire, UK
Filter paper	Fisher Scientific, Loughborough, UK

Equipment	Manufacturer
Balance MXX-212	Denver Instrument GmbH, Göttingen, Germany
Combs (0.75 or 1 mm)	Bio-Rad Laboratories Ltd., Hertfordshire, UK
Glass coverslips	VWR International Inc., Chicago, USA
Glass plates (0.75 or 1 mm)	Bio-Rad Laboratories Ltd., Hertfordshire, UK
Freezing container	Nalgene Labware, Thermo Fisher Scientific, Basingstoke, UK
Gel electrophoresis tank, Mini-proteanII	Bio-Rad Laboratories Ltd., Hertfordshire, UK
Incubator	Binder GmbH, Tuttlingen, Germany
Labofuge H00 R Heraeus	Thermo Fisher Scientific, Basingstoke, UK
Magnetic stirrer	Falc instruments, Tremglio, Italy
Microcentrifuge (Centrifuge 5415 R)	Eppendorf UK Limited, Cambridge, UK
Microscopy slides	Carl Zeiss AG, Oberkochen, Germany
Mini Trans-Blot cell	Bio-Rad Laboratories Ltd., Hertfordshire, UK
Neubauer counting chamber	VWR International Inc., Chicago, USA
OMEGA plate reader	BMG Labtech, Offenburg, Germany
pH meter (pH209)	Hanna instruments
Pipettes	Starlab, Milton Keynes, UK and Gilson Scientific Ltd., Bedfordshire, UK
Pipette boy	Integra Biosciences Ag, Zizers, Switzerland
Power supply (Power Pac HC)	Bio-Rad Laboratories Ltd., Hertfordshire, UK
Rotator plate (Luckham 802 suspension mixer)	Luckham Ltd., Sussex, UK
Shaker plate (IKA-VIBRAX-VXR, Type VX7)	IKA-Werke GmbH & CO. KG, Staufen, Germany
Tweezers	VWR International Inc., Chicago, USA

UVP UV gel doc (Gel doc – It TS Imaging System)	Ultra-Violet Products Ltd, Cambridge, UK
UVP UV gel doc (Gel doc – It TS Imaging System)	Ultra-Violet Products Ltd, Cambridge, UK
X-ray hypercassettes	Amersham Bioscience, GE Healthcare Ltd., Buckinghamshire, UK

Appendix IV: DNA sequences endcoding shRNAs used to stably transfect U373 glioblastoma cells

- shGPR56.2 (21 bp): GAACCGACATGCTGGGAGATT
- shGPR56.4 (21 bp): ACTGACCTCTGTGAGATTCAT
- shNON-CODING(21 bp): GGAATCTCATTCGATGCATAC

Appendix V: Sequence of wild type GPR56, 693 aa

MTPQSLLQTTLFLLSLLFLVQGAHGRGHREDFRFCSQRNQTHRSSLHYKPT
PDLRISIENSEEALTVHAPFPAAHPASRSFPDPRGLYHFCLYWNRHAGRLH
LLYGKRDFLLSDKASSLLCFQHQEESLAQGPPLLATSVTSWWSPQNISLPS
AASFTFSFHSPPHTAAHNASVDMCELKRDLQLLSQFLKHPQKASRRPSAAP
ASQQLQSLESKLTSVRFMGDMVSFEEDRINATVWKLQPTAGLQDLHIHSRE
EEQSEIMEYSVLLPRTLFQRTKGRSGEAEKRLLLVDFSSQALFQDKNSSQV
LGEKVLGIVVQNTKVANLTEPVVLTFQHQLQPKNVTLQCVFWVEDPTLSSP
GHWSSAGCETVRRETQTSCFCNHLTYFAVLMVSSVEVDAVHKHYLSLLSY
VGCVVSALACLVTIAAYLCSRVPLPCRRKPRDYTIKVHMNLLLAVFLLDTSFL
LSEPVALTGSEAGCRASAIFLHFSLLTCLSWMGLEGYNLYRLVVEVFGTYV
PGYLLKLSAMGWGFPIFLVTLVALVDVDNYGPIILAVHRTPEGVIYPSMCWIR
DSLVSYITNLGLFSLVFLFNMAMLATMVVQILRLRPHTQKWSHVLTLLGLSLL
GLPWALIFFSFASGTFQLVVLYLFSIITSFQGFLIFIWYWSMRLQARGGPSPL
KSNSDSARLPISSGSTSSSRI

Appendix VI: Stably transfected HEK293 control cells stained for GPR56 and TG2.

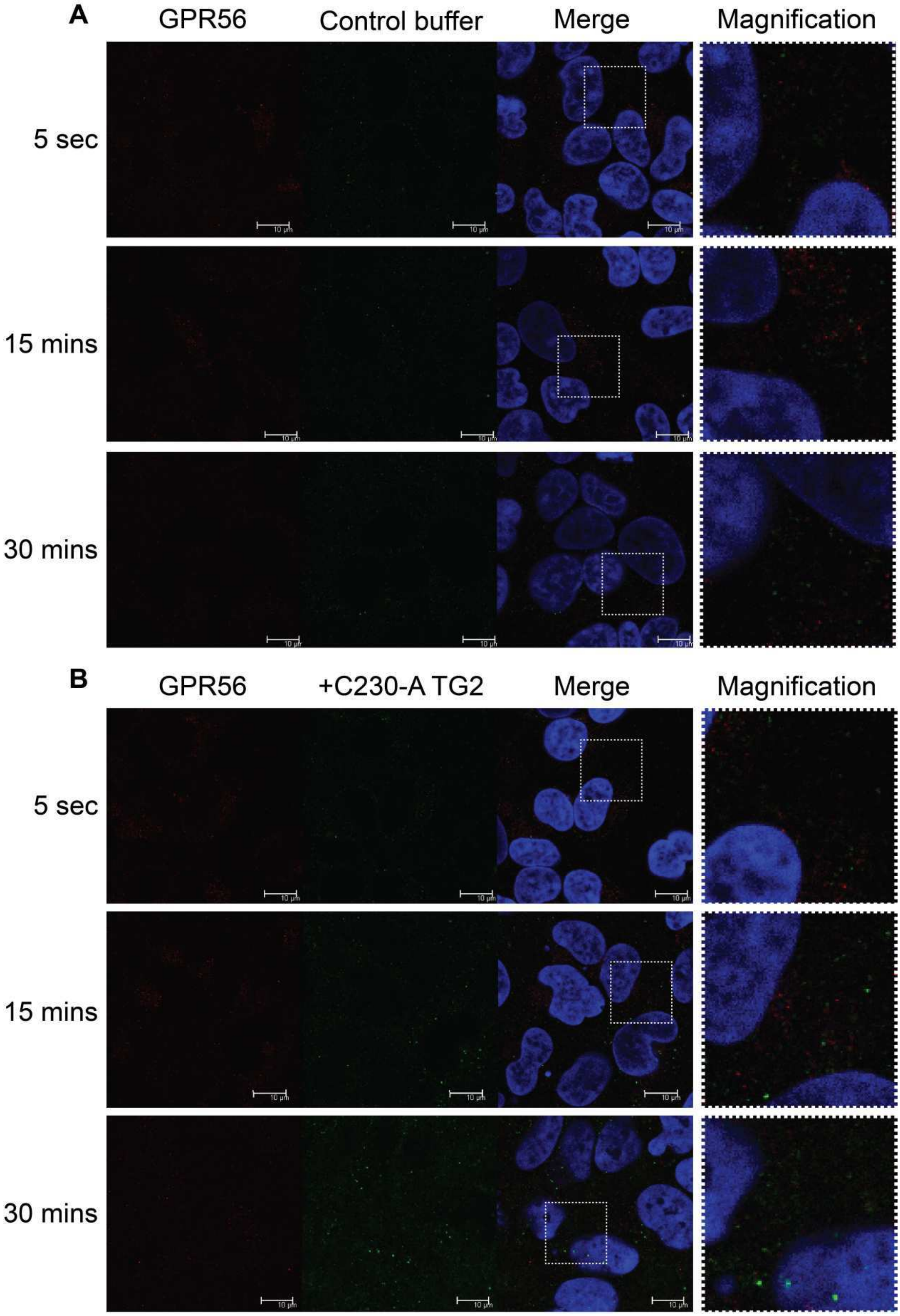
A
GPR56
Control buffer
Merge
Magnification
5 sec
15 mins
30 mins
B
GPR56
+C230-A TG2
Merge
Magnification
5 sec
15 mins
30 mins
10 µm

Figure Appendix VI: Stable HEK293 control cells stained for GPR56 and TG2.

The GPR56 inducible cell line was seeded onto poly-L-lysine coated glass coverslips and cultured for 48 h without antibiotics prior to 1 h serum starvation. Cells were then treated for 5 sec, 15 mins or 30 mins with (A) control buffer or (B) 20 µg/ml C_{230}-A TG2. Cells were fixed and permeabilised and GPR56 was stained with anti-N-GPR56 (red; R&D Systems) and anti-sheep Alexa568 antibody (Jackson ImmunoResearch). C_{230}-A TG2 was stained with monoclonal anti-TG2 (green; Thermo Scientific) and anti-mouse Alexa488 antibodies (Jackson ImmunoResearch).

(A)&(B) Cells are negative for GPR56 expression and TG2 staining at any time.